CRANFIELD UNIVERSITY

Andrew Upton

Methods, measurements, and novel materials for improving depth filtration processes used in drinking water treatment.

SCHOOL OF WATER ENERGY AND ENVIRONMENT

EngD
Academic Year: 2020 - 2021

Supervisor: Prof. Peter Jarvis
Associate Supervisor: Prof. Bruce Jefferson
June 2021

CRANFIELD UNIVERSITY

STREAM INDUSTRIAL DOCTORATE CENTRE
Cranfield Water Science Institute

EngD

Academic Year 2020 - 2021

Andrew Upton

Methods, measurements, and novel materials for improving depth filtration processes used in drinking water treatment.

Supervisor: Prof. Peter Jarvis
Associate Supervisor: Prof. Bruce Jefferson
June 2021

This thesis is submitted in partial fulfilment of the requirements for the degree of EngD.

ABSTRACT

Rapid media filtration is used to treat most surface water sources for municipal drinking water supply. This thesis presents results of an investigation into how media filters in Scottish Water, built decades ago to different standards, can meet increasingly stringent water quality requirements.

A new method for efficient assessment of filter performance and diagnosis of issues using online data were developed. A recursive partitioning algorithm applied to operationally relevant predictor variables was shown to efficiently and effectively characterise the conditions associated with elevated turbidity over an extended period of operation. Tree models can then be used to communicate a diagnosis in operational terms to aid the efficient management of individual pathogen barriers in a multi-barrier system.

Robust rapid filtration requires effective coagulation. An investigation was conducted at a water treatment works (WTW) to understand the influence of zeta potential. The effective zeta potential window was modelled & observed to change with conditions. The online measurement of zeta potential was shown to be useful for process optimisation by providing a quantitative measurement with a mechanistic basis for coagulation conditions. This provides advantages over jar testing which may poorly represent the system under investigation.

Pilot and full-scale trials of an alternative expanded aluminosilicate media show that the additional bed expansion achieved by replacing sand with the lower density material can, at comparatively low cost, improve the performance of rapid gravity filters with a common design limitation. The effective application of new finer grade expanded aluminosilicate was shown at pilot and full scale.

This thesis presents a suite of efficient solutions to ensure aging 20th century filters robustly meet challenges in 21st century. This is achieved by improving understanding of how and why specific constraints limit the performance of existing RGFs and developing strategic solutions to overcome common limitations to process performance.

Keywords:

Coagulation, Filtration, Media, Water treatment, Filter, Turbidity

ACKNOWLEDGEMENTS

Generous funding from the EPSRC and Scottish Water enabled this project to take place.

Thank you to Pete and Bruce, for your guidance, patience and good humour and for giving me this life-changing opportunity.

I owe a huge thanks to Graeme for the incredible generosity of support that you have given me and faith you have shown in the project. Thanks also for your guidance and all your work driving what success has come from this project.

Thank you Amanda & Tania for everything you have done to welcome, help and organise me. I'd like to thank Ed for the many nudges he has given me in the right direction over the last few years. I want to thank Paul for his relentlessly enthusiastic support, advice and guidance. Many thanks to Stewart and Nic for their guidance and advice and the fantastic data which has directed much of this project and multiplied the value of the work many times over. Thanks to Ross, Craig, Colin, Cammy & Chris, Jack and Peter for putting up with me on site and having the faith to put it into practice.

Thank you to Mum & Dad for your encouragement and support over the years.

Thank you Louise for your love and support, encouragement and patience and for the many ways you made this a possibility.

Louise & Magnus thank you for giving me the only title that matters.

TABLE OF CONTENTS

LIST OF FIGURES

LIST OF SUPPLEMENTARY FIGURES

LIST OF TABLES

LIST OF SUPPLEMENTARY TABLES

LIST OF EQUATIONS

LIST OF ABBREVIATIONS

abs	absorbance
ANOVA	Analysis of variance
AR-1	Autoregressive order 1
CART	Classification And Regression Tree
CBHL	Clean Bed Head Loss
D10	Diameter of 10th percentile particle
D50	Diameter of 50th percentile particle
DAF	Dissolved Air Flotation
DBP	Disinfection-by-product
DOC	Dissolved organic carbon
EBV	Empty bed volume
GAM	Generalised additive model
GAMM	Generalised additive mixed model
HC	High density crushed
HL	Head loss
HRS	Hours
LME	Linear mixed-effects
MAD	Median Absolute Deviation
MAPE	Median Absolute Percentage Error
MGCV	Mixed Generalised Additive Model Computation Vehicle
MTBF	Mean time between failures
MTTR	Mean time to recovery
mV	milli volt
NC	Normal density crushed
NCBHL	Normalised Clean Bed Head Loss
NOM	Natural Organic Matter
NTU	Nephelometric Turbidity Units
OLS	Ordinary least squares
PACl	Poly-aluminium chloride
PCA	Principal Components Analysis
RGF	Rapid Gravity Filter
RMSE	Root Mean Squared Error

RPC	Receiver Operating Characteristic
RSQ	coefficient of variation
SG	Specific Gravity
T_{goal}	targeted turbidity value
TOC	Total Organic Carbon
T_p	pth percentile turbidity
TRI	Turbidity Robustness Index
UFRV	Unit filter run volume m3/m2/run
UV	Ultraviolet
UV_{254}	UV at 254 nm
VIF	Variance Inflation Factor
V_{mf}	minimum velocity required to achieve fluidisation
VNHL	Volume Normalised Head Loss
WTW	Water treatment works

1 Introduction

1.1 Background

The purpose of water treatment for municipal supply is to remove, or render harmless, contaminants from environmental water sources to provide wholesome drinking water that presents minimal public health risk. Removal of contaminants is commonly achieved through the destabilisation and precipitation of dissolved and colloidal material (coagulation) followed by aggregation (flocculation) and physical separation of the resulting particulate matter (clarification & filtration). Residual pathogens are deactivated, and their re-growth suppressed with chlorine. In most large potable water supply systems, rapid media filtration processes are the final barrier for removal of particulates before water reaches the tap. This thesis focuses on filtration in Scottish Water through investigation of the technical and strategic causes for sub-optimal process operation and considers solutions for improving filtration performance.

Filter performance is commonly gauged by measuring the turbidity into and out of the process. Turbidity is an indicator of the cloudiness of the water caused by colloids and particulates and is usually measured as the light scattered at 90° measured in nephelometric turbidity units (NTU). Though turbidity does not describe the quantity and character of suspended particles at concentrations of interest in water, it is cheaply measured and remains a ubiquitous indicator of physical water treatment performance. The World Health Organisation suggests that prior to chlorination water should average below 0.2 NTU and not exceed 0.5 NTU for large drinking water supplies (WHO, 2015). The recent recast of the revised EU Drinking Water Directive has proposed that turbidity should be considered a biological parameter which should be monitored online (European Parliament, 2019). Elevated turbidity is considered indicative of sub-optimal performance, increased risk of pathogen passage, reduced disinfection performance and elevated risk of gastrointestinal illness (Huck *et al.*, 2001; Léziart *et al.*, 2019; Mann *et al.*, 2007).

Rapid media filtration systems are typically large concrete constructions with a long operational life which are expensive to build and modify. Civil components have typically had an estimated asset life of 60 years, with the filter media and mechanical elements estimated to be replaced every 20 years (Water Industry Commission for

Scotland, 2009). Several changes have occurred since the design and construction of most of the filters in use today, these include:

1. The regulation of water quality over time has become increasingly more stringent. Specifically, the recast Drinking Water Directive includes turbidity as a microbiological parameter, with a limit of 1 NTU that should be maintained at less than 0.3 NTU for 95% of samples and should not exceed 0.5 NTU for 15 consecutive minutes (European Parliament, 2019).

2. The concentration of natural organic matter (NOM) in surface waters has increased in northern Europe and America (Pagano *et al.*, 2014). This increasing loading of NOM has challenged filters beyond the operational expectations at the time of design.

3. The standard of filter design and approaches to operation have progressed since many of the filters in use today were built. For example, it has become more common to design filters with dual media or with a larger coarse media. Media beds are typically backwashed at higher rates or using the combination of air and water. After washing, the first few bed-volumes of water do not typically enter supply but are instead “run to waste”.

It is the responsibility of water utilities to make the most effective use of their assets, providing good value to society by keeping them operational for their full design life (and beyond in many cases). Innovative solutions are required to enable ageing filters to be able to meet higher water quality expectations in the face of more challenging conditions. This must also be considered alongside the level of investment which is appropriate for treatment systems with limited remaining design life. The focus of this research was to develop and apply new approaches in order to deliver filter performance fit for the 21st century from filters that were designed for the 20th century.

1.1.1 Rapid media filtration in water treatment

Records suggest that the use of sand as a media to filter water has been practised for over 4000 years (Baker, 1949). Today, there are broadly three types of media filters which can be considered in terms of the primary mechanism which underpins their operation: 1) Depth filters use an inert media to collect particles which are then physically removed; 2) adsorption contactors exploit surface properties of a media to

remove specific contaminants, and 3) biological filters which provide a substrate for microorganisms grow on and then break down contaminants. This thesis is concerned with the application of rapid depth filtration.

The story of developments in depth filtration is one of relatively limited and slow progress constrained by limited incentives, risk aversion and relatively long-lived and expensive assets. However, one major innovation in media filtration was the development of rapid filtration from slow filtration processes. Rapid filtration relies predominantly on physical and chemical processes for removal of contaminants, this distinguishes them from slow filters for which biological processes are also vital (Ives, 1970). Rapid filtration is typically used to remove colloidal particles between 0.01 and 10µm, normally using sand media with an effective size which is typically over 500µm with pores in the region of 35-50µm (Amirtharajah, 1988). In order to ensure that particles are removed by physical means, water for rapid media filtration should be treated by coagulants to de-stabilise and aggregate particles prior to their collection on media grains.

To maintain effective particle removal rapid filters typically require careful operation and maintenance. Performance deterioration can occur if the condition of the filter deteriorates, or if aspects of filter design may mean that it is incapable of meeting performance requirements, or due to the way that the filter or pre-treatment stages are operated. Figure 1 illustrates the main components of a rapid depth filter and some of the issues which can affect performance.

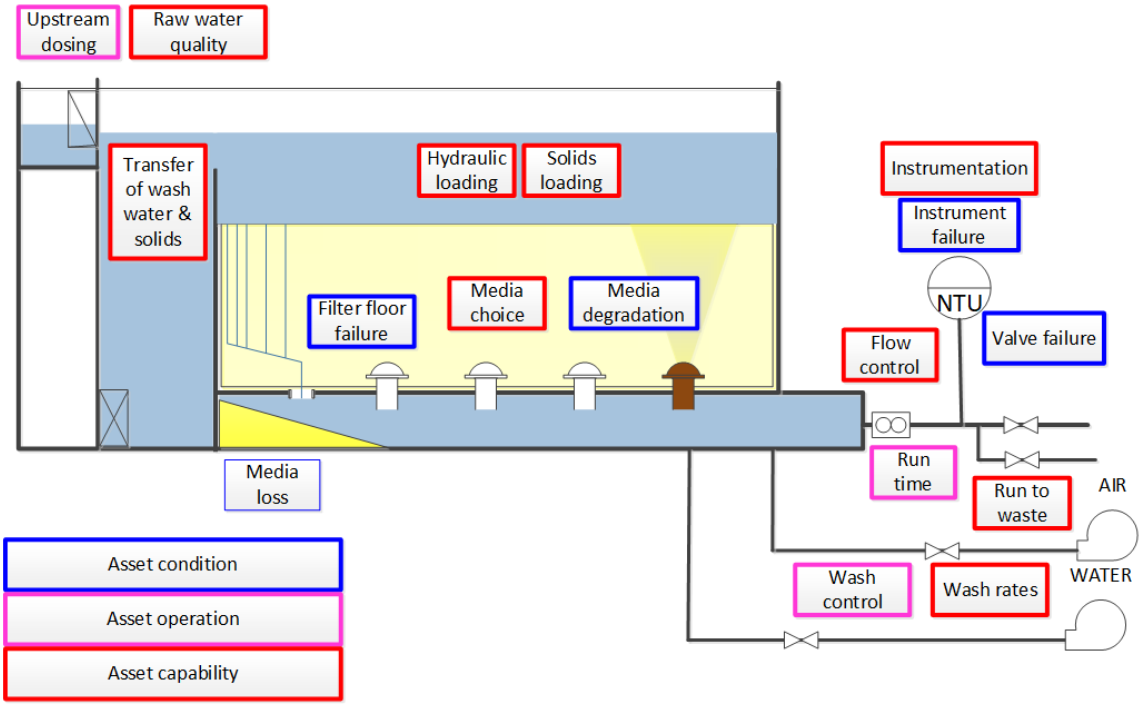

Figure 1 Diagram showing a typical depth filter including some of the issues which can affect performance, depending on the asset condition (blue), operation (pink) and capability (red).

The major advances in rapid filtration in the last century have been the adoption of dual and multi media filters in the 1960s and the shift to deep-bed coarse mono-media filtration in the 1990s (Hendricks, 2006). More recently the inclusion of run-to-waste facilities have reduced risks associated with high levels of particles commonly observed at the start of a filter run. These changes to process design have been accompanied by advances in monitoring and control which have been followed by reduction in the numbers of operators and engineers overseeing filtration processes. The relatively slow rate of innovation is due to the combination of long asset life expectancy, understandable risk aversion in public health engineering and the acceptable performance of a relatively narrow set of standard designs. Another barrier to innovation is that filtration is a technology that is relatively simple to implement and operate acceptably but complicated to fully optimise. A depth filter in water treatment should operate robustly, performing well during adverse conditions (Huck and Coffey, 2004). Filtration is difficult to optimise because there are complex interacting physical and chemical processes occurring that influence the efficacy of particle removal. This is further complicated by the fact that some of the components such as the media bed

are fixed for long periods of time whilst the condition of the water to be treated fluctuates. Some of the important variables that govern filtration performance include:

- The physico-chemical properties of the media surface including surface charge, surface activation, chemical species.
- The physical properties of the media grain including size, density, shape, friability and roughness.
- The aggregate properties of the media grains within localised areas of the filter bed govern properties such as porosity and the transition between regions with different properties though the profile of the bed.
- Characteristics of the water to be treated including temperature, corrosivity and solids load.
- The hydraulic and solids loading rate and the rate of change of these variables.
- Characteristics of the particles and aggregates to be removed including size, charge, strength and density.
- Physical forces imparted on the media during the filter wash to dislodge deposited solids.
- The characteristics of the particles dislodged from the media during the filter wash, including size and density.
- Factors governing the efficiency of the transport of dislodged solids from the filter.

1.1.2 Measurements for quantifying filter performance

There are two common bases for characterising the performance of a filtration system, these are the quality of filtered water and the efficiency. The most common means of assessing filtered water quality is through the measurement of turbidity. Turbidity quantifies the extent to which suspended particles scatter light subject to their concentration, size and colour (Anderson, 2005). Efficiency of filters can be considered in terms of productivity or water efficiency; contaminant capture in terms of particles or mass of solids capture; hydraulically in terms of head loss; or cost in terms of capital

and operational expenditure. This project is primarily concerned with the performance of filters in terms of turbidity in relation to a target of 0.1 NTU in filtered water. As an optical property, the turbidity of a sample does not directly link to a health risk. However, turbidity has been associated with the presence of bacteria, the shielding of micro-organisms from disinfection, causing additional chlorine demand, increasing disinfection-by-product (DBP) formation and promoting biological growth in distribution systems (LeChevallier, Evans and Seidler, 1981; McCoy and Olson, 1986). In the UK, the prescribed value for turbidity is 4 Nephelometric Turbidity Units (NTU) and water must be below 1 NTU to demonstrate sufficient preliminary treatment prior to disinfection and upon leaving the WTW (Scottish Statutory Instruments, 2014; Statutory Instruments, 2016) .

Turbidity measurement in filtration is ubiquitous and therefore has the advantage of already being relatively consistently measured and recorded. The specification of low turbidity in filtered water as being < 0.1 NTU (LeChevallier and Kwok-Keung, 2004). The use of a turbidity value of 0.1 NTU as a benchmark for good performance, though broadly considered to be reasonable and appropriate, can be criticised on three fronts: sensitivity, specificity and substitutability.

Sensitivity: in treated waters turbidity instruments are working at the lower range of their capability so that random error may be in the same order of magnitude as the observed value (Russell, 2014). Gregory (1994) concludes that conventional turbidity measurements are not sufficiently sensitive to particles in the *Cryptosporidium* oocyst size range. There is typically inconsistency in the readings given by turbidity instruments of different design (Letterman *et al.*, 2004). In addition, the reduction in disinfection efficiency by turbidity particles has been shown to be dependent upon the material which generates light scatter (Farrell *et al.*, 2018; Léziart *et al.*, 2019).

Specificity: turbidity is a function of the surface area and refractive index of the particles within a given system, rather than their risk. Previous investigators have concluded that turbidity is not a quantitative indicator of *Cryptosporidium* removal capability or strongly related to particle counts (Bridgeman, Simms and Parsons, 2002; Huck *et al.*, 2002a). As turbidity describes the relative extent to which suspended particles scatter light due to the combined effects of concentration, size and colour of suspended particles it is not a conserved quantity in the way that other measurements of water

quality are, such as suspended solids (Bridgeman *et al.*, 2002; Davies-Colley and Smith, 2001). Equivalent turbidity values have been shown to be representative of different particle concentrations, dependent on the composition of the turbidity material (Farrell *et al.*, 2018; Léziart *et al.*, 2019).

Substitutability: particle counters have been demonstrated to have greater sensitivity to filter breakthrough than turbidimetry (Hargesheimer *et al.*, 1998). However, it is not the case that a particle counter is a substitute for turbidity monitoring, rather a supplement as they have been demonstrated to measure different things which are not linearly related (Bridgeman *et al.*, 2002). Though limitations to the sensitivity of turbidity have been observed in comparison to particle count monitoring, its simplicity, reliability and economy ensure that turbidity remains the most widely used parameter for monitoring filter performance (Gregory, 1994; Hartshorn *et al.*, 2014; Huck *et al.*, 2001).

In water supply systems in the developed world public health risk is primarily associated with contamination or challenge events and the frequency of typical regulatory monitoring is ineffective at capturing such events (Rizak and Hrudey, 2007). On-line turbidity meters, which provide a record to evidence filtration performance with a degree of granularity far greater than can be achieved by regulatory sampling, have been widely interpreted to indicate removal performance of water-borne pathogens (Lusardi and Consonery, 1999).

The World Health Organisation suggests that prior to chlorination large municipal supplies should average below 0.2 NTU and not exceed 0.5 NTU (WHO, 2015). A best practice target of 0.1 NTU has previously been proposed to limit the risk of pathogen passage (EPA, 1998).

1.1.3 Key particle properties

Contaminant particles of primary concern in water treatment consist of suspended, colloidal, and dissolved materials with varied properties. Colloidal particles and dissolved molecules are driven to continuous (Brownian) movement due to thermal agitation and other natural and engineered hydrodynamics. Bratby (2016) summarises that this motion results in interactions between colloids, dissolved molecules, and ions

on convergent trajectories and interaction between particles and static surfaces from which there are three important potential outcomes:

- Electrostatic or steric repulsion could alter particle trajectory preventing collision.
- Particles could collide and separate again and return on a different trajectory.
- Molecules or ions could collide and become chemically adsorbed by ionic, covalent, hydrogen, dipolar bonding or van der Waals attraction.

Removal of contaminant particles by conventional coagulation, flocculation and filtration processes is dependent on the manipulation of properties such that the number of collisions, or the success in terms of attachment of these collisions, is increased. The property that allows colloidal particles to persist in a dispersion is known as stability. Colloidal stability primarily arises from the presence of surface charge and hydration of surface layers of a colloid (Stumm and Morgan, 1996). Stability is therefore achieved either from properties which reduce the likelihood of interaction with other particles or properties which reduce the likelihood that any given interaction would result in aggregation.

The water molecule exists as a dipole, with positive charge arising from the two hydrogen atoms and negative charge arising from the oxygen atom's free electrons. This property of water serves to bind water molecules at the interface of solids and results in the orientation of water molecules in the vicinity of a charged surface. Particles with significant surface charge co-ordinate water molecules and ions in proximity into an electrical double layer (Chapman, 1913; Gouy, 1910; in Stumm and Morgan, 1996). The first layer, or Stern layer, consists of water molecules and ions adsorbed onto the solid surface due to chemical interactions. The second layer is known as the diffuse layer and consists of a cloud of ions and counter ions balanced to neutralise this particle charge. This co-ordination prevents particles converging to a proximity which would allow weak intermolecular Van der Waals forces to drive particle attachment (Stumm and Morgan, 1996). This particle stability must be overcome in order for effective filtration to be achieved.

1.1.4 Pre-treatment for rapid filtration

The pre-treatment to de-stabilise particles is the most important variable affecting filtration efficiency (Amirtharajah, 1988). Coagulation in water treatment is typically achieved by dosing aluminium or iron salts or pre-polymerised coagulants such as poly-aluminium chloride (PACl). When dosed, trivalent metal ions become rapidly hydrolysed into different species depending upon the process conditions. These hydrolysis products then interact to destabilize the particle system. The efficacy of these different hydrolysis products varies considerably. Use of pre-hydrolysed metal salts improves control of the hydrolysis species formed and so can be used for more reliably maintaining effective coagulation conditions over a range of pH and temperature conditions particularly in low turbidity waters (Van Benschoten and Edzwald, 1990).

Colloidal and dissolved contaminants can become destabilised by the addition of coagulants through four key mechanisms which vary depending on the particles involved and the coagulant used (Bratby, 2016; Hendricks, 2006).

- Double layer compression: by increasing the ionic strength of a solution the thickness of the double layer is reduced.
- Charge neutralisation: Cationic coagulant hydrolysis products are incorporated within the diffuse layer weakening the electrostatic repulsion between particles.
- Adsorption destabilisation: Dissolved cationic metal hydrolysis species become adsorbed to the negatively charged surfaces of particles directly reducing the effective surface charge.
- Particle bridging: Polymerised ions can act to de-stabilise particles during coagulation by forming a bridge between particles.
- Enmeshment: At sufficient concentration and pH, coagulant metal ions precipitate and form a weak amorphous structure which enmeshes colloids and particles.

For effective aggregation of destabilised particles to take place, sufficient collisions between particles must occur. Flocculation is a two-stage process. Firstly, peri-kinetic flocculation arises from the random movement of particles due to thermal agitation and has limited effect once flocs grow beyond a certain size. Secondly, orthokinetic

flocculation requires agitation, promoting particle interactions by introducing velocity gradients.

1.1.5 Detachment and shear

The accumulation of deposits over the course of a filter run, described in phenomenological models, results in narrowing of pores within the media and a consequential increase in the interstitial flow velocity for any given approach velocity. Increasing velocity increases the drag force on the deposited particles and detachment and shear occurs when these drag forces are greater than the forces of attachment or the strength of the floc (Amirtharajah, 1988).

1.1.6 Theories of filtration

Fundamental theories of depth filtration start with an assumption of an idealised homogenous uniform stable particle filtration system and describe mass or particle population transfer from the liquid phase to the filter media with depth (Equation 1). This has been further developed to describe the interaction of (contaminant) particles and collectors (media grains) in terms of two stages, namely transport and attachment. These transport and attachment efficiencies, quantified in fundamental theories of filtration, can be used to characterise the relationship between physical characteristics of a filtration system and performance of the filtration process from the filter coefficient (λ) as defined in Equation 2 (Yao, Habibian and O'Melia, 1971).

Equation 1 Fundamental filtration model (Iwasaki, 1937)

$$-\frac{\delta C}{\delta L} = \lambda C$$

Where: C = particle concentration or mass (nbr/L or mg/L), L = depth within the filter media (m), and λ is the filter coefficient.

Equation 2 definition of the filter coefficient (Yao *et al.*, 1971)

$$\lambda = \frac{3(1-\Phi)\eta\alpha}{2d_c}$$

Where: Φ = porosity, η = transport efficiency, α= attachment efficiency and d_c = diameter of the collector (m)

Transport, or the movement of the contaminant particle to the surface of the collector is governed by the physical characteristics of the system. The efficiency of attachment is then governed by physio-chemical surface effects. Transport mechanisms within

depth filtration include straining, sedimentation, interception, diffusion, inertia and hydrodynamic action (illustrated in Figure 2 from Ives, 1970).

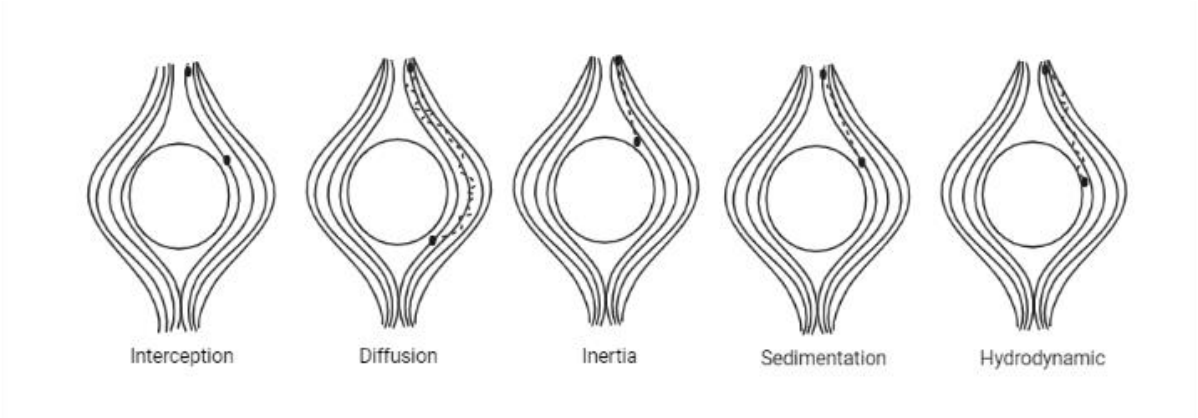

Figure 2 Illustration of fundamental transport mechanisms adapted from Ives (1970)

Models to estimate transport efficiency on the basis of physical properties typically simplify transport as the sum of three mechanisms: diffusion, interception and gravity Equation 3 (Yao *et al.*, 1971). Other mechanisms of transport are considered to be negligible.

Equation 3 Equation for single collector efficiency (Yao *et al.*, 1971)

$$\eta_0 = \eta_D + \eta_I + \eta_G$$

Where: η_D is the transport by diffusion, η_I is the transport by interception, and η_G is the transport due to gravity.

Trajectory theories have been developed to adapt fundamental theories of transport to the dynamic hydraulic properties of filters during the run (Rajagopalan and Tien, 1976; Tufenkji and Elimelech, 2004). One established approach is described by equations relating transport, by different mechanisms, to physical characteristics of the system including: the aspect ratio (Equation 4), Peclet number (Equation 5), Van der Waals number (Equation 6), attraction number (Equation 7), gravity number (Equation 8) and porosity (Equation 9). The dominant mechanisms of diffusion (Equation 10), interception (Equation 11) and gravity (Equation 12) can then be quantified by relating them to the physical characteristics and their sum can be used to estimate transport efficiency (Equation 3).

Equation 4 Aspect ratio between particle and collector sizes

$$N_R = \frac{d_p}{d_c}$$

Where: d_p = particle diameter (m) and d_c is the collector diameter (m)

Equation 5 Peclet number quantifying the ratio of transport by convection and diffusion

$$N_{Pe} = \frac{Ud_c}{D_\infty}$$

Where: U = fluid approach velocity (m/s), D_∞ = bulk diffusion coefficient (m/s^2)

Equation 6 Van der Waals number quantifying the ratio of van der Waals interaction energy to particle energy

$$N_{vdW} = \frac{A}{kT}$$

Where: A = Hamaker constant (J), k = Boltzmann constant (1.381x10-3 J/K), T = fluid absolute temperature (K)

Equation 7 attraction number; represents combined influence of van der Waals attraction forces

$$N_A = \frac{A}{12\pi\mu a_p^2 U}$$

Where: A = Hamaker constant (J), a_p = particle radius (m), U = fluid approach velocity (m/s), μ = absolute fluid viscosity (kg/m-s),

Equation 8 gravity number; ratio of Stokes particle settling velocity to approach velocity of the fluid

$$N_G = \frac{2}{9}\frac{a_p^2(\rho_p - \rho_f)g}{\mu U}$$

Where: ρ_p=particle density (kg/m^3), ρ_f=fluid density (kg/m^3), g = acceleration due to gravity (m/s^2)

Equation 9 porosity parameter

$$A_s = \frac{2(1-\gamma^5)}{2-3\gamma+3\gamma^5-2\gamma^6}$$

Where: $\gamma = (1-\Phi)^{1/3}$, and Φ = porosity

Equation 10 Diffusion transport mechanism

$$\eta_D = 2.4A_S^{1/3}N_R^{-0.081}N_{Pe}^{-0.715}N_{vdW}^{0.052}$$

Equation 11 Interception transport mechanism

$$\eta_I = 0.55 A_S N_R^{1.675} N_A^{0.125}$$

Equation 12 Gravitational transport mechanism

$$\eta_G = 0.22 N_R^{-0.24} N_G^{1.11} N_{vdW}^{0.053}$$

Fundamental models can be used to illustrate how changes to media materials and design may impact filter performance. For example, increasing size or porosity will reduce the removal rate requiring an increased depth to achieve the same rate of particle removal (Figure 3). However, smaller, less-porous media incur high head loss and may become blinded by larger particles. Equally, these models can also be used to illustrate how converting from a mono media to a dual media filter can reduce the risk of blinding but retain a high rate of particle removal within the depth of filter. However, it should be noted that fundamental models, whilst useful for understanding some properties of filters are typically ineffective at predicting the performance of real filters (Crittenden *et al.*, 2012). The real-life accuracy of fundamental models is limited because change to the characteristics of particles, pores and surface chemistry occurs over a filter run in a non-uniform way which cannot readily be observed (Amirtharajah, 1988; Ives, 1970).

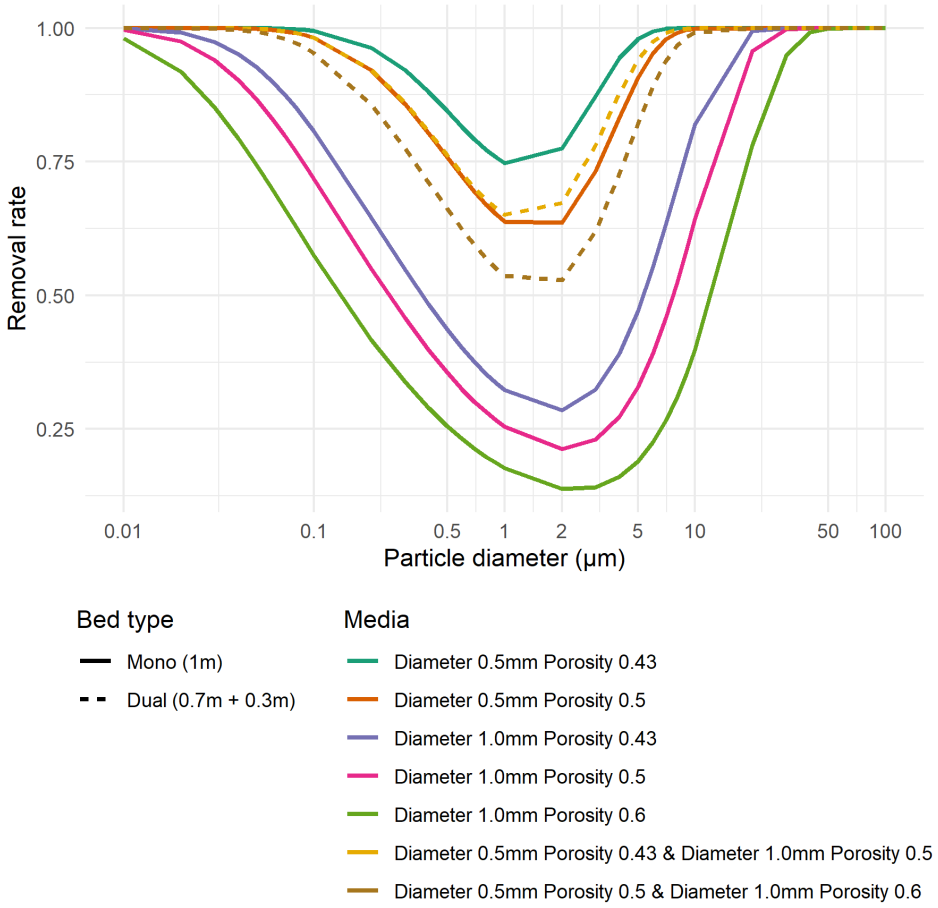

Figure 3 Simulated removal rates for particles of different size based on fundamental modelling. Removal rate approximated using the method of Rajagopalan and Tien (1976) **with the following assumptions: Partcicle density = 1050 Kg/m3, temperauture = 10°C, attachment efficiency = 1.**

Limitations in the applicability of fundamental models led to the development of alternative approaches to filtration modelling which allow for the filter coefficient to develop over the course of a filter run, recognising that deposited material changes the porosity and surface characteristics within the media (Equation 13) (Amirtharajah, 1988; Ives, 1970). Phenomenological models developed from these principles describe change over time *t*(s) and vertical distance Z(m) in the measurable characteristics of a filtration system in terms of the concentration of suspended solids *C*(Z,t), the accumulation of deposits within the bed σ(Z,t) and the development of a hydraulic gradient *i*(Z,t) (Hendricks, 2006). These equations are used to describe the development and progression through the depth of media of a saturated zone of solids in which the attachment and detachment rates are equal, along with a wave front covering a zone of deposit accumulation and suspended particle reduction. This

results in a class of models which is more applicable to reliable design but may be of limited use for generalisation (Amirtharajah, 1988)

Equation 13 Phenomenological model of filter coefficient Ives (1970)

$$\lambda = \lambda_0(1+\frac{\beta\sigma}{f})^y(1-\frac{\sigma}{f})^z(1-\frac{\sigma_u}{f})^x$$

Where: β is a geometric constant describing filter grain packing, σ = specific deposit (m), f = specific deposit porosity, x,y & z are estimated empirically.

Though filtration theory is not capable of capturing all of the complex interactions between the variables listed above, it provides a useful framework to identify potential mechanisms which can be exploited with the aid of experimentation to improve performance. From the theory covered above it can be inferred that media selection requires a trade-off between transport efficiency and solids handling capacity. Though coarse porous media have advantages in terms of solids handling capacity and hydraulic efficiency this is limited in practice by bed depth and sensitivity to ineffective pre-treatment.

1.1.7 Context of the sponsoring organisation in the research

This research was supported by Scottish Water, a large publicly owned water utility delivering the public water supply in Scotland. The majority of water supplied by Scottish Water comes from surface water sources which is then treated by coagulation and filtration. These filtration works are spread across a large area, treating source waters of varying quality. Scottish Water was formed in 2002 from the amalgamation of regional water authorities which were themselves earlier amalgamations of local water authorities. Most of the filters in use by Scottish Water today were built at some point in the last 70 years by one of the former local or regional water authorities. This means that there are filters with a variety of designs, ages and condition which have been inherited by Scottish Water. The objective of this project was to identify how a target of 0.1 NTU could be maintained in filtered water within the Scottish Water region. Recently a programme of surveys has assessed and collated the design and operation of WTWs across Scotland and characterised the design limitations. Many of the filters in operation today do not meet current design practice. Many have poor hydraulic control, insufficient backwash and no run-to-waste facility. Upgrading or replacing these assets to meet current design standards would incur considerable cost and

Water utilities are required to manage these risks whilst providing good value to customers.

1.2 Aims & Objectives

The aim of this work was to determine and specify the causes for sub-optimal effluent turbidity from depth filtration processes and develop solutions to ensure robust filter operation. The realization of this aim was pursued through the following objectives:

1. Develop novel methods for assessment of filtration performance and diagnosis of the potential causes of operational issues associated with rapid gravity filters using online data.
2. Develop methods for modelling and optimising upstream coagulation using online zeta potential measurement, and demonstrate how this influences filtration performance
3. Understand the potential application of a novel aluminosilicate filter media within Scottish Water filtration systems.

1.3 Thesis overview

An EngD is similar to a PhD but is aimed to prepare students for a career in industry. It combines industrially relevant research with novel scientific investigation and a taught course programme. Students spend most of the programme on placement within a sponsoring company. In order to achieve the sponsor's aim it was necessary to engage with scientific, design and operational causes of sub-optimal filtration and pre-treatment processes.

This thesis is presented as three experimental sections (chapters 2-4) and a management chapter that discusses the implementation of the knowledge gained from the previous chapters (Chapter 5). The experimental chapters are intended to be self-contained and formatted in a style similar to that of a journal article. However, the word limit typically demanded by journal papers is relaxed in order to allow more detailed explanation of relevant scientific concepts and methodology.

The current submission status of the papers is summarised in Table 1. All chapters were written by Andrew Upton and edited by Professors Peter Jarvis and Bruce Jefferson. All experimental work and data analysis was planned and completed by Andrew Upton.

In order to deliver improvements in the performance of filtration processes across Scottish Water it was first necessary to understand where and why filtration performance was sub-optimal. The first chapter addresses objective 1 and presents novel methods for the performance assessment and diagnosis of filtration issues using online data. The investigation critically appraises the existing available methods for assessing filtration performance and presents a novel data driven decision support system for the prioritisation of preventative maintenance of filters. This chapter has been published in the Chemical Engineering Journal (Upton *et al.*, 2017).

Maintaining optimal pre-treatment of water was identified as being key to maintaining filtration performance. The second chapter addresses objective 2 and presents the findings of research into the application of new online charge

measurement instrumentation for identifying and maintaining optimal pre-treatment conditions for robust filtration performance.

Key legacy constraints in the design of the backwash system in many filters were identified. The third chapter presents research on using an alternative filter media material in pilot scale experiments to determine how it can be applied to mitigate legacy filtration design risks associated with filtration backwash.

Chapter 5 discusses in more detail how and where the alternative media material could be applied to address design limitations across the asset base at Scottish Water and the potential savings available.

Chapter 6 synthesises the investigations presented in the previous chapters into a cohesive discussion.

Chapter 7 concludes the key findings of the research and identifies the key areas of research required to further improve filtration performance and operation.

Table 1 Current status of paper submissions

Ch No	Paper No	Objective No	Title	Journal	Status
2	1	1	Rapid gravity filtration operational performance assessment and diagnosis for preventative maintenance from on-line data	Chemical Engineering Journal	Published 2017 313 250-260
3	2	2	Online zeta potential measurement for maintaining optimal coagulation conditions in low turbidity and low alkalinity surface water	Water Research	In preparation
4	3	3	Improving the performance of sand filters with constrained up-wash rates using low-density expanded clay media.	Water and Environment Journal (or similar)	In preparation
5	-	3	Economic improvement of filtration performance for Scottish Water using low density media	-	-
6	-	1,2,3	Discussion: Implications of the work for water treatment in the UK	-	-
7	-	1,2,3	Conclusions and future work	-	-

1.4 References

Amirtharajah, A. (1988). Some theoretical and conceptual views of filtration. *Journal of the American Water Works Association*, *80*(12), 36-46.

Anderson, C.W. (2005). Turbidity, in *National field manual for the collection of water-quality data*. 9th edn. Reston, VA: USGS, pp. 1–55.

Baker, M.N. (1949) *The quest for pure water: the history of water purification from the earliest records to the twentieth century*. New York: American Water Works Association.

Bratby, J. (2016). *Coagulation and Flocculation in Water and Wastewater Treatment*. 3rd edn. London: IWA Publishing.

Bridgeman, J., Simms, J. S., & Parsons, S. A. (2002). Practical and theoretical analysis of relationships between particle count data and turbidity. *Journal of Water Supply: Research and Technology—AQUA*, *51*(5), 263-271.

Chapman, D. L. (1913). A contribution to the theory of electrocapillarity. *The London, Edinburgh, and Dublin Philosophical Magazine and Journal of Science*, *25*(148), 475-481.

Crittenden, J. C., Trussell, R. R., Hand, D. W., Howe, K., & Tchobanoglous, G. (2012). *MWH's water treatment: principles and design*. Hoboken, New Jersey: John Wiley & Sons.

Davies-Colley, R. J., & Smith, D. G. (2001). Turbidity suspended sediment, and water clarity: A review. *Journal of the American Water Resources Association*, *37*(5), 1085-1101.

EPA. (1998).*Optimizing Water Treatment Plant Performance Using the Composite Correction Program*. 1998 edn. Cincinati: US Environmental Protection Agency

European Parliament. (2019) *European Parliament legislative resolution of 28 March 2019 on the proposal for a directive of the European Parliament and of the Council on the quality of water intended for human consumption (recast) (COM(2017)0753 – C8-0019/2018 – 2017/0332(COD))*. *Official Journal of the European Communities*. (COM(2017)0753 – C8-0019/2018 – 2017/0332(COD)). European Parliament Legislative Observatory, European Union, European Union

Gouy, M. (1910). Sur la constitution de la charge électrique à la surface d'un électrolyte. *Journal de Physique Théorique et Appliquée.*, *9*(1), 457-468.

Great Britain. The Water Supply (Water Quality) Regulations 2016: Elizabeth II. Chapter 614 (2000) London: Her Majesty's Stationery Office. Available at:https://www.legislation.gov.uk/uksi/2016/614/contents/wales (Accessed: 26/11/2021).

Gregory, J. (1994). Cryptosporidium in water: treatment and monitoring methods. *Filtration & Separation*, *31*(3), 283-268.

Hargesheimer, E. E., McTigue, N. E., Mielke, J. L., Yee, P., & Elford, T. (1998). Tracking filter performance with particle counting. *Journal of the American Water Works Association*, *90*(12), 32-41.

Hartshorn, A. J., Prpich, G., Upton, A., Macadam, J., Jefferson, B., & Jarvis, P. (2015). Assessing filter robustness at drinking water treatment plants. *Water and Environment Journal*, *29*(1), 16-26.

Hendricks, D. W. (2006). *Water Treatment Unit Processes Physical and Chemical*; Boca Raton, Florida CRC Press.

Huck, P. M., & Coffey, B. M. (2004). The importance of robustness in drinking-water systems. *Journal of Toxicology and Environmental Health Part A*, 67(20-22), 1581-1590.

Huck, P.M., Emelko, M.B., Coffee, B.M.M, Maurizio, D.D. and O'Melia, C.R. (2001). *Filter operation effects on pathogen passage*. Denver: AWWA Research Foundation and American Water Works Association.

Huck, P. M., Coffey, B. M., Anderson, W. B., Emelko, M. B., Maurizio, D. D., Slawson, R. M., ... & O'Melia, C. R. (2002). Using turbidity and particle counts to monitor Cryptosporidium removals by filters. *Water Science and Technology: Water Supply*, *2*(3), 65-71.

Ives, K. J. (1970). Rapid filtration. *Water Research*, *4*(3), 201-223.

Iwasaki, T., Slade, J. J., & Stanley, W. E. (1937). Some notes on sand filtration [with discussion]. *Journal of the American Water Works Association*, *29*(10), 1591-1602.

LeChevallier, M. W., & Au, K. K. (2004). *Water treatment and pathogen control*. London: IWA Publishing.

LeChevallier, M. W., Evans, T. M., & Seidler, R. J. (1981). Effect of turbidity on chlorination efficiency and bacterial persistence in drinking water. *Applied and Environmental Microbiology*, *42*(1), 159-167.

Léziart, T., Dutheil de la Rochere, P. M., Cheswick, R., Jarvis, P., & Nocker, A. (2019). Effect of turbidity on water disinfection by chlorination with the emphasis on humic acids and chalk. *Environmental Technology*, *40*(13), 1734-1743.

Lusardi, P. J., & Consonery, P. J. (1999). Factors affecting filtered water turbidity. *Journal of the American Water Works Association*, *91*(12), 28-40.

Mann, A. G., Tam, C. C., Higgins, C. D., & Rodrigues, L. C. (2007). The association between drinking water turbidity and gastrointestinal illness: a systematic review. *BMC Public Health*, *7*(1), 1-7.

McCoy, W. F., & Olson, B. H. (1986). Relationship among turbidity, particle counts and bacteriological quality within water distribution lines. *Water Research*, *20*(8), 1023-1029.

Rajagopalan, R., & Tien, C. (1976). Trajectory analysis of deep-bed filtration with the sphere-in-cell porous media model. *AIChE Journal*, *22*(3), 523-533.

Rizak, S. N., & Hrudey, S. E. (2007). Strategic water quality monitoring for drinking water safety. *Water*, *34*(4), 67-71.

Russell, S., Jonsson,J. & Watts, M. (2014) UC9882:*A critical appraisal of existing guidance on online monitor performance data*. Swindon. WRc

Scotland. The Public Water Supplies (Scotland) Regulations: Elizabeth II. No 364 (2014) London: Her Majesty's Stationery Office. Available at: https://www.legislation.gov.uk/ssi/2014/364/contents/made (Accessed: 26/11/2021).

Stumm, W. and Morgan, J.J. (1996) *Aquatic chemistry: Chemical equilibria and rates in natural waters*. 3rd edn. Chichester, UK: Wiley.

Tufenkji, N., & Elimelech, M. (2004). Correlation equation for predicting single-collector efficiency in physicochemical filtration in saturated porous media. *Environmental Science & Technology*, *38*(2), 529-536.

Upton, A., Jefferson, B., Moore, G., & Jarvis, P. (2017). Rapid gravity filtration operational performance assessment and diagnosis for preventative maintenance from on-line data. *Chemical Engineering Journal*, *313*, 250-260.

Van Benschoten, J. E., & Edzwald, J. K. (1990). Chemical aspects of coagulation using aluminum salts—I. Hydrolytic reactions of alum and polyaluminum chloride. *Water Research*, *24*(12), 1519-1526.

Water Industry Commission for Scotland. (2009) *The Water Industry Commission for Scotland Scottish Water Scottish Water Reporter's Report SR10 2 ND Draft Business Plan Appendix B-Asset Inventory and System Performance*. Stirling. Water Industry Commission for Scotland. Available at: https://www.watercommission.co.uk/UserFiles/Documents/SR10 2DBP App B - Asset Inventory v02 (Final 020409).pdf (Accessed: 17 May 2019).

WHO. (2015) *Guidelines for drinking-water quality,* 4th edn, Geneva. World Health Organization.

Yao, K. M., Habibian, M. T., & O'Melia, C. R. (1971). Water and Waste Water Filtration. Concepts and Applications. *Environmental Science & Technology*, *5*(11), 1105-1112.

2 Rapid gravity filtration operational performance assessment and diagnosis for preventative maintenance from on-line data

2.1 Abstract

Rapid gravity filters, the final particle barrier in many water treatment systems, are typically monitored using on-line turbidity, flow and head loss instrumentation. Current metrics for assessing filtration performance from on-line turbidity data were critically assessed and observed not to effectively and consistently summarise the important properties of a turbidity distribution and the associated water quality risk. In the absence of a consistent risk function for turbidity in treated water, using on-line turbidity as an indicative rather than a quantitative variable appears to be more practical. Best practice suggests that filtered water turbidity should be maintained below 0.1 nephelometric turbidity units (NTU), at higher turbidity we can be less confident of an effective particle and pathogen barrier (EPA, 1998; Logsdon *et al.*, 2002). Based on this simple distinction, filtration performance has been described in terms of reliability and resilience by characterising the likelihood, frequency and duration of turbidity spikes greater than 0.1 NTU. This view of filtration performance is then used to frame operational diagnosis of unsatisfactory performance in terms of a machine learning classification problem. Through calculation of operationally relevant predictor variables and application of the Classification and Regression Tree (CART) algorithm, the conditions associated with the greatest risk of poor filtration performance can be effectively modelled and communicated in operational terms. This provides a method for an evidence-based decision support which can be used to efficiently manage individual pathogen barriers in a multi-barrier system.

2.2 Introduction

Rapid gravity filters provide the final barrier to particulates in most large municipal water supply systems. Public health risk arising from large water supply systems is primarily associated with short duration contamination or challenge events, such as those associated with extreme weather events, which are poorly captured by regulatory sampling programmes (Rizak and Hrudey, 2007). Breakthrough and transient periods of high turbidity have been associated with increased concentrations of oocysts, suspended solids and spore forming bacteria in distribution systems

(Gauthier *et al.*, 2003; Huck *et al.*, 2002b). In addition, turbidity is widely interpreted and assumed to indicate removal performance of water-borne environmental pathogens (Foladori *et al.*, 2015; Lusardi and Consonery, 1999). Therefore, on-line turbidity meters provide a record to evidence filtration performance with a degree of granularity far greater than can be achieved by regulatory sampling.

Turbidity quantifies the extent to which suspended particles scatter light subject to their concentration, size and colour (Anderson, 2005). As an optical property, turbidity is not a direct health risk but has been associated with the presence of bacteria, the shielding of micro-organisms from disinfection, causing additional chlorine demand, increasing disinfection-by-product (DBP) formation and promoting biological growth in distribution systems (Lechevallier *et al.*, 1981; McCoy and Olson, 1986). In the UK, the prescribed value for turbidity is 4 nephelometric turbidity units (NTU) at the customer's tap, with an indicative limit of 1 NTU for water leaving the treatment works (Statutory Instruments, 2000). The World Health Organisation suggests that prior to chlorination large municipal supplies should average below 0.2 NTU and not exceed 0.5 NTU (WHO, 2015). A best practice target of 0.1 NTU has been proposed to limit the risk of pathogen passage (EPA, 1998). Water utilities aim to maintain low filtered water turbidity in order to minimise risk of bacteriological failure, reduce the cost of additional chemical dosing and lower DBP formation (Huck *et al.*, 2001). Though limitations to the sensitivity of turbidity have been observed in comparison to particle count monitoring, its simplicity, reliability and economy ensure that turbidity remains the most widely used parameter for monitoring filter performance (Gregory, 1994; Hartshorn *et al.*, 2014; Huck *et al.*, 2001).

Visualisation of turbidity records is routinely used to assess and diagnose performance (Martin, 2014). Typically, efforts by operators and scientists to monitor and improve the performance of filtration processes in terms of turbidity have used averages, percentile statistics, or compliance with a target value over various periods (DeMers and LeBlanc, 2003; Egerton, Hall and Watts, 1999; Huck *et al.*, 2001; Logsdon *et al.*, 2002). To aid consistent and objective management, investigators and practitioners have developed turbidity robustness indices (TRIs) to improve understanding of performance (EPA, 1998; Hartshorn *et al.*, 2014; Li and Huck, 2008). However, these metrics have not routinely been applied in practice. One of the aims of the research was to assess the suitability and reliability of these indices. Alternative approaches to

performance assessment can be based around the best practice target of 0.1 NTU (EPA, 1998). Performance can then be described in terms of the likelihood, frequency, and duration of quality target breaches. Such an approach, allows the application of basic reliability engineering metrics such as the mean time between failures (MTBF) and the mean time to recovery (MTTR) which can be applied to indicate reliability and resilience.

Once detected, a process fault is typically diagnosed by one of the following: by reference to prior information in quantitative or qualitative models of the process; by using historical data; or by combining one or more approach (Venkatasubramanian *et al.*, 2003a). Purely quantitative modelling approaches to diagnosis of filtration performance are impractical because the underlying complex non-linear particle separation process is not accurately described by theory and measurement. Phenomenological and theoretical filtration models often rely on measurements which are not routinely collected in full scale water treatment (Gitis *et al.*, 2010; Yuan and Shapiro, 2011). Turbidity, for example, is not a quantitative measurement. The formalisation of qualitative knowledge into models is challenged by behavioural complexity of the process, inflexibility to new conditions and the generation of spurious diagnoses (Venkatasubramanian *et al.*, 2003b). Process history based methods have been broadly categorised as quantitative or qualitative depending upon the method by which historical data are transformed and applied within the diagnostic system (Venkatasubramanian *et al.*, 2003c). Current guidance suggests a form of manual qualitative trend analysis for rapid gravity filter fault diagnosis. This requires the time-consuming manual inspection and interpretation of filter monitoring trends in order to identify potential issues and confirmation with further physical inspections and process investigation (Logsdon *et al*., 2002). This investigation proposes a quantitative method to identify key operational issues associated with elevated filtrate turbidity, applicable over extended periods to provide easily interpretable diagnostic models for rapid gravity filtration operation and maintenance decisions. Such models can guide investigations reducing the time and financial and environmental cost incurred.

The magnitude of the failure was not included into the analysis. As these methods are applied to turbidity levels below what can be resolved organoleptically, using the magnitude of failure implicitly assumes a relationship between turbidity and risk. There does not appear to be a scientific basis to assume that risk is a consistent function of

turbidity between 0 and 1 NTU. Firstly, turbidity is a function of the surface area and refractive index of the particles within a given system. Previous investigators have concluded that turbidity is not a quantitative indicator of *Cryptosporidium* removal capability and is not strongly related to particle counts (Bridgeman *et al.*, 2002; Huck *et al.*, 2002a). Gregory (1994) concludes that conventional turbidity measurements are not sufficiently sensitive to particles in the oocyst size range. There is typically inconsistency in the readings given by turbidity instruments of different design (Letterman, Johnson and Viswanathan, 2004). The reduction in disinfection efficiency by turbidity particles has been shown to be dependent upon the material which generates light scatter (Farrell *et al.*, 2018; Léziart *et al.*, 2019).

Treatment operators and managers need efficient, effective, robust and justifiable tools and methods for the aggregation and interpretation of large volumes of filter monitoring data into useful information from which evidence based decisions can be made (Logsdon *et al*., 2002). Using a turbidity target, such as the best-practice level of 0.1 NTU, we can frame the analysis of control system data as a classification problem whereby we identify the conditions associated with greater likelihood of high filtrate turbidity. Tree based methods use recursive binary splitting of the feature space to fit a stepwise function. Classification trees have been chosen for this application based on their primary virtue which is interpretability (James *et al.*, 2013). This is key for the efficient and successful retrospective implementation of such a decision support tool for operators and managers facilitating more effective management of individual pathogen barriers. Further advantages of the classification tree methods are that they work effectively using discrete and continuous variables of any distribution and are insensitive to outliers (Hastie, Tibshirani and Friedman, 2009).

The primary criticisms of classification trees are comparatively poor accuracy, a tendency to over-fit, instability and poor capture of additive structure (Hastie *et al.*, 2009). The objective of this investigation was to develop workable methods which can be applied to improve operational and preventative maintenance decision making on water treatment assets and for this reason interpretability trumps accuracy in this application. Though it is likely that alternative classification methods may produce better classification accuracy, the generation of the classification tree models allows far more broadly accessible communication and sense checking of the diagnosis. The

tendency of classification trees to over-fit the data can be mitigated by appropriately using k-fold cross validation to estimate the extent of model pruning required.

Though classification trees have been implemented by numerous algorithms, the two most popular methods are the classification and regression tree approach (CART) and the C4.5 and C5.0 algorithms (Kuhn and Johnson, 2013). The main distinctions between the implementation of these methods are the use of different functions to inform the split location, alternative pruning procedures, the possibility for multiway splits on categorical predictors and the potential for conversion to rules. CART has been widely applied and popular due to its accessibility and ease of interpretation when applied to non-linear processes (Hastie *et al.*, 2009). CART has been applied to understanding and managing water contamination events and mechanisms (Frederick *et al.*, 2016; Thoe *et al.*, 2014). Through recursive partitioning of explanatory variables, the conditions associated with an outcome of interest can be simplified and presented in an interpretable tree format using the classification and regression tree (CART) algorithm (Breiman *et al.*, 1984). The CART algorithm is used in this study to produce interpretable models describing the operational conditions associated with the occurrence of elevated filtrate turbidity.

The aims of this paper were therefore to develop intelligent, data-driven decision support systems by assessing and developing existing performance metrics for summarising the performance of filtration processes in terms of turbidity and utilising other typical sources of data to identify the likely causes.

2.3 Materials and methods

Data was extracted from the control system at a water treatment plant in Scotland treating a mix of two upland surface water sources by coagulation, flocculation, dissolved air flotation, rapid gravity filtration and chlorination. A data flow diagram is included in the supplementary materials (Figure_Apx 1). Data for the whole of 2015 describing turbidity, flow, level and head loss for four filters as well as raw water temperature and clarified water turbidity data was extracted at 30 second intervals. Data handling and analysis was performed using a PostgreSQL 9.4 database, R 3.2.0, and RStudio (PostgreSQL Global Development Group, 2015; R Core Team, 2015; RStudio, 2017). The key R packages used were lubridate (Grolemund and Wickham, 2011), ggplot2 (Valero-Mora, 2010), dplyr (Wickman *et al.*, 2021), RPostgreSQL

(Conway *et al.*, 2013), caret (Khun *et al.*, 2011) and rpart (Therneau and Atkinson, 2015).

Data for individual filters were split into in-service and out of service periods and individual filter runs were delineated based on threshold values for flow, level and head loss. Prior to analysis the turbidity time series at 30 second intervals was cleaned to remove specific artefacts. High turbidity values likely associated with trapped bubbles or detachment of biofilm within the sample line were removed, then a Hampel filter was applied over the natural log transformed turbidity time series with a window length of 15 observations and a threshold of 3 standard deviations. This removed outliers, attributable to measurement, data collection and sampling error, from the local trend over a rolling window. Removed data was replaced with the local median value. This process removed false low and high outliers from bubbles passing through the measurement cell preventing them from influencing assessment of the frequency and duration of real turbidity spikes in the filtered water. Bubbles can cause interference with the measurement of turbidity by causing light scatter as particles would or resulting in temporary loss of flow to an instrument. In this case, as is typical, the sample was passed through a degasser before the instrument but this was not completely successful.

A number of performance statistics were applied to turbidity data in order to communicate the relative merits of different approaches. The simple descriptive statistics applied were the mean, median, standard deviation, 90th, 95th and 99th percentiles. To describe the distribution of turbidity data over a period of operation a number of turbidity robustness metrics (TRIs) have been proposed evolving from the original TRI_E Equation 14 proposed by Huck (2001)

Equation 14 Original form of the Turbidity Robustness Index E (E is an arbitrarily chosen distinctive letter) (TRIE) metric

$$TRI_{\mathrm{P}E} = \frac{1}{2}\left[\frac{T_p}{T_{50}} + \frac{T_{50}}{T_{goal}}\right]$$

Where: T_{goal} = targeted turbidity value, T_p. =pth percentile turbidity value (e.g.95th%ile)

The TRI function summarises a distribution of turbidity data in a single value by taking a quotient of percentiles as a proxy for variance and right skew, the quotient of the

median and a goal value to locate the distribution followed by averaging of these two terms. This metric has been applied to demonstrate changes in clarifier and filter performance (Hurst *et al.*, 2004; Zhang *et al.*, 2012). Subsequent modifications to improve metric performance were proposed in Equation 15, which involved weighting the terms of the original metric to provide outcomes more consistent with expectations and an algorithm was applied to assign the weights (Li and Huck, 2008). A further investigation simplified the allocation of weighting based on the time below the turbidity goal Equation 16 (Hartshorn *et al.*, 2014).

Equation 15 Calculation of Turbidity Robustness Index D (D is an arbitrarily chosen distinctive letter) (TRI_D) metric

$$TRI_{90D} = \left[A_1 \frac{T_{90}}{T_{50}} + A_2 \frac{T_{50}}{T_{goal}}\right]$$

Where:

$$if\ W \leq N\ \&\ T_{90}/T_{50} \leq T_{50}/T_{goal}\ \ A_1 = 0.9, A\_2 = 0.1\ else$$
$$if\ W \leq N\ \&\ T_{90}/T_{50} > T_{50}/T_{goal}\ \ A_1 = 0.1, A_2 = 0.9\ else$$
$$if\ W > N\ \&\ T_{90}/T_{50} \leq T_{50}/T_{goal}\ \ A_1 = 0.1, A_2 = 0.9\ else$$
$$if\ W > N\ \&\ T_{90}/T_{50} > T_{50}/T_{goal}\ \ A_1 = 0.9, A_2 = 0.1$$

and

N = 0.5

and

$$W = \left(\frac{T_{50}}{T_{goal}} + \frac{T_{60}}{T_{goal}} + \frac{T_{70}}{T_{goal}} + \frac{T_{80}}{T_{goal}} + \frac{T_{90}}{T_{goal}}\right) * 10$$

Equation 16 Calculation of Turbidity Robustness Index J (J is an arbitrarily chosen distinctive letter) (TRI_J) metric

$$TRIJ_p = \left[\left(1 - \frac{G\%}{100}\right) * \frac{T_p}{T_{50}}\right] + \left[\frac{T_{50}}{T_{goal}} * \frac{G\%}{100}\right]$$

Where: G% = time below turbidity goal, Tp = p^{th} percentile turbidity

A new approach to managing filtration can be developed from a binary view of performance based on compliance with 0.1 NTU. The simple discrete failure rate aggregates two distinct aspects of performance, reliability and resilience. Though limited, common metrics can be used to summarise these different aspects of performance. Reliability, or the frequency of failure events over a given period, is often characterised using the mean time between failures (MTBF) Equation 17. Resilience, the time that a system takes to return to acceptable performance when a failure event does occur, can be described using the mean time to recovery (MTTR) Equation 18.

Equation 17 Mean time between failures (MTBF)

$$MTBF = \frac{\sum_{i=0}^{i=n}(s_i - f_{i-1})}{3600 * n}$$

Where: MTBF = Mean Time Between Failures (hrs), s_i = time from origin datum for first observation within turbidity i^{th} spike > 0.1NTU, f_i-1 time from origin datum for final observation within (i-1^{th}) turbidity spike > 0.1NTU(seconds)

Equation 18 Mean time to recovery (MTTR)

$$MTTR = \frac{\sum_{i=0}^{i=n}(f_i - s_i)}{3600 * n}$$

Where: MTTR = Mean Time To Recovery (hrs), s_i = time from origin datum for first observation within turbidity i^{th} spike > 0.1NTU, f_i time from origin datum for final observation within (i^{th}) turbidity spike > 0.1NTU(seconds)

In order to facilitate differential diagnosis of operational filtration issues a number of relevant variables were derived from the time-stamped observations from other signals (see Table 2). Head loss was normalised against a standardised temperature (10°C) and flow in order to provide a more useful comparison of media condition using the method described by Logsdon *et al.* (2002). As head loss is strongly correlated with the number of hours in service this effect was removed by fitting a second-order linear regression model to describe head loss within each filter run in terms of the volume of water filtered since the last wash (Equation 19). Prior to fitting the model, outlying head loss observations more than 2 standard deviations from the within-run mean were removed. An illustrative example of a fitted model is shown in Figure 4. Average r-squared values for the head loss models in the four filters were 0.98, 0.96, 0.93 and 0.99 in filters A-D respectively. The coefficients for these head loss models were then extracted and used as explanatory features in the diagnostic models. The model intercept, used to estimate normalised clean bed head loss, was converted to a z-score within the group of runs for each filter for use in diagnostic modelling of multiple filters. The slope coefficients were used to characterise head loss accumulation and change in rate during the run.

Equation 19 Normalised head loss

$$Normalised\ Head\ Loss = \beta_0 + \beta_1 v + \beta_2 v^2 + \varepsilon$$

Where: v = volume filtered since wash, β_i = regression coefficient as identified by minimising sum of squared residuals, ε = error

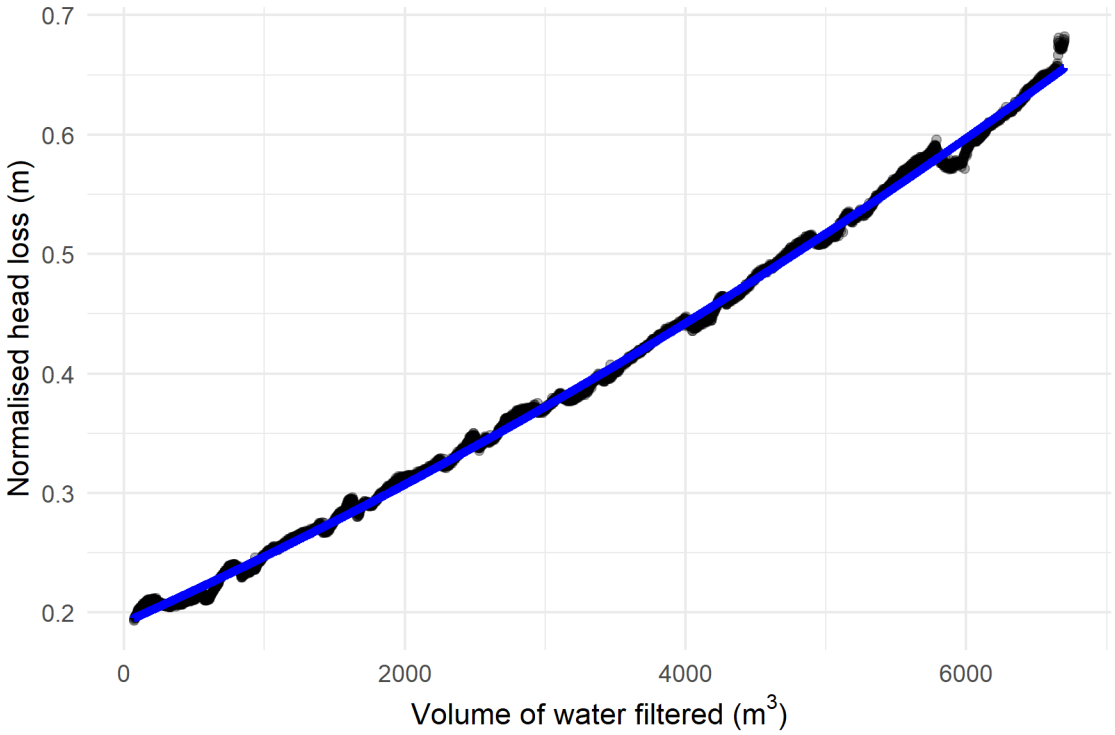

Figure 4 Illustrative example of a linear model relating normalised head loss to volume of water treated.

Useful information from the potential explanatory variables was then extracted using a classification algorithm. An implementation of the CART algorithm was applied to build simple explanatory classification models of the conditions associated with “HIGH” >0.1 NTU and “OK” ≤ 0.1 NTU filtrate (Breiman *et al.*, 1984). CART applies recursive binary partitioning to split a multi-dimensional predictor space of *P* distinct predictor variables X_1, X_2,…,X_p into *J* distinct non-overlapping *P* dimensional rectangular regions R_1,R_2,…,R_J with an assigned classification in the response variable for each region. The data is split on the point of an explanatory variable which minimises “risk” calculated from the loss adjusted Gini purity. The Gini index is a measure of class imbalance (Equation 20). Due to the underlying public health objective of water treatment false negative classifications are more undesirable than false positives. Therefore, a loss matrix was applied during model training which weighted the penalty of false negatives by a factor of 10 giving the loss adjusted Gini purity. Portioning is then carried out such that the location *s* on the predictor X_j is selected recursively such that the loss adjusted Gini purity is maximised. At each step, all possible locations for *s* on all *P* predictor variables is assessed and the point with the maximum value for loss adjusted Gini purity is selected. Regions are partitioned recursively until the

number of observations in each R is less than 20, otherwise the splitting would result in a terminal node of fewer than 7 observations.

Equation 20 Standard Gini index for node purity

$$G = \sum_{k=1}^{K} \hat{p}_{mk}(1 - \hat{p}_{mk}),$$

Where:
$\hat{p}_{mk}$ = proportion of observations in the m^{th} region that are from the k^{th} class

In order to simply and effectively describe the underlying data the size of the classification model tree needs to be restricted. The extent to which the model is pruned is determined by the complexity parameter which is the cost assigned to each additional terminal node. The smallest tree that minimises the sum of the loss adjusted Gini purity and complexity cost is then selected. The value of the complexity parameter was tuned using 10-fold cross validation using the area under the receiver operating characteristic (ROC) curve to assess model fit and select the best value. The performance of the final model was tested by applying the model to 20 percent of the data retained for testing by comparing the predicted and observed classes.

The CART algorithm was used to review a period of filter operation and characterise the occurrence of elevated turbidity in order to aid understanding of past filter performance. A classification tree model was trained for each filter each week where the probability of exceeding 0.1 NTU was greater than 1 in 1000, which is equivalent to a single 30 second measurement in 20.16 hours. Failure rates below this level are of less concern for public health, and less predictable, as error in measurement and data systems is likely to contribute a greater proportion of failing measurements as the total failure rate decreases. The approach was then tested again over each monthly period looking at all of the filters in the bank in order to explore more general operational issues common between filters over an extended period.

Table 2. Predictive features for CART diagnostic model.

Explanatory variable	Description
Hours In Run	The time (hours) elapsed between the start of the filter run and the time at which turbidity is observed. Performance issues can often be linked to issues during the ripening or breakthrough phases of the filter cycle. If failure is more likely later in the run it may indicate that breakthrough is occurring, in which case shortening the filter run could reduce water quality risk. If turbidity is high early in the run it may indicate that the effectiveness of pre-treatment should be investigated.
Flow Trend	A two-hour average flow (l/s) to the filter bank captures the hydraulic loading to the treatment system. If high hydraulic loading is predictive of high turbidity it may indicate that a filter or process stage is hydraulically overloaded.
Max Bank Flow Increase	The maximum filter bank flow (l/s) increase over 30 minutes during previous 90 minutes. This captures increases in hydraulic loading to the whole system. Rapid changes in flow through the treatment process can cause control and performance challenges. If rapid flow changes are predictive of high turbidity, then this may indicate that control philosophies should be modified to reflect the sensitivity to flow rate changes.
Bank Flow Proportion	The proportion of total flow to a filter bank treated by an individual filter indicates if the distribution of flow between filters is associated with performance. If the proportion of flow treated is predictive of high turbidity it may indicate that a filter is overloaded and that the hydraulic control should be adapted to equalise loading between filters or to reduce loading to a filter with a specific condition issue.
Flow Shock	The difference between the instantaneous rate of flow and the average over the run (l/s) captures periods of additional hydraulic

	loading such as those during washing of another filter. Hydraulic shocking causes deposits to shear from filter media and break through a filter bed. If hydraulic shocking is predictive of high turbidity, improvements to hydraulic control of the bed may improve water quality risk.
Clarified Turbidity Trend	An average clarified turbidity since the start of the run provides an indication of the solids loading. Turbidity in the filter influent is indicative of solids loading. If high solids loading is resulting in high turbidity, it may indicate that improvements to the performance of pre-treatment processes may reduce water quality risk.
Clarified Turbidity Spike	The maximum difference between 30-minute average clarified turbidity and “Clarified Turbidity Trend” experienced since the start of the run to capture shock solids loading. In some processes, inconsistency in the quality of clarified water can be caused by poor control de-sludging or other cyclic control effects. If short duration turbidity spikes in the influent water are correlated with high turbidity in the filtered water then it may indicate that improved control of upstream processes may reduce water quality risk.
Temperature	Water temperature is known to affect particle separation and filter washing. If poor performance is correlated with high temperature, it may indicate that the media is not being effectively cleaned when backwash viscosity is reduced. If poor filter performance is correlated with low temperature, it may indicate that low collision rates and collision energy is inhibiting treatment performance. Temperature was measured in the raw water inlet.
Clean Bed Head Loss	Head loss at the start of the run normalised for flow and temperature as indicated by the intercept of the head loss model Equation 19. Normalised clean bed head loss is a good indicator of the effectiveness of filter washing and of media loss. If low clean bed head loss is correlated with high turbidity it may indicate that media loss should be checked. If elevated filter effluent turbidity is

	associated with high clean bed head loss then it may indicate that filter backwash performance may need investigating.
Scaled Clean Bed Head Loss	The within filter z score of “Clean Bed Head Loss” used to capture variation in post-wash media condition rather than differences between filters. Clean bed head loss may not be directly comparable between filters either due to physical differences between filters or sensor calibration. It is possible therefore to scale clean bed head loss estimates to indicate the variation in this parameter within the range seen for an individual filter. This may provide a more effective predictor of elevated turbidity.
Head loss Coefficient 1	The growth m/m^3 of normalised head loss over the course of the filter run indicates the rate at which hydraulic resistance accumulates within the bed. The linear coefficient indicates the rate of head loss accumulation with volume of water treated. High rates of normalised head loss accumulation may indicate higher solids loading.
Head loss Coefficient 2	The change in rate of hydraulic resistance accumulation with volume filtered over the course of a filter run is symptomatic of the distribution of deposited solids within a filter bed. If breakthrough is associated with a negative quadratic term, then this may indicate that the rate of head loss accumulation is declining, and solids might be breaking through the filter.

2.4 Results

2.4.1 Filtration performance data

An overview of the turbidity data for the four filters assessed is presented in time series and cumulative distribution format (Figure 5). The time series indicates higher turbidity and therefore worse performance at the start and end of the year. The cumulative distribution indicates that filters A and D are the best and worst performers, respectively (Figure 5). To provide a more detailed view for comparison, data for every 10th week was selected and plotted both as a time series (Figure 6) and a cumulative distribution (Figure 7). In week 1, it can be seen that turbidity from filters B-D

deteriorates rapidly during the filter run and exhibits several turbidity spikes throughout the run, with the data for cumulative distribution of turbidity clearly indicating the worst performance for filter D. Improved performance can be seen through weeks 11 and 21 where there was lower turbidity. By week 31, turbidity spiking was only evident for filter C. No large turbidity spikes were evident during week 41. During week 51 turbidity appeared to deteriorate during the run for filter D. These examples illustrate variation in turbidity profiles and distributions in filters with inconsistent performance.

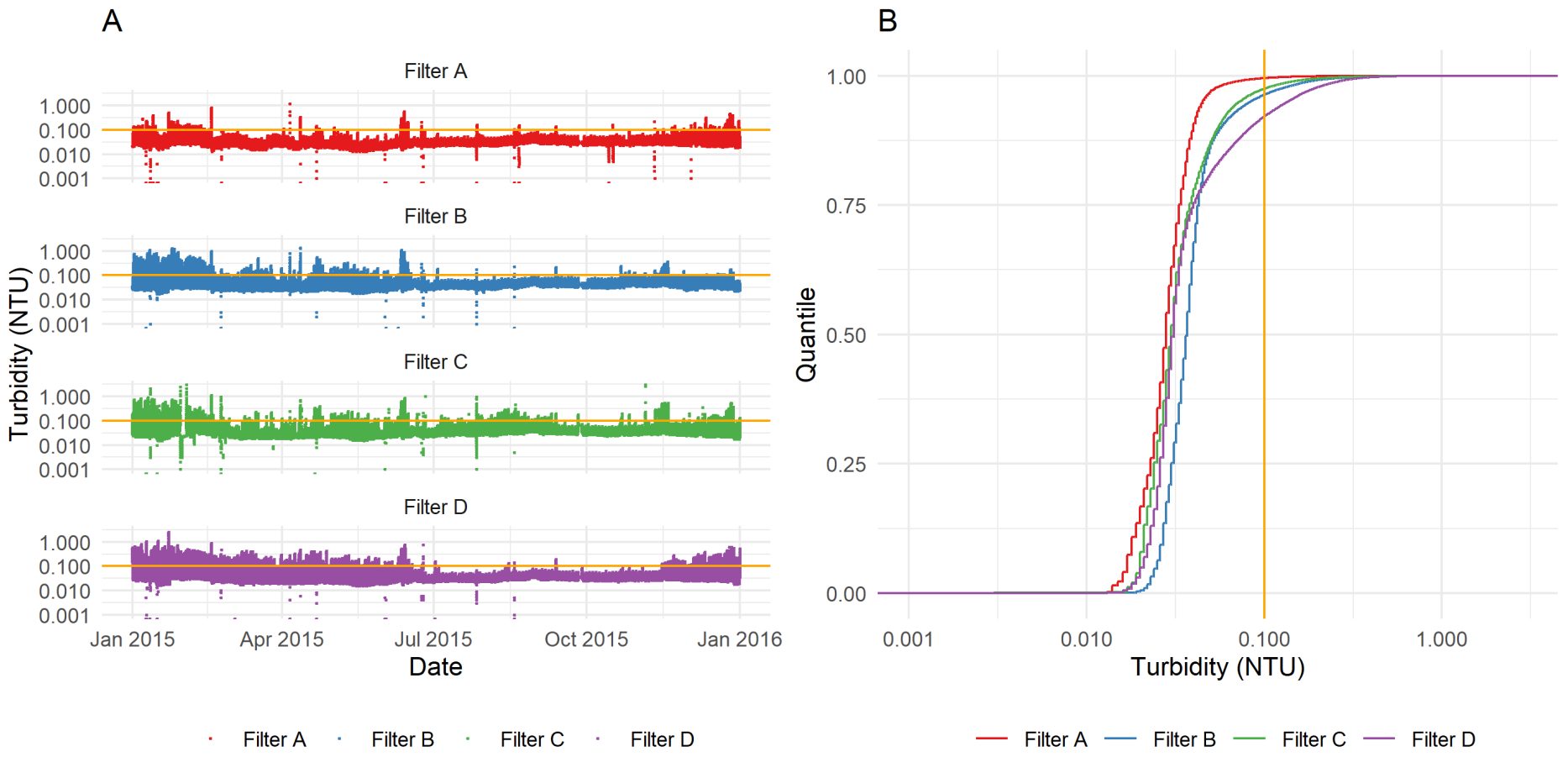

Figure 5 Filtrate turbidity data for 2015 plotted as a time series (A) and cumulative distribution (B). For clarity, part A has been included at larger size in the supplementary materials (7.1A.2). Target value of 0.1 NTU is indicated by orange line.

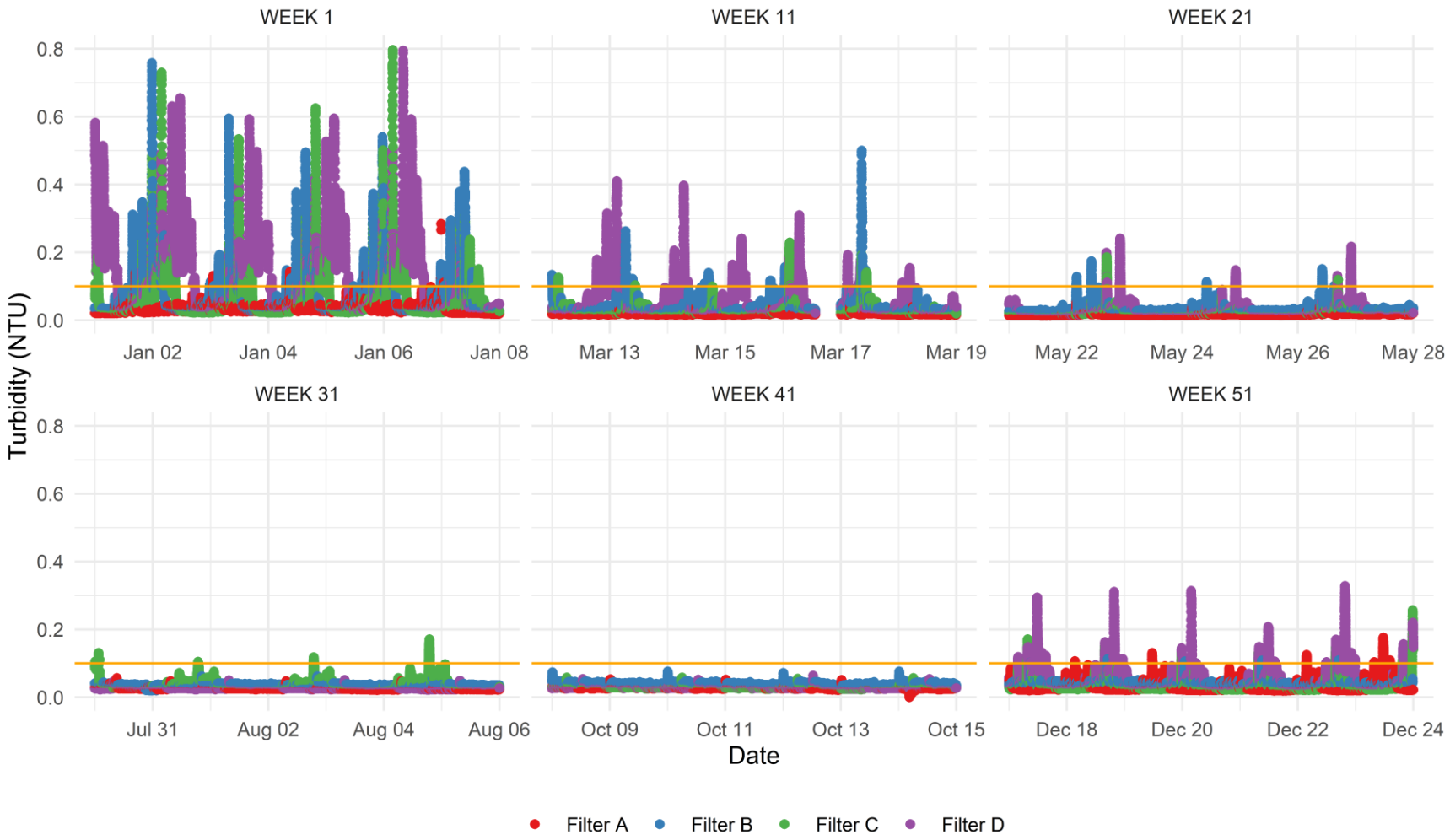

Figure 6 Turbidity time series for selected weeks to demonstrate variation in filter performance. Target value of 0.1 NTU is indicated by orange line.

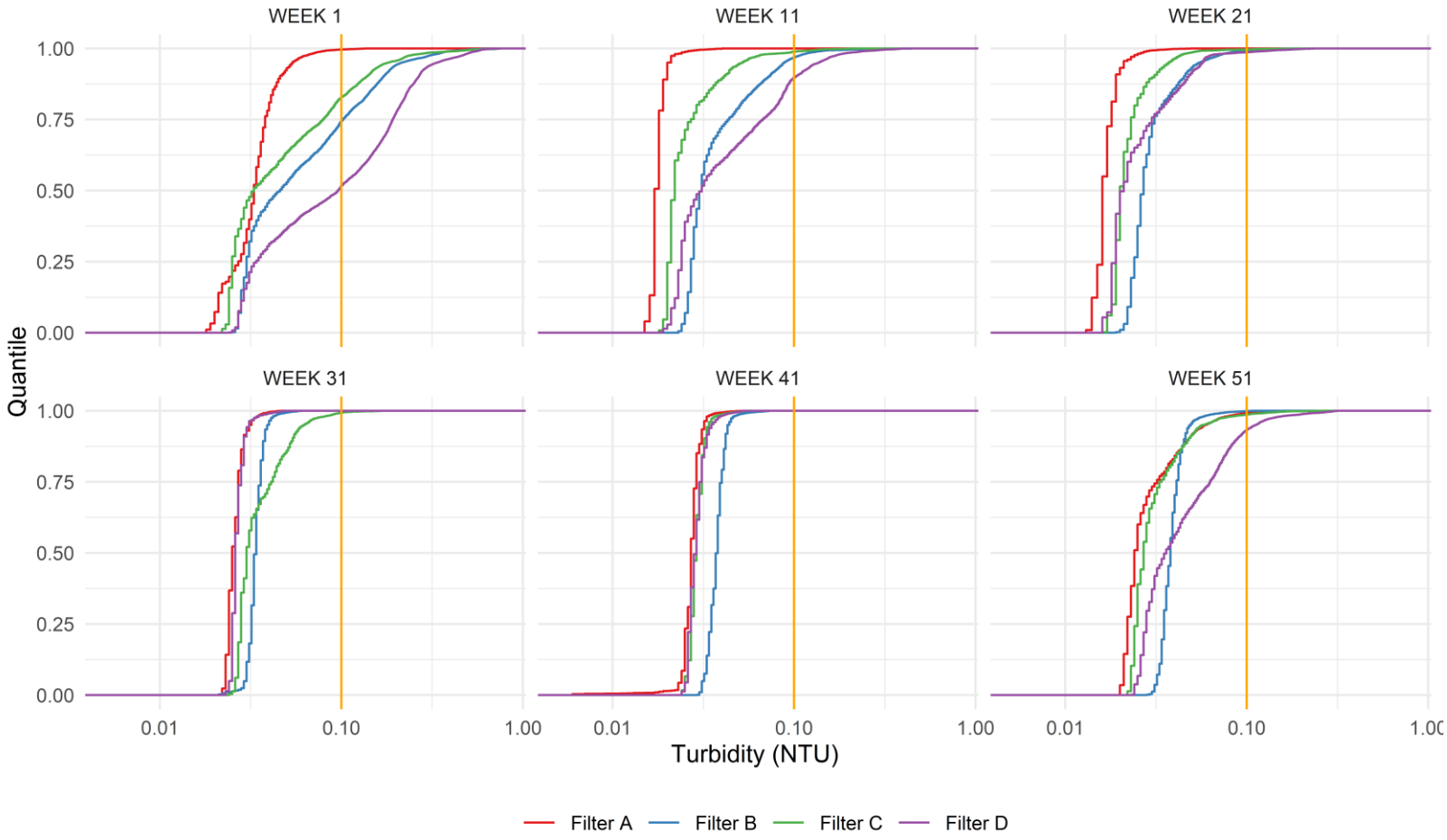

Figure 7 Cumulative turbidity distributions for selected weeks to demonstrate variation in filter performance. Target value of 0.1 NTU is indicated by orange line.

2.4.2 Assessment of performance metrics

A number of summary statistics including mean, median, standard deviation, 90th, 95th and 99th percentiles, were calculated using the filtrate turbidity data for each week of the 2015 period (Figure 8). Similarly, values returned by the TRID and TRIJ metrics at the 90^{th}, 95^{th} and 99^{th} percentile have been compared for the same data (Figure 8). Superficially, there is a broad consensus in the performance metrics which show typically poor performance at the start of the year, which improves mid-year before deteriorating at the end of the year. However, Spearman's rank correlations between metric scores illustrate the varying levels of agreement (Table 3). The TRIJ metric at all percentiles shows greater agreement with the mean than the TRID. However, the standard deviation is more strongly associated with the TRID than the TRIJ. Though both the TRIJ and TRID show a strong relationship between the values returned for different percentiles, greater consistency between metrics applied at different percentiles is shown by the TRIJ metric than the TRID. Only moderate correlations between TRID and TRIJ scores are apparent indicating diverging perspectives on filtration performance. Using the same data, the failure rate, mean time between failure and mean time to recovery based on a filter achieving the best practice target of 0.1 NTU are shown in Figure 9. The failure rate shows a pattern similar to the traditional performance metrics, with performance improving during the first part of the year before declining slightly at the end. The number of hours that the filter operates, on average, before exceeding 0.1 NTU clearly shows variation in the reliability of different filters (Figure 9 B). Filter A is shown to be most consistently reliable and filter D is shown to have periods of both good and poor reliability. For much of the year, however, filters B and C exhibit a turbidity spike greater than 0.1 NTU at least once every two days. The average duration in hours of turbidity spikes, illustrative of process resilience, indicates that turbidity spikes are typically less than half an hour in duration (Figure 9 C). However, this is not the case for filter D at the start of the year, or occasionally in filter A, which both exhibit periods above 0.1 NTU lasting over an hour. The expression of performance in terms of rates and time is more intuitively comparable than values derived from weighted quotients of percentiles of the turbidity distribution.

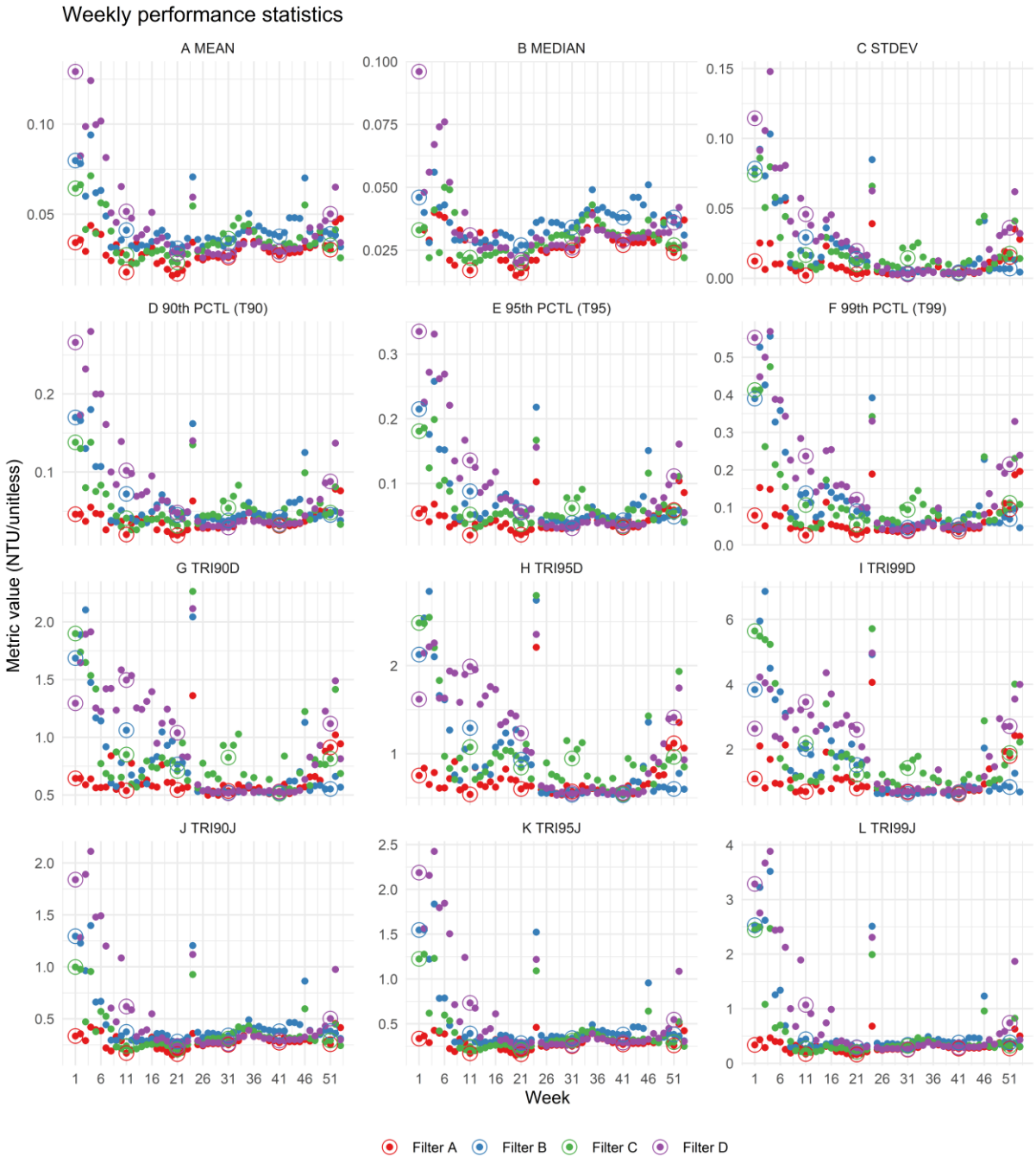

Figure 8 Values returned by performance statistics. The points corresponding to the six selected weeks are circled. Each sub-plot is reproduced at a larger size in the supplementary materials (7.1A.3).

Table 3 Spearman's rank correlation coefficient between performance statistics

	MEAN	MEDIAN	STDEV	90th PCTL (T90)	95th PCTL (T95)	99th PCTL (T99)	TRI90D	TRI95D	TRI99D	TRI90J	TRI95J	TRI99J
MEAN	1.00	0.81	0.63	0.90	0.85	0.74	0.52	0.49	0.46	0.97	0.98	0.97
MEDIAN	0.81	1.00	0.20	0.55	0.47	0.33	0.03	-0.01	-0.03	0.85	0.82	0.74
STDEV	0.63	0.20	1.00	0.82	0.89	0.96	0.92	0.93	0.94	0.51	0.55	0.66
90th PCTL (T90)	0.90	0.55	0.82	1.00	0.98	0.88	0.79	0.75	0.70	0.81	0.83	0.88
95th PCTL (T95)	0.85	0.47	0.89	0.98	1.00	0.94	0.85	0.84	0.79	0.75	0.77	0.84
99th PCTL (T99)	0.74	0.33	0.96	0.88	0.94	1.00	0.86	0.87	0.91	0.63	0.67	0.77
TRI90D	0.52	0.03	0.92	0.79	0.85	0.86	1.00	0.98	0.92	0.39	0.42	0.53
TRI95D	0.49	-0.01	0.93	0.75	0.84	0.87	0.98	1.00	0.95	0.36	0.40	0.5
TRI99D	0.46	-0.03	0.94	0.70	0.79	0.91	0.92	0.95	1.00	0.34	0.38	0.51
TRI90J	0.97	0.85	0.51	0.81	0.75	0.63	0.39	0.36	0.34	1.00	1.00	0.96
TRI95J	0.98	0.82	0.55	0.83	0.77	0.67	0.42	0.40	0.38	1.00	1.00	0.97
TRI99J	0.97	0.74	0.66	0.88	0.84	0.77	0.53	0.50	0.51	0.96	0.97	1.00

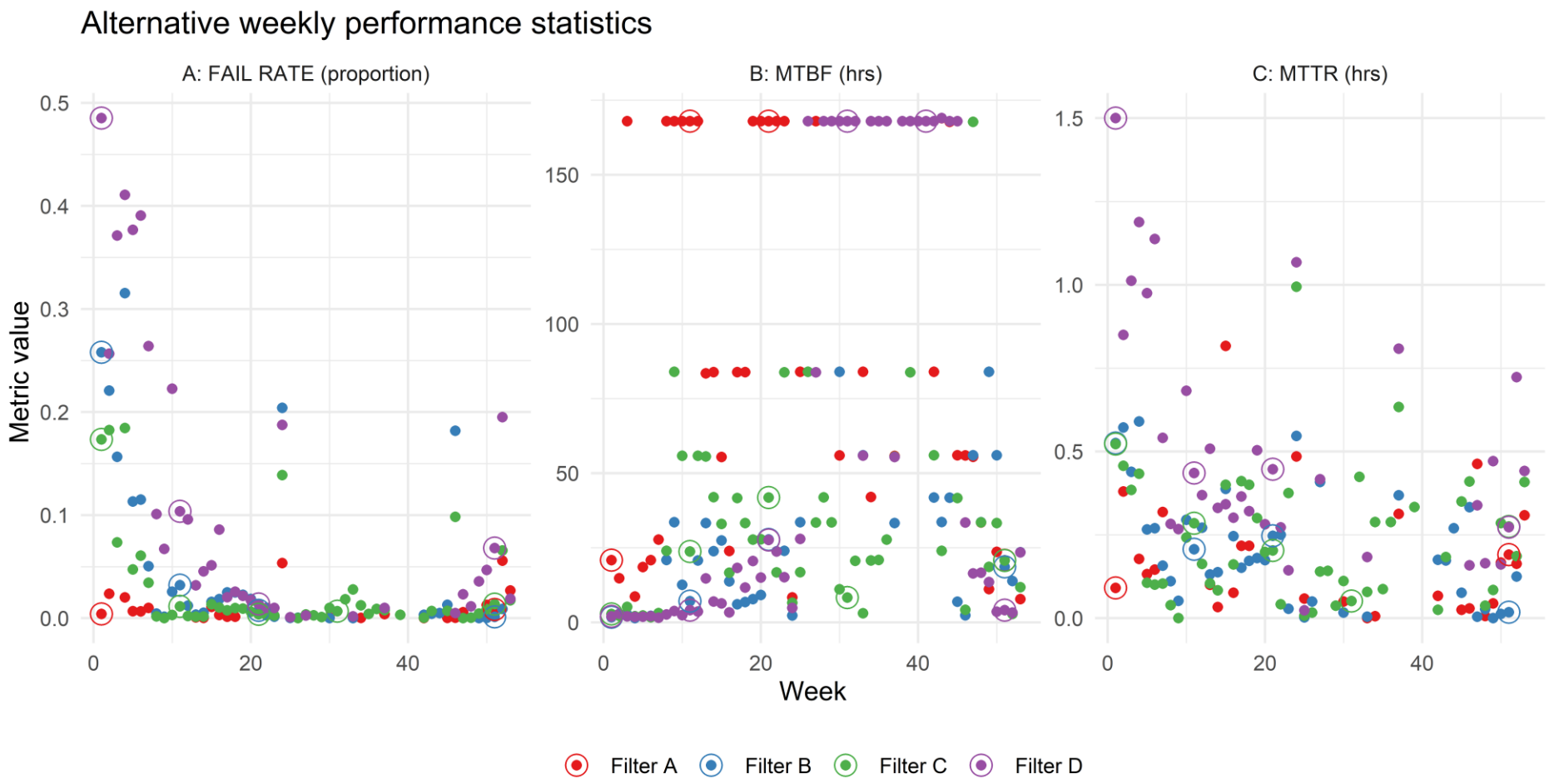

Figure 9 Performance assessment based on a binary classification of turbidity. The points corresponding to the six selected weeks are circled

2.4.3 Filter performance diagnosis

Diagnosis of the cause of poor filtration performance is key to managing and reducing water quality risk. In order to demonstrate the effectiveness of classification trees, an example of a weekly model for Filter D Week 21 is shown in Figure 10. Each circular node describes a split in the data describing filter operation. The first split divides observations into those which are associated with a hydraulic shock, whereby the instantaneous flow rate was greater than 1.2 times the mean flow for the filter over the run. Such conditions may have resulted in the shearing of flocs and deposits within the bed.It was this point that most effectively split the turbidity observations in the training data into those which were greater than or less than 0.1 NTU. Each rectangular leaf node describes the performance of the filter given the particular conditions as described by the nodes above. Three lines of text in the leaf node describe the probability of a “HIGH” (>0.1 NTU) turbidity reading, the complimentary probability of “OK” turbidity and the overall probability over the period of interest that those conditions would be observed. Based on the diagnostic model presented in Figure 10 the priority actions to manage filtered water turbidity would be to reduce the hydraulic shocking or run length. The simplest short-term intervention would be to reduce filter run time to less than 42 hours. However, to avoid hydraulic shocking and improve water efficiency, modifications to hydraulic control would be beneficial. The filters use inlet penstocks and a hydraulic step to control flow split between filters. Outlet flow control for the filters is modulated to maintain a level set point in the individual filter using a Proportional-Integral-Derivative (PID) control loop. An interim risk reduction would be to adjust parameters such that the volume of the tank was used to buffer the rate of flow change. Ultimately the hydraulic control philosophy of the filters is unsatisfactory and would benefit from modification such that the flow from all the filters was adjusted to maintain a level in the common inlet channel and equal flow across filters in service.

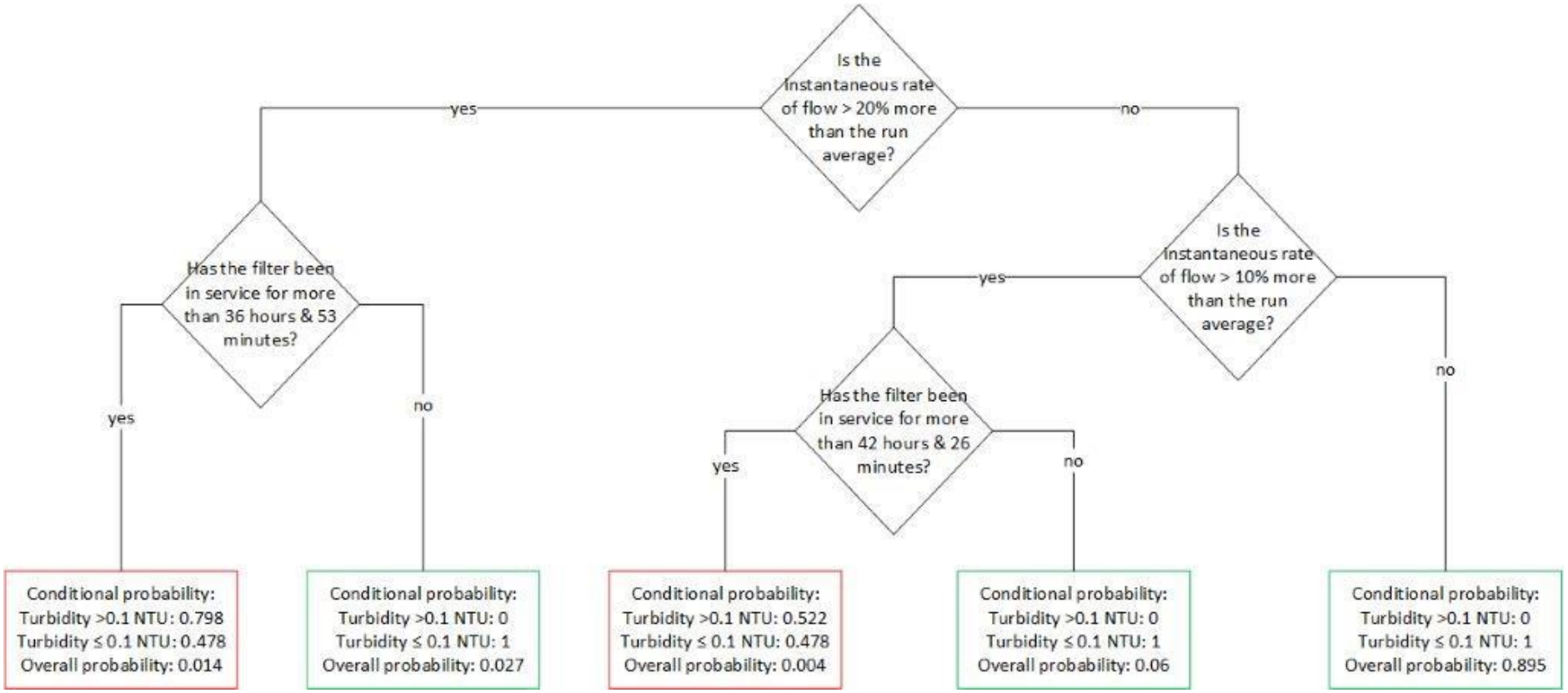

Figure 10 Example classification tree model for Filter D Week 21

The outputs from the fitted weekly models showed that they provided a highly accurate description of the conditions associated with correct classification for >75% of observations in the worst performing model and average accuracy between 94% and 99% depending on the filter (Table 4). Average true positive rates for high turbidity values were greater than 91% for all filters. The classification tree approach is not limited to informing on week to week operation of individual filters. An additional categorical variable indicating the specific filter was added to the model and clean bed head loss was scaled for each of the filters using a z score.

Table 4 Summary of weekly models for individual filters performance

Filter	Count (weeks)	accuracy (min, ave, max)	sensitivity (min, ave, max)	specificity (min, ave, max)
Filter A	18	0.91, 0.99, 1	0.74, 0.93, 1	0.91, 0.99, 1
Filter B	32	0.8, 0.96, 1	0.47, 0.91, 1	0.75, 0.95, 1
Filter C	42	0.76, 0.97, 1	0.56, 0.91, 1	0.71, 0.97, 1
Filter D	35	0.81, 0.94, 1	0.81, 0.96, 1	0.78, 0.92, 1

We can see that the monthly models typically have good accuracy >0.75, however model sensitivity (from the true positive rate) was lower in some of the months that experienced better filter performance (Table 5). In July, only 55% of high observations were explained by the model however, the failure rate was only 0.1%. The classification tree model for the month of January was plotted to provide an example (Figure 11). This shows that those filters treating more than 24% of the flow to the bank had a 0.48 probability of producing “HIGH” turbidity water after 15 hours, indicating that earlier washing was required at this hydraulic loading. At the case study WTW, splitting of the flow to the filters was controlled by an upwards penstock at the inlet to each filter box, while outlet flow is controlled to maintain a constant level within the filter. There was a 0.28 probability of high turbidity in the first hour and 20 minutes, suggesting an undesirably long ripening period. Between 1.3 and 15 hours into a run, filter D had a 0.19 probability of producing “HIGH” turbidity water if it had experienced a spike in clarified water turbidity of greater than 0.12 NTU above the trend. Classification trees such as those demonstrated here can effectively identify and clearly communicate the conditions associated with poor filtration performance. This can aid the identification of activities to manage filtered water quality. On the basis of the diagnostic model presented in Figure 11 there are multiple performance issues which would benefit from the following priority actions:

- High turbidity is associated with unequal hydraulic loading.
    - In this system the hydraulic loading to the filters can be modified by:
        - Adjusting the set-points of the inlet penstocks.
        - Upgrading the hydraulic control philosophy.
- High ripening turbidity:
    - Investigate backwashing. Residual turbidity within the filter at the end of the backwash cycle may indicate insufficient rinsing of deposits from the bed.
    - Reduce the rate of flow change at the start of a run. Known as a “slow start”, a low initial filtration rate can improve the filter coefficient during the ripening phase.
    - Consider investing in a run-to-waste so that poor quality initial water does not enter supply.
- Spike loadings of turbidity in the clarified water appear to be linked with high turbidity from filter D.
    - Further investigation into the condition of filter D including media cores and backwash observation would be recommended.
    - Investigation into the cause of elevated clarified water turbidity is recommended.

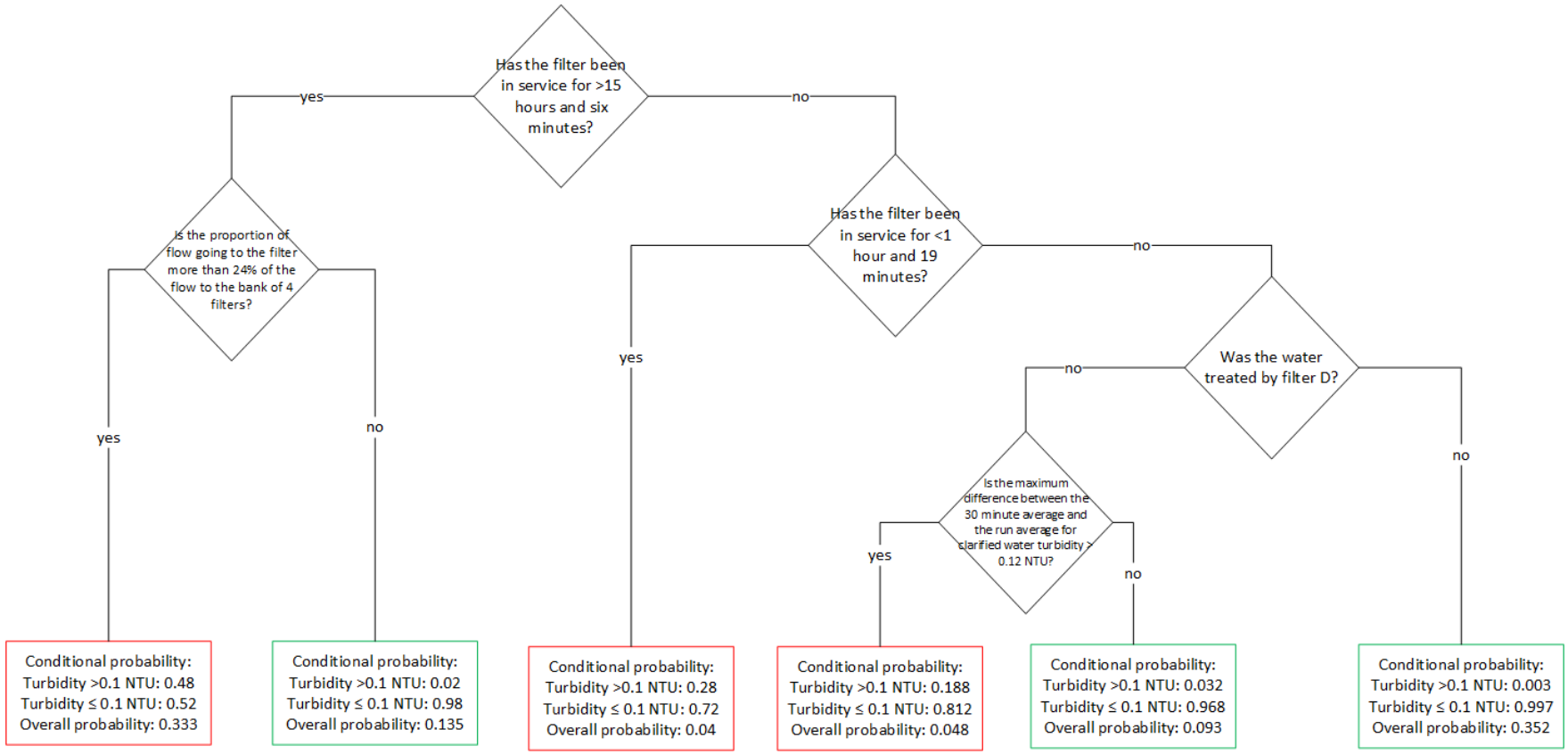

Figure 11 Example classification tree model filter bank in January 2015

Table 5 Summary of monthly models for individual filters performance

Month	>0.1 NTU %	accuracy	sensitivity	specificity
Jan	15.00	0.75	0.96	0.70
Feb	7.10	0.85	0.81	0.86
Mar	2.60	0.94	0.93	0.94
Apr	1.50	0.96	0.74	0.96
May	0.80	0.99	0.84	0.99
Jun	2.90	0.95	0.87	0.96
Jul	0.10	1.00	0.55	1.00
Aug	0.30	1.00	0.89	1.00
Sep	0.20	0.99	0.95	0.99
Nov	1.70	0.98	0.85	0.98
Dec	2.40	0.92	0.81	0.92

2.5 Discussion

The cyclic operation and dynamic characteristics of filtration typically produce a fluctuating turbidity trend from which a relative comparison of performance may not be visually intuitive (Figure 5 and Figure 6). To aid clearer comparison, turbidity data are often plotted as a cumulative distribution, though information is lost describing the time and operational context (Figure 5). The underlying processes giving rise to filtrate turbidity vary as do properties of the resultant distributions (Figure 6 and Figure 7). An appropriate method for the quantification of performance through the aggregation of this data is important for the effective management of the treatment process which requires the effective comparison of performance over time and between filters in order to direct preventative maintenance.

2.5.1 Performance assessment

Though widely used, the average turbidity (mean or median) is not the most appropriate property of the distribution upon which to compare filter performance (Figure 8 A, B). This is because unless a filter is suffering acute and prolonged periods of poor performance, average turbidity is likely to be below 0.2 NTU. Without visibility of the underlying distribution, it is not clear if differences in mean turbidity arise from turbidity spikes of concern or bias at the lower end of the measurement range. For example, average turbidity of 0.05 NTU from one system or period of operation cannot consistently be assumed to represent lower

risk than turbidity of 0.07 NTU from another. The insensitivity of the mean and median statistics are demonstrated when comparing the performance of filters B and C during weeks 31 and 41, where both statistics fail to capture the significant spiking which occurs in the filtrate turbidity of filter C during week 31 (Figure 6 and Figure 7). The median and mean are sensitive, however, to the comparatively higher turbidity recorded during normal operation in filter B which, with the limitations of the measurement, hold little useful information and are likely to arise from measurement error.

The standard deviation of turbidity (Figure 8 C) is generally effective and appropriate for comparing the variation in the right tailed distributions of filtrate turbidity during inconsistent performance. However, the statistic may not always appropriately compare distributions with varying kurtosis. It is common to select a high percentile value with which to compare performance (Figure 8 D, E, F). As turbidity time series exhibit inconsistent skewness and kurtosis between groups and over time, comparison of a single percentile value will not be a consistent basis for comparison (Figure 7). Two distributions, one with a short fat tail and another with a long thin tail may return an equal 95th percentile but reflect quite different turbidity risk. A process may completely fail for 4% of the period without impacting on the performance as measured by the 95th percentile. The choice of a high percentile (T90 - T99) affects the relative assessment of performance between filters B and C during week 1 (Figure 8 D, E, F). The 90th and 95th percentiles for filter B are greater than those of filter C, however, the 99th percentile for filter C is greater than filter B. There remains no clear empirical or theoretical link that supports the assessment of overall performance on the basis of a single percentile value.

Turbidity robustness indices have developed from the TRIE with additional terms and weighting procedures but fall short of addressing distortions arising from variation in tail shape. The relative performance of filters as described by the TRID (Li and Huck, 2008) and TRIJ (Hartshorn *et al.*, 2014) metrics are illustrated in Figure 8 (G-L). The first term of the TRI metrics takes the quotient of two percentiles in a manner analogous to the uniformity coefficient applied to filter

media (Logsdon *et al.*, 2002). Such an approach may function when comparing similarly shaped distributions, but is not reliable when the skewness and kurtosis of the underlying distributions are inconsistent. As a lower median turbidity (denominator) will result in a larger quotient there is an unjustified penalty for better average turbidity given the same high percentile value. The weakness of the TRID in this regard is clear when comparing week 1 (Figure 8 G-I) where filter D has a TRI90D less than for filters B and C which is clearly counter intuitive upon examination of the time series and distributions (Figure 6 and Figure 7). The second term common to the TRI metrics takes the median and divides it by the goal turbidity, typically between 0.1 and 0.3 NTU. Assuming a consistent target turbidity, this term does not serve to usefully differentiate performance any more than taking the median. The differentiating elements of the original TRIE metric could therefore be simplified to T90/T50 + T50 which, given the limitations of using percentiles, is unlikely to be the best approach for comparing performance. Though the additional procedures for weighting terms implemented in the TRID metric remove some cases where nonsense TRIE values would be returned, the examples identified demonstrate that the method is fallible. Though the TRIJ introduces a simpler and more stable method for weighting terms, the use of arbitrary percentile values continues to exhibit an influence on the relative assessment of performance between filters with turbidity distributions of different shape (Figure 8 J-L).

A more appropriate approach is to apply best practice guidance which indicates that turbidity greater than 0.1 NTU is indicative of a filtration performance issue (EPA, 1998). Breaching this limit can be considered as “failure”, such a binary approach is appropriate given uncertainties in the relationship between turbidity and water quality risk, allowing a simple and effective way to incorporate performance comparison on the basis of time. The failure rate against a goal of 0.1 NTU is a good metric for filtration performance as it is understandable, comparable, insensitive to measurement error and easily applied (Figure 9 A). For example, in week 1 filter D spent almost twice as much time over 0.1 NTU than filter B. The reliability of a filtration process can be compared by contrasting the average duration of acceptable performance between turbidity spikes

(Equation 17). The performance of filters spiking more frequently can be described as being less reliable. The MTBF shows that filter A typically appears to be more reliable than the other filters throughout the year, with a longer average interval between turbidity spikes (Figure 9 B). Poor performance may be a result of frequent spikes in filtrate turbidity, or less frequent but more extended periods of poor performance, the causes of which are likely to be functionally different and therefore of interest in the management of the process. Insight in this regard can be gained by examining the interval between turbidity events. However, it should be acknowledged that as high turbidity events are likely to cluster, the mean time between failures is an indicator only. The resilience of the performance of a filter can be compared by contrasting the average duration of turbidity spikes observed (Equation 18). Filters which on average return to acceptable performance in a shorter time can be considered to be more resilient. Filter D can be seen to be the least resilient early in the year with turbidity spikes lasting on average over an hour (Figure 9 C).

The alternative measures of filtration performance described offer a sensible and intuitive approach to characterising the aspects of performance which are effectively measured using turbidity. The main advantage of these approaches is that they do not depend on consistent skewness of the turbidity distribution to be comparable. Furthermore, when applying the failure rate (MTBF and MTTR) there is no reliance on an implicit assumption that risk is a consistent linear function of turbidity. There is merely an assumption that turbidity above 0.1 NTU is consistently indicative of greater risk than turbidity less than 0.1 NTU. Assessment of filter performance on the basis of turbidity could be further improved by the effective definition of a risk function for turbidity.

2.5.2 Diagnosis

In order to effectively manage filtration performance, an understanding of the causes of poor performance is required. Diagnosis of filtration issues is typically achieved through interpretation of turbidity time series and normalised starting head loss. Approaches to the interpretation of turbidity trends over the period of a filter run are well described and have been used to characterise a number of

filtration issues (Logsdon *et al.*, 2002). However, these methods are manual, time consuming and subjective which can restrict their application. Through automation of the analysis, such interpretation can be applied much more broadly to understanding marginal treatment performance concerns. Addressing such performance issues in individual treatment stages by preventative maintenance, the likelihood of acute compound treatment failures can be reduced (Venkatasubramanian *et al.*, 2003a). In this research the assessment of filtration performance as “HIGH” if >0.1 or “OK” if ≤ 0.1 NTU facilitates the framing of diagnosis of these issues as a machine learning classification problem, where other sources of process data are used to build explanatory models. The CART algorithm allows the training of simple and interpretable classification tree models which effectively describe the conditions which are associated with greater risk of poor filtration performance. These models can be readily used to review the operation and control of filtration processes. The classification and regression tree algorithm provides an easily interpretable output for non-linear processes which are affected by outlying observations, conditions which challenge linear diagnostic models (James *et al.*, 2013; Sotomayor and Odloak, 2005).

The common operational causes of poor filtration performance such as hydraulic balancing, surging, ineffective backwashing, excessively long filter runs and ineffective pre-treatment are well known (Logsdon *et al.*, 2002). Explanatory features describing these issues can be calculated from typical operational monitoring signals at a WTWs (Table 2). Supplying these features to the algorithm, rather than raw data trends, results in more interpretable models which are readily translated into remedial actions. As an example, it was evident that high turbidity from filter D during week 21 occurred with an 80% probability during times of hydraulic shock of more than 19.3% later than 36.9 hours into the filter run (Figure 10). After 42.4 hours, a smaller hydraulic shock of only 10% was associated with a 52% chance of turbidity spiking above 0.1 NTU. Flow increases are known to cause additional shear, increasing the rate of detachment of particles from the media, with the effect growing more pronounced later in the run (Cleasby, Williamson and Baumann, 1963; Han, Fitzpatrick and Wetherill, 2009a). From this, it is possible to infer that filter performance could be improved

at this time by improving flow distribution or shortening the filter run. The high accuracy, sensitivity (true positive rate) and specificity (true negative rate) of the models tested provides confidence that amelioration of the conditions suggested by the model are likely to improve performance (Table 4).

In January, across the filter bank, poor performance occurred in a number of circumstances (Figure 11). Typically, there was high turbidity in the first 1.3 hours of the filter run. A number of issues have been associated with extended ripening periods, these include over-washing, low solids in the clarified water, low temperature, hydraulic overloading and ineffective particle destabilisation (Logsdon *et al.*, 2002; Suthaker, Smith and Stanley, 1998; Tobiason and Melia, 1988). Reducing the initial rate of filtration is a typical process intervention in such circumstances, and more modern filters typically have a run to waste facility (Logsdon *et al.*, 2002). Flow distribution to the individual filters was clearly important later in the run with those treating more flow exhibiting greater probability of breakthrough later in the run. Balancing flows to the four filters is likely to improve the performance. Filter D was more likely to produce high turbidity water during normal filter operation after the ripening period particularly in the event of a sudden turbidity loading from a clarification issue. Further investigation indicated that flows to filter D were higher than those to the other three filters making it more vulnerable to fluctuations in clarified water quality. The simple tree model shown in Figure 11 describes conditions associated with 96% of the elevated turbidity observations during January, clearly identifying operational opportunities for improving performance. The monthly models were successful at describing challenge conditions for the bank of filters with accuracy and sensitivity typically over 80%, consistently demonstrating the potential for useful insight for process management (Table 5).

Though the methodology discussed has been shown to identify a range of issues related to poor performance, certain types of process fault may not be apparent using this approach. For example, long-term changes to filter characteristics which occur uniformly across filters. This includes media erosion which typically takes place over years and so is not likely to be captured. Rapid changes, such

as sudden loss of media or change in backwash performance which impact on performance should be indicated by the influence of normalised clean bed head loss in the diagnostic model.

Other investigations focussed on other processes have developed and employed more sophisticated approaches to fault diagnosis and adaptive model based control (Venkatasubramanian *et al.*, 2003a; Kim *et al.*, 2013; Foscoliano *et al.*, 2016; Tidriri *et al.*, 2016). Despite the additional capabilities of many such historical data driven control and diagnostic systems described in the literature there remains an implementation gap. By-definition, such methods are likely to be implemented through integration of software with existing assets and control systems. Interaction with existing proprietary control systems is awkward or costly by design. An inherently simpler tree-based method as described can flexibly facilitate operators and engineers to deliver performance improvements in many distributed assets with considerably lower barriers to implementation.

2.6 Conclusions

It is the conclusion of this investigation that:

- Simple performance metrics which describe the likelihood, frequency and duration of turbidity spikes using compliance rate, mean time between failures and mean time to recovery provide an appropriate and effective indication of filter performance, avoiding spurious scoring and comparisons arising from current methods.
- The diagnosis of operational causes of elevated filtrate turbidity were framed as a machine learning classification problem which is a more efficient and scalable approach than traditional manual interpretation of turbidity time series. The CART algorithm is demonstrated to be an effective diagnostic method generating highly accurate models describing conditions associated with elevated filtrate turbidity. Weekly models for individual filters and monthly models across the whole filter bank typically described conditions associated with elevated turbidity with accuracy over 90%.

- By engineering and using operationally relevant predictor variables these diagnostic models were intuitive to interpret and translate into operational and preventative maintenance decisions.
- A weekly model for an individual filter was shown to clearly identify and communicate that elevated turbidity was largely associated with hydraulic loads greater than 1.2 times the within run average after 36.8 hours of operation or hydraulic shocks greater than 1.1 times the within run average after 42.4 hours of operation. Identifying these conditions clearly indicates that that filter run times or hydraulic load fluctuations late in the run should be reduced. A monthly model describing performance across the filter bank identified that high turbidity occurred during the ripening of all filters and that turbidity breakthrough was an issue after 15 hours except where filters were hydraulically underloaded compared to their neighbours. Furthermore, Filter D exhibited elevated turbidity earlier in the run during clarified turbidity spikes. Such conditions indicate that flow balancing, and the optimisation of pre-treatment and backwashing should be investigated to deliver performance improvements.
- The methods described can be readily applied to inform operational and preventative maintenance decisions.

2.7 References

Anderson, C.W. (2005). Turbidity, in *National field manual for the collection of water-quality data*. 9th edn. Reston, VA: USGS, pp. 1–55.

Breiman, L., Friedman, J., Olshen, R., & Stone, C. (1984). *Classification and regression trees.* Boca Raton, Florida: Taylor & Francis Group.

Bridgeman, J., Simms, J. S., & Parsons, S. A. (2002). Practical and theoretical analysis of relationships between particle count data and turbidity. *Journal of Water Supply: Research and Technology—AQUA*, *51*(5), 263-271.

Cleasby, J. L., Williamson, M. M., & Baumann, E. R. (1963). Effect of filtration rate changes on quality. *Journal of the American Water Works Association*, *55*(7), 869-880.

Conway, J., Eddelbuettel, D., Nishiyama, T., Prayaga, S. K., & Tiffin, N. (2013). RPostgreSQL: R interface to the PostgreSQL database system. R package version 0.4.

DeMers, L. D., & LeBlanc, J. Z. (2003). Louisiana systems take on the optimization challenge. *Journal of the American Water Works Association*, *95*(6), 48-52.

Egerton, A., Hall,T. & Watts, M. (1999) *99/DW/06/9 Statistical Process Control and Other Techniques for Managing Cryptosporidium Risk in Water Treatment.* London: UK Water Industry Research Limited

Farrell, C., Hassard, F., Jefferson, B., Leziart, T., Nocker, A., & Jarvis, P. (2018). Turbidity composition and the relationship with microbial attachment and UV inactivation efficacy. *Science of the Total Environment*, *624*, 638-647.

Foladori, P., Bruni, L., Tamburini, S., Menapace, V., & Ziglio, G. (2015). Surrogate parameters for the rapid microbial monitoring in a civil protection module used for drinking water production. *Chemical Engineering Journal*, *265*, 67-74.

Foscoliano, C., Del Vigo, S., Mulas, M., & Tronci, S. (2016). Predictive control of an activated sludge process for long term operation. *Chemical Engineering Journal*, *304*, 1031-1044.

Frederick, L., VanDerslice, J., Taddie, M., Malecki, K., Gregg, J., Faust, N., & Johnson, W. P. (2016). Contrasting regional and national mechanisms for predicting elevated arsenic in private wells across the United States using classification and regression trees. *Water Research*, 91, 295-304.

Gauthier, V., Barbeau, B., Tremblay, G., Millette, R., & Bernier, A. M. (2003). Impact of raw water turbidity fluctuations on drinking water quality in a distribution system. *Journal of Environmental Engineering and Science*, *2*(4), 281-291.

Gitis, V., Rubinstein, I., Livshits, M., & Ziskind, G. (2010). Deep-bed filtration model with multistage deposition kinetics. *Chemical Engineering Journal*, *163*(1-2), 78-85.

Great Britain. The Water Supply (Water Quality) Regulations 2000: Elizabeth II. Chapter 3184 (2000) London: Her Majesty's Stationery Office. Available at:https://www.legislation.gov.uk/uksi/2000/3184/contents/made (Accessed: 26/11/2021).

Gregory, J. (1994). Cryptosporidium in water: treatment and monitoring methods. *Filtration & Separation*, *31*(3), 283-268.

Grolemund, G., & Wickham, H. (2011). Dates and times made easy with lubridate. *Journal of statistical software*, *40*(1), 1-25.

Han, S., Fitzpatrick, C. S., & Wetherill, A. (2009). The impact of flow surges on rapid gravity filtration. *Water Research*, *43*(5), 1171-1178.

Hartshorn, A. J., Prpich, G., Upton, A., Macadam, J., Jefferson, B., & Jarvis, P. (2015). Assessing filter robustness at drinking water treatment plants. *Water and Environment Journal*, *29*(1), 16-26.

Hastie, T., Tibshirani, R., & Friedman, J. (2009). *The elements of statistical learning*. 2nd edn. Springer.

Huck, P.M., Emelko, M.B., Coffee, B.M.M, Maurizio, D.D. and O'Melia, C.R. (2001). *Filter operation effects on pathogen passage*. Denver: AWWA Research Foundation and American Water Works Association.

Huck, P. M., Coffey, B. M., Anderson, W. B., Emelko, M. B., Maurizio, D. D., Slawson, R. M., ... & O'Melia, C. R. (2002a). Using turbidity and particle counts to monitor Cryptosporidium removals by filters. *Water Science and Technology: Water Supply*, *2*(3), 65-71.

Huck, P. M., Coffey, B. M., Emelko, M. B., Maurizio, D. D., Slawson, R. M., Anderson, W. B., ... & O'Melia, C. R. (2002b). Effects of filter operation on Cryptosporidium removal microbial pathogens. *Journal of the American Water Works Association*, *94*(6), 97-111.

Hurst, A. M., Edwards, M. J., Chipps, M., Jefferson, B., & Parsons, S. A. (2004). The impact of rainstorm events on coagulation and clarifier performance in potable water treatment. *Science of the Total Environment*, *321*(1-3), 219-230.

James, G., Witten, D., Hastie, T., & Tibshirani, R. (2013). *An introduction to statistical learning*. New York: Springer.

Kim, H. S., Moon, T. S., Kim, Y. J., Kim, M. S., Piao, W. H., Kim, S. J., & Kim, C. W. (2013). Evaluation of rule-based control strategies according to process state diagnosis in A2/O process. *Chemical Engineering Journal*, *222*, 391-400.

Kuhn, M. (2011). caret: Classification and Regression Training. R package version 6.0-78. https://github.com/topepo/caret/

Kuhn, M., & Johnson, K. (2013). Classification trees and rule-based models. In *Applied Predictive Modeling* (pp. 369-413). Springer, New York, NY.

LeChevallier, M. W., Evans, T. M., & Seidler, R. J. (1981). Effect of turbidity on chlorination efficiency and bacterial persistence in drinking water. *Applied and Environmental Microbiology*, *42*(1), 159-167.

Letterman, R. D., Johnson, C. E., & Viswanathan, S. (2004). Low–Level Turbidity Measurements: A Comparison of Instruments. *Journal of the American Water Works Association*, *96*(8), 125-137.

Léziart, T., Dutheil de la Rochere, P. M., Cheswick, R., Jarvis, P., & Nocker, A. (2019). Effect of turbidity on water disinfection by chlorination with the emphasis on humic acids and chalk. *Environmental Technology*, *40*(13), 1734-1743.

Li, T., & Huck, P. M. (2008). Improving the evaluation of filtration robustness. *Journal of Environmental Engineering and Science*, *7*(1), 29-37.

Logsdon, G., Hess, A., Chipps, M. J., & Rachwal, A. (2002). *Filter maintenance and operations guidance manual*. Denver: Awwa Research Foundation and American Water Works Association.

Lusardi, P. J., & Consonery, P. J. (1999). Factors affecting filtered water turbidity. *Journal of the American Water Works Association*, *91*(12), 28-40.

Martin, B. (2014) *Treatment plant & distribution system optimization programs annual data summary report*. Denver. American Water Works Association.

McCoy, W. F., & Olson, B. H. (1986). Relationship among turbidity, particle counts and bacteriological quality within water distribution lines. *Water Research*, *20*(8), 1023-1029.

PostgreSQL Global Development Group. (2015) *PostgreSQL* 9.4. PostgreSQL Global Development Group.

R Core Team. (2015) *R: A Language and Environment for Statistical Computing* Vienna, Austria. available at https://www.r-project.org/

Rizak, S. N., & Hrudey, S. E. (2007). Strategic water quality monitoring for drinking water safety. *Water*, *34*(4), 67-71.

Rstudio. (2017) *RStudio: Integrated development environment for R (Version 0.97.311)* Boston, MA.

Sotomayor, O. A., & Odloak, D. (2005). Observer-based fault diagnosis in chemical plants. *Chemical Engineering Journal*, *112*(1-3), 93-108.

Suthaker, S., Smith, D. W., & Stanley, S. J. (1998). Optimisation of filter ripening sequence. *Journal of Water Supply: Research and Technology—AQUA*, *47*(3), 107-118.

Therneau, T.M. and Atkinson, E.J. and Ripley, B. (2017). rpart: Recursive Partitioning and Regression Trees. R package version 4.1-11. https://CRAN.R-project.org/package=rpart

Thoe, W., Gold, M., Griesbach, A., Grimmer, M., Taggart, M. L., & Boehm, A. B. (2014). Predicting water quality at Santa Monica Beach: evaluation of five different models for public notification of unsafe swimming conditions. *Water Research*, *67*, 105-117.

Tidriri, K., Chatti, N., Verron, S., & Tiplica, T. (2016). Bridging data-driven and model-based approaches for process fault diagnosis and health monitoring: A review of researches and future challenges. *Annual Reviews in Control*, *42*, 63-81.

Tobiason, J. E., & O'melia, C. R. (1988). Physicochemical aspects of particle removal in depth filtration. *Journal of the American Water Works Association*, *80*(12), 54-64.

Venkatasubramanian, V., Rengaswamy, R., & Kavuri, S. N. (2003a). A review of process fault detection and diagnosis: Part II: Qualitative models and search strategies. *Computers & Chemical Engineering*, *27*(3), 313-326.

Venkatasubramanian, V., Rengaswamy, R., Kavuri, S. N., & Yin, K. (2003b). A review of process fault detection and diagnosis: Part III: Process history based methods. *Computers & Chemical Engineering*, *27*(3), 327-346.

Venkatasubramanian, V., Rengaswamy, R., Yin, K., & Kavuri, S. N. (2003c). A review of process fault detection and diagnosis: Part I: Quantitative model-based methods. *Computers & Chemical Engineering*, *27*(3), 293-311.

WHO. (2015) *Guidelines for drinking-water quality,* 4th edn, Geneva. World Health Organization.

Wickham, H. (2016). *ggplot2: Elegant Graphics for Data Analysis*. New York: Springer-Verlag.

Wickham, H., François,R., Henry, L., and Müller, K. (2020). dplyr: A Grammar of Data Manipulation. R package version 1.0.0. https://CRAN.R-project.org/package=dplyr

Yuan, H., & Shapiro, A. A. (2011). A mathematical model for non-monotonic deposition profiles in deep bed filtration systems. *Chemical Engineering Journal*, *166*(1), 105-115.

Zhang, K., Achari, G., Sadiq, R., Langford, C. H., & Dore, M. H. (2012). An integrated performance assessment framework for water treatment plants. *Water Research*, *46*(6), 1673-1683.

3 Online zeta potential measurement for maintaining optimal coagulation conditions in low turbidity surface water

3.1 Abstract

Zeta potential is an established tool for observing and informing charge-neutralisation conditions required for effective coagulation of pathogens and natural organic matter (NOM). Theory and practice has established that contaminant minimisation should occur within a range of zeta potentials close to the iso-electric point, but the factors controlling the boundaries of this region are not well understood. Variation in sensitivity to zeta potential window was observed and modelled using on-line monitoring data from a full-scale water treatment works (WTW). Residual charge of only ±5 mV was shown to result in deterioration in performance of clarification and filtration processes suggesting that online measurement of zeta potential can provide a sensitive measure of coagulation performance. Explanatory models and simulation indicated that the size of the optimal zeta potential window varied with temperature, flow rate, turbidity, NOM concentration and pH. Supplementary jar testing suggested that, depending on conditions, performance deterioration with slight changes of zeta potential were driven by changes in secondary mechanisms including collision rate, adsorption and floc strength. These results provide a basis for greater understanding and improved operation of non-ideal reactors and more sensitive control of coagulation processes. This may potentially enable the more effective and economic operation of coagulation systems in a charge neutralisation regime with potential for reducing capital costs, chemical use and sludge.

3.2 Introduction

The effective particle destabilisation by coagulation-flocculation is critical for successful removal of particles, pathogen and natural organic matter (NOM) removal in conventional clarification-filtration water treatment processes used in most large water supply systems (Huck *et al.*, 2001; Lechevallier *et al.*, 1981). Failure to effectively remove particles and dissolved organic matter can result in excessive consumption of chlorine and shielding of micro-organisms during disinfection, as well as increased potential for disinfection by-product (DBP) formation (LeChevallier, Evans and Seidler, 1981; Golea *et al.*, 2017). The behaviour of colloidal particles is

governed by attractive and repulsive forces. Particles are stable in natural waters predominantly as a result of their hydrophilic nature and from electrostatic repulsion (Bratby, 2016). Interaction between the hydrated surfaces of hydrophilic colloids and the consequential aggregation is inhibited by the layer of water molecules. Attractive van der Waals forces are driven by the properties of the colloid as accounted for by the Hamaker constant. Repulsive forces are a product of surface charge and ionic properties of the aqueous phase. The accumulation of counter-ions in two layers, at the surface and in a diffuse layer of the aqueous phase in proximity to a charged particle gives rise to electrostatic stability. Colloids can be stable in water through retaining surface charge or hydration. Counter ions held fixed at the colloid surface are known as the Stern layer. The thickness of this layer is defined as the Stern plane and is the distance from the colloid of ½ the radius of the counter ion. Ions outside the Stern plane but still co-ordinated by colloidal charge make up the diffuse layer. Due to the difficulty in directly measuring the potential at the Stern plane, the potential at the shear plane between Stern and diffuse layers, known as the zeta potential, is used instead (Bratby, 2016). The net effect of van der Waals attraction and double later repulsion forces are described by DLVO (Derjaguin and Landau, Verwey and Overbeek) theory (Derjaguin and Landau, 1941; Verwey, 1947).

Coagulants destabilise charged colloids by compressing the double layer of counter ions, adsorbing onto the surface of colloids or enmeshing colloids in precipitate. After dosing, traditional trivalent aluminium and iron salts transition from free ions to insoluble metal hydroxide precipitates which are more effectively adsorbed at the colloid surface (Bratby, 2016). Due to the complexity and difficulty in observing interactions between coagulant hydrolysis products and ligands within natural waters, a quantitative description of coagulant demand based on first principles which is applicable in practice remains elusive (Davis and Edwards, 2014; Ratnaweera and Fettig, 2015). Approaches to coagulation and flocculation can be broadly categorised in two ways: 1) sweep flocculation; and 2) charge neutralisation. In sweep flocculation, a higher pH is maintained to promote the precipitation of the metal salt, increasing the rate of particle collisions and resulting in entrapment of particles and colloid within metal hydroxide precipitates (Hendricks, 2006). Alongside this, adsorption of dissolved compounds onto the solid precipitate also occurs. The charge-neutralisation regime operates at a lower pH than sweep flocculation and are conditions where the minimum

amount of metal salt are added which can sufficiently reduce the net charge on colloids and particles to minimise repulsive forces and promote aggregation. However, this is an oversimplification because coagulant-colloid interactions are influenced by: the character and surface properties of the contaminant colloids, the extent of hydrolysis of the coagulant, and the concentrations of both contaminant colloid and coagulant. At intermediate pH it is possible for either regime to dominate depending on the coagulant concentration. It is also possible that over-dosing of cationic coagulants can result in surface charge reversal and the re-stabilisation of colloidal particles (Bratby, 2016). Flocculation, the aggregation of destabilised particles, is also vital for the effective performance of water treatment processes. Flocculation is the net product of collision, attachment, entrapment, detachment, shear, erosion, and settlement processes.

The objective for water utilities is to identify and maintain optimal coagulation & flocculation conditions which enable downstream separation processes to remove contaminants to acceptable levels, whilst minimising unnecessary chemical use and sludge-handling as environmental conditions change. It is therefore advantageous to operate coagulation processes in the charge neutralisation regime, particularly for water sources of low alkalinity. Another important aspect to consider for low turbidity waters sources is that the floc formation process can be slow, particularly at low temperatures (< 5°C), making water treatment more sensitive to small changes in coagulant dose (Xiao *et al.*, 2008a). Low colloid concentrations characterised by low turbidity may not have sufficient collision opportunities to produce aggregates from particles even when completely destabilised (Stumm and Morgan, 1996). The coagulant dose required is dynamic and dependent upon the prevailing characteristics of the raw water alkalinity, contaminant particles and NOM (Sharp *et al.*, 2006). Such changes in water quality are caused by the increased mobility of terrestrial dissolved organic carbon (DOC), extreme weather events, catchment change, reservoir turnover and algal blooms. Manipulation of coagulant dose is the primary way by which water treatment operatives respond to changing raw water quality.

Determination of the optimal dose for the prevailing raw water quality has historically been achieved through empirical testing using the jar test procedure. Here, source water samples are coagulated on a bench-top mixing device using a range of coagulant and pH conditions to determine the most appropriate chemical doses to apply for any given water. Dissatisfaction with this method arises because it can be

slow, reactive, inaccurate and a poor representation of the hydraulic conditions present in real treatment systems. It is therefore typical to rely on subjective visual floc sizing methods to compare coagulation success which can be problematic in the case of low turbidity waters as there may not be a visible floc (Brink *et al.*, 1988). The optimal size of floc for dissolved air flotation processes is 10 - 30µm (Edzwald, 1995), a size which is smaller than can be effectively resolved by the naked eye. To overcome the limitations of jar testing, investigators have sought to optimise and control coagulation through empirically evaluating treatment systems using parameters such as turbidity and UV absorbance. These parameters can be measured on-line and be used to develop control systems (feed-forward and feedback) that link to the coagulant dose. While these tools have greatly improved the ability to respond to changes in water quality, they do not directly measure the effectiveness of the coagulation process. For example, an increase in the UV absorbance of water may not increase the coagulant demand of the water and such monitors are unable to detect NOM compounds that do not absorb UV light.

For coagulation processes operating in a charge-neutralisation dominated regime, electro-kinetic measurements of the dosed water can provide information describing the success of colloidal destabilisation (Black and Willems, 1961; Pilipovich *et al.*, 1958). The streaming current monitor is a well-established measurement technique successfully applied for feedback control of charge-neutralisation coagulation in many water treatment systems (Dentel and Kingery, 1988; Jefferson *et al.*, 2004). Current generated by the transient attachment of charged particles to surfaces within a reciprocating piston is linearly related to the zeta potential of that system (Dentel and Kingery, 1988). The main limitations of streaming current application for control are that the coating and abrasion of sensor surfaces, changes in particle size and a change in the ionic strength can cause instrumental drift and occasional erratic performance (Barron *et al.*, 1994). This instrumental drift can be managed with regular instrument maintenance and cleaning, meaning that feedback control is still possible. Interpreting streaming current readings and using this to understand coagulation performance is challenging as there is no consistent scale. Therefore, such a system requires external validation in order to confirm that the streaming current value is optimal.

Electrophoretic determination of zeta potential is frequently carried out by laser Doppler electrophoresis at a constant 20˚C (Tucker *et al.*, 2015). Unlike the streaming current instruments, electrophoretic measurements do not depend on moving mechanical measurement surfaces. As a result, it offers the potential for greater sensitivity in charge measurement than streaming current monitors. In addition, electrophoretic determination of zeta potential has the advantage of having a consistently meaningful mV scale and is an established bench top monitor used for understanding coagulation performance of water treatment (Black and Willems, 1961). The key long-held concerns identified with the use of zeta potential as a measure of coagulation success are that there is no single value which is universally effective for aggregation and that an optimal zeta potential value must be obtained experimentally, typically on the basis of the lowest residual turbidity (Bratby, 2016; Hendricks, 2006; O'Melia, 1969). Previous investigations at bench and pilot scale have identified optimal windows for zeta potential within which performance variation is independent of variation in charge but the location and size of these windows are system dependent (Jefferson *et al.*, 2004). Typically, a zeta potential window between -10 and +5 mV has been observed to apply for charge neutralisation coagulation for NOM laden water sources (Sharp *et al.*, 2005). However, the range of effective coagulant dose comprising the destabilisation zone is known to reduce with lower colloid concentrations (Stumm and Morgan, 1996).

There is a paradox in optimising coagulation using electrophoretic measurements. Zeta potential is derived from measurements of the electrophoretic mobility which is a function of particle charge. Particle systems that approach net neutral surface charge will therefore exhibit reduced electrophoretic mobility relative to random movement. Where the objective of coagulation is to neutralise the charge of colloidal particles to minimise inhibition of particle interaction then measurements in this region will have relatively large error and be less sensitive. Conversely in systems where coagulant is added in excess of charge neutralisation to promote the enmeshment of particles within a sweep floc the quality of electrophoretic measurements will be better, but the measurements won't be of value for understanding the dominant mechanism of coagulation (Xiao, Zhang and Lee, 2008b). For zeta potential measurements to be of value for informing and optimising coagulation performance the charge neutralisation mechanism must be predominant (Bratby, 2016).

In recent years, instrument manufacturers have developed an on-line sampling system for zeta potential, allowing for a much higher frequency of measurement and more efficient data collection. This provides greater opportunity to understand and optimise treatment systems, potentially enabling improved performance from imperfect reactors. The aim of this work was to demonstrate how comparatively small changes in the zeta potential within previously identified operational windows could impact the downstream water quality at a full-scale water treatment works (WTWs). The work then modelled online data from a full scale trial to understand how the effective operational window for zeta potential varied according to prevailing conditions. Additional jar testing of the two sources at varying temperature and mixing conditions at an optimal coagulant dose provided contextual information to understand the constraints of this approach.

3.3 Methods

3.3.1 Study site

The WTWs used in this study was a conventional 34 mega litres per day (Ml/d) plant treating water from two upland reservoirs (Sources A & B) in central southern Scotland. Coagulation is achieved using 18% Al_2O_3 poly-aluminium chloride solution (PACl) at 40% basicity without pH correction at typical doses in the region of 1 - 1.6 mg/L as Al. Exact doses could not be reliably determined for the period of the investigation as the rate of coagulant delivery was affected by the driving head in the coagulant storage tank and recorded coagulant doses rates were based on flow tests from a measurement vessel at relatively low driving head. Duty-standby coagulant storage tanks, pumps and lines dose the PACl into the inlet pipe which then enters a convoluted chamber where water recovered from the wash water settlement tanks is returned. The flow splits into one of three flocculation lanes (with approximately 5-10 minutes retention) before passing into a dissolved air flotation (DAF) stage and combining in a single clarified water channel. Water is then filtered by one of eight rapid gravity filters before disinfection with chlorine and pH correction. The study site was chosen because improvements to the performance of physical treatment processes were required. The known performance constraints at the case study site include inadequate flocculation time, hydraulic overloading of the DAF process, and seasonally poor filtration in winter. Online zeta potential measurements of coagulated

water were collected using a Malvern Zetasizer WT. Additional on-line instrumentation was used for collecting data for turbidity, pH, temperature, colour and UV_{254} absorbance. Online UV_{254} absorbance data were collected using ABB AV410 & AV420 online DOC monitors which provide a turbidity corrected UV_{254} absorbance reading by reference to absorbance at 405nm.

3.3.2 Data preparation & management

Data from on-line instrumentation was extracted from the control system between October 2016 and April 2018. This was achieved through the manual transfer of SCADA historian files to a separate PC via a mobile USB drive. Control system files were then converted to text before they were combined with data logged from additional trial instruments in a PostgreSQL 9.5 database (PostgreSQL Global Development Group, 2016). A data processing diagram is included in supplementary materials (Figure_Apx 15). Further data analysis was conducted using R software, primarily using the *tidyverse* packages for data manipulation and Mixed Generalised Additive Model Computation Vehicle (MGCV) packages for generalised additive modelling (CRAN, 2013; Wickham, 2017; Wood, 2012). Implausible and extreme data values were removed by imposing plausible limits from visual analysis of the data. For example, pH values >14 were indicative of sensor or signal error and so were removed. Time indexes for data series were shifted relative to the raw water series data set in proportion to the estimated water residence time in each of the processes (coagulation: 3 minutes; clarification: 20 minutes; filtration: 1 hour). Water quality signals taken at different frequencies (between 30 – 300 seconds) were then averaged at consistent three-hourly intervals. Outliers were removed using a Hampel filter calculated over a rolling window of 13 observations (+/- 18 hours). The Hampel filter was configured to replace the seventh value of each window with the median if the median absolute deviation (MAD) exceeded two standard deviations. The data set was then split into a training and test set. The first 12 months of the data were allocated for model training and the remaining data were used for model assessment. Single missing values were interpolated by carrying the last observation forward. Longer stretches of missing data were interpolated with an automated random forest algorithm based process which was applied separately to the training and test sets to avoid leakage of information from the test data into the training data (Stekhoven, 2013). Periods of interpolated data are indicated in Figure 12. Further pre-processing

including power transformations and calculation of principal components used the caret package (Max *et al.*, 2011).

3.3.3 Statistical modelling

The purpose of this investigation was to improve understanding of how the performance of treatment processes were affected by change in zeta potential and to understand if the effective operational window for a full-scale treatment system varied with the prevailing conditions. To do this, regression models were fitted using data describing treatment conditions to explain variation in treated water quality. Variation in treated water quality was measured by clarified UV absorbance, clarified water turbidity, filtered water turbidity, and filtered water aluminium. Variables characterising treatment conditions used in the predictive models were raw water turbidity, raw water UV absorbance, raw water pH, water temperature, raw water flow, return water turbidity, return water flow, filter run time, coagulated water pH and coagulated water zeta potential.

Correlations between predictor variables can result in unstable regression models and this multicollinearity can cause errors resulting in unstable predictions and inference errors. To address observed multicollinearity and instability during model selection the predictor variables were pre-processed. All parameters for pre-processing were calculated on the training set alone and then later used to process the test data for model performance assessment. Predictor variables were first transformed using a Yeo-Johnson power transformation which is similar to a Box-Cox transformation but is applicable to negative numbers with lambda fitted by maximum likelihood (Equation 21) (Yeo and Johnson, 2000).

Equation 21 Yeo-Johnson transformation

$$y_i^{(\lambda)} = \begin{cases} \left((y_i + 1)^{\lambda}\right)/\lambda & if\ \lambda \neq 0, y \geq 0 \\ log(y_i + 1) & if\ \lambda = 0, y \geq 0 \\ -[(-y_i + 1)^{(2-\lambda)} - 1]/(2 - \lambda) & if\ \lambda \neq 2, y < 0 \\ -log(-y_i + 1) & if\ \lambda = 2, y < 0 \end{cases}$$

Where: λ = a power transformation identified by maximum likelihood.

The resulting power transformed variables were scaled between 0 and 1 and then principal components were computed to explain 90% of the variance. Principal components analysis (PCA) is a linear transformation which produces a set of

orthogonal standardised variables in a new coordinate system which explain progressively decreasing proportions of variation in the original data. Further details explaining the calculation of principal components can be found in James *et al.* (2013).

Where possible it is preferred to use simple and familiar modelling approaches. However, in this investigation a modelling approach appropriate for observational studies of non-linear, autocorrelated processes with colinear variables was required. The advantage of using online instrumentation from a live WTWs was the large amount of data could be collected, and the results from the investigation could be rapidly applicable in practice. This came at the cost of experimental flexibility and the ability to collect independent data. Water treatment processes are complex and non-linear. However, the inherent assumption when using a linear model is that the relationship between the dependent and independent variables can be linearised through use of transformations and or polynomials. Where a linear approximation of a non-linear system results in errors which are not random (i.e., they have a pattern) the assumptions of Ordinary Least Squares (OLS) regression modelling are violated and parameter estimates are likely to be unreliable.

In this investigation generalised additive mixed models (GAMMs) were used to understand water treatment performance in the context of varying operational conditions, including zeta potential. GAMMs combine generalised additive models and mixed effects models to allow effective non-parametric, non-linear modelling of data with inherent dependency structures. First it is helpful to start with the definition of an OLS model that describes a linear relationship between X & Y shown in Equation 22 and on the assumption that residuals from the model are independent and normally distributed (Equation 23).

Equation 22 General form of a linear regression model

$$Y_i = \alpha + \beta x_i + \varepsilon_i$$

Where: Y_i = Value of the response variable, α = intercept β = slope coefficient ε = Error

Equation 23 Error structure for OLS regression model

$$\varepsilon_i \sim N(0, \sigma^2)$$

Where: σ = Standard deviation $N(0, \sigma^2)$ = Independently normally distributed with a mean of 0 and a variance of σ^2

The underlying processes, generating values measured by online instruments at WTWs, violate assumptions of independence, meaning that the use of ordinary least squares (OLS) regression models resulted were not appropriate. A serial dependence structure in this data means that use of OLS would result in correlated residuals that would have increased the risk of incorrectly concluding that relationships occurred when they do not (Zuur, 2009). Serial dependence was controlled for using a mixed modelling approach with the assumption of an autoregressive error structure of order 1 (AR-1). Using this approach, the residual at time s as a function of the residual at *s*-1 and noise can be modelled as Equation 24 and therefore have the correlation structure shown in Equation 25.

Equation 24 AR-1 error structure

$$\varepsilon_s = \rho\varepsilon_{s-1} + \eta_s$$

Where: ε = error, ρ = autocorrelation coefficient, s = time s, η = error (assumes independent & normally distributed)

Equation 25 AR-1 correlation structure

$$cor(\varepsilon_s, \varepsilon_t) = \begin{cases} 1 & if\ s = t \\ \rho^{|t-s|} & else \end{cases}$$

Where: t = time t

Generalised additive models (GAMs) are generalised linear models using a linear predictor which is the sum of smooth functions fitted to the independent variables. The general form for a GAM is shown in Equation 26 (Hastie and Tibshirani, 1986). GAMs were selected because they are broadly applicable, require few assumptions about the nature of the modelled relationship and are extendable to a mixed modelling approach (Zuur, 2009).

Equation 26 Generalised form for a GAM

$$y_i = \alpha + f_1(X_{i1}) + f_2(X_{i2}) + \cdots + f_p(X_{ip}) + \varepsilon_i$$

Where: y_i = is the value of the dependent variable (y) at index (i), α = the model intercept, f_1= smooth function 1, X_{i1}= the ith value of the first independent variable, p = denotes an index of smooth functions and independent variables, ε_i = model error between fitted & observed values of y at index i.

A wide range of smoothing functions can be used within generalised additive models and these functions are most intuitively understood as piecewise regressions. This

means that the space relating dependent and independent variables is broken down into subsections for which a local polynomial linear function is approximated and a smoothing term is then produced from the combination of these local linear functions. A more involved explanation of the thin plate and tensor interaction smoothing functions used can be found in Wood (2017).

Residuals from the generalised additive regression models exhibited significant correlation, therefore a mixed effect extension of GAMs known as generalised additive mixed modelling (GAMM) was used. GAMs and GAMMs were estimated using the MGCV package in R (Wood, 2012). All of the GAMMs used in this investigation used an AR-1 error structure and therefore can be described using the general form shown in Equation 27 which combines the general form of a GAM (Equation 26) with AR-1 errors (Equation 24) and therefore have the correlation structure shown in Equation 25.

Equation 27 Generalised form for a GAMM (AR1)

$$y_i = \alpha + f_1(X_{i1}) + f_2(X_{i2}) + \cdots + f_p(X_{ip}) + \varepsilon_{is}$$

$$\varepsilon_{is} = \rho\varepsilon_{is-1} + \eta_{is}$$

Where: y_i = is the value of the dependent variable (y) at index (i), α = the model intercept, f_1= smooth function 1, X_{i1}= the i_{th} value of the first independent variable, p = denotes an index of smooth functions and independent variables, ε_{is} = model error between fitted & observed values of y at index I and time s., ρ = autocorrelation coefficient, η = error which is independent & normally distributed

Each of the GAMMs was fitted according to the following procedure (Figure_Apx 16)

- The cleaned data was split into a training and test set, with data collected during the first year used for training and data collected subsequently used for model testing.
    - Three hourly average values for relative UV absorbance, clarified water turbidity, filtered water turbidity, filtered water aluminium were used as dependent variables.
    - Three hourly averages for zeta potential, coagulated water pH, flow, temperature, raw water UV absorbance, raw water turbidity, raw water pH and filter run time were used.
- After Yeo-Johnson transformation and scaling, principal components explaining 90% of the variation in the explanatory variables were calculated.

- Turbidity and residual aluminium dependent variables were natural log transformed.
- GAMMs with an AR-1 error structure were fit using all of the principal components and all two-way interactions.
- Residuals were checked for autocorrelation.
- Performance of the models was assessed using the hold-out test data for observations taken after the training data.

3.3.4 Jar-testing

Bulk raw water samples from Source A were collected in 25L high-density polyethylene (HDPE) containers from the WTW in Scotland and transported by vehicle overnight to the laboratory at Cranfield University without temperature control. Raw water samples were then stored at 5(+/- 3) ˚C in a walk-in refrigerator. Half the samples were removed from the cold room several hours prior to testing and analysis to allow them to reach room temperature, the other half were analysed direct from the cold room maintaining the low temperature with an ice bath. All jar testing was conducted on the water within three days of sampling. A sample of the PACl coagulant was taken from the WTW at the same time as the water samples and stored in a 250 mL HDPE bottle for transport.

Jar testing was conducted on samples of water from Sources A & B using PACl without pH correction (procedure as used at the WTW). An initial set of tests was conducted to identify the coagulant dose required to achieve a zeta potential of 0 mV for each water source. This set of jar tests was conducted in 1L cylindrical beakers using a PB 900 6 impeller variable speed jar tester with 76 x 25 mm flat paddle impellers. 1L of raw water was added to each of six jars. These jars were then stirred at 200 rpm during the rapid mix phase, where coagulant was added at increasing concentration. The concentration was increased by 0.2 mg/l increments. PACl was added to each jar using a micropipette. Once all of the jars were dosed with coagulant, the mixing was continued for a further 10 seconds before the mixing speed was dropped to 20 rpm. An aliquot from each jar was then immediately extracted using a syringe rinsed with DI water, before analysis for zeta potential using a Malvern nanosizer. The coagulant dose and resultant zeta potential was recorded and plotted in order to identify the

coagulant dose required to achieve a zeta potential of 0 mV by interpolation, this dose (1mg/l for source A, 2.1 mg/l for source B) was then used for all subsequent jar tests.

Subsequent jar tests for floc size analysis were conducted one at a time using a single cylindrical jar and stirrer of a two paddle PB-980 series jar tester. Sample volumes, jars and paddle dimensions remained consistent with the first set of jars. Floc size was monitored over the jar test using a Malvern Mastersizer 2000. The sample was drawn through the optical cell of the Mastersizer by a peristaltic pump using 5 mm ID tubing at a flow rate of 1.5 L/hr. Repeated jar tests were then conducted to examine the effect of temperature and mixing conditions in different waters whilst the coagulant dose remained fixed at the dose required to achieve neutral zeta potential. Triplicate jar tests were completed with a full factorial 3x2 design. Variables investigated were:

- temperature: 5 and 20 ˚C (maintained with an ice bath or at room temperature),
- Slow stir speed: 20 and 50 rpm,
- With & without a rapid mix: (10 seconds at 200rpm).

3.3.5 Analysis of jar test data

The jar testing experiments conducted required the repeated measurement of floc-size within the same suspension which would result in strong serial dependence between residuals. Particle collisions and aggregations within a suspension have a random component and jar-testing has non-random sources of error which cannot be adequately eliminated or measured. This means that the floc growth observed under controlled conditions in a single jar is one outcome out of the distribution of outcomes which would be observed if the test conditions were replicated infinitely. For example, random Brownian motion will influence the floc growth rate in a jar test as will the non-random location along the radius of a stirred jar at which the coagulant enters the water. These and other influences will impact the precipitation of the micro-floc and the rate of early collisions and therefore the rate of aggregation. Consecutive observations of any growth process are also not independent with the floc size observed at one time point being dependent in part on the size of the floc at the previous time point. For this reason floc size data was modelled by comparing discrete time points at five minute intervals. For each time point a linear regression model of

the form shown in Equation 28 including interactions between all experimental variables was fit. Interactions were removed sequentially if not significant and models presented in standard regression tables including coefficient estimates, standard errors, observations and performance statistics.

Equation 28 Equation for linear model of D_{50} floc size for jar test data

$$D_{50} = \alpha + \beta_T T + \beta_R R + \beta_F F + \beta_{TR} TR + \beta_{TF} TF + \beta_{RF} RF + \beta_{TRF} TRF + \varepsilon$$

Where: D_{50} = median floc diameter, T = Temperature included as a categorical variable either LOW (7.5°C ± 2) or HIGH (19.5°C), R = Rapid mix included as a categorical variable indicating if a 200rpm rapid mix for 10 seconds was used ,F = Flocculant mixing speed included as a categorical variable indicating if the flocculant mixing speed was 20 or 50rpm

3.4 Results & Discussion

3.4.1 Summary of operational data

Source A was from a deep upland reservoir and was of low turbidity ($\bar{x}$ = 0.9 NTU, 95th%ile = 2.86 NTU) and low total organic carbon (TOC) ($\bar{x}$ = 3.57 mg/l, 95th%ile = 4.17 mg/l) but high specific ultra violet absorbance (SUVA = $UV254_{abs}$/ TOC) ($\bar{x}$ = 4.8 L/mg/m, 95th%ile =5.7 L/mg/m) (Table_Apx 1). The shallower source B had higher solids from turbidity ($\bar{x}$ = 1.55, 95th%ile = 2.76), colour ($\bar{x}$ = 42, 95th%ile =54) and TOC ($\bar{x}$ = 6.6, 95th%ile =8.2) concentrations and similar SUVA ($\bar{x}$ = 4.7 L/mg/m, 95th%ile =5.3 L/mg/m) (Table_Apx 1). Originally designed to receive a 50-50 contribution of sources, the WTW tends to operate with slightly more of source A in the summer to reduce sludge production and reduce taste and odour issues. It is operational practice, during the winter, to blend the two sources more equally in order to improve the formation of flocs. Over the period of the investigation there was an increase in the concentration of UV absorbing organic compounds in the raw water as well as a general trend of increasing coagulated water zeta potential, going from -4 to +2 mV, and increasing pH from 6.3 to 6.7 (Figure 12). Increasing UV absorbance in the raw water and changes in the coagulation pH observed over the period of investigation were indicative of underlying changes to the coagulation regime at the case study site.

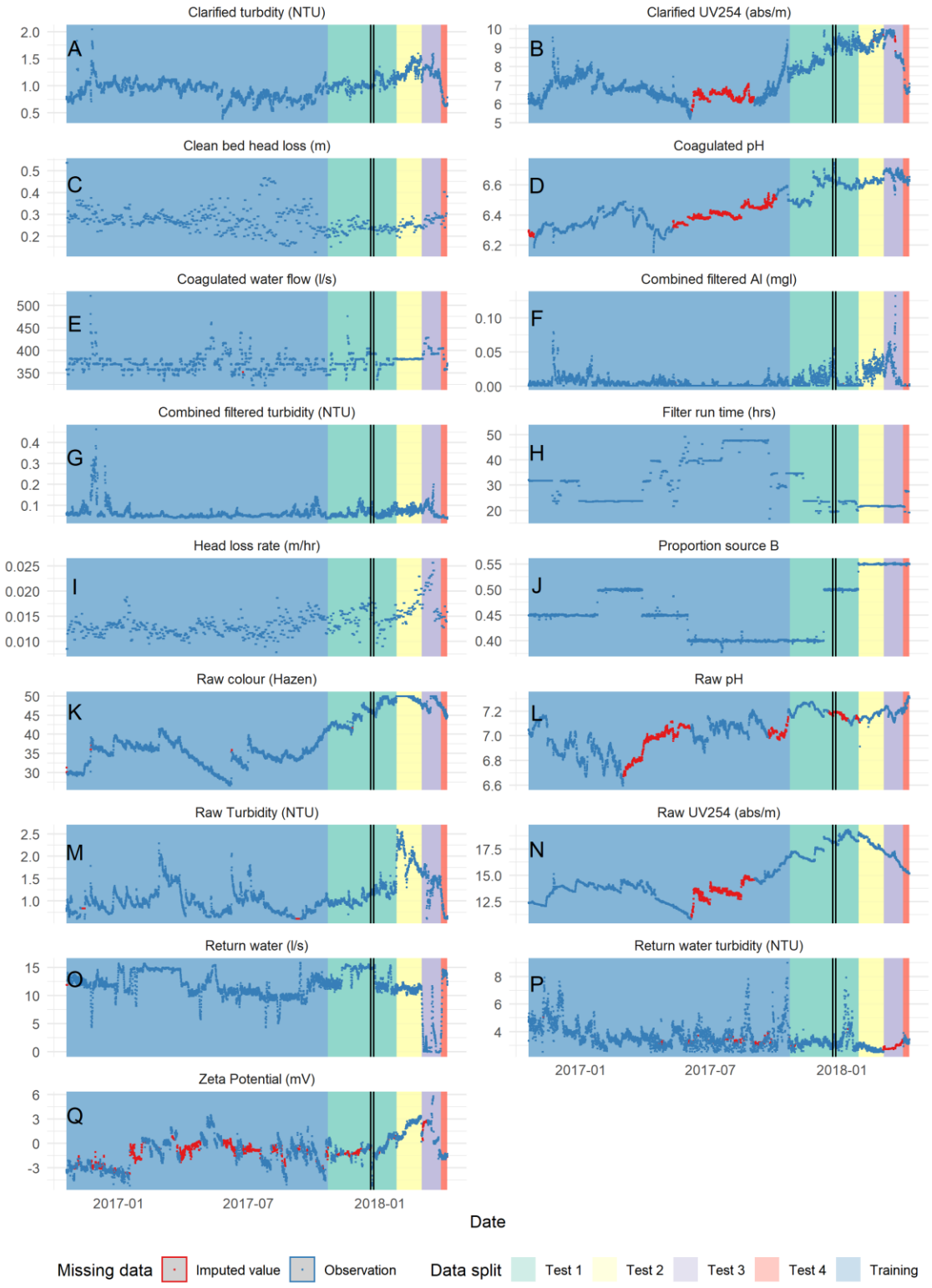

Figure 12 Change in the water quality variables over the study period. Red points show interpolated values. Data was divided into training and test data as indicated by background colour on plots. Vertical black lines indicate the period covered in the short term example used in Figure 13. For reference larger sized versions for each sub-plot are included in the supplementary materials (Individual water quality trends).

3.4.2 Short term example of sensitivity to zeta potential change

At certain points during the experimental period, the coagulation process appeared very sensitive to changes in zeta potential. For example, over a six-day period the coagulant dose was changed four times, resulting in changes in the zeta potential between 0 and -6 mV (Figure 13A). In turn, there were also changes in downstream water quality. As the zeta potential went from -6 mV to approaching neutral charge, there was a decrease in the clarified UV absorbance in the water (Figure 13B). A similar correlation was seen for the clarified turbidity and the aluminium in the filtered water over the study period (Figure 13B). The reduction in zeta potential between -6 and -1 mV corresponds to an observable drop of 2 UV absorbance units (m^{-1} or cm^{-1}) and the reduction of combined filtered turbidity from 0.12 to 0.06 (NTU). With three-hourly averaging, a quadratic linear model relating zeta potential to clarified UV_{254} absorbance explained 96% ($p<2.2x10^{-16}$) of the variation in clarified water UV absorbance. Testing of the residuals failed to demonstrate that there was no serial correlation in the residuals of this model (Durbin-Watson test 1.927, p = 0.292), suggesting that significance of p values would not be accurate. Though as autocorrelation at a single timestep was, for practical purposes, small (r = 0.035) it is reasonable to assume a significant relationship.

This example illustrates the value of online measurement of zeta potential, as opposed to bench-top measurements. This was because at charge-neutralisation zeta potential, the relative variance of the values observed is high (Figure_Apx 32). Zeta potential is derived from measurements of electrophoretic mobility. Therefore, at particle charges approaching zero charge the movement of charged particles reduces and therefore error in the measurement of that movement becomes larger in comparison. By taking frequent and repeated measurements of conditions, the precision of measurement approaching charge neutralisation conditions can be improved by averaging. This helps to distinguish the true signal from the noise of random measurement errors. The main confounding factor in this example is that no base is currently added to control pH independently of the coagulant dose. With additional suppression of the pH resulting from a higher dose of the coagulant it is possible that this may have resulted in a relative increase in the formation of coagulant species of higher charge resulting in a higher zeta potential value. However, as the coagulant used was a pre-hydrolysed PACl the speciation of hydrolysis products was

expected to be relatively insensitive to small changes in pH compared to alum. The slight drop in coagulation pH from 6.75 to 6.65 as a response to the increased coagulant dose was correlated with zeta potential and the downstream water quality measurements. This collinearity between covariates complicates the attribution of variance in downstream water quality to the zeta potential achieved in coagulation. Though there was evidently a drop in pH (from 6.75 to 6.65) with increasing coagulant pump stroke (60 to 69%), clarification performance approaches a plateau at a higher pH (pH 6.6) than would typically be considered optimal for charge-neutralisation with an alum-based coagulant (pH 6.1) (Bratby, 2016). Investigators have also observed that the pH of minimum solubility of PACl is typically higher than that of alum and that low temperature increases the pH at which minimum solubility occurs (Pernitsky and Edzwald, 2003).

Collinearities are inherent in studies observing working treatment process which cannot be experimentally manipulated, and in this example it is not possible to reliably resolve pH and zeta potential effects. Robustly drawing more general conclusions requires analysis of more data and appropriate modelling techniques to resolve the effects.

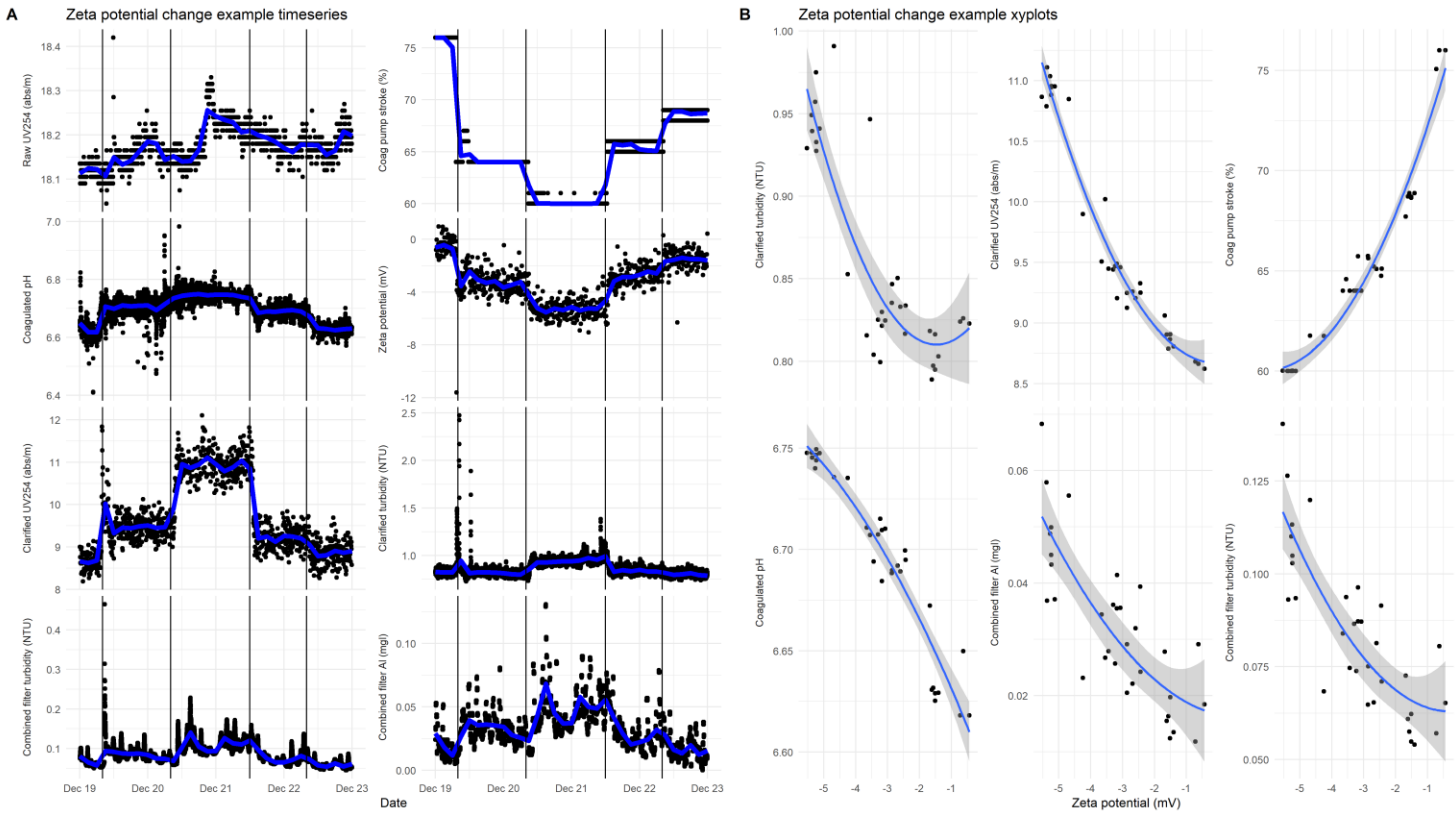

Figure 13 A short-term example of water quality change with zeta potential. Time series in part A show the changing conditions over time with coagulant dose alterations indicated by vertical lines. Part B shows three-hourly average data is then plotted with zeta potential on the x-axis and different water quality variables on the y axis. A fitted line shows the expected value of each variable based on a quadratic least squares linear model, the shaded region indicates the standard error. Other treatment conditions during this period were: Coagulated water flow 393 l/s, raw water turbidity: 1.2 NTU; colour: 45 °Hazen; temperature: 3.7°C.

3.4.3 Longer-term impact of varying zeta potential in context

When the data was considered and aggregated over a longer period, there were still apparent relationships between zeta potential and water quality parameters over the range of temperature and flow conditions experienced during the trial (Figure 14). Linear and quadratic least-squares regression lines illustrate the relationship between zeta potential between -6 to +4 mV and treatment performance as indicated by the proportional removal of UV254 absorbance (Figure 14 A), the clarified turbidity (Figure 14 B), residual aluminium (Figure 14 C) and combined filtered water turbidity (Figure 14 D). Significance figures and r squared (R^2) values are not quoted as these linear models do not effectively capture the serial dependence of measures or other important effects (such as temperature), rendering these statistics unreliable. Relative UV254abs removal in clarification appears to be greatest at a zeta potential between -1 & 0 mV, with apparent performance deteriorating exponentially with positive and negative zeta potential. As the zeta potential approached 0 mV, the removal of UV254 absorbance increased to a range between 45 and 80%. As the zeta potential became more positive, removal decreased to below 50% at +4 mV. Changes in clarified turbidity and residual aluminium reduced on average as the zeta potential approached zero and deteriorated in quality between 0 - 6 mV.

The relationships between zeta potential and downstream water quality variables were apparently affected by temperature and flow (Figure 14). An association with temperature was more clearly observable for the quality of clarified water than filtered water, with warmer temperatures resulting in improved organic matter removal and lower clarified water turbidity. The influence of temperature on process performance is not straightforward in this study because it is operational practice that the blend of water sources is adjusted seasonally such that the contribution of source B is greater at lower temperatures. Given that this was an observational study and confounding variables could not be experimentally controlled, statistical modelling was required to reliably estimate the effect of different environmental and operational variables.

Figure 14 Downstream water quality observed over the zeta potential range seen in this study.

Panel A shows the relative removal of UV254 absorbing material; B shows the clarified turbidity; C shows the residual aluminium in the filtered water, and; D shows the filtered turbidity. Temperature is indicated by the colour of the data points and plant flow is indicated by the size of the data points. The expected value of y from a quadratic linear model y = zeta + zeta^2 +E is indicated by the blue line in each plot with standard errors indicated by the shaded region. To further clarify the influence of small changes in zeta potential over this region each sub plot is reproduced at a larger size in Figure_Apx 32,Figure_Apx 33,Figure_Apx 34 & Figure_Apx 35 An alternative presentation of the data using boxplots of y over the range of zeta potentials observed are also plotted in Figure_Apx 36.

3.4.4 GAMM Models explaining downstream water quality

PC-GAMMS with all two-way interactions were fit relating principal components of raw water quality variables to the downstream water quality variables. These models are presented in Table 6. Pairwise dot plots and correlations between original explanatory variables and principal components are shown in supplementary materials (7.1B.6). Plots of the smooth functions of the models identified in Table 6 are presented in supplementary materials (7.1B.7).

The models provided a good explanation of Clarified UV absorbance (r^2 = 0.91) and reasonable explanation of filtered water Aluminium residuals (r^2 = 0.58) but relatively poor explanation of turbidity in the clarified and treated water (r^2 <0.2) over the training set (Table 7). More complex interaction structures failed to improve the explanatory power. Median absolute percentage error (MAPE) of the model fits indicate that typically the models explaining clarified turbidity, UV254 absorbance and combined and filtered water turbidity had small errors of 2-13% for training data 4 -30 % depending on test set. Training set MAPE for residual aluminium was higher (53% training, 75-187% in depending on test set) but the Root Mean Squared Error of 0.01 mg/l Al for training data and < 0.03 mg/l Al for test data suggests that the model is still potentially informative. As the residual aluminium levels were typically low, measurement error is likely to have influenced the data and provided an additional challenge to defining an effective model.

The reduced model performance between coagulated and filtered water is likely due to additional variance associated with the condition and control of the filters during the investigation period which were less effectively captured in the independent variables used to build the models. The case study WTW was known to have issues with filter washing performance and hydraulic control (Upton *et al.*, 2017). Poor model fitting and predictive performance of the clarified water turbidity when compared to UV absorbance is potentially attributable to a more complicated mechanism controlling the variation in turbidity or measurement interference. Clarified water turbidity values did appear to demonstrate some relationship with sample flow rate which had some reliability issues. UV instrumentation was installed for the purpose of this investigation whereas clarified water turbidity instruments were pre-existing instruments linked to the WTW control system and telemetry alarms.

Table 6 PC GAMM regression table showing model coefficients and (standard errors)

Summary of PC-GAMMs

	Downstream water quality models			
	$\log_e$ Clarified Turbidity (NTU)	Clarified UV254 (abs/m)	$\log_e$ Filtered Turbidity (NTU)	$\log_e$ Filtered Al (mg/l)
	(1)	(2)	(3)	(4)
X(Intercept)	-0.116***	6.690***	-2.834***	-5.766***
	(0.029)	(0.016)	(0.040)	(0.050)
S(PC1)	-0.030**	-0.146	0.116*	-0.431***
	(0.013)	(0.102)	(0.061)	(0.048)
S(PC2)	0.058***	0.131***	0.009	-0.134***
	(0.012)	(0.021)	(0.021)	(0.049)
S(PC3)	-0.006	0.057***	0.022***	0.204***
	(0.004)	(0.020)	(0.008)	(0.028)
S(PC4)	-0.014***	-0.059***	-0.019*	-0.088***
	(0.005)	(0.011)	(0.010)	(0.033)
S(PC5)	0.010**	0.082***	-0.018	0.042
	(0.005)	(0.011)	(0.029)	(0.035)
S(PC6)	0.007**	0.034	0.018***	0.121***
	(0.003)	(0.034)	(0.006)	(0.022)
Ti(PC1,PC2)	-0.063	-0.416	0.070	0.509
	(0.187)	(0.949)	(0.399)	(0.849)
Ti(PC1,PC3)	-0.048	1.111***	0.459***	2.105***
	(0.049)	(0.226)	(0.173)	(0.385)
Ti(PC1,PC4)	-0.035	-0.655***	0.079	0.220
	(0.094)	(0.240)	(0.188)	(0.680)
Ti(PC1,PC5)	0.182	-0.032	-0.027	-0.545
	(0.183)	(0.492)	(0.196)	(0.661)

Ti(PC1,PC6)	-0.127**	1.076***	0.158	0.941***
	(0.056)	(0.266)	(0.099)	(0.365)
Ti(PC2,PC3)	-0.253***	0.002	0.152	0.039
	(0.057)	(0.355)	(0.116)	(0.463)
Ti(PC2,PC4)	-0.267**	2.151***	0.044	0.220
	(0.119)	(0.408)	(0.164)	(0.578)
Ti(PC2,PC5)	0.121	-0.282	0.457*	0.217
	(0.226)	(0.434)	(0.249)	(0.630)
Ti(PC2,PC6)	0.033	0.158	-0.077	0.584
	(0.073)	(0.383)	(0.103)	(0.410)
Ti(PC3,PC4)	-0.245***	-0.075	0.014	-0.013
	(0.068)	(0.389)	(0.116)	(0.565)
Ti(PC3,PC5)	-0.065	0.577*	-0.169	-0.141
	(0.084)	(0.332)	(0.108)	(0.538)
Ti(PC3,PC6)	-0.072**	0.581***	-0.051	0.433
	(0.031)	(0.218)	(0.078)	(0.455)
Ti(PC4,PC5)	-0.007	0.587***	0.011	0.373
	(0.085)	(0.219)	(0.155)	(0.568)
Ti(PC4,PC6)	-0.045	0.946**	-0.056	0.330
	(0.048)	(0.456)	(0.092)	(0.394)
Ti(PC5,PC6)	-0.073	-1.108***	-0.190*	-0.655
	(0.048)	(0.283)	(0.114)	(0.472)
Observations	2,911	2,911	2,911	2,911
Log Likelihood	5,070.551	1,812.073	3,000.303	-1,308.570
Akaike Inf. Crit.	-10,021.100	-3,504.145	-5,880.606	2,737.139
Bayesian Inf. Crit.	-9,662.526	-3,145.570	-5,522.031	3,095.714
Note:	*p<0.1**p<0.05***p<0.01			

Table 7 Summary table of model performance summary statistics on training set and 4 periods of test data. Error statistics include root mean squared error (RMSE), r^2 (RSQ) and median absolute percentage error (MAPE).

Training & test set model performance statistics

	Model	Training set			Test set 1			Test set 2			Test set 3			Test set 4		
	Error Structure	RMSE	RSQ	MAPE	RMSE	RSQ	MAPE	RMSE	RSQ	MAPE	RMSE	RSQ	MAPE	RMSE	RSQ	MAPE
Clarified Turbidity (NTU)	AR1	0.16	0.07	13	0.15	0.21	12	0.42	0.49	31	0.29	0.45	17	0.12	0.81	14
Clarified UV254 (abs/m)	AR1	0.17	0.91	2	0.72	0.63	6	0.64	0.51	5	1.92	0.18	11	0.54	0.78	4
Filtered water Al (mg/l)	AR1	0.01	0.58	53	0.01	0.19	76	0.02	0.44	86	0.03	0.06	75	0.00	0.03	187
Combined filtered turbidity (NTU)	AR1	0.03	0.17	13	0.02	0.16	16	0.02	0.07	16	0.03	0	33	0.01	0.38	30

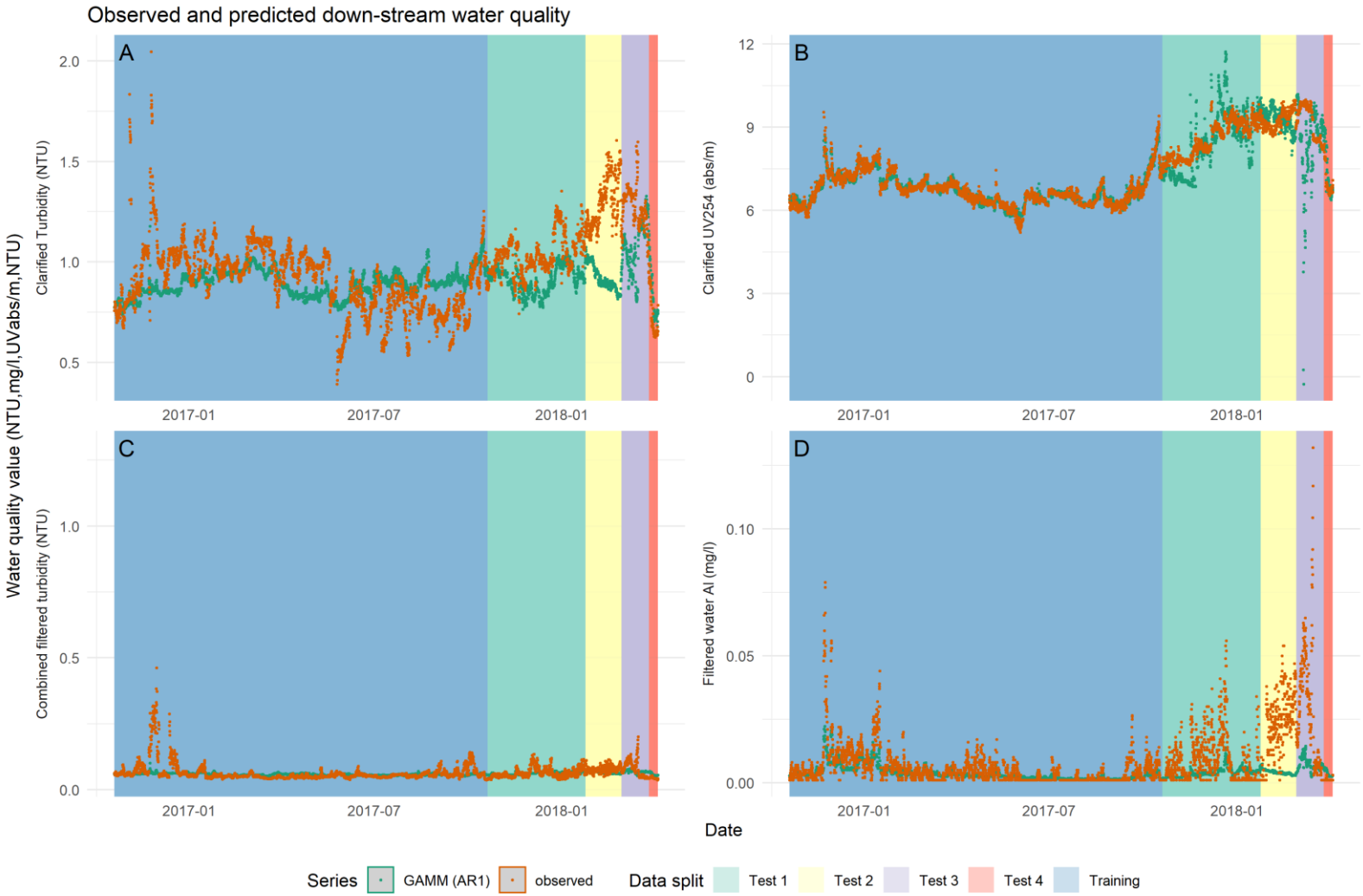

Figure 15 Observed and predicted values of downstream water quality variables using PC-GAMMs. A: clarified turbidity, B: UV254 absorbance, C combined filtered turbidity, D bottom right filtered water aluminium. Series are split into training data and test data 1-4.

When the models from the first year's data were applied to the test set, the performance was varied between the different models and the period of operation over which conditions were predicted. The test data was split into four parts as changing operational practice resulted in variation in predictive performance (Figure 15). Conditions during the first test set 1, shaded green, were most similar to those seen during the training period in blue.

GAMMs predicting clarified turbidity, filtered water turbidity and the relative removal of UV absorbing species showed relatively good performance in terms of MAPE at 16% or below, but could account for only one fifth of the variance in turbidity in the clarified or filtered water over this period. The r^2 of the GAMM predicting clarified UV absorbance was comparatively good at 0.63 (Table 7).

During test set two, the blend of water sources changed, with an increased proportion of source B (55%) than was observed during the model training period, and the temperature was consistently low (<4 °C). The zeta potential was increasingly positive over this period potentially indicating coagulant overdose, whilst the coagulation pH at 6.6, was higher than during the training period. Prediction performance for clarified turbidity was poor during this period with an RMSE 0.42 NTU reflecting that the negative impact of re-stabilisation was not adequately captured in the predictive model. Similarly predicted filtered water aluminium was lower than that observed RMSE 0.02. Prediction errors of clarified UV254 absorbance remained low during this period (MAPE 5%) but the r^2 (0.51) was also reduced.

Test set three covers an extended period where supernatant return to the head of works was suspended. There were no equivalent conditions which were encountered during the first year of the investigation during which the model was trained. This is reflected in the poor r^2 values (0.45 clarified turbidity, 0.18 clarified UVabs, 0.06 residual Aluminium and 0 filtered water turbidity). There is an apparent impact from the recycle flow which could be estimated over a certain range of flows and conditions within the training data but this did not extend well to flows stopping altogether. The poor predictive performance is illustrative of some of the challenges inherent in building predictive models for automatic coagulation control. Conditions in test set four had deviated so far from those observed during model training that the modelled

relationship between coagulation conditions and treatment performance was no longer applicable.

Test set four covers the period after the supernatant return flow was restored, five months after the last measurement used to fit the GAMM models During test period four, the coagulation pH (6.6 - 6.7) and contribution of source B (55%) was higher than at any point during the period used to fit the model. However, prediction performance was good indicating the models were approximating the performance of the treatment processes reasonably well during this time (RMSE: 0.12 NTU clarified, 0.01 NTU filtered, 0.00 mg/l filtered Al and 0.54 UV254 abs/m Table 7).

Broadly, in terms of explanatory and predictive performance, the models relating coagulation conditions to clarified water UV absorbance appears to be useful and of interest. Uncontrolled sources of variance within the filters and instrument issues mean that modelling of the turbidity or filtered water aluminium data was not on the whole effective or useful. A further challenge to predictive performance was an underlying change in the chemistry and operational regime of the process between the training and test periods. The test period was characterised by higher pH in the raw (pH 7.2) and coagulated water (pH 6.6), higher UV absorbance (15-18 abs/m) in the raw water, a typically positive zeta potential and periods with interrupted supernatant return. For much of the test period, the blend of water treated was different to that treated during the training period. This meant that the colloid concentration, as inferred from the water UV absorbance and turbidity, were higher in the test period than much of the training period. Greater colloid concentrations are likely to have resulted in a wider operational zeta potential window, and variations in particle separation performance arising in downstream processes are likely to have been more significant. It appears that the coagulation regime at this WTW varies in the extent to which it relies on charge neutralisation and adsorption regimes and there was a shift towards reliance on adsorption during the test period which could not be effectively modelled using the training data.

A further development of this investigation as it progressed, was that when it became clear that the process was sensitive to relatively small drops in zeta potential, to values below -3 mV, the operation of the plant was changed to maintain a zeta potential above -3 mV after January 2017 (Figure 12). Goodheart’s law suggests that when a measure

becomes a target it ceases to become a good measure. Improved operational practice in the light of this new information reduced the amount of variance in coagulation performance, reducing the opportunity to model the influence of variation in zeta potential.

3.4.5 Simulations from GAMM models explaining treatment performance

Where GAMM models of the process could be shown to provide a good explanation of the treatment system they were then used to isolate and present the effects of interest. Model simulations of different water quality and operational conditions were used to aid interpretation and facilitate inference about relationships between coagulation and the performance of the case study WTW. Simulations were conducted to illustrate the influence of zeta potential and coagulation pH on downstream water quality under different conditions observed within the training period for the coagulation models. The modelled relationship between of zeta potential (-6 and +3) and clarified UVabs is presented over a 5x2 matrix of conditions in (Figure 16). The thicker line in the middle shows the predicted mean value with the shaded area denoting the 95% confidence interval. On this basis conditions with non-overlapping confidence intervals are observed to have a statistically significant difference in performance. Varying pH is presented at 6.2 and 6.5 as different colours. Temperature 0.4 temperature (4°C and 14°C), flow (350 & 380 l/s), raw UV (12 & 15 abs/m) turbidity (0.8 & 1.2 NTU) are presented as a matrix of sub-plots A:P. Flow and temperature conditions vary between the columns and colloid concentrations and composition varies between the rows.

At lower raw UV254 absorbance (12 abs/m) and a pH of 6.5 if the temperature is low (4°C) or the flow is high (380 l/s) there was a significant reduction in clarified UV254 as zeta potential increases over the range of -6 to 2 mV (Figure 16: A,C,D,I,K &L). This suggests when primary colloid concentrations are low, and the pH is high, adsorption and enmeshment mechanisms are important and the increasing dose associated with increasing zeta potential is resulting in improved treatment performance as a result of an elevated collision rate. At pH 6.5 and a temperature of 14°C and a flow rate of 350 l/s there appears to be no significant variation in clarified UV absorbance over the zeta potential range observed for any of the variations in colloid concentrations (Figure 16: B,F,J,H). This suggests that with longer flocculation

times and higher temperatures, coagulation performance is no longer collision-limited and does not benefit from additional coagulant particles. At the lower pH of 6.2 and lower raw water UV254 concentrations (12 abs/m), change in clarified water UV254 absorbance over the range of zeta potentials observed was not typically significant. At pH 6.2 reduction in clarified UV254 between -6 and 3 mV occurred either at relatively higher raw water UV254 and turbidity (15 abs/m & 1.2 NTU) (Figure 16: M,N,O&P) or at high UV254 and high temperature (Figure 16: F &H). This would suggest that an increased coagulant to NOM ratio, captured by the change in zeta potential, improved floc strength or improved adsorption in a way that was in some way moderated by temperature. Previous investigators have observed improved floc strength with an increased coagulant to NOM ratio (Sharp *et al.*, 2006). Some patterns in mean clarified UV absorbance indicated a potential relationship between zeta potential and treated water quality when the water was colder (4°C) and primary colloid concentrations were lower (UV 12 abs/m). However, sparsity of the data under these conditions led to large confidence intervals and therefore the trend was not significant (Figure 16: A, I and K). This was a key draw-back of completing the investigation on a live WTW, where conditions anticipated to cause treatment issues were not readily captured. Variation in zeta potential between -6 and +3 mV was not observed to significantly change the performance of charge neutralisation coagulation on a consistent basis but variation in treatment performance in this region appears to be correlated with likely changes in alternative adsorption and enmeshment mechanisms within the charge neutralisation window.

Variation in clarified and filtered water turbidity over the range of zeta potentials observed is presented in Figure_Apx 49 and Figure_Apx 50 but no statistically significant relationship was observed. This may have been as a result of a combination of poor data quality for the clarified filter model and the mis-specification of the model. It is likely that this could indicate variation in treated water turbidity resulting from small changes in zeta potential were relatively insignificant when compared to other causes of variation within this system.

Variation in filtered water aluminium is presented in Figure 17. Under most conditions there was an apparent trend in reduced residual aluminium with increased zeta potential, however under most conditions presented this trend was slight with the average remaining <10µg/l over the range observed. When the water was cold (4°C)

increased residual aluminium in the filtered water at negative zeta potentials was most apparent, though expected average values remained < 15µg/l.

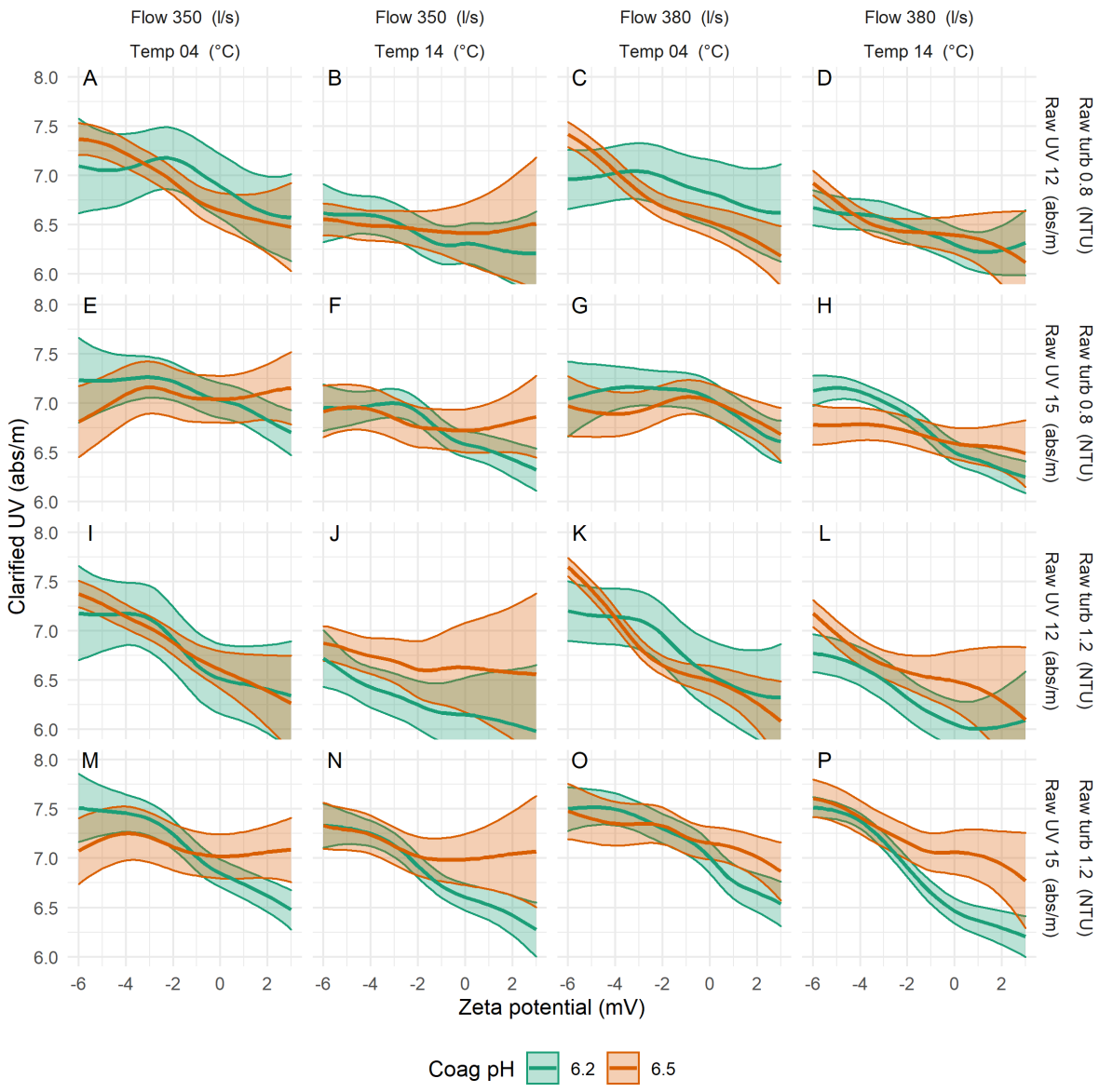

Figure 16 Simulation results from PC-GAMM model showing mean and 95% confidence interval predictions for clarified UV (abs/m) over a range of zeta potentials (-6 to +3) at pH 6.2 & 6.5 at different temperature (4°C & 14°C), flow (350 & 380 l/s), raw UV (12 & 15 abs/m) turbidity (0.8 & 1.2 NTU) other variables were held constant supernatant return flow (15 l/s) supernatant turbidity (3.5 NTU) filter run time (30 hrs).

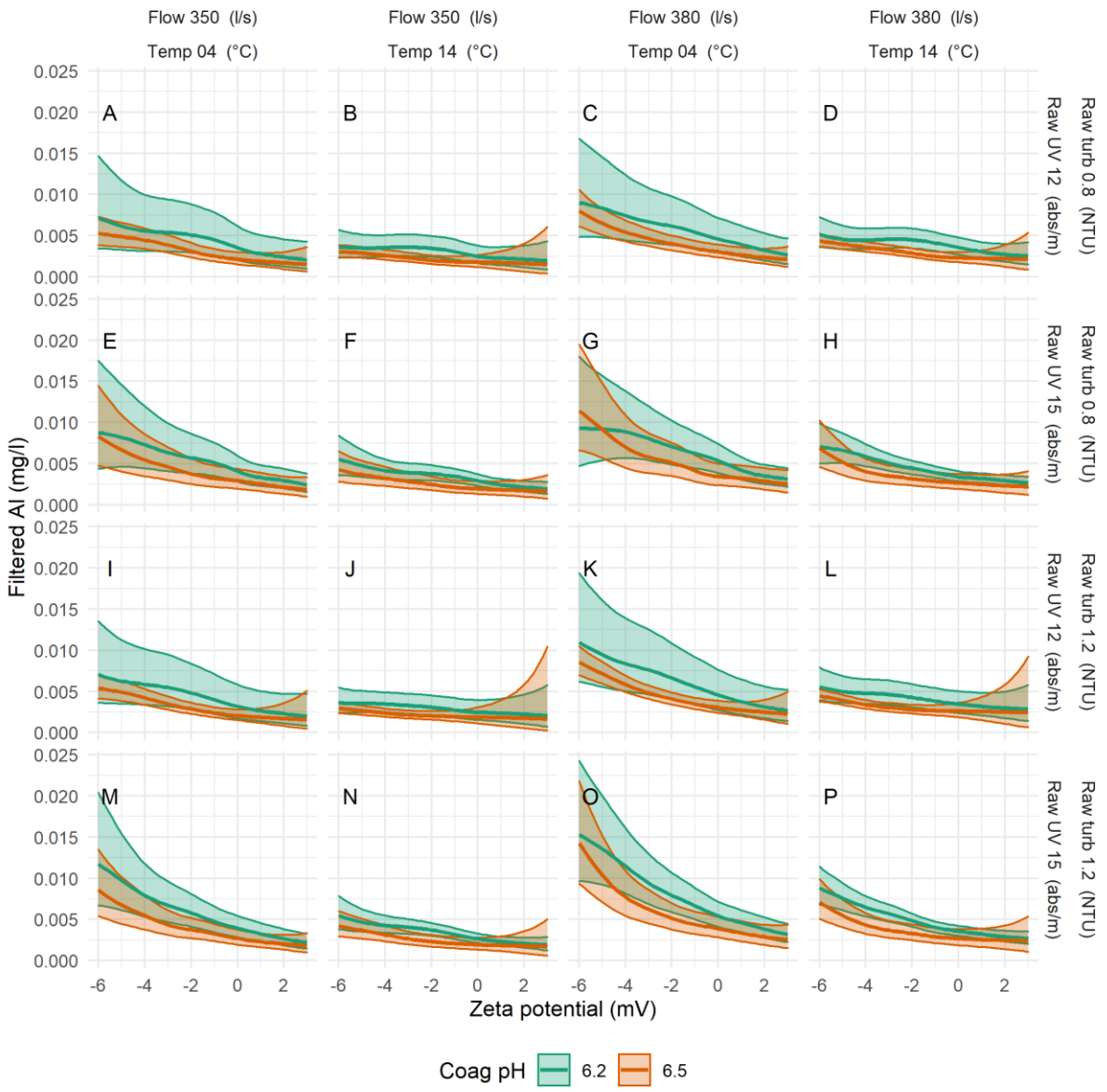

Figure 17 Simulation results from PC-GAMM model showing mean and 95% confidence interval predictions for filtered water residual aluminium (mg/l) over a range of zeta potentials (-6 to +3) at pH 6.2 & 6.5 at different temperature (4°C & 14°C), flow (350 & 380 l/s), raw UV (12 & 15 abs/m) turbidity (0.8 & 1.2 NTU) other variables were held constant supernatant return flow (15 l/s) supernatant turbidity (3.5 NTU) filter run time (30 hrs)

.

3.4.6 Jar testing to understand influence of temperature and mixing conditions at optimal dose

Modelling of WTW performance indicated that temperature, collision rate, hydraulic loading and shear were important factors in understanding the effective operational window for zeta potential of a given water treatment system. Jar testing of the two source waters at different temperatures and mixing conditions with a consistent dose showed the importance of mixing on effective floc formation at WTW A. Coagulation and flocculation testing of the two water sources showed that the influence of temperature and mixing on flocculation performance, as measured by D_{50} floc size, was contingent on the raw water being treated. Literature suggests that a floc size between 10 to 30 µm is required for effective DAF operation (Edzwald, 1995). Flocculation performance for the lower turbidity and DOC source A varied with temperature and mixing conditions but for source B, flocculation varied with mixing conditions but not temperature.

The mean and range of D_{50} floc sizes changed over time during the jar tests (Figure 18). At high temperatures and a floc speed of 20 RPM the floc formed from source A floc continued to grow for 15 minutes stabilising at 40 µm with or without rapid mixing. At high temperatures and a floc speed of 50 RPM, floc growth had stopped after 10 minutes, plateauing at a D_{50} size of 24µm when the rapid-mix was deployed. Without the rapid mix, floc size reached 15µm. This suggests that a looser floc structure formed when the water temperature was higher which was weaker and growth was shear limited. Flocculation of source A at low temperatures was faster at a higher flocculant mixing speed of 50 RPM, reaching 24µm in 10 minutes. At 20 RPM with no rapid mix, floc formation was slower but ultimately reached the D_{50} of 26µm after 14 minutes. If an initial rapid mix had been used, the final floc size was larger at 33µm. This suggests that flocs from source A at low temperature were sensitive to both collision rate and shear limitations to floc growth.

Source B showed more rapid floc growth compared to source A, growing to between 28-60µm in 8 minutes for all conditions tested. This was likely to result from the greater collision rate in a system with greater numbers of primary,

coagulant and precipitate particles. Limited mixing resulted in the largest flocs from source B at all temperature conditions (60-67 µm). At 50 rpm, the D_{50} for flocs formed in source B typically remained below 40µm. The reduced size of flocs at a higher mixing rate indicates that growth was shear limited under all temperature conditions.

The results of linear regression models relating floc size to temperature and mixing conditions show that for source A, low temperature resulted in a significantly reduced floc size ($p < 0.01$) at all time points with the D_{50} estimated to be between 11-19 µm smaller at 7.5 °C than at 19.5 °C depending on the flocculation time (Table 8). Source B, however, showed no significant impact of temperature on floc size (Table 9). Previous investigations into the impact of temperature on coagulation & flocculation processes have reported smaller floc and worse performance at lower temperatures (Fitzpatrick, Fradin and Gregory, 2004; Morris and Knocke, 1984; Xiao *et al.*, 2008a). These studies have studied the flocculation of synthetic kaolin suspensions and have suggested that temperature effects most significantly impact upon enmeshment mechanisms of aggregation (Morris and Knocke, 1984). Studies have also shown that pre-hydrolysed coagulants such as PACl are less sensitive to low temperatures than traditional hydrolysing metal salts (Fitzpatrick *et al.*, 2004; Jiang and Graham, Graham and Harward, 1996; Van Benschoten and Edzwald, 1990). This would suggest that treatment of source A is more reliant on bridging and enmeshment mechanisms and, for that reason, is more sensitive to temperature whereas treatment of source B can be achieved effectively with charge – neutralisation alone.

Effective rapid mixing is commonly regarded as essential for the effective operation of coagulation (Bratby, 2016). However, Edzwald (2013) concluded that rapid mixing was not necessary for sweep flocculation but was required for effective charge neutralisation. This has been questioned by other investigators who have observed that sweep flocculation and enhanced coagulation could be optimised at low mixing energy regimes (Vadasarukkai and Gagnon, 2015). Rapid mixing did not appear to provide a significant overall benefit to the

flocculation in jar tests of source A using flocculation times of 5, 10 and 15 minutes (Table 8, models 1-3). However, there was significant ($p < 0.05$) but slight benefit associated with rapid mixing at 20 minutes floc time, increasing floc size by 3.4 µm (13%). This small increase may be associated with more effective dispersal or stronger floc structural characteristics initiated in the initial high shear environment. Rapid mixing appeared to result in reduced floc size in jar tests of source B water, with a 9µm reduction ($p<0.05$) in floc size after 15 minutes flocculation time when rapid mixing was deployed (Table 9). This may indicate that rapid mixing for ten second at 200 RPM within a jar test may have resulted in some irreversible floc breakage on exposure to increased shear rates for floc formed from source B. This may indicate that the relatively high DOC of source B resulted in a weaker floc structure. Relatively high NOM concentration and NOM to coagulant ratio has been previously demonstrated to increase the fragility of flocs (Jarvis, *et al.*, 2005; Jarvis *et al.*, 2005).

An increase in jar test flocculant mixing speed from 20 to 50 rpm was associated with significantly ($p<0.01$) reduced floc size for flocculation times of ten minutes or greater in source A and source B. After 10 minutes, an increase in flocculant mixing from 20 to 50 RPM was associated with a 15µm reduction in the D_{50} floc size. The impact of mixing on flocs from source A was more complicated as it was contingent upon temperature. At 7.5 °C after 10 minutes flocculation at 50 RPM this was associated with flocs 9 µm larger than those seen at 20 rpm. However, after 20 minutes the 50 RPM mixing regime was associated with flocs 1µm smaller than at 20 RPM. This indicates that at low temperatures more mixing of source A earlier in the flocculation process provided some benefit from a higher collision rate, but later contributed to shear-limiting of floc size. At higher temperatures for source A, and all temperatures for source B, the increased mixing rate was not observed to provide a benefit earlier in flocculation and was only associated with greater shear limiting of floc size. Overall, the greater variation in floc size seen for source B was likely to arise from the greater growth potential associated with higher solids in combination with a greater sensitivity to shear between 20-50 RPM.

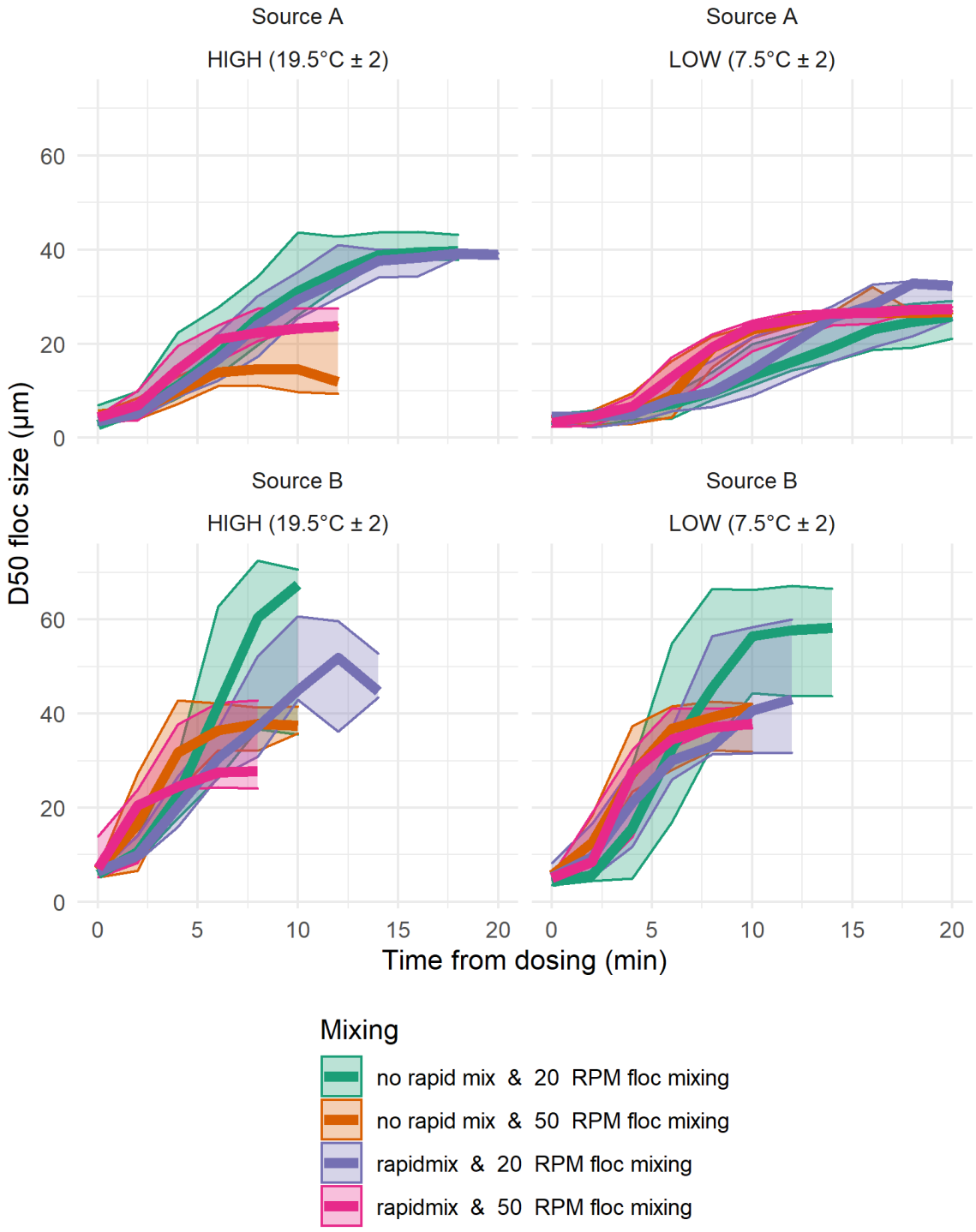

Figure 18 D_{50} floc growth data for different temperatures at different flocculant mixing speeds and with and without rapid mixing. Thick lines show median value of the D_{50} floc across all replicates with shaded areas showing range of observed D_{50} values. Individual floc growth curves under different jar test conditions are shown in Figure_Apx 51.

Table 8 Linear models of D_{50} floc size for jar tests of source A. Coefficient estimates are shown with standard errors in brackets.

	Dependent variable: D_{50} (µm)			
	Floc size at time intervals in jar test at fixed dose			
	5 minutes	10 minutes	15 minutes	20 minutes
	(1)	(2)	(3)	(4)
LOW (7.5°C ± 2)	-7.665*** (1.141)	-17.511*** (2.135)	-15.932*** (2.260)	-11.754*** (2.118)
Rapid mix	-1.359 (1.611)	1.683 (1.512)	2.315 (1.600)	3.428** (1.500)
50 RPM floc mixing	-1.330 (1.611)	-11.118*** (2.135)	-18.109*** (2.260)	-19.047*** (2.118)
Rapid mix:50 RPM floc mixing	5.084** (2.275)			
LOW (7.5°C ± 2):50 RPM floc mixing		19.879*** (3.016)	21.641*** (3.192)	18.325*** (2.992)
Constant	14.833*** (1.273)	30.525*** (1.738)	37.526*** (1.839)	37.828*** (1.724)
Observations	26	26	26	26
R^2	0.725	0.771	0.785	0.804
Adjusted R^2	0.672	0.728	0.744	0.767
Residual Std. Error (df = 21)	2.892	3.833	4.057	3.802
F Statistic (df = 4; 21)	13.814***	17.701***	19.203***	21.562***
Note:	*p<0.1,**p<0.05***p<0.01			

Table 9 Linear models of D_{50} floc size for jar tests of source B. Coefficient estimates are shown with standard errors in brackets.

	Dependent variable: D_{50} (µm)		
	Floc size at time intervals in jar test at fixed dose		
	5 minutes	10 minutes	15 minutes
	(1)	(2)	(3)
LOW (7.5°C ± 2)	-4.387 (2.891)	-0.866 (3.879)	-0.282 (3.458)
Rapid mix	-2.123 (2.875)	-7.419* (3.858)	-9.238** (3.439)
50 RPM floc mixing	4.570 (2.891)	-14.884*** (3.879)	-15.401*** (3.458)
Constant	31.168*** (2.938)	55.347*** (3.943)	56.445*** (3.515)
Observations	26	26	26
R^2	0.206	0.456	0.552
Adjusted R^2	0.098	0.382	0.491
Residual Std. Error (df = 22)	7.330	9.836	8.769
F Statistic (df = 3; 22)	1.905	6.140***	9.034***
Note:	*p**p***p<0.01		

3.4.7 Implications for process scientists and engineers

At the case study WTW of the sensitivity of treatment to slight changes in zeta potential were observed and a specific short-term example has been presented, where a target zeta potential of 0 mV would be optimal for removal of DOC and a small deviation from that to -5mV resulted in deterioration in treated water quality. As pH was not independently controlled, the mechanism driving this performance change could not be identified. It could not be ruled out that changes in NOM structure occurred over the pH change observed and the resulting influence on adsorption and steric effects were responsible for changes in the

treatment performance. Conformations of humic acids have been observed to change with pH, resulting in an increase in adsorption sites, and therefore exerting a greater coagulant demand at higher pH (Davis and Edwards, 2014; Stumm and Morgan, 1996).

Rapid deterioration in treatment performance as zeta potential becomes positive has also been observed and is associated with transition from charge neutralisation to colloidal re-stabilisation (Stumm and O'Melia, 1968). Similarly, a narrower window for destabilisation with decreasing coagulant and colloid concentration is a well established phenomenon (Stumm and O'Melia, 1968). This explanation was not sufficient to explain the variation in treatment performance observed at the case study WTW. Presenting data over the period of the investigation showed that as zeta potential deviated from 0 mV deterioration in treated water quality was more likely. However, this deterioration was inconsistent and moderated by other factors including temperature and flow. Prior to this work, the challenge has been to understand what controls the size of the operational window for zeta potential and how this can be manipulated to improve the robustness of treatment (Jefferson *et al.*, 2004). This investigation has demonstrated that online zeta potential measurement and appropriate modelling techniques can be used to quantify how the effective operational window changes with prevailing conditions for a specific treatment system. This allows not only dose optimisation but identification of alternative mixing strategies to overcome treatment constraints.

It is typically understood that the minimum effective coagulant dose is determined stoichiometrically by the coagulant demand of NOM (Stumm and O'Melia, 1968). However, it is likely that the case study system was at times collision limited. In practical terms this means that floc size is constrained by too low a concentration of particles resulting in too few opportunities for the agglomeration of particles within the available retention time of the flocculator. Under collision limited conditions, increased concentrations of NOM have been associated with a reduction in the minimum effective coagulant dose as precipitated organic matter improves the collision rate (Shin, Spinette and O'Melia, 2008). It is therefore

possible that zeta potential variation, within what has previously been observed as the stable operational window, is caused by the collision rate from additional precipitated polymeric aluminium hydroxide and aluminium-NOM particles. If this is the case, the online zeta potential analyser is providing information which enables the optimisation of coagulation within a collision limited system by allowing an increase in the collision rate up until the boundary of the re-stabilisation zone is reached. Essentially this involves dosing beyond the point required by pure charge-neutralisation coagulation and increasing the number of particles with coagulant particles and additional precipitation of dissolved organic matter. Up until the point of zero charge there is a trade-off between collisions, adsorption and operational cost. At doses beyond the iso-electric point there is a trade-off between collision rate, treatment cost and re-stabilisation. Online zeta potential has been shown to be an informative operational aid for navigating this region.

Examining the marginal deterioration of flocculation rate of a low turbidity water at zeta potentials near 0 mV in a jar test is problematic. Not only are the incremental increases in coagulant concentration small, the region of interest for optimising charge-neutralisation coagulation systems is where the measurement error for electrophoretic mobility is greatest. However, the advantage of online measurement of zeta potential in this instance was in the collection of a much greater amount of data allowing an average to be taken of several samples and, with appropriate modelling of the treatment system, a more sensitive and informative measure of coagulation performance to be derived.

Jar testing provided some further evidence that variation in coagulation-flocculation performance was not controlled by dose alone. Under apparently collision limited conditions faster flocculant mixing increased the growth of flocs but ultimately resulted in shear-limiting of floc size. This is likely to mean that the optimal mixing regime would be contingent upon the quality of water treated and the retention time within the flocculation tanks. The data from jar testing also supports observations from the modelling of the full-scale process showing that the combination of low temperature, low particle concentration and limited

flocculation had the potential to negatively affect the performance of flocculation. This has been previously shown to affect the performance of downstream separation processes (Morris and Knocke, 1984).

In the well mixed batch reactor conditions of the jar test, the growth of floc in source A was extended to as long as 20 minutes at cold temperatures under optimal charge conditions. This exceeded the available process time at the case study WTW. The jar testing results clearly reflect the justification for the operational decision to increase the proportion of source B during the winter due to the poor floc formation in source A which results in higher clarified water turbidity. However, jar tests also indicate that though benefits from the higher collision rate can be gained from using more of source B there is an apparent trade-off against solids loading and floc strength. Using more source B would result in a greater solids load of weaker floc and greater potential for shear in the DAF. These observations identify the potential opportunities to explore the use of polymer to improve floc strength during conditions of low coagulant: NOM ratios as well as nucleating particles to overcome collision limiting when treating low colloid concentrations at low temperatures.

It is likely that there are more complex physical mechanisms (collision and shear rates) driving turbidity variation in clarified water than can be measured by UV absorbance (a turbidity corrected measurement), which is likely to be more dependent upon adsorption mechanisms. This may explain why modelling of turbidity was less successful than clarified UV254 absorbance. The turbidity adjusted UV254 absorbance measurement would be sensitive to the adsorption of dissolved aromatic organic matter and would be less sensitive to the resultant particles. Turbidity measurements would be affected to a greater extent by primary particles, coagulant particles, precipitated NOM-coagulant complex particles and the fragmentation of flocs.

This investigation suggests that where there is an operational requirement to overcome complex raw water challenges, or other process constraints, zeta potential can provide a valuable source of data to aid understanding of coagulation performance within a nominally charge-neutralisation regime. Bench

scale methods for optimization, such as jar testing, are time consuming and slow. Jar testing in a small completely stirred tank reactor can also be a poor representation of the hydraulics and shear forces at play in full scale treatment systems where the combination of non-ideal plug flow and stirred tank reactors may be present. The methods presented in this paper suggest that process modelling using online zeta potential may allow treatment plants to be more productive and adapt operations to meet challenges from changing raw water quality without building additional process capacity. Furthermore, in systems with low turbidity, the large number of replicate measurements that the online instrument provides allows greater precision when optimising charge neutralisation in collision limited low particle systems which exhibit greater sensitivity to changes in coagulation conditions.

3.5 Conclusions

- Online zeta potential enables increased frequency of monitoring of coagulation allowing improved precision which can facilitate operational insights when compared to bench testing for charge-neutralisation coagulation of low turbidity water sources.

- Online monitoring of zeta potential has shown that under certain conditions changing coagulant dose with resulting zeta potential suppression of between -4 to 0 mV can have a material impact on WTW performance and treated water quality. Though the methods used in this investigation could not confirm the mechanism driving this performance change, modelling of full scale and jar test data indicate that depending on prevailing conditions likely performance benefits resulted from increased collision rate, increased adsorption or improved floc strength.

- WTWs with shorter process residence times which experience colder waters and relatively low raw water particle concentration are likely to exhibit performance which is less robust in response to variation in zeta potential achieved in coagulation than other treatment systems. The improved precision of charge measurements provided by online zeta

potential measurements may facilitate greater coagulation efficiency in the charge neutralisation window. It is likely that this would be achieved through supplementary adsorption and bridging mechanisms. Improved precision (through averaging multiple measurements) of online monitoring compared to bench-top instruments would more effectively enable operators to prevent re-stabilisation.

- The sensitivity to zeta potential and the effective operational window for treatment and coagulant dose appears contingent upon collision rate. It is likely that this will have implications on the relative costs and benefits associated with using different charge measurements for optimising treatment. In treatment systems which are more robust to sub-optimal coagulation conditions streaming current is likely to be adequate, whereas in more sensitive systems the greater precision and interpretability of online zeta potential measurements are likely to provide an additional benefit.

- Using a PCA-GAMM model to relate online zeta potential measurements with other online quality and operational control measurements can enable the identification of the effective operational zeta potential window for a treatment system with a given prevailing water quality, operational constraints and treatment goals. This is particularly the case where conditions and constraints vary such that the optimal treatment strategy may change between charge-neutralisation and sweep-flocculation.

3.6 References

Barron, W., Murray, B. S., Scales, P. J., Healy, T. W., Dixon, D. R., & Pascoe, M. (1994). The streaming current detector: A comparison with conventional electrokinetic techniques. *Colloids and Surfaces A: Physicochemical and Engineering Aspects*, *88*(2-3), 129-139.

Black, A. P., & Willems, D. G. (1961). Electrophoretic studies of coagulation for removal of organic color. *Journal of the American Water Works Association*, *53*(5), 589-604.

Bratby, J. (2016). *Coagulation and Flocculation in Water and Wastewater Treatment*–3rd edn. London: IWA Publishing.

Brink, D. R., Choi, S. I., Al-Ani, M., & Hendricks, D. W. (1988). Bench-Scale Evaluation of Coagulants for Low Turbidity Water. *Journal of the American Water Works Association*, *80*(4), 199-65.

CRAN. (2013) *The R Project for Statistical Computing*., *The R Project for Statistical Computing.* available at http://www.r-project.org

Davis, C. C., & Edwards, M. (2014). Coagulation with hydrolyzing metal salts: mechanisms and water quality impacts. *Critical Reviews in Environmental Science and Technology*, *44*(4), 303-347.

Dentel, S. K., & Kingery, K. M. (1988). *An evaluation of streaming current detectors*. Denver: AWWA Research Foundation.

Derjaguin, B., & Landau, L. (1993). Theory of the stability of strongly charged lyophobic sols and of the adhesion of strongly charged particles in solutions of electrolytes. *Progress in Surface Science*, *43*(1-4), 30-59.

Edzwald, J. K. (1995). Principles and applications of dissolved air flotation. *Water Science and Technology*, *31*(3-4), 1-23.

Edzwald, J. K. (2013). Coagulant mixing revisited: theory and practice. *Journal of Water Supply: Research and Technology—AQUA*, *62*(2), 67-77.

Fitzpatrick, C. S. B., Fradin, E., & Gregory, J. (2004). Temperature effects on flocculation, using different coagulants. *Water Science and Technology*, *50*(12), 171-175.

Golea, D. M., Upton, A., Jarvis, P., Moore, G., Sutherland, S., Parsons, S. A., & Judd, S. J. (2017). THM and HAA formation from NOM in raw and treated surface waters. *Water Research*, *112*, 226-235.

Hastie, T., & Tibshirani, R. (1986). Generalized Additive Models. *Statistical Science*, *1*(3), 297-310.

Hendricks, D. W. (2006). *Water Treatment Unit Processes Physical and Chemical*; Boca Raton, Florida. CRC Press.

Huck, P.M., Emelko, M.B., Coffee, B.M.M, Maurizio, D.D. and O'Melia, C.R. (2001). *Filter operation effects on pathogen passage*. Denver: AWWA Research Foundation and American Water Works Association.

James, G., Witten, D., Hastie, T., & Tibshirani, R. (2013). *An introduction to statistical learning*. New York: Springer.

Jarvis, P., Jefferson, B., & Parsons, S. A. (2005a). Breakage, regrowth, and fractal nature of natural organic matter flocs. *Environmental Science & Technology*, *39*(7), 2307-2314.

Jarvis, P., Jefferson, B., & Parsons, S. A. (2005b). How the natural organic matter to coagulant ratio impacts on floc structural properties. *Environmental Science & Technology*, *39*(22), 8919-8924.

Jefferson, B., Sharp, E. L., Goslan, E., Henderson, R., & Parsons, S. A. (2004). Application of charge measurement to water treatment processes. *Water Science and Technology: Water Supply*, *4*(5-6), 49-56.

Jiang, Q. J., & Graham, N. J. D. (1996). Coagulation of upland colored water with polyferric sulphate compared to conventional coagulants. *Journal of Water Supply: Research and Technology – AQUA 4*(3), 143-154.

Kuhn, M. (2011). caret: Classification and Regression Training. R package version 6.0-78. https://github.com/topepo/caret/

LeChevallier, M. W., Evans, T. M., & Seidler, R. J. (1981). Effect of turbidity on chlorination efficiency and bacterial persistence in drinking water. *Applied and Environmental Microbiology*, *42*(1), 159-167.

Morris, J. K., & Knocke, W. R. (1984). Temperature effects on the use of metal-ion coagulants for water treatment. *Journal of the American Water Works Association*, *76*(3), 74-79.

O'Melia, C. R. (1969). A review of the coagulation process. *Public works*, *100*(5), 87-98.

Pernitsky, D. J., & Edzwald, J. K. (2003). Solubility of polyaluminium coagulants. *Journal of Water Supply: Research and Technology—AQUA*, *52*(6), 395-406.

Pilipovich, J. B., Black, A. P., Eidsness, F. A., & Stearns, T. W. (1958). Electrophoretic studies of water coagulation. *Journal of the American Water Works Association*, *50*(11), 1467-1482.

PostgreSQL Global Development Group. (2015) *PostgreSQL* 9.4. PostgreSQL Global Development Group,

Ratnaweera, H., & Fettig, J. (2015). State of the art of online monitoring and control of the coagulation process. *Water*, *7*(11), 6574-6597.

Sharp, E. L., Banks, J., Billica, J. A., Gertig, K. R., Henderson, R., Parsons, S. A., ... & Jefferson, B. (2005). Application of zeta potential measurements for coagulation control: pilot-plant experiences from UK and US waters with elevated organics. *Water Science and Technology: Water Supply*, *5*(5), 49-56.

Sharp, E. L., Banks, J., Billica, J. A., Gertig, K. R., Henderson, R., Parsons, S. A., ... & Jefferson, B. (2005). Application of zeta potential measurements for coagulation control: pilot-plant experiences from UK and US waters with elevated organics. *Water Science and Technology: Water Supply*, *5*(5), 49-56.

Sharp, E. L., Parsons, S. A., & Jefferson, B. (2006). Seasonal variations in natural organic matter and its impact on coagulation in water treatment. *Science of the Total Environment*, *363*(1-3), 183-194.

Shin, J. Y., Spinette, R. F., & O'melia, C. R. (2008). Stoichiometry of coagulation revisited. *Environmental Science & Technology*, *42*(7), 2582-2589.

Stekhoven, D.J. (2013). missForest: Nonparametric Missing Value Imputation using Random Forest. R package version 1.4. available at http://cran.r-project.org/web/packages/missForest/index.html.

Stumm, W. and Morgan, J.J. (1996) *Aquatic chemistry: Chemical equilibria and rates in natural waters*. 3rd edn. Chichester, UK: Wiley.

Stumm, W., & O'Melia, C. R. (1968). Stoichiometry of coagulation. *Journal of the American Water Works Association*, *60*(5), 514-539.

Tucker, I. M., Corbett, J. C. W., Fatkin, J., Jack, R. O., Kaszuba, M., MacCreath, B., & McNeil-Watson, F. (2015). Laser Doppler Electrophoresis applied to colloids and surfaces. *Current Opinion in Colloid & Interface Science*, *20*(4), 215-226.

Upton, A., Jefferson, B., Moore, G., & Jarvis, P. (2017). Rapid gravity filtration operational performance assessment and diagnosis for preventative maintenance from on-line data. *Chemical Engineering Journal*, *313*, 250-260.

Vadasarukkai, Y. S., & Gagnon, G. A. (2015). Application of low-mixing energy input for the coagulation process. *Water Research*, *84*, 333-341.

Van Benschoten, J. E., & Edzwald, J. K. (1990). Chemical aspects of coagulation using aluminum salts—I. Hydrolytic reactions of alum and polyaluminum chloride. *Water Research*, *24*(12), 1519-1526.

Verwey, E. J. W. (1947). Theory of the stability of lyophobic colloids. *The Journal of Physical Chemistry*, *51*(3), 631-636.

Wickham, H., Averick, M., Bryan, J., Chang, W., McGowan, L. D. A., François, R., ... & Yutani, H., (2019). Welcome to the tidyverse. *Journal of Open Source Software*, 4(43), 1686, https://doi.org/10.21105/joss.01686

Wood, S. N. (2017). *Generalized additive models: an introduction with R*. 2nd edn. London: CRC press.

Wood, S.N. (2011) Fast stable restricted maximum likelihood and marginal likelihood estimation of semiparametric generalized linear models. *Journal of the Royal Statistical Society* (B) 73(1):3-36

Xiao, F., Ma, J., Yi, P., & Huang, J. C. H. (2008a). Effects of low temperature on coagulation of kaolinite suspensions. *Water Research*, *42*(12), 2983-2992.

Xiao, F., Zhang, X., & Lee, C. (2008b). Is electrophoretic mobility determination meaningful for aluminum (III) coagulation of kaolinite suspension?. *Journal of Colloid and Interface Science*, *327*(2), 348-353.

Yeo, I. K., & Johnson, R. A. (2000). A new family of power transformations to improve normality or symmetry. *Biometrika*, *87*(4), 954-959.

Zuur, A. F., Ieno, E. N., Walker, N. J., Saveliev, A. A., & Smith, G. M. (2009). *Mixed effects models and extensions in ecology with R*. New York: Springer.

4 Improving the performance of sand filters with constrained up-wash rates using low-density expanded clay media.

4.1 Abstract

Rapid gravity sand filters (RGF) form the final barrier to particles and pathogenic micro-organisms in many large municipal water supply systems. Many RGFs are in operation that were designed before advances in filtration theory and practice that occurred during the 1980s and 1990s, or have been built intentionally with design limitations. Previous investigations and fullscale application of expanded aluminosilicate (Filtralite^{TM}) as a replacement for sand have demonstrated potential to improve the performance of deep-bed filters, particularly in RGFs with poorly designed cleaning systems.

This research investigated the application of aluminosilicate media of a much smaller size grade than has been previously researched. Pilot scale filtration trials were undertaken at two water treatment works in Scotland comparing different aluminosilicate media configurations with conventional media arrangements. The results showed that filtration performance gains and the mechanisms driving them were contingent on filter design and influent solids loading conditions. Pilot trials showed that a fine dual Filtralite bed (0.5-1 mm & 0.8-1.6 mm) with a porosity that was 26% greater than the equivalent grade of sand anthracite delayed particle breakthrough by more than 50%.

The availability of finer aluminosilicate grades of media combined with improved understanding of its application broadens the range of conditions where switching media from sand to aluminosilicate can economically deliver water quality and performance improvements in existing filters. Pilot trials showed that depending on the solids loading conditions, filter type and backwash system the processes driving improved performance varied. Much of the performance gain associated with use of Filtralite was associated with the improved removal of deposits during backwash. The expansion for the low-density media rather than the greater porosity and surface roughness, a result consistent with what has been published previously.

These findings can be applied to many of the RGFs currently in operation in the UK. In many cases, these performance gains can be achieved at a fraction of the cost of upgrading backwash systems and hydraulic control regimes. Such a replacement strategy would allow many older filter structures and supporting mechanical and electrical components to be adapted to meet the increasing demands of more stringent water quality standards and deteriorating raw water quality.

4.2 Introduction

Rapid gravity filtration (RGF) is a batch process where water is passed through a fixed bed of granular media, traditionally silica sand, providing a large surface area and void-space for the collection of flocculated colloidal and precipitated solids. After a period of operation, the accumulated solids are backwashed from the bed, recovering the surface area and voids for attachment of particles during the next run. If not effectively backwashed, deposits accumulate within the filter, resulting in a deterioration in media condition and performance (Van Staden and Haarhoff, 2011). Deposits retained within the media bed increase interstitial velocity and shear, as well as lowering attachment efficiency, reducing filtration performance. Retained deposits can also, in some applications, be used to increase attachment efficiency reducing the ripening period. Hydraulic shock, overloading of solids and inadequate pre-treatment can cause the release of accumulated solids into treated water, a process known as breakthrough. Breakthrough of particles from filters has been associated with increased concentrations of microorganisms in filtered water and supply systems (Hendricks, 2006; Huck *et al.*, 2002b). Ineffective clearing of deposits from the media voids reduces the solids handling capacity of the filter and over time can lead to operational issues such as mud-balling and wormholes. Reduction in filter run times can result in a cycle of hydraulic overloading of filter wash water systems, deteriorating recycle water quality and increasing public health risk and/or the emergency discharge of wash water to the environment (Huck *et al.*, 2001; Mann *et al.*, 2007).

Filter washes typically progress in stages to: 1) dislodge accumulated solids from the surface of media grains; 2) transport dislodged solids out of the filter box; and 3) re-grade the media bed to ensure hydraulic efficiency. First, air is passed through the bed to agitate the media grains and dislodge deposits, in what is known as the air scour. More modern filters backwash with a combination of air and water. The

promotion of maximum shear conditions, known as “collapse pulse” backwashing are well established, with the combination of air and water at between 25 and 50% of the minimum fluidisation velocity (V_{mf}) having been demonstrated to be most effective (Amirtharajah, 1993). Following the air-scour or combined phase, a rinse is applied to transport dislodged solids into the dirty wash-water collector. Critically, for this investigation there are two potentially limiting processes in the performance of a back-wash: the removal of deposits from media grains, the transport of deposits from the filter by rinsing. It should be noted that in experimental methods Amirtharajah uses a high-rate rinse capable of 20-25% bed expansion to transport dislodged solids from the bed (Ambergey *et al.*, 2003; Amirtharajah *et al.*, 1990). Effective backwashing is crucial for filter operation and is affected by media density, size, friability, voidage and water temperature (Fitzpatrick, 1998). The type of backwashing is typically dependent on the type of rapid filter media design, which can be broadly characterised into three types:

1. ***Traditional mono-media filters***: Traditionally rapid filters used a fine sand with an effective size (10^{th} percentile of the grain diameter distribution) of 0.5 - 0.6 mm and a bed depth of 1 m or less. Some of these systems wash at a rate below fluidisation, others are washed to expand the bed by more than 20%. Broadly speaking, operation of filters in the US typically use higher wash rates than those used in Europe (Beverly, 2005; Hendricks, 2006; Brandt *et al.*, 2016). Many of these filters now use a separate air-scour that has been retro-fitted into older filters. The high surface area of small media grains means that good quality water can be produced from a relatively shallow bed. However, the hydraulic and solids loading capacity of these filters is much lower than later designs.

2. ***Deep bed mono-media filters***: These filters use a single larger grade media with a typical effective size greater than 0.95 mm used in a deep bed depth of 1 m or greater to compensate for the reduced surface area of the larger media (Beverly, 2005). Coarse media has greater hydraulic efficiency. This configuration is less likely to blind than finer sand by more efficiently collecting solids through the depth profile of the bed. However, the reduced collision rate leads to a shallow wave front of accumulated deposits within the bed, hence the requirement for a deeper filter bed. In addition, polymer is frequently applied

in order to retain fine floc and prevent early breakthrough of particles. Most deep-bed filters are washed with a combination of air and water to induce collapse-pulse conditions which allow effective cleaning of media grains. However, there is considerable divergence in how these filters are cleaned with respect to the fluidisation achieved during backwash, with some systems designed to expand the bed and others rinsing at a sub-fluidisation velocity with or without supplementary surface washing.

3. ***Dual and multimedia filters***: These filters exploit the density difference between two or more media materials of different particle size and density. Larger and low density media is retained at the top of the bed above a layer, or layers, of finer higher density media. Such filters allow for more effective and efficient particle capture in the filter bed. Dual media filters rely on effective bed expansion beyond the fluidisation velocity and the difference in settlement rates of the media to re-grade the filter in order to maintain the hydraulic efficiency of the filter (Beverly, 2005; Hendricks, 2006).

RGFs are generally large, expensive, and long-lived concrete structures and many of the RGFs operating today were designed and built several decades ago when water quality standards were lower. Many filters in operation today pre-date the advances that have been made, such as the use of deep bed coarse media filtration and collapse-pulse backwashing. Furthermore, changes in raw water quality have placed filtration processes under increased pressure. For example, the concentration of natural organic matter (NOM) in surface waters has increased in northern Europe and America over the last decades (Pagano, Bida and Kenny, 2014). The precipitation and flocculation of these materials in water treatment results in increased solids loading, challenging the performance of filters which were designed and built before the water quality had changed (Eikebrokk, Vogt and Liltved, 2004; Jarvis *et al.*, 2005a). The increased NOM content in flocs also weakens them, making them more difficult to remove during clarification and filtration (Jarvis *et al.* 2005). The shearing and breakthrough of weaker NOM flocks limits the solids handling capacity of a filter compared to denser and stronger mineral floc, however, this can be mitigated with the use of polymers (Rebhun, Fuhrer and Adin, 1984). However, the use of polymer on filters which are ineffectively backwashed can exacerbate deteriorating filter condition and performance through the formation of mud balls (Logsdon *et al.*, 2002).

To satisfy changing requirements and realise the full life of civil assets, it is not uncommon for older filters to be modified or upgraded to overcome limitations of the original design. One type of upgrade, the conversion of mono media filters with a fluidising backwash into dual media filters using anthracite to increase the solids handling capacity is well established. Such upgrades typically require not only replacement of the media, but also an increase in the up-flow velocity of the wash water to re-grade the dual media bed. Addressing the constraints in the availability and delivery of backwash water can be a considerable capital cost. The central rationale of this work was to therefore demonstrate how and where low-density media can be used to improve water quality and avoid the requirement for large capital expenditure to upgrade RGF backwash facilities.

There are several media alternatives to sand for use in RGFs including: anthracite, garnet, crushed glass, pumice, quartz, slate, polystyrene and expanded aluminosilicate (Davies-Colley and Wheatley, 2012; Schöntag and Sens, 2015; Suthaker, Smith and Stanley, 1995). Increasing solids loading capacity in a filter by adding a layer of pumice or anthracite to a mono-media sand filter is a long established method for improving the robustness of a filter(Ives, 1970). Aluminosilicate media offers an advantages over these materials because of its reduced friability and increased porosity (Davies, 2012). The most common aluminosilicate product on the market is known by the commercial name Filtralite. The use of Filtralite as a filter material for drinking water applications was pioneered in the late 1990s and is now well established (Eikebrokk and Saltnes, 2001). Typically, Filtralite media with a particle diameter >0.8 mm have been used in water treatment to improve the hydraulic loading and solids handling capacity of deep bed filters. Filtralite has been used effectively to improve the hydraulic efficiency of roughing filters using a fine 0.6-1.2 mm sand and anthracite media to be replaced by larger Filtralite media whilst retaining the same wash rate (Mikol *et al*., 2007). Lower density media, including Filtralite, has also been reported to wash more effectively than sand reducing wash frequency (Bayley *et al*., 2006). Though more effective washing has been observed during comparisons at consistent backwash conditions, improvements in filtration performance due to Filtralite have been attributed primarily to increased porosity, favourable shape and surface characteristics and consequently the support of biofilm within the media (Bayley *et al*., 2006; Mikol *et al*., 2007; Saltnes, Eikebrokk and

Ødegaard, 2002). As previous published investigations involving Filtralite have used media > 0.8 mm in diameter, filtered water turbidity results have not been advantageous compared to conventional fine sand filters in media beds ≤1 m deep (Mikol *et al.*, 2007; Saltnes *et al*., 2002). Fundamental filtration theory indicates that the greater porosity will result in lower particle capture efficiency (Rajagopalan and Tien, 1976; Tufenkji and Elimelech, 2004). As a consequence, following investigators have paired Filtralite with finer and lower porosity media which also has higher density (Cescon *et al*., 2016; Davies and Wheatley, 2012). In recent years, a finer Filtralite grade (0.5-1 mm) with lower porosity has become available making it more appropriate for use in older filters that are of relatively shallow bed depth (<1 m) and require greater collection efficiency to maintain water quality.

The benefit of using Filtralite in sufficiently deep filters with backwash systems capable of delivering combined air and water collapse-pulse backwashing and rinse rates greater than 45 m/h is well established. In these conditions it is possible to replace coarse sand (≥ 0.85-1.7 mm) with a dual media of Filtralite HC (0.8-1.6 mm) and Filtralite NC (1.5-2.5 mm). In these ideal conditions performance benefits in terms of hydraulic efficiency and solids handling capacity have been attributed to additional voidage from larger, irregularly shaped media with greater porosity and lower sphericity (Mikol *et al.*, 2007). These ideal conditions are not replicable in many existing filters with performance challenges. Though the advantages of Filtralite in terms of backwash performance have been observed previously, these investigations have compared the performance of Filtralite to sand over an extended period with consistent backwash conditions and concluded that further research was required to identify the mechanisms enabling the advantages associated with Filtralite (Bayley *et al.*, 2006; Mikol *et al*., 2007). The aims of this work were therefore to further understand water quality improvement associated with replacement of sand with Filtralite in the context of legacy constraints in the design of backwash systems and new finer grades of Filtralite.

4.3 Materials and methods

4.3.1 Study sites

Pilot scale investigations were undertaken at two surface WTWs (A and B) in Scotland, with full scale trials following at WTW A:

4.3.2 WTW A: DAF - Dual Media RGF

WTW A treats a blend of two surface water sources by coagulation with poly-aluminium chloride (PACl), dissolved air flotation (DAF), and RGFs. The RGFs at this works had originally been designed to use a 0.5 to 1 mm diameter sand media. During a previous upgrade the media had been changed to a combination of 0.6 - 1.2 mm sand and pumice (original size unknown). The filters are washed by a separate air and water wash. The backwash pumps can deliver an up-flow velocity of 23 m/hr, which is insufficient to effectively re-grade the sand-pumice media resulting in a largely mixed bed. The air scour rate is 20 m/hr. Seasonal water quality issues arise at low temperature due to hydraulic overload of flocculation and flotation stages. To improve performance, the source water blend is changed seasonally; this results in changes to the clarified water quality throughout the year (Table 11). Poor flocculation performance when the water is cold, and floc carry-over in combination with hydraulic shocking of the filter bed has been associated with premature turbidity breakthrough during the winter and *Cryptosporidium* detections.

4.3.3 WTW B Direct filtration

WTW B is a direct filtration plant coagulating with alum and flocculating with a cationic polymer. The filters comprise a BSS 10/18 (0.85-1.7 mm) coarse mono media sand filter at a depth of 1000 mm. These filters are washed with air (55 m/hr), then combined air (55 m/hr) and water (7 m/hr, approximately 13% of the D90 v_{mf} at 15°C) for 10 minutes. The large grade of sand media and the low water rise rate allows an extended combined air and water wash during which water spills into the launder with minimal media loss. This is followed by a rinse with an upwash velocity of 17 m/hr for 5 minutes which is not high enough to fluidize the bed. The up wash is supplemented by a concurrent surface wash. This type of deep-bed coarse sand filter was popular in the 1990s, during a period of considerable investment in water treatment in the UK.

4.3.4 Pilot plant

The pilot plant consisted of three 3 m high columns with an internal diameter of 150 mm. The columns were operated in parallel. Flow to each filter was supplied by a common sample line. This was fed from the clarified water during trials at WTW A and from the flocculated water during trials at WTW B. An independent in-line peristaltic pump for each column provided flow control & additional driving head. All pumps and

valves were operated manually. A schematic of the pilot filter arrangement for each filter is shown in Figure 19. An air compressor with mass flow meter provided air-scour and a pump provided backwash water. Filtration tests were carried out using configurations of sand, Filtralite and anthracite media (Figure 20 and below for further descriptions). The physical properties of the media used in the trial are shown in Table 10 and particle size distributions from sieve testing are shown in Figure_Apx 53 (British Standards Institution, 1989).

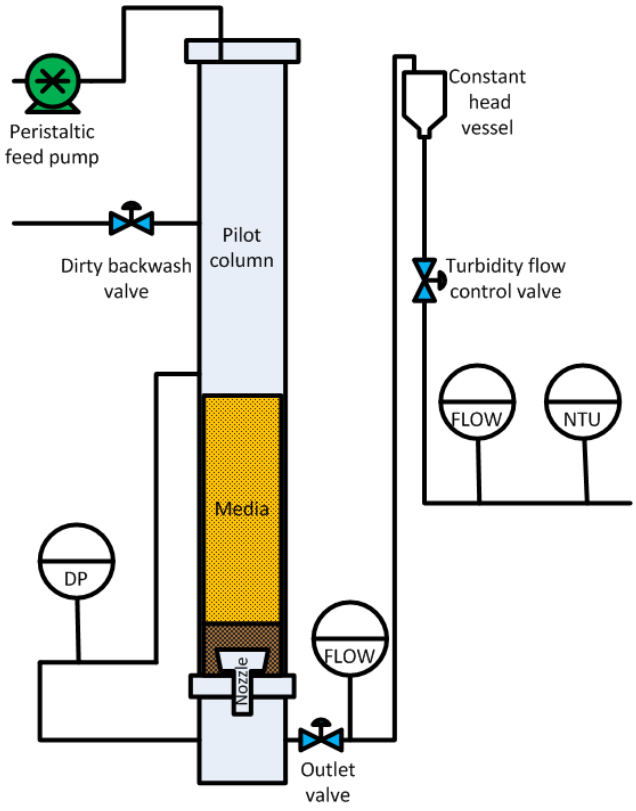

Figure 19 Schematic of filtration pilot plant for a single filter column.

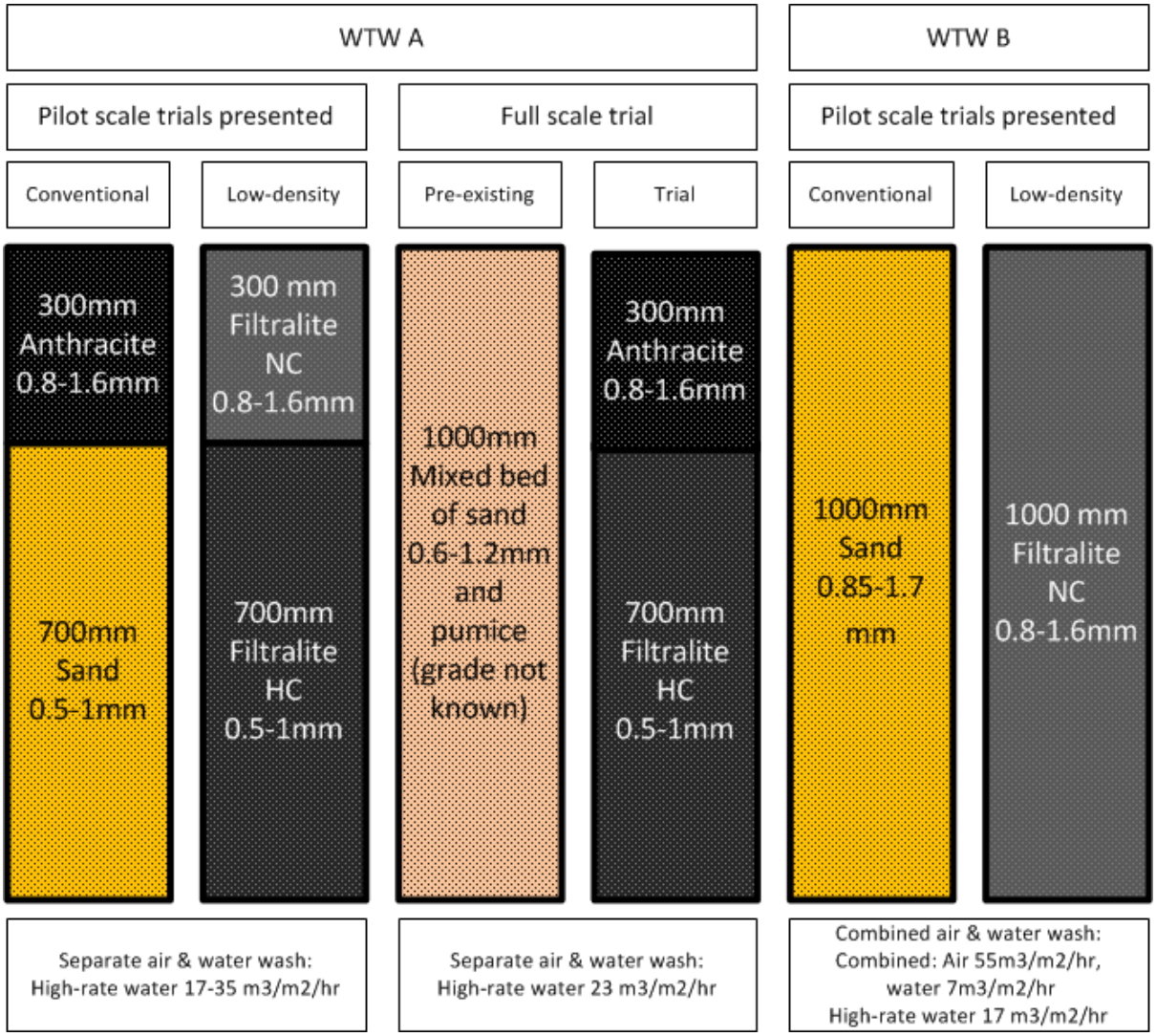

Figure 20. Summary of media trial configurations.

Table 10. Summary of the key physical properties of media tested in pilot trials.

Material	Sizes / Grade Tested (mm)	Effective size (D_{10}) (mm)	D_{90} (mm)	Uniformity coefficient (D_{60}/D_{10})	Density (kg/m^3)	Porosity
Sand	0.5-1.0	0.6[3]	0.9	1.27	2650[1]	0.43[2]
Sand	0.85-1.7	1.0[1]	1.74	1.36[3]	2650[1]	0.43[2]
Filtralite HC	0.5-1.0	0.52[3]	0.95	1.46[3]	1800[1]	0.55[1]
Anthracite	0.8-1.6	0.85-1[1]		<1.5[1]	1400[1]	0.5[2]
Filtralite NC	0.8-1.6	0.98[3]	1.46	1.34[3]	1260[1]	0.61[1]

1. Suppliers data
2. Textbook value (Crittenden *et al.*, 2012)
3. Sieve testing

4.3.5 Media trials

4.3.5.1 Pilot trials at WTW A: (DAF - Dual Media RGF)

Pilot scale trials at WTW A compared a column with 700 mm filter sand (0.5-1 mm, 2650 kg/m^3) below 300 mm of anthracite (0.8-1.6 mm, 1400 kg/m^3) to a filter column containing 700 mm of Filtralite HC (0.5-1 mm, 1800 kg/m^3) below 300 mm of Filtralite NC (0.8-1.6 mm, 1260 kg/m^3). Both media beds were supported by a 100 mm layer of gravel (10 mm). Feed water was sourced from the clarified water channel. Performance of the media was compared at hydraulic loading rates between 4.5 m/hr and 6 m/hr and with backwashes at 17, 23, 27 and 34 m/hr. Selected runs were repeated in an attempt to capture deteriorating condition effects inherent in sub optimal backwash trials. The trials presented for WTW A took place between January and August at water temperatures ranging from 4 to 16 °C. The conventional and test filter columns were operated in parallel at the same time on the same feed water. The air scour was maintained at 20 m/hr for all washes to reflect the conditions at full scale. The blend of the two sources treated at WTW A varied marginally over the course of the pilot trial, with a slight increase in the raw water turbidity and colour during winter when there was an increase in the proportion of Source B to half of the flow (Table 11). This resulted in a slightly higher turbidity in the clarified water going onto the filters

during winter, with an average of 0.7 NTU compared to 0.6 and 0.5 NTU in spring and summer.

Table 11. Averages for WTW A water quality over the pilot study period based on different seasonal blends

Blend Source A: Source B	WTW Flow (l/s)	Clarified turbidity (NTU)	Raw water turbidity (NTU)	Raw colour (Hazen)
Spring Blend 55:45	381	0.6	0.9	32.1
Summer Blend 60:40	367	0.5	1.0	33.6
Winter Blend 50:50	363	0.7	1.2	37.6

4.3.5.2 Full scale trials at WTW A: DAF - Dual Media RGF

On the basis of successful pilot trials at WTW A, full-scale trials of lower-density media were initiated at the site. Data was extracted from the control system describing the performance of the trial filter containing a bed of Filtralite HC 0.5-1 mm (700 mm) and Anthracite 0.8-1.6 mm (300 mm) and a neighbouring filter containing the old media an ungraded mixture of 14/25 sand & pumice of unknown size at a total depth of 1m. Both filters were backwashed at the maximum available rate of 21 m/hr. Anthracite was chosen in preference to coarser grade Filtralite in order to minimise the risk of media loss, a fraction of Filtralite NC 0.8-1.6 is buoyant upon initial contact with water and can remain buoyant for several weeks.

4.3.6 Pilot trials at WTW B Direct filtration

Pilot column trials were conducted to compare the performance of a 1000 mm deep bed of 10/18 filter sand (0.85-1.7 mm 2650kg/m^3) with a 1000 mm bed of low-density Filtralite (0.8-1.6 mm 1260kg/m^3). A hydraulic loading rate of 4 m/hr was maintained for all the pilot tests matching that of the WTW. Sand was backwashed under conditions as far as possible approximating to those of the full-scale site. The combined wash phase combined air (55 m/hr) and water (7 m/hr) for 10 minutes. In addition to a combined air and water wash, WTWs B uses a surface wash to assist the transport of dislodged solids from the filter box; this operation could not be directly replicated using the pilot filter columns. As the pilot plant was not capable of simulating

a surface-wash the duration of the 17 m/hr rinse was doubled to 10 minutes in an attempt to correct for this effect.

4.4 Data analysis

Filter operation and filtered water quality was monitored and logged for each column using online monitors for turbidity, particle count, flow and differential pressure. This data was downloaded and stored within an SQLite database (Hipp, 2020). A run log, recording the details of each filter run including the start and end times and backwash conditions was kept and added as a table within the database.

As pilot trials are time consuming to complete the acquisition of data is limited. Observations within the same filter run have inherent dependencies so aggregate measures of filter operation and performance of individual runs required for realistic estimates of modelling error.

Normalised clean bed head loss (NCBHL), a widely applied indicator of filter backwash performance, was calculated using the procedure described in Logsdon *et al*. (2002) to the mean of values measured in the first hour of operation after backwashing (Equation 29). Volume normalised head loss (VNHL) applies this approach over the whole run after dividing by the volume of water treated in units of empty bed volumes (EBV) (Equation 30). VNHL was used as a metric of hydraulic performance, with lower values indicative of greater distribution of deposits over the profile of the bed. The effective run productivity, or breakthrough, was defined for pilot trials at WTW A, as the empty bed volume after which the particle counts consistently increased by more than 10% in a 4 hour period.

Equation 29. Flow normalised head loss:

$$H_F = H_{QT}\left(\frac{Q_N}{Q}\right)$$

Where: H_f = flow normalised head loss (m), H_{QT}= measured head loss at flow rate Q and temperature, T (°C), Q_N= flow rate used as standard for normalization (m/hr), Q = measured flow rate ($m^3/m^2/h$)

$$H_N = H_F\left(\frac{\mu_T}{\mu}\right)$$

Where: H_N = flow and temperature normalised head loss (m), μ_T = absolute viscosity of water at the normalised (standardized) temperature (kg/m/s), μ - absolute viscosity of water at the mean weekly water temperature (kg/m/s)

Equation 30. Volume normalised head loss (VNHL):

$$VNHL = \frac{\sum_{i=1}^{n}\left(\frac{H_{N_i} - CBHL}{Vi}\right)}{n}$$

Where: H_{Ni} = flow and temperature normalised head loss at observation *(m), CBHL = Clean bed head loss (m),* V_i = Volume filtered at observation *I (EBV), n =* Number of observations

As the performance of the filters during pilot trials at WTW A varied depending on the seasonal blend of water. Linear mixed models were used to correct for within blend dependency and maximise the statistical power of the analysis of the whole period. Model identification was performed according to the method set out in Zuur (2009). Additional ordinary least squares (OLS) regression models using data from only the most challenging winter period at WTW A were undertaken. Models were fitted to the three performance variables using the explanatory fixed effect variables describing media bed type and wash-rate. In the experiments media performance in pilot trials at WTWA were compared at a range of wash rates which were practically relevant to the application of the low density material in existing filters and the objectives of the research. In response to criticism of the original version of this thesis additional data analysis was performed with wash rates normalised for minimum fluidisation velocity. Therefore, wash rate was modelled as an explanatory variable in two ways in separate models: firstly as an absolute value of the filtration velocity (m/hr) and secondly relative to the minimum fluidisation velocity of the lower layer of media. The minimum backwash velocity required to achieve fluidisation (V_{mf}) was calculated using the procedure of Wen & Yu as described Logsdon *et al.* (2002) shown in Equation 31 and Equation 32. It should be recognised that correcting for density, after the fact, rather than in the experimental design, introduced collinearity into the statistical models as media choice was correlated with wash-rate after correction for density. These collinearities were checked using the variance inflation factor (VIF). VIF values between 3-3.5 for individual seasonal blends and 2 across all pilot runs between flow normalised wash rate and media were considered to be acceptably low and no further correction was made.

Equation 31. Calculation of velocity of minimum fluidisation V_{mf} (Logsdon *et al.*, 2002)

$$V_{mf} = \frac{\mu}{\rho d_{eq}}(33.7^2 + 0.0408Ga)^{0.5} - \frac{33.7\mu}{\rho d_{eq}}$$

Where: V_{mf} = minimum velocity required to fluidise the bed (m/hr), μ = absolute viscosity (kg/m/s),ρ = mass density of fluid (kg/m3)

Equation 32. Calculation of Galileo number (Logsdon *et al.*, 2002)

$$Ga = \frac{{d_{eq}}^2 \rho(\rho_s - \rho)g}{\mu^2}$$

Where: g = acceleration due to gravity (m/s^2), μ = absolute viscosity (kg/m/s),ρ = mass density of fluid (kg/m3), ρ_s = mass density of media grains (kg/m3), d_{eq} = equivalent diameter of the filter (90^{th} percentile used)

Pilot trials at WTW A aimed to understand the comparative performance of media under a range of backwash rates. Trials took place across different seasons with the pilot columns treating a different blend of water in each season. This meant that performance of the media varied across the seasons in a way that was not the original focus of the experiments. To efficiently and reliably model data across all seasons a mixed effects model was used. Mixed effects models allow the analysis of a phenomenon of interest across data collected amongst different groups (Zuur, 2009). In this case the phenomenon of interest was the impact of wash rate on the performance of two media but the characteristics of the water treated changed over the period of the trial meaning that there were correlations between the blend treated and the performance of the filter columns. The errors from an ordinary least squares regression model fit to all of the data would not be independent. This can be avoided by aggregating the data within the test condition across the different groups, however by doing this, lots of the information is lost. It is also possible to fit individual models within each of the groups, however this results in a large number of models and given there are comparatively few data points within each group the uncertainty of each model would be high. A normal OLS model has only fixed effects such as the intercept and slope which the modelling procedure estimates. It is possible to specify a more complicated fixed effects model which included the grouping factor as a fixed effect, but where there is an interaction between the grouping variable and another fixed effect of interest this would need to be captured in the model increasing the number of parameters and the complexity of interpreting them. Mixed effects modelling allows the inclusion of a random intercept and or slope for each group and therefore the

estimation of the fixed effects of interest across all observations. Each of the three performance variables; bed volumes at breakthrough,

One particular performance characteristic, volume filtered at breakthrough, was an issue particularly during treatment of the winter blend but not the others. To effectively understand and communicate the differential performance of media and the impact of backwashing during this critical period additional modelling was carried out. The volume filtered at breakthrough during treatment of the winter blend only was also modelled using ordinary least squares regression.

Data was analysed using the R statistical programming environment. Mixed effects models were fitted with the lme4 package (Bates *et al.*, 2017; R Core Team, 2015). Plots and tables were generated using the ggplot2 and stargazer packages (Hlavac, 2015; Wickham, 2010). Code used for the analysis is included at (https://github.com/APU2/CH4-FILTRALITE).

4.5 Results and discussion

4.5.1 Pilot trials 1: Sand-anthracite filter with insufficient backwash (WTW A)

4.5.1.1 Effective run volume

On average, across filter runs where particle breakthrough was observed, Filtralite media delayed breakthrough by 74 empty bed volumes (EBVs) when compared to the conventional sand and anthracite filter (Figure 21, Table 12 model 1). This represented a 57 % increase in run length or an additional 12 hours at a filtration rate of 6 m/hr, when compared to the sand and anthracite filter. While Filtralite HC 0.5-1 mm has 26 % greater porosity than sand, this difference does not appear to explain the delay to breakthrough observed. Breakthrough of particles was primarily associated with treatment of the winter blend and was less frequently observed for either media during the spring and summer blends. This led to censoring of the data as the volume filtered at breakthrough was only captured when breakthrough took place. Pilot runs which were stopped after several days due to head loss, rather than quality deterioration were not included in the models of breakthrough. As filter runs where breakthrough did not occur were more common for Filtralite the benefit of using Filtralite, in terms of delaying breakthrough, is likely underestimated though this is of limited practical

importance as head loss would limit run duration. When treating the winter blend particle breakthrough was observed in 18/19 pilot runs of the sand anthracite media and in 12/16 of the Filtralite pilot runs. When treating the summer blend particle breakthrough was observed in 12/22 sand pilot runs and 1/24 Filtralite pilot runs. Though only a 0.2 NTU difference between seasons in the average turbidity of the clarified water was observed in online measurements, visual inspection of grab-samples showed the presence of larger (sludge blanket knockdown, solids load not quantified) particles. Larger particles are typically less effectively represented by turbidity which is a surface area driven measurement (Anderson, 2005). It is also likely that the floc formed during treatment of the winter blend would be weaker as a result of increased TOC and lower temperature (Bache and Gregory, 2010). Greater delay to breakthrough with increasing wash rate was apparent for both media. For Filtralite the volume treated at breakthrough increased from 143 to 213 EBVs (equivalent to 23 to 36 hrs run time at 6 m/hr) as the backwash rate increased from 17 to 34 m/hr. Equivalent figures for the sand filter were 68 and 137 (equivalent to 11 to 23 hrs run time at 6 m/hr) EBV (Table 13 model 1). When the backwash rate was normalised to the V_{mf} there was an apparent convergence between media in the expected volume treated at breakthrough where relative wash rates were equal (Figure 22).

When data for observed breakthrough was analysed using a linear mixed model, using the blend of water treated as a random effect, there was a significant difference in the volume of water treated at breakthrough and the media used ($p<0.01$) of approximately 74 EBVs, while the wash rate had no significant impact. The absence of a significant relationship between absolute wash rate and breakthrough would support the hypothesis that the performance benefit associated with the use of Filtralite was a result of collector characteristics rather than wash performance. However, the relationship is somewhat more complicated than we can see that during treatment of the winter blend there is a clear relationship between wash rate and breakthrough (Figure 21). During treatment of the spring and summer blends it is likely that breakthrough was not observed due to a relatively low solids load and a stronger floc. A simplified mass balance of a filtration process shows that the quality of filtered water will deteriorate if the solids load exceeds the available capacity of a filter to contain it (Equation 33 & Equation 34). The available capacity of a filter bed is reduced by any residual deposits which remain after a backwash. This may not be an issue if the solids

load is less than the residual solids handling capacity of an incompletely cleaned filter and such conditions are likely to have occurred during treatment of the summer blend.

Using the same mixed modelling approach and normalising wash rate for the density of the lower layer of media using V_{mf} the estimated effect of the media choice reduced to 25.8 EBVs and the difference was no longer significant (p = >0.1, 95% CI -17.4 – 69.1). However, there was a significant (p = <0.01, 95% CI 7.6 – 43.4) relationship between the normalised wash rate and EBVs to breakthrough, independent of the media type (Table 12, model 2). The absence of any statistically significant (p > 0.1) effect of media on breakthrough associated with scaling wash rate to the fluidisation velocity (of the lower layer) provides some indication that the improved transport and removal of deposited solids from an expanded media bed was the key factor in the filtration performance improvement in this application rather than the shape or void characteristics of the media. For example, during treatment of the higher solids loading in the winter blend, it was hypothesised that there was an accumulation of solids in the lower layers of the filter. If these layers are not effectively expanded during backwash, the media will be poorly cleaned resulting in accumulation of solids and an earlier onset of breakthrough. The use of the lower density Filtralite media was able to mitigate this problem through greater bed expansion (and cleaning) during the backwash. It is likely that, over time, the condition of an unexpanded bed would deteriorate such that even at reduced solids loading rate a greater difference in performance would still become apparent. However, the nature of experimental design where the wash conditions were varied between runs to avoid potential influence of experimental treatments correlating with environmental conditions meant that such cumulative inter-run effects were not captured.

Equation 33. Simplified mass balance for rapid gravity filter run

$$M_{out} = M_{in} * (1 - \eta) + \begin{cases} M_e & M_e > 0 \\ 0 & M_e < 0 \end{cases}$$

Where: M_{out} = Effluent mass of solids during a filter run (kg), M_{in} = Influent mass of solids during a filter run (kg), M_e = Excess solids (kg), η = Filtration efficiency

Equation 34. Definition of excess solids load

$$M_e = S_{cb} - M_r - M_{in} * \eta$$

Where: M_{in} = Influent mass of solids during a filter run (kg), S_{cb} = Available solids storage capacity of a clean filter bed (kg), M_r = Residual solids not removed during backwash, η = Filtration efficiency

As the breakthrough performance during treatment of the winter blend was clearly different and did not have the impact of censoring that occurred during treatment of the spring and summer blends additional modelling of the data collected during this period was performed. Ordinary least squares regression modelling of breakthrough time for all filter runs as a function of media type and wash rate (m/hr) during the winter period alone indicated that, during this period, an increase in 1m/hr in wash rate resulted in an additional 4.1 EBVs in filter run prior to breakthrough for both media. No significant interaction was observed between wash rate and media indicating that the relative benefits of increasing wash rates were consistent between media. During treatment of the winter blend alone Filtralite was associated with a significant 76.3 EBV ($p < 0.01$) increase in filter run volume (Table 13, model 1). As with the mixed models, normalising the wash rate by the V_{mf} of the media served to remove any significant ($p > 0.1$) performance effect associated with media choice (Table 13, model 2). When modelling only the high solids winter blend, increasing wash rate was associated with a significant ($p < 0.01$) increase in the effective filter run volume irrespective of normalisation for media density (Table 13, model 1 and 2). Modelling of breakthrough performance during the treatment of the winter blend alone indicates that delay to breakthrough was driven by more effective removal of deposits during backwash. For this reason under backwash rate constrained conditions at sufficiently high solids loading the lower density of Filtralite effectively extended the effective run time when compared to sand.

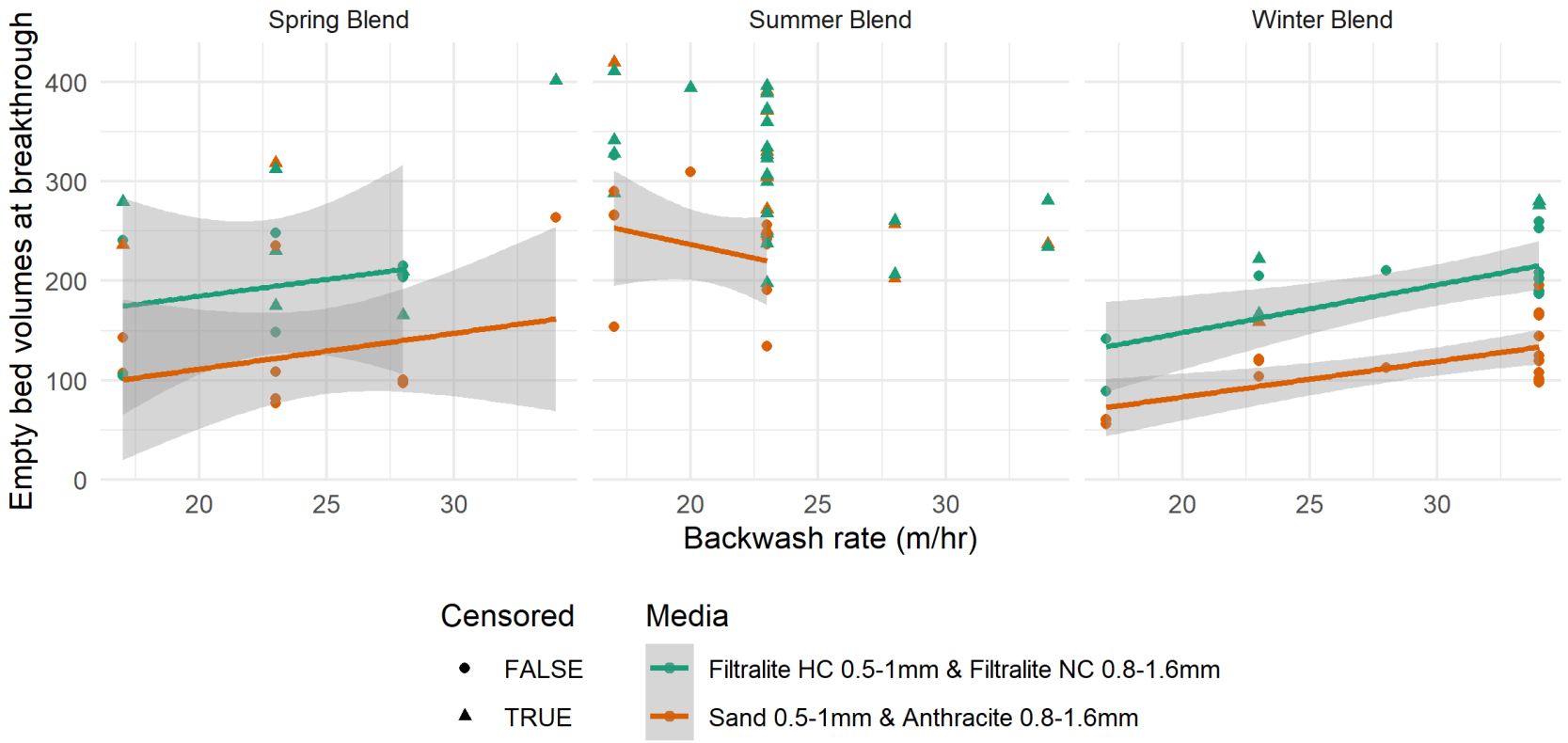

Figure 21. Empty bed volumes filtered at start of particle breakthrough plotted against high rate backwash rate for the two media across of each of the seasonal blends. Lines indicate linear model fit with shaded area showing standard error of expected value. Censored runs (where the pilot run was ended before breakthrough started) are shown as triangles and excluded from model fitting.

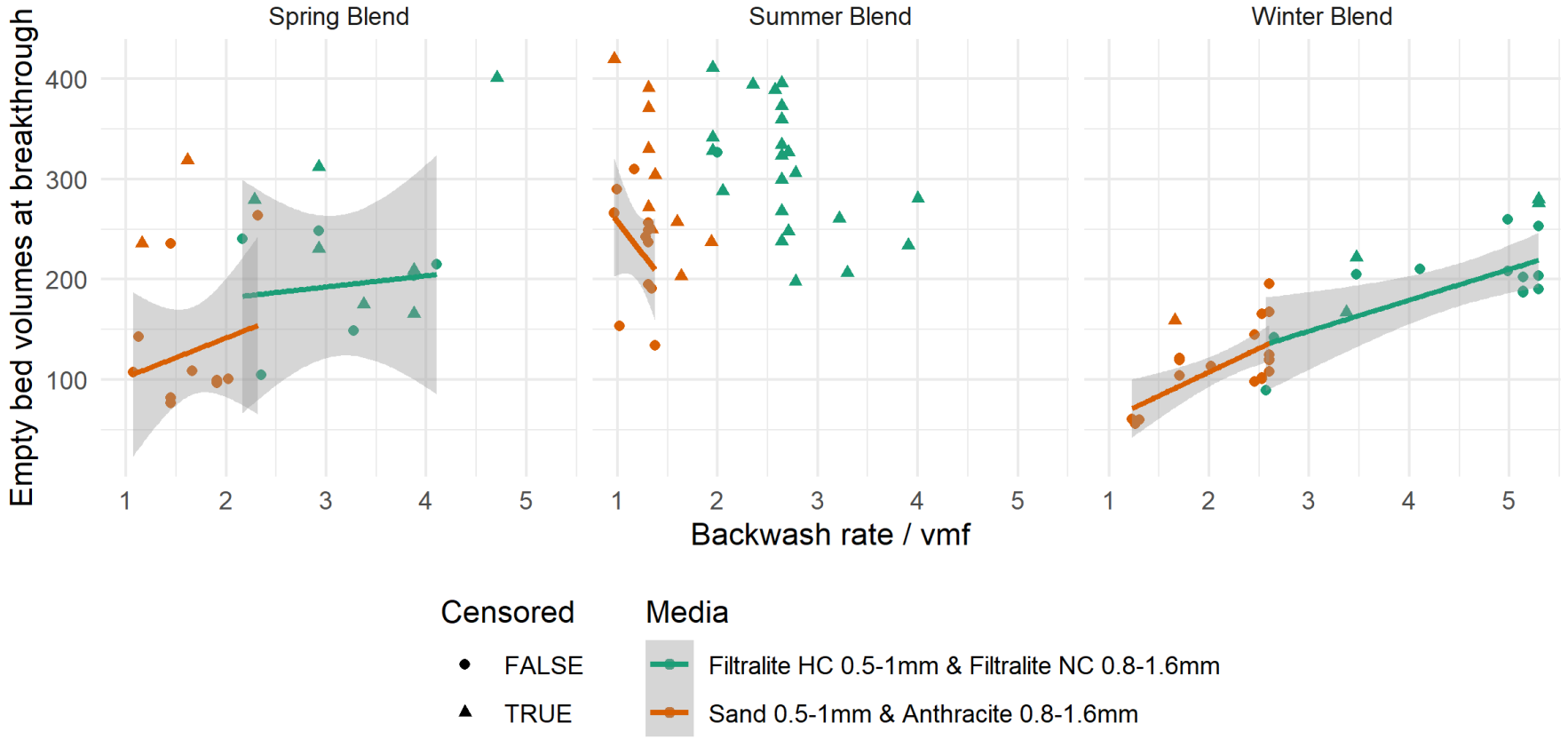

Figure 22. Empty bed volumes filtered at start of particle breakthrough plotted against the ratio of high rate backwash rate to minimum fluidisation velocity for the two media across of each of the seasonal blends. Lines indicate linear model fit with shaded area showing standard error of expected value. Censored runs where the pilot run was ended before breakthrough started are shown as triangles and not used to fit linear OLS regression model.

Table 12. Linear mixed-effects models relating backwash (BW) rate and media to filter column performance, across all seasonal blends, in terms of: bed volumes before breakthrough (BT), Normalised Clean Bed Head Loss (NCBHL), Volume Normalised Head Loss (VNHL). Coefficient estimates are shown with 95% confidence intervals in brackets.

	Dependent variables : Particle breakthrough, Normalised Clean Bed Head Loss & Volume Normalised Head Loss					
	BT (Hrs) RI&S	BT (Hrs) RI	NCBHL (m) RI	NCBHL (m) RI	VNHL (mm/bv) RI	VNHL (mm/bv) RI&S
	(1)	(2)	(3)	(4)	(5)	(6)
BW rate (m/hr)	0.6		-0.005***		0.05*	
	(-4.8, 6.1)		(-0.01, -0.004)		(-0.01, 0.1)	
BW rate/ V_{mf}		25.5***		-0.1***		0.004
		(7.6, 43.4)		(-0.1, -0.05)		(-0.8, 0.8)
Media = Filtralite	73.6***	25.8	-0.03***	-0.02	5.6***	3.3***
	(49.3, 98.0)	(-17.4, 69.1)	(-0.05, -0.02)	(-0.1, 0.02)	(3.8, 7.5)	(2.6, 4.0)
BW rate/ V_{mf}: Media = Filtralite				0.03***		
				(0.01, 0.04)		
BW rate: Media = Flitralite					-0.1**	
					(-0.2, -0.02)	
Constant	130.4	116.4**	0.5***	0.5***	2.0***	3.4***
	(-70.4, 331.3)	(22.7, 210.0)	(0.4, 0.5)	(0.4, 0.5)	(0.5, 3.6)	(2.3, 4.5)
Observations	60	60	106	106	106	106
Log Likelihood	-306.7	-307.7	206.4	205.3	-171.8	-159.7
Akaike Inf. Crit.	627.5	625.4	-402.9	-398.6	355.5	333.3
Note:	*p<0.1; **p<0.05; ***p<0.01					

Table 13. Ordinary least-squares regression models relating breakthrough of particles to media and wash-rate conditions. Censored filter runs where breakthrough did not occur were excluded. Coefficient estimates are shown with 95% confidence intervals in brackets.

	Dependent variable: Particle breakthrough

	OLS	
	(1)	(2)
Media = FL	76.3***	-3.8
	(54.7, 97.9)	(-43.9, 36.4)
BW rate (m/hr)	4.1***	
	(2.5, 5.6)	
BW rate/ V_{mf}		35.6***
		(21.2, 50.0)
Constant	-2.2	38.4**
	(-50.1, 45.8)	(4.2, 72.6)
Observations	30	30
R^2	0.7	0.7
Adjusted R^2	0.7	0.7
Residual Std. Error (df = 27)	29.6	30.1
F Statistic (df = 2; 27)	38.5***	36.8***
Note:	*p<0.1; **p<0.05; ***p<0.01	

4.5.1.2 Normalised clean bed head loss

Analysis of normalised clean bed head loss (NCBHL) further supports the assertion that the main performance gains observed during pilot trials at WTW A were due to the more effective transportation of deposits from the bed facilitated by expansion of the lower layer of Filtralite media when compared to the sand equivalent during the backwashing. Figure 23 shows that during treatment of the higher solids winter blend, across all backwash rates, the clean bed head loss for the Filtralite was approximately 0.02 m lower for the Filtralite media than it was for the sand anthracite. However, during treatment of the spring blend the difference in CBHL between media increases with increasing wash rate, below a rinse rate of 20 m/hr there appears to be no difference. During treatment of the summer blend difference in CBHL decreases with increasing wash rate, at rinse rates above 25 m/hr there appears to be marginal difference between media. After adjusting for media density and expressing the wash rate in relation to the velocity of minimum fluidisation (v_{mf}) clean bed head losses for Filtralite are equivalent or higher for the Filtralite than for the sand anthracite media (Figure 24). For the spring and summer blends, at wash rates approximately double the v_{mf} of both media, which corresponds to the lowest wash rates (17 m/hr) for the Filtralite and the highest wash rates (34 m/hr) for sand - anthracite, Filtralite exhibits higher clean bed head loss by approximately 0.05 m. During treatment of the winter blend and backwashing at a rate approximately 2.5 times the v_{mf}, both media exhibit similar levels of head loss. These results both indicate that increased wash rates reduced the starting head loss of filters for both media. For any given wash-rate lower head loss was observed from the Filtralite media. Though clean bed head loss is commonly used to indicate media cleanliness this appears to be somewhat more complicated when comparing dual media at velocities which achieve less than a complete re-grade. Variations in the particle size distribution over the profile of the bed due to changes in the depth of the transition layer appear to have a greater impact on the Filtralite media than sand-anthracite, this is illustrated by wider standard errors (Figure 23 & Figure 24).

Linear mixed models relating NCBHL to wash rate and media type showed that increasing the wash rate significantly ($p < 0.01$) reduced the normalised starting head loss. For example, the expected NCBHL on average across all treated blends for sand

anthracite was 0.415 m at 17 m/hr wash rate, while this decreased to 0.33 at a wash rate of 34 m/hr. Whereas for Filtralite the expected NCBHL on average across all blends was 0.385 m at a wash rate of 17 m/hr dropping to 0.3 m at 34 m/hr. This was further evidence for the more effective back washing and media regrading that was achievable for the lower density media (Table 12, models 3 and 4). As seen for particle breakthrough, the media type had a significant ($p < 0.01$) impact on head loss when the wash rate was expressed in absolute terms but this effect was not significant ($p > 0.1$) when wash rate was normalised for the V_{mf} of the lower media layer bed (Table 12, models 3 and 4). There was a significant ($p < 0.01$) interaction between media type and V_{mf} normalised wash rate with the NCBHL of sand reducing by an additional -0.03m for each increase in wash rate equivalent to the v_{mf} (Table 12, models 3 and 4). However, it should be noted that the high normalised backwash rates (>2.5) were only achievable for the Filtralite media and the very highest normalised backwash rates resulted in the lowest head loss. The case of treatment of the winter blend resulted in a different pattern, with convergence of the NCBHL at a scaled backwash rate of 2.5. It was only during the treatment of the winter blend that the wash rate for sand was regularly more than double the velocity of minimum fluidisation.

The sand/anthracite filter had a consistently lower head loss accumulation rate across the trial period between 2.1 and 4.8 mm/EBV, while the Filtralite filter had a higher and more variable head loss accumulation between 4.2 and 11 mm/EBV (Figure 26). The higher head loss accumulation rate observed in the Filtralite bed would have led to shorter run times than sand-anthracite when treating the summer blend (Figure_Apx 65). However, in practical terms, the key performance constraint was the breakthrough of particles during treatment of the winter blend as this would limit the filter run time the most

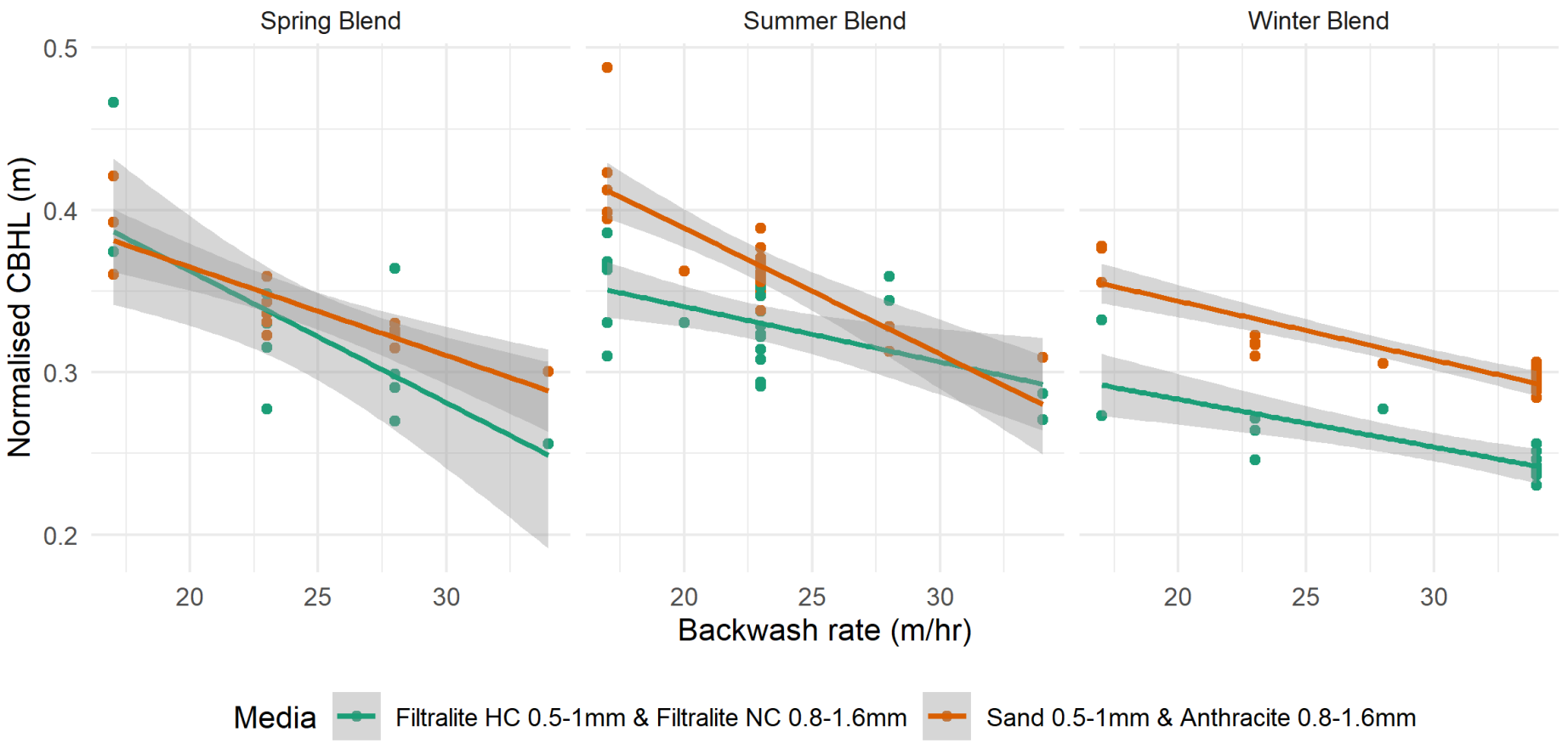

Figure 23. Normalised clean bed head loss plotted against backwash rate for the two media across of each of the seasonal blends. Lines indicate linear model fit with shaded area showing standard error of expected value.

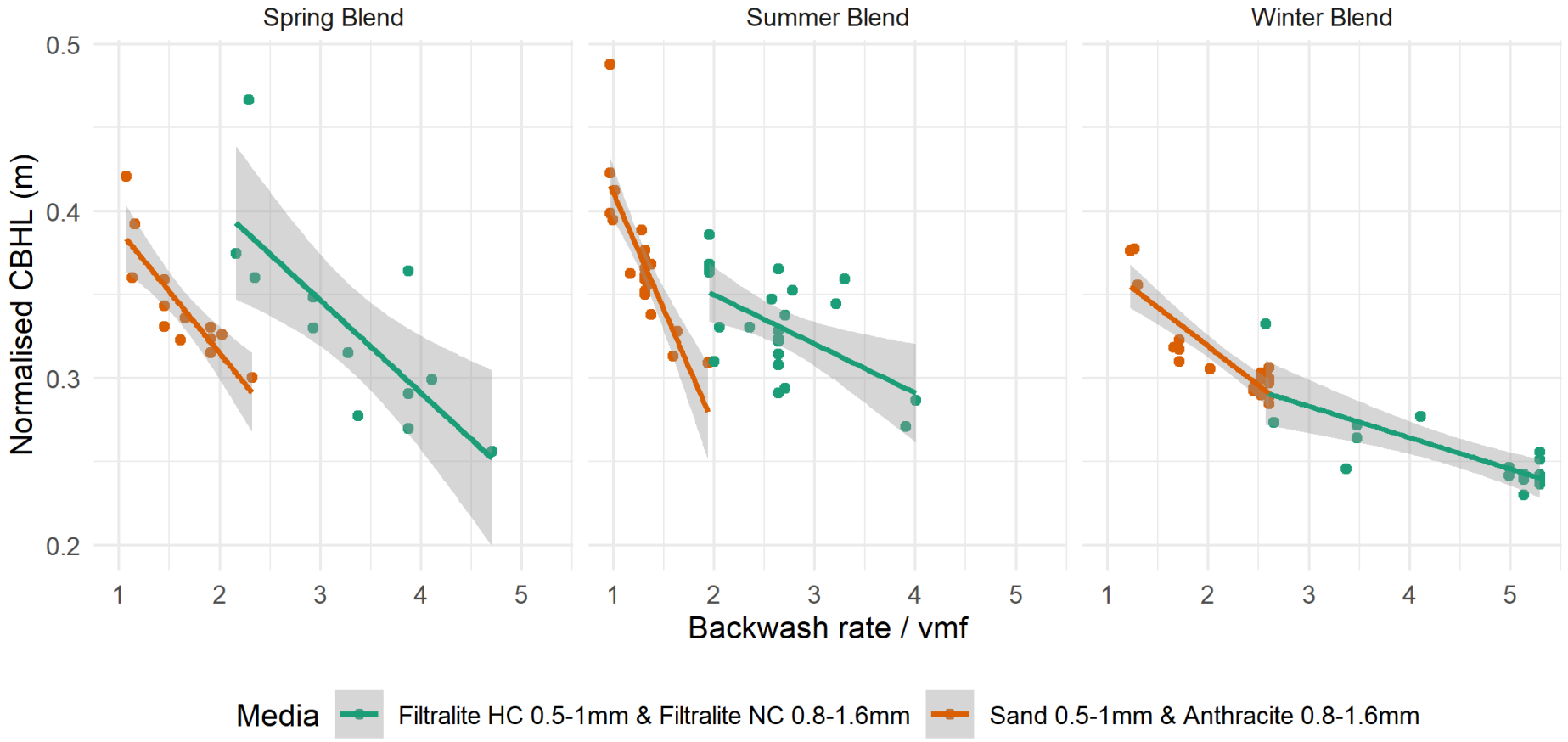

Figure 24. Normalised clean bed head loss plotted against the ratio of high rate backwash rate to minimum fluidisation velocity for the two media across of each of the seasonal blends. Lines indicate linear model fit with shaded area showing standard error of expected value.

4.5.1.3 Volume normalised head loss rate

It is in contrast to previous investigations which involved comparison of larger grades of Filtralite to sand anthracite that the Volume Normalised Head Loss Rate (VNHLR) from the Filtralite bed was higher than that for sand during treatment of each of the blends and across all wash rates (Figure 26). Previous trials using the larger grades have reported lower rates of head loss to sand and anthracite (Davies, 2012; Mikol *et al.*, 2007; Saltnes *et al.*, 2002). There was no strong or consistent relationship between backwash rate and VNHL apparent during treatment of any of the seasonal blends with or without normalising wash rate to the V_{mf} (Figure 25,Figure 26). The higher rate of head loss accumulation by Filtralite, of 6.6 mm/EBV on average compared to 3.27 mm/EBV for sand anthracite, was not consistent with arguments suggesting that improved performance of this media was being driven by higher media porosity. The difference in average VNHL between the two media was greatest during treatment of the summer blend (sand 3.34 mm/EBV, Filtralite 7.65 mm/EBV), this may indicate that higher head loss may in part be driven by additional biofilm formation on the Filtralite media.

Linear mixed models relating VNHL to media and backwash rate suggest that VNHL was significantly ($p < 0.1$) higher than seen for the sand (Table 12, models 5&6). The significant ($p < 0.05$) interaction between absolute backwash rate and media shows that as the backwash rate increased, the difference between head loss accumulation rates of the two media decreased (Table 12, model 5;Figure 25). This may indicate that a more complete re-grading of the Filtralite media may be the reason for the lower hydraulic performance of Filtralite relative to sand. After normalising the wash rate for the V_{mf} of the lower layer, the main effect of using Filtralite was still estimated to significantly ($p < 0.01$) increase the rate of head loss accumulation by 3.3 mm/EBV. There was, however, no longer a significant interaction between media choice and head loss accumulation rate ($p > 0.1$), further indicating that size sorting of the media was an important factor in driving the higher head loss.

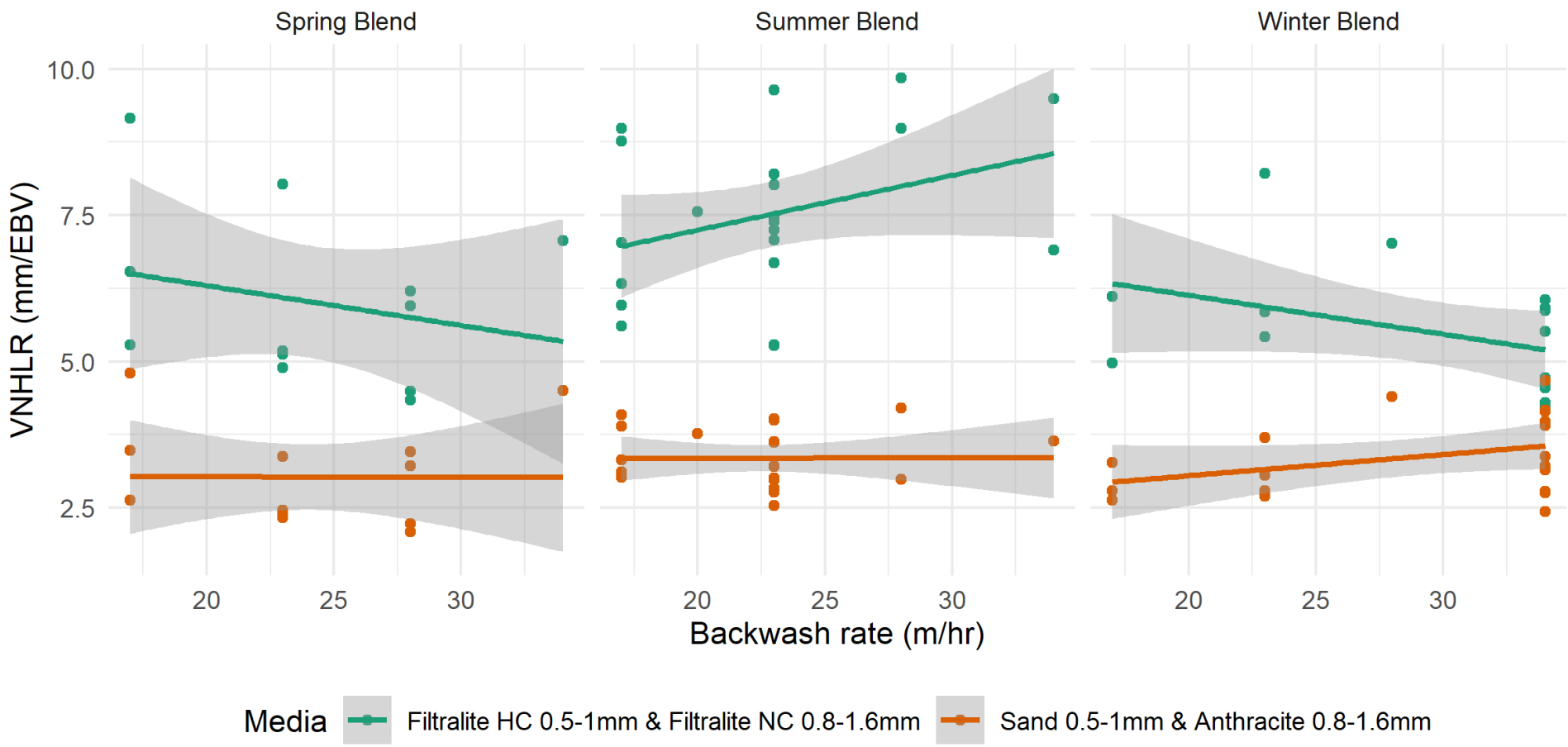

Figure 25. Average of the Volume Normalised Head Loss Rate (VNHLR) (mm/EBV) plotted against backwash rate for the two media across of each of the seasonal blends. Lines indicate linear model fit with shaded area showing standard error of expected value.

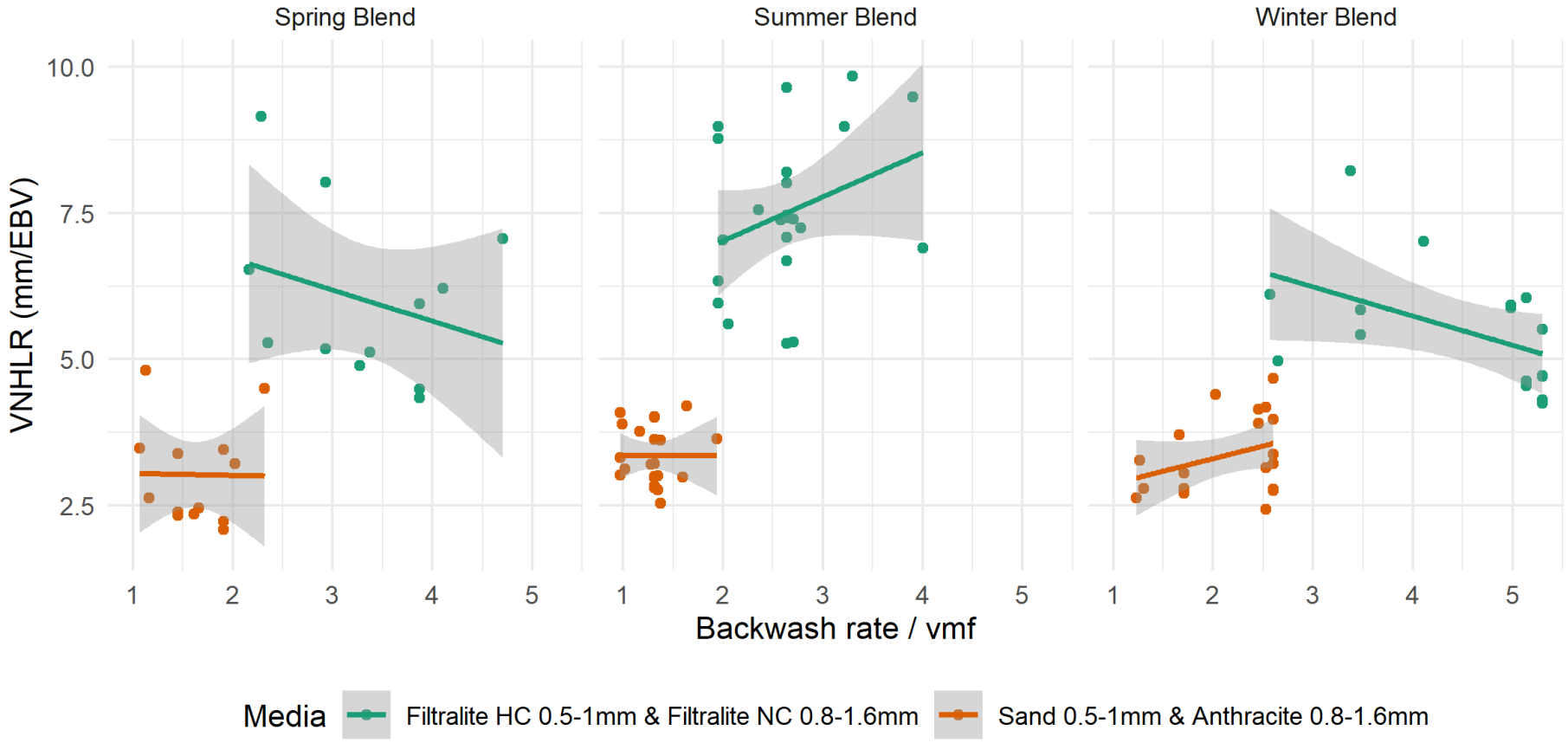

Figure 26 Average of the Volume Normalised Head Loss Rate (VNHLR) (mm/EBV) plotted against the ratio of high rate backwash rate to minimum fluidisation velocity for the two media across of each of the seasonal blends. Lines indicate linear model fit with shaded area showing standard error of expected value.

4.5.1.4 Summary of pilot trials at WTWA

The results presented thus far show that where backwash rates are constrained and solids loading is sufficiently high there are potential performance gains associated with the replacement of sand with Filtralite. Considerable advantage was shown, in terms of delayed breakthrough and media cleanliness at a given wash-rate, associated with the use of Filtralite dual media compared to sand and anthracite where the lower layer is 0.5-1 mm and the upper layer is between 0.8 and 1.6 mm. The fact that, when wash-rates were normalised against minimum fluidisation velocity, there appeared to be no difference in the time to breakthrough between media suggests that the improved performance was driven by improved washing, rather than the primary particle properties of the clean beds. This is supported by the clean bed head loss which was lower at each wash rate for the Filtralite media, but if the wash rates were normalised for the v_{mf} the clean bed head loss was the same as, or higher than, that of the sand – anthracite for the grades tested.

However, the advantages of delayed breakthrough and lower initial head loss did come at the cost of increased loss of head during the filter run. Though it was the conclusion of the investigators that the performance advantage was likely due to the improved washing of the lower density media there are other candidate mechanisms. Greater porosity could provide additional volume for solids to be deposited. Particle characteristics, such as low sphericity or smaller effective size could improve the particle collection efficiency of the media. Poor re-grading performance could result in a low porosity interface region between the media layers resulting in a high localised particle collection efficiency and high head-loss. Greater size sorting of the lower density media could result in a smaller effective size improving particle collection efficiency, but reducing hydraulic efficiency. Six candidate characteristics which could contribute to a performance advantage are summarised in Table 14 and the outcome in terms of the assessed performance metrics which would be expected if each of the characteristics was driving the performance benefit is compared to the observed outcome. Though it is possible that all the characteristics identified could contribute to some extent to the observed performance none, apart from lower media density resulting in improved filter washing, are consistent with the observed results.

Table 14. Summary of observed and expected outcomes if different media characteristics were responsible for driving performance. The colour of text indicates if the expected result for a potential mechanism is consistent with the observed results (Red = inconsistent with experimental observations, Green = consistent with experimental observations, orange = neither consistent or inconsistent with experimental observations.

Potential mechanisms	Time to BT	CBHL	VNHL
Observed in pilot trials at WTW A	Strongly significant increase with wash rate for winter blend.	Strongly significant decrease with wash rate	Weak & inconsistent relationship with wash rate
Porosity responsible for performance	No significant relationship with wash rate.	No significant relationship with wash rate.	No significant relationship with wash rate.
Particle shape responsible for performance	No significant relationship with wash rate.	No significant relationship with wash rate.	No significant relationship with wash rate.
Lower effective size. responsible for performance	No significant relationship with wash rate.	No significant relationship with wash rate.	No significant relationship with wash rate.
Low porosity interface layer responsible for performance	Decreases with wash rate	Decreases with wash rate	Decreases with wash rate
Size sorting of lower layer responsible for performance	Increases with wash rate	Increases with wash rate	Increases with wash rate
Lower density (resulting in improved washing) responsible for performance	Increases with wash rate	Decreases with wash rate	No significant relationship with wash rate.

4.5.2 Full scale trial: Sand-anthracite filter with insufficient backwash

After the pilot trials, the low-density media was trialled at full scale at WTW A. A dual media filter consisting of Filtralite HC (700 mm deep, media size 0.5-1 mm) below anthracite (300 mm and 0.8-1.6 mm) replaced a single sand-pumice filter at WTW A. This was a slightly different configuration to the pilot testing that was conducted. Filtralite NC has a low density and porous structure which entrains air and this results in buoyancy of a fraction of the material upon initial contact with water. Over time, with soaking, the effective density of a Filtralite NC particle approaches that of anthracite (Eikebrokk and Saltnes, 2001). As pilot trials indicated that the main performance advantage from new media at WTWA was the effective cleaning of the lower (previously sand) layer anthracite was selected for use instead of Filtralite NC of the same size to minimise any risk associated with media loss and reduce the time and cost associated with media replacement.

During the full-scale trial the performance of the new media was compared to the performance of a neighbouring bed which retained the previous sand (0.6-1.2 mm) and pumice (unknown mm) media. The performance was initially trialled during treatment of the winter blend which has historically challenged filtration performance and progressed in four phases. First the filters were operated with the same hydraulic loading rate and backwashed on a time at between 21 and 37 hours, run times were reduced as plant performance deteriorated towards the end of the year. During phase 2 the filter run time for the trial media was extended up to 48 hours whilst the comparison filter run time remained between 20 – 25 hours. In the third phase backwashing was initiated at the same time whilst the hydraulic loading rate on the trial filter was increased by 20%. During phase 4 the new filter media continued to be operated at a higher hydraulic loading rate as the raw water blends were changed until the media in the comparison filter was replaced in August 2018. The performance improvement associated with using Filtralite - anthracite is summarised with run statistics including mean flow, max head loss, run time, the 95 percentile turbidity (95 %ile), mean turbidity and unit filter run volume (UFRV) (Figure 27, Table_Apx 4). Through phases 1-3 the water temperature dropped and this was accompanied by increasing turbidity in the clarified water (Figure 27 K &L) this period has been historically associated with poor filter performance and repeated low level detections

of *Cryptosporidium*. Reduced pre-treatment performance due to short flocculation times and shallow dissolved air flotation tanks is a known issue at this WTW.

Use of the lower density media resulted in a improvements in UFRV during key periods of operational challenge without elevated turbidity (Figure 27 A-D &J). During phase 2 the average UFRV for the Filtralite anthracite (141 EBVs) bed was 72% greater than that for the pre-existing media (83 EBVs). The turbidity observed during phase 2 from the trial bed (mean of run means 0.04, mean of run 95th %iles 0.09 NTU) was typically equivalent to the comparison filter (mean of run means 0.04, mean of run 95th %iles 0.10 NTU). During phase 3 the trial media produced an additional 16 empty bed volumes of water whilst producing lower turbidity water with an average mean run turbidity of 0.03 NTU compared to 0.05 for the old media. The extent of turbidity spiking was also reduced with the 95th percentile for each filter run averaging at 0.04 NTU compared to 0.13 NTU for the older media. Through phase 4 as the water temperature increased and the blend of water treated was changed and the solids loading onto the filters reduced the productivity of the low-density media remained higher but no benefit in terms of run-average turbidity was observed. The lower density media did appear to consistency reduce the extent of turbidity spiking, for each of the three trial phases the mean of the 95th%ile filter run turbidity was lower for the Filtralite trial (P1 0.04, P2 0.09, P3 0.04, P4 0.05) than for the pre-existing media (P1 0.06, P2 0.10, P3 0.13, P4 0.07). Broadly the quality benefits observed at full scale were in line with that observed during pilot trials.

During the early weeks of the full scale alternative media trial, elevated ripening phase turbidity was apparent for the low density bed when compared to the pre-existing sand anthracite but the difference reduced as the trial progressed (Figure 27 E). The turbidity of the first four bed volumes of each filter run was, on average 0.18 for the trial media and 0.04 for the pre-existing media during phase 1 but this reduced to a 0.03 NTU difference by phase 3. The relatively high ripening turbidity of the new trial media during the initial stages of the trial could have been due to the release of fine particles and the chemical and biological conditioning of media particles over this period. It is likely that slightly higher ripening turbidity observed for the trial media compared to the sand in phase 4 of the trial is likely due to reduced packing density from greater bed expansion and relative backwash efficiency. The normalised clean bed head -loss for the new media increased from 0.04 m to 0.2 m over the trial period

with the most rapid increase taking place over the first 6 weeks and a slower rate of increase thereafter (Figure 27 G). The NCBHL observed in the pre-existing media varied considerably with temperature over the trial period. Over the trial period between November and March the NCBHL for the pre-existing media decreased from 0.3 to 0.2 m, indicative of improved backwash performance, over a period with declining water temperature from 11°C to 2°C and therefore increasing backwash bed expansion (Figure 27 G). There is no temperature adjustment of the backwash rate at WTW A. Over the trial period presented the Volume Normalised Head Loss (VNHL), as defined in Equation 30, exhibit different behaviour for the trial media but both mirror the trend observed in (Figure 27 H & G). VNHL for the trial media exhibits a rapid decline from 11 mm/EBV early in phase 1 to averaging 4 mm/EBV in phase 3. It is likely that this is due to the increasing loss of media fines from the bed during the backwash as the water cools. A useful observation from the full-scale trial, particularly in that it deviates from what was observed in pilot scale testing, is that the VNHL for the trial media (3.3 mm/EBV) was lower than the pre-existing media (6.8 mm/EBV) during phase 4. This indicates that over time deposits accumulating between washes in the conventional media could potentially lead to poorer hydraulic performance over the summer. It is likely that the presence of this deposited material did lead to more effective particle capture and lower average filtered water turbidity at the end of phase 3 during July (Figure 27, C). The occasional breakthrough of this material did also lead to more spikes being observed in filtered water turbidity meaning that on average during phase 3 the 95^{th} percentile turbidity for each run the pre-existing media was higher (0.07 NTU) than the low density trial media (0.05 NTU).

Figure 27. Comparison of filter run summary statistics between filter 6 with the trial media and filter 7 with the pre-existing media during the full-scale trial at WTW A. Plots compare: A- run time (hours), B- filtration rate (m/hr), C- average turbidity (NTU), D- 95th percentile turbidity (NTU), E- ripening turbidity summarised by 95th percentile turbidity during first 4 bed volumes of the run (NTU), F- terminal turbidity summarised by average turbidity during final hour of run (NTU), G-Normalised Clean Bed Head Loss (m), H- Volume Normalised Head Loss (mm/EBV), I- Terminal Normalised Head Loss (m), J- Unit Filter Run Volume (m3/m2/run).

Overlayed filter run turbidity profiles from the full-scale trial filter using Filtralite-anthracite are shown in comparison to the neighbouring filter using the pre-existing 14/25 filter sand (0.6-1 mm) and pumice (Figure 28). The treated water turbidity is shown for the Filtralite - anthracite filter treating an additional 20% flow (4 m/hr compared to 3.3 m/hr) compared to the existing sand-pumice filter (Figure 28a) and an extended filter run of up to 48 hours for the Filtralite - anthracite filter bed (Figure 28b). The turbidity spikes which can be seen in the filter profile for both types of media were associated with hydraulic shocking consistent with that seen in previous investigations (Glasgow and Wheatley, 1998; Han *et al.*, 2009a; Huck *et al.*, 2001). Despite greater hydraulic loading the Filtralite - anthracite can be seen to reduce the extent and delay the onset of turbidity spiking in the trial filter in response to these flow surges.

This case study demonstrates the useful application of a low-density media to improve filtration performance by mitigating design constraints with the existing process. The 0.5-1 mm Filtralite HC & 0.8-1.6 mm anthracite could be more effectively backwashed at the available wash rate (21 m/hr). Ineffective cleaning of the pre-existing 0.6-1.2 mm sand & pumice (unknown size) media resulted in the retention of deposits between filter washes. Variation in the condition of the pre-existing media due to poor washing led to elevated clean bed head loss and breakthrough of particles. The low density dual media configuration prevented elevated solids in the clarified water during cold temperatures from breaking through. As a result of this trial, the replacement of the media in all the filters at the WTWs has now been completed based on the successful trial. The effective performance recovery of the media during the filter backwash means that filter run times are no longer constrained during cold water conditions, reducing the volume of backwash water produced, meaning that the backwash water system is no longer hydraulically overloaded. In order to manage *Cryptosporidium* risk daily sampling of the final water at WTW A has been conducted since 2015. Between 2015 and 2018 there were on average 2.5 *Cryptosporidium* detections (low level) each year. At the time of re-writing (Feb 2021) there has only been 1 *Cryptosporidium* detection (low-level & associated with a specific coagulant

dosing issue) in the final water with continued daily sampling since the media replacement was completed.

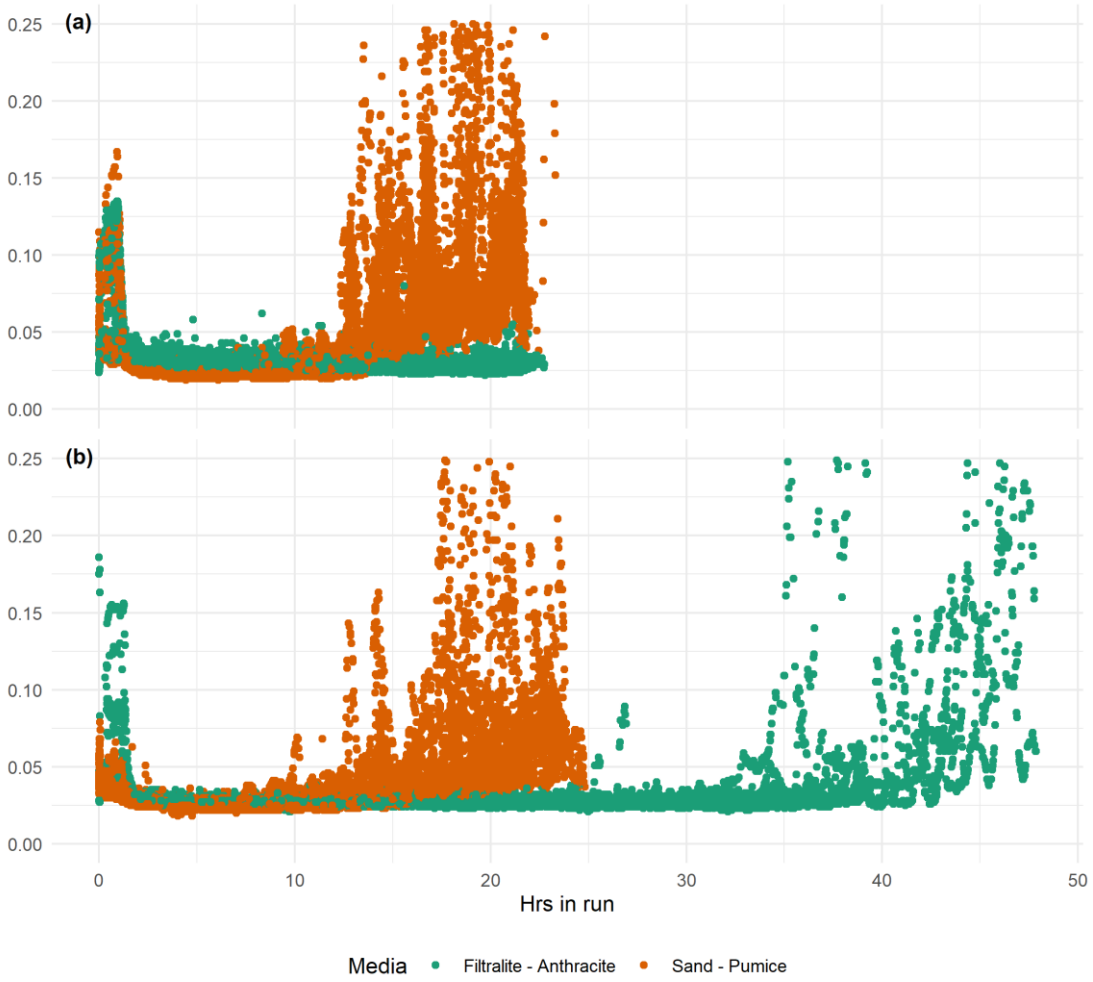

Figure 28. Overlaid filter run turbidity profiles from multiple runs during full scale trial of low density media at WTW A. Performance of trial filter using Filtralite HC 0.5-1 mm & Anthracite 0.8-1.6 mm is contrasted to its immediate neighbour which continued to use the previous 14/25 silica sand and pumice media. a) comparison of the performance of the two filters during phase 3 when the trial filter 6 is treating 20 % more flow than filter 7 but filter run times were set to 24 hrs. b) comparison of the performance during phase 2 at equal flow but when the run duration for filter 6 was extended.

4.5.3 Pilot trials 2: Direct coarse mono-media filter with combined air & water phase and sub-fluidising rinse

Further pilot trials were conducted at WTW B to assess the potential replacement of coarse sand in a deep-bed non-fluidising mono-media sand filter with a similar-sized lower-density media which would effectively fluidise at the backwash rate delivered in these filters (17 m/hr). These pilot trials were conducted during August and September when water temperature was at its highest and therefore bed expansion would be at its lowest. Filtration rates were maintained at 4 m/hr throughout. Turbidity profiles of pilot trials comparing the performance of sand to Filtralite showed that the lower density Filtralite media reliably produced acceptable quality water for more than 36 hours whilst the sand media frequently failed to produce water of acceptable quality and at most managed to produce water of acceptable quality for 24 hours (Figure 29). Analysis of variance for mean filter performance in the 24th hour (92-96 empty bed volumes) of operation showed turbidity for the Filtralite column (0.05 NTU) was on average 0.66 NTU less than the sand column (0.72 NTU) (0.05 NTU) (one-way ANOVA, $p= 3x10^{-4}$). In addition to the apparent quality benefits the hydraulic performance of the Filtralite in the pilot trials was considerably better than sand. The more effective recovery of void space in the media resulted in consistently lower head loss accumulation as well as lower CBHL (Figure 30). Head loss for the Filtralite (1.19m) during the 24^{th} hour was on average 1.54 m less than the sand (2.73 m) (one-way ANOVA, $p= 3x10^{-8}$). On average the CBHL for Filtralite was 0.2m compared to 0.5m for sand. Average VNHL for the Filtralite bed was 10.5 mm/EBV compared to 22.6 mm/EBV for sand. The performance of sand within the pilot column was considerably worse than the performance of the full-scale filters at WTWB which at the time were treating the same feed water to below 0.1 NTU at a hydraulic loading rate of 3.6 m/hr for 22 hours. Though the backwash rates used in the pilot plant replicated those used on the full-scale filters transport of solids from the bed at full scale was supported with a surface wash which was not effectively replicated in the pilot column. Despite using a larger volume of rinse water (to compensate for the lack of a surface wash in the pilot columns

which was used in the full scale filter), backwash performance of the sand media was insufficient to maintain consistent filtration performance.

Despite backwashing of the Filtralite mono-media filter using separate air and water wash phases (compared to air & water used for the sand) and a reduced volume of wash water Filtralite was able to operate at a UFRV (to 0.1 NTU) of >150 m^3/m^2 (min 152, avg 180 m^3/m^2) typically double or more than that of either the sand column (<80 m^3/m^2) or the filters on the full-scale plant (80 m^3/m^2), which could take advantage of the cross-wash facility. The Degremont Aquazur V Filter applies a combined air and water backwash to promote a collapse pulse condition during the filter wash and a surface wash to clear dirt from above the media. Considering the observations seen in the pilot trials with the fine-grained HC Filtralite materials, it was likely that increases of 100 % or more in the solids handling capacity of the larger Filtralite media grades was not solely attributable to a 40 % relative increase in primary porosity compared to sand. Differences in the recoverable porosity due to the increased efficiency of washing of the primary filter was assumed to contribute to this performance improvement. It has been shown previously that filters using a combination of air and water generate greater turbulence which is effective for dislodging solids from media grains (Amirtharajah, 1993). This additional turbulence, however, is likely to reduce the efficiency of transport of dislodged solid through the water column and into the launder (Han *et al.*, 2009b). Effective expansion of a lower density media not only prevents re-capture of floc dislodged during the air scour & collapse-pulse phase, but also increases the vertical velocity of the water column in the freeboard area of the filter increasing the speed of transport of dislodged solids into the backwash channel.

There are two key engineering arguments against the expansion of a coarse sand filter during the rinse phase of a wash. Firstly, the wash rate required is very high which increases energy costs and limits the maximum plan area of a filter for a given size of WTW. The second is that expansion of the bed will re-grade the media such that the smallest grains will rise to the top of the bed reducing the hydraulic efficiency of the bed and lead to high head loss. These arguments do

not appear to apply to the conversion of sand filters to Filtralite media. The lower density of Filtralite means that expansion occurs at much lower rise rates making bed expansion practical and economical in large filters. Secondly, head losses after expansion of Filtralite remain lower than the equivalent grade of sand which has not been fluidised during the backwash (Figure 30). This is at least partially attributable to the higher porosity of the filter media. However, it may be worth considering the role of an apparent variation in density between Filtralite particles in preventing size-sorting as apparent differences in density were visually observed, but not quantified, in this investigation. Tailored experiments will be of value to ascertain if variance in particle density is reducing the size sorting of Filtralite during the backwash. If so, this is a property which could be exploited further to engineer more ideal deep-bed mono-media materials. By mixing media materials of the same particle size distribution, but with an advantageous density difference, it could be possible to retain the benefits of bed-expansion during the rinse whilst reducing the hydraulic disadvantages associated with size-sorting.

Pilot trials indicated that it was possible to overcome limitations to the washing of deep bed coarse non-fluidising sand filters such as those at WTW B, which typically have an upwash rate of 14 to 18 m/hr. Pilot trials have shown that though operating with only a separate air and water wash, the Filtralite could be recovered more effectively with the available air and water rates than can be achieved by the combined air and water washing of sand. However, previous investigators have concluded that, over the medium to long term, filters require backwashing with combined air and water in order to maintain the condition of the media bed (Chipps *et al.*, 1995). In order to effectively switch from a coarse sand non-fluidising bed to a fluidising low density Filtralite bed, some operational changes to the back wash would be required. In the example of WTWB it would no longer be possible to operate with extended combined air and water wash phase (i.e. with water spilling over weirs / launders during the combined phase) or a concurrent rinse and surface wash as this would risk excessive loss of the low-density media.

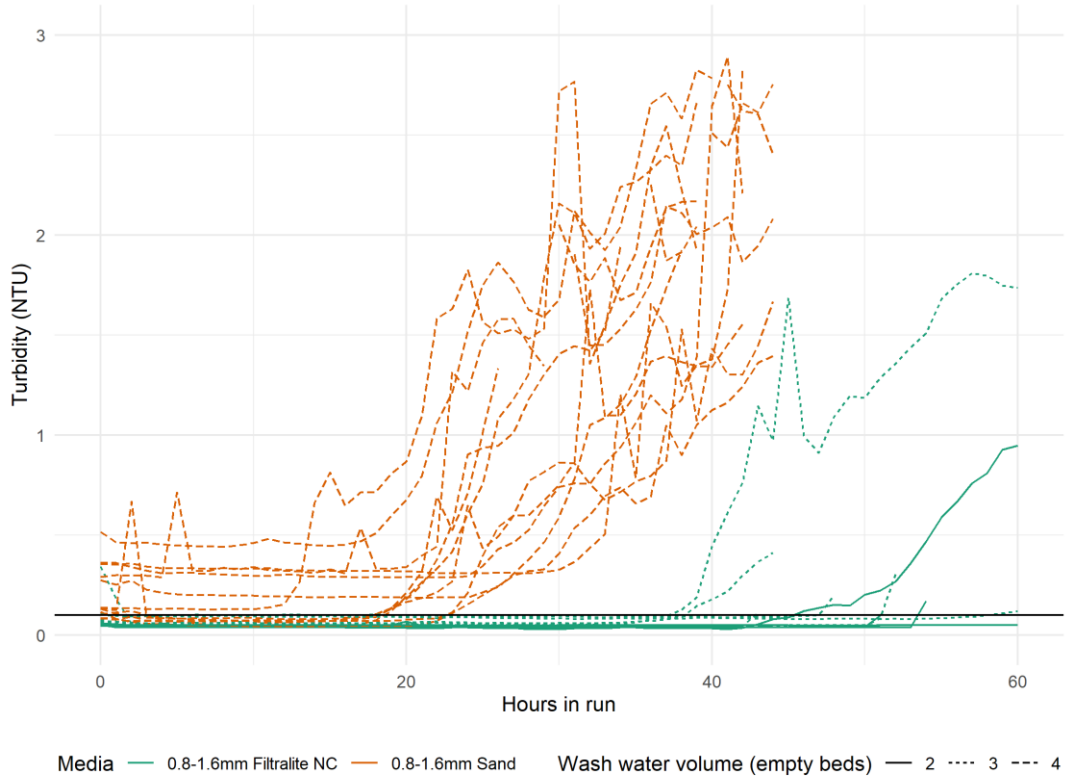

Figure 29. Turbidity profiles for pilot trials at WTW B. The hourly average turbidity values for pilot filter runs are plotted comparing filtered water quality from the sand and Filtralite media. Consistently lower turbidity and delayed breakthrough is apparent from the Filtralite media.

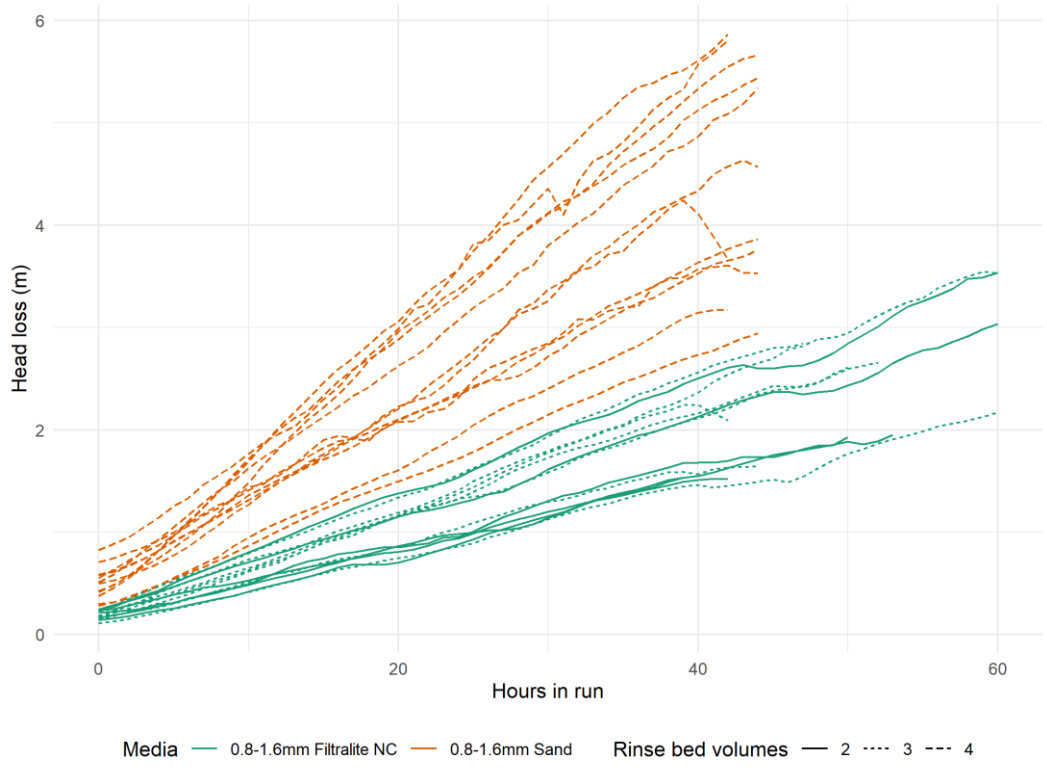

Figure 30. Head loss profiles for pilot trials at WTW B. The hourly average differential pressure values for pilot filter runs are plotted comparing hydraulic performance of the sand and Filtralite media. Consistently lower head loss is apparent from the Filtralite media.

4.6 Discussion

The results of the investigation presented in this paper go some way to explaining the driving mechanisms for performance benefit in certain circumstances. It is however likely that the driving mechanism for performance benefits from Filtralite in comparison to sand are contingent on three broad scenarios of which the results presented in this investigation are relevant to the third:

1. Under conditions where wash performance is not a constraint and Filtralite replaces sand of equal size and depth fundamental filtration theory indicates that a higher porosity media will have a lower particle capture efficiency reducing the potential for blinding (Rajagopalan and Tien, 1976). Where there is sufficient depth to maintain the same quality hydraulic and solids handling benefits are likely available due to the increased voidage

and more efficient storage across the depth of the bed. Further benefits may be available due to shape characteristics.

2. In conditions where the wash performance is effective for the grade of sand used in addition to the benefits in scenario 1 additional hydraulic and solids handling benefits are available if the lower density Filtralite allows the effective use of a larger media or dual media configuration which would not be effectively washed if conventional sand was used. Mikol et al (2007) show, that replacement of a fine (0.6-1.2 mm) sand and anthracite (1.7-2.5 mm) media in a roughing filter with a dual media combination of (0.8-1.6 and 1.5-2.5 mm) improved hydraulic performance with a rinse of 3.75 EBVs at 45 m/hr. Implicitly described is a filter with a hydraulic performance issue arising from blinding of the fine sand which has been overcome by the use of a larger Filtralite media, and for which an equivalent increase in the size of the sand would have compromised the re-grading of sand and anthracite layers at the available wash rate.

3. In conditions where the existing backwash facilities are inadequate and are limiting the performance of sand it is possible to deliver operational and water quality benefits from using material of lower density which can be more effectively washed at the available backwash rate.

The observations from pilot trials in this are broadly in line with brief observations from previously conducted pilot trials that Filtralite can be used as other low density media are to improve performance of filters with sub-optimal backwashing (Bayley *et al.*, 2006; Mörgeli and Ives, 1979). However, the use of Filtralite is not as widespread as the backwash design issues which it can be used to mitigate. Given the tendency for many fluidising filters in the UK to be designed to achieve bed expansion of less than 4%, and the widescale occurrence of non-fluidising coarse mono-media filters (including those without a supplementary surface wash), the application of lower density filter media offers the opportunity to improve the performance a large-number of filters in the UK. Reported unfavourable water quality resulting from using coarse media in relatively shallow (<1m) filter beds that are common to many UK mono-media filters (depths below

800 mm) has likely in the past contributed the limited use of Filtralite (Davies and Wheatley, 2012; Kawamura, 1999). With a growing range of alternative Filtralite products, of different grades and density, and an improved understanding of the mechanisms that drive performance gains from low density media it is now possible to specify a low-density media solution to a broader range of filtration issues.

In the presented research, pilot and full-scale trials have demonstrated the successful exploitation of the lower density of Filtralite to deliver operational and water quality benefits for filters where the combination of existing media and backwash systems were limiting filtration performance. The first pilot and full-scale trials (WTWA) illustrate the effective application of a dual media including 1800 kg/m^3 Filtralite HC 0.5-1 mm rather than sand of equivalent size. Improved backwashing of the lower density media allowed the filters to operate with an extended run time by delaying the breakthrough of solids during the critical operational period with seasonally high solids load. We can deduce, from the fact that head loss accumulation was greater for the Filtralite than for the sand throughout this trial, that the mechanism driving this improvement was not the greater reported voidage of Filtralite. The observation that the performance gains of the Filtralite, in comparison to sand, reduced at higher backwash rates suggests that this was a result of the relatively effective backwash of filtralite at lower backwash rates.

The second (WTWB) demonstrates the conversion of a sand filter that was not effectively fluidised during the rinse into one that could be fluidised and more effectively rinsed while using the same wash rate. Performance gains were seen with respect to increased filter run time while achieving a similar or better filtered water quality. These improvements were based on exploiting the density difference between two granular media materials that resulted in improved cleaning and grading of media during the filter backwash given the pre-existing constraints of the backwash system.

The trials conducted in this investigation indicate that low density media is likely to be worth considering as a solution to the following operational challenges:

- Where solids loading leads to premature filter breakthrough or rapid head loss development in an existing fine sand filter. If run times or water quality risk are impacted and backwash rates are insufficient to re-grade a sand-anthracite filter, use of a fine grade of Filtralite may allow conversion of a filter into an effective dual media filter without upgrading the backwash system.

- Where inadequate backwash flow has resulted in ineffective regrading of a sand-anthracite filter bed, use of Filtralite will afford opportunities for improvements in water quality.

- Filters consisting of a deep layer of a coarse media that have backwash rates that do not enable full fluidisation rinse-rates would also benefit from conversion to a lower density media which will expand with the available backwash rates. Those filters that have a large distance to transport dislodged solids (in other words with a deep free board) and without a surface wash would particularly benefit such an upgrade.

- In circumstances where shorter filter run times has caused hydraulic overloading of the wash water system causing an increased risk of environmental pollution or excessive process water losses.

If the drivers for considering an alternative media are one of those listed, it is then necessary to identify the key design constraints which impact the selection of a media replacement. These have been identified as: the availability of driving head; hydraulic and solids loading; the rise rate that can be achieved by the backwash pump and wash water pipework; the maximum water temperature; and the height of the launder from the filter floor(Beverly, 2005; Logsdon *et al.*, 2002). In many cases the cost and complication associated with increasing the wash rate to achieve an equivalent level of performance will be considerable. There can be economic, environmental and water quality advantages to the use of low-density media, but the relative importance of these advantages is likely to be site specific. In systems where it is possible just to install a new pump in order to improve performance with greater bed expansion, the economics of replacing all

of the media may not be advantageous. However, when upgrading ageing filters, built decades ago, there are many hidden costs associated with increasing the backwash rate. Firstly, it may not be possible to source enough backwash water. It is not uncommon to source wash water directly from the filtered water channel, and depending on the filtration area per filter, the number of filters and the size of the sand, the backwash rate can exceed the plant flow. In such cases, where additional large concrete tanks need to be built to store the backwash water, replacement of the media becomes a relatively low cost option. Similarly, the pipework, underdrain and power supplies to a WTW may be insufficient to allow the additional pumping required to achieve greater expansion of the sand. Where media replacement is required and conducted at the end of the sand filter's operational life, the filter upgrade to low density media can be achieved at a fraction of the cost of realising the same or lower levels of performance from conventional media through improved washing.

Improving media expansion within a filter bed by switching to a lower density media is not without risk and the greatest risk is that of media loss over the weir. Dry Filtralite NC (0.8-1.6 mm) has a reported mean density of 1280 kg/m^3. However, the variance in grain size and density is such that before the material is fully saturated there is a buoyant fraction. Careful material handling and additional preparation of this media is required for effective use at full scale. The risk of media loss in some of the applications described can be reduced by using anthracite in combination with the higher density Filtralite NC, as demonstrated during the full-scale trial at WTW A. If bed expansion or depth is to be increased it is necessary to have adequate freeboard between the surface of the media and the launder. Many older filters use a nozzle with slits larger than the diameter of the media grain. Such nozzles require a support media which retains the filtration media to prevent it from passing through the nozzle. In many cases these older nozzles can be replaced with ones that have a greater number of finer slits, which retain the media whilst maintaining similar head loss characteristics without the need for support media. Therefore, the depth gained can be used for expanding the bed with the secondary advantage of increasing the driving head.

4.7 Conclusions

- Mono-media 0.5-1 mm or 0.6-1.2 mm sand filters backwashed at >22 m/hr in order to achieve <5% bed expansion can be successfully converted to dual media filters with extended run times by using the combination of Filtralite HC (0.5-1 mm) and either Filtralite NC or Anthracite (0.8-1.6 mm) without requirement for upgrades to backwash provision.

- Under backwash constrained conditions 17-34 m/hr Filtralite (HC 1800kg/m^3 at 0.5-1 mm) in combination with lower density Filtralite (NC 0.8-1.6 mm) or Anthracite (0.8-1.6 mm) can be used to improve the solids handling capacity of a sand-anthracite bed of an equivalent grade.

- Deep-bed coarse non-fluidising 10/18 sand (0.85-1.7 mm) filters with rinse rates in the region of 15-18 m/hr can be converted to fluidising mono-media filters with greater solids handling capacity using Filtralite NC (0.8-1.6 mm). This is particularly advantageous if there is no surface wash facility.

- More effective washing of a Filtralite media relative to sand for a given grain size and wash rate enables Filtralite to more effectively recover its primary porosity and accept a greater solids loading, delaying breakthrough of turbidity.

- The improved wash performance achieved by switching to Filtralite media was shown to mitigate the water quality risk associated with sub-optimal hydraulic control of a rapid gravity filter and the premature breakthrough of weak NOM floc in full scale trials.

- The improved understanding of the mechanisms driving the comparative performance advantage associated with using Filtralite can allow municipal water suppliers to more effectively exploit the material to economically improve the filtration performance of filters with outmoded design.

4.8 References

Amburgey, J. E., Amirtharajah, A., Brouckaert, B. M., & Spivey, N. C. (2003). An enhanced backwashing technique for improved filter ripening. *Journal of the American Water Works Association*, *95*(12), 81-94.

Amirtharajah, A. (1993). Optimum backwashing of filters with air scour: a review. *Water Science and Technology*, *27*(10), 195-211.

Amirtharajah, A., McNelly, N., Page, G., & McLeod, J. (1990). *Optimum backwash of dual media filters and GAC filter-adsorbers with air scour.* Denver: AWWA Research Foundation

Anderson, C.W. (2005). Turbidity, in *National field manual for the collection of water-quality data*. 9th edn. Reston, VA: USGS, pp. 1–55.

Bache, D. H., & Gregory, R. (2010). Flocs and separation processes in drinking water treatment: a review. *Journal of Water Supply: Research and Technology—AQUA*, *59*(1), 16-30.

Bates, D., Maechler, M., Bolker, B., & Walker, S. (2014). lme4: Linear mixed-effects models using Eigen and S4. R package version 1.1-7. available at https://cran.r-project.org/package=lme4

Bayley, R. G. W., Chipps, M. J., Steele, M. E., White, R., Mikol, A., & Fitzpatrick, C. S. B. (2006). 'Alternative low density media for use in biological roughing filtration prior to slow sand filtration'. in Gimbel, R., Graham, NJD and Collins, MR (Ed.s), *Recent Progress in Slow Sand and Alternative Biofiltration Processes,* London: IWA Publishing, 460-464.

Beverly, R. P. (2011). *Filter troubleshooting and design handbook*. Denver: American Water Works Association.

Brandt, M. J., Johnson, K. M., Elphinston, A. J., & Ratnayaka, D. D. (2016). *Twort's water supply*. Oxford: Butterworth-Heinemann.

British Standards Institution. (1989) *BS 1796-1: Test sieving*. London:BSi.

Cescon, A., Jiang, J. Q., Haffey, M., Moore, G., & Callaghan, K. (2016). Assessment of recycled glass and expanded clay in a dual media configuration for drinking water treatment. *Separation Science and Technology*, *51*(14), 2455-2464.

Chipps, M. J., Bauer, M. J., & Bayley, R. G. (1995). Achieving enhanced filter backwashing with combined air scour and sub-fluidising water at pilot and operational scale. *Filtration & Separation*, *32*(1), 55-63.

Crittenden, J. C., Trussell, R. R., Hand, D. W., Howe, K., & Tchobanoglous, G. (2012). *MWH's water treatment: principles and design*. Hoboken, New Jersey: John Wiley & Sons.

Davies, P. D., & Wheatley, A. D. (2012). Pilot plant study of alternative filter media for rapid gravity filtration. *Water Science and Technology*, *66*(12), 2779-2784.

Davies, P.D. (2012) *Alternative filter media in rapid gravity filtration of potable water*. PhD thesis. Loughborough University. available at https://dspace.lboro.ac.uk/2134/12183

Eikebrokk, B., & Saltnes, T. (2001). Removal of natural organic matter (NOM) using different coagulants and lightweight expanded clay aggregate filters. *Water Science and Technology: Water Supply*, *1*(2), 131-140.

Eikebrokk, B., Vogt, R. D., & Liltved, H. (2004). NOM increase in Northern European source waters: discussion of possible causes and impacts on coagulation/contact filtration processes. *Water Science and Technology: Water Supply*, *4*(4), 47-54.

Fitzpatrick, C. S. B. (1998). Media properties and their effect on filter performance and backwashing. *Water Science and Technology*, *38*(6), 105-111.

Glasgow, G. D., & Wheatley, A. D. (1998). The effect of surges on the performance of rapid gravity filtration. *Water Science and Technology*, *37*(2), 75-81.

Han, S. J., Fitzpatrick, C. S. B., & Wetherill, A. (2009). Simulation on combined rapid gravity filtration and backwash models. *Water Science and Technology*, *59*(12), 2429-2435.

Han, S., Fitzpatrick, C. S., & Wetherill, A. (2009). The impact of flow surges on rapid gravity filtration. *Water Research*, *43*(5), 1171-1178.

Hendricks, D. W. (2006). *Water Treatment Unit Processes Physical and Chemical*; Boca Raton, Florida. CRC Press.

Hipp, R.D. (2020) *SQLite.* available at https://www.sqlite.org/index.html

Hlavac, M. (2015). stargazer: *Well-Formatted Regression and Summary Statistics Tables.* R package version 5.2. http://CRAN.R-project.org/package=stargazer

Huck, P.M., Emelko, M.B., Coffee, B.M.M, Maurizio, D.D. and O'Melia, C.R. (2001). *Filter operation effects on pathogen passage*. Denver: AWWA Research Foundation and American Water Works Association.

Huck, P. M., Coffey, B. M., Emelko, M. B., Maurizio, D. D., Slawson, R. M., Anderson, W. B., ... & O'Melia, C. R. (2002). Effects of filter operation on Cryptosporidium removal microbial pathogens. *Journal of the American Water Works Association*, *94*(6), 97-111.

Ives, K. J. (1970). Rapid filtration. *Water Research*, *4*(3), 201-223.

Jarvis, P., Jefferson, B., & Parsons, S. A. (2005). How the natural organic matter to coagulant ratio impacts on floc structural properties. *Environmental Science & Technology*, *39*(22), 8919-8924.

Kawamura, S. (1999). Design and operation of high-rate filters. *Journal of the American Water Works Association*, *91*(12), 77-90.

Logsdon, G., Hess, A., Chipps, M. J., & Rachwal, A. (2002). *Filter maintenance and operations guidance manual*. Denver:Awwa Research Foundation and American Water Works Association.

Mann, A. G., Tam, C. C., Higgins, C. D., & Rodrigues, L. C. (2007). The association between drinking water turbidity and gastrointestinal illness: a systematic review. *BMC Public Health*, *7*(1), 1-7.

Mikol, A., Fitzpatrick, C. S. B., Chipps, M. J., Steele, M. E. J., & Bayley, R. G. W. (2007). Novel dual media combination for drinking water treatment. *Water Science and Technology: Water Supply*, *7*(5-6), 131-139.

Mörgeli, B., & Ives, K. J. (1979). New media for effluent filtration. *Water Research*, *13*(10), 1001-1007.

Pagano, T., Bida, M., & Kenny, J. E. (2014). Trends in levels of allochthonous dissolved organic carbon in natural water: a review of potential mechanisms under a changing climate. *Water*, *6*(10), 2862-2897.

R Core Team. (2015) *R: A Language and Environment for Statistical Computing* Vienna, Austria. available at https://www.r-project.org/.

Rajagopalan, R., & Tien, C. (1976). Trajectory analysis of deep-bed filtration with the sphere-in-cell porous media model. *AIChE Journal*, *22*(3), 523-533.

Rebhun, M., Fuhrer, Z., & Adin, A. (1984). Contact flocculation-filtration of humic substances. *Water Research*, *18*(8), 963-970.

Saltnes, T., Eikebrokk, B., & Ødegaard, H. (2002). Contact filtration of humic waters: performance of an expanded clay aggregate filter (Filtralite) compared to a dual anthracite/sand filter. *Water Science and Technology: Water Supply*, *2*(5-6), 17-23.

Schöntag, J. M., & Sens, M. L. (2015). Effective production of rapid filters with polystyrene granules as a media filter. *Water Science and Technology: Water Supply*, *15*(5), 1088-1098.

Suthaker, S., Smith, D. W., & Stanley, S. J. (1995). Evaluation of filter media for upgrading existing filter performance. *Environmental Technology*, *16*(7), 625-643.

Tufenkji, N., & Elimelech, M. (2004). Correlation equation for predicting single-collector efficiency in physicochemical filtration in saturated porous media. *Environmental Science & Technology*, *38*(2), 529-536.

Van Staden, S. J., & Haarhoff, J. (2011). The use of filter media to determine filter cleanliness. *Physics and Chemistry of the Earth, Parts A/B/C*, *36*(14-15), 1135-1140.

Wickham, H. (2010). *ggplot2: Elegant Graphics for Data Analysis*. New York: Springer-Verlag.

Zuur, A. F., Ieno, E. N., Walker, N. J., Saveliev, A. A., & Smith, G. M. (2009). *Mixed effects models and extensions in ecology with R*. New York: Springer.

5 Management Chapter: Economic assessment of replacing sand filter media with a low density equivalent at Scottish Water drinking water treatment works

5.1 Executive summary

The effective capture and retention of particles and pathogens within filters is crucial to the provision of safe compliant drinking water and the stable and economic operation of potable water distribution networks. Media filters are the final physical barrier in most large water supply systems. Poor performance of filters can lead to increased risk of customer exposure to pathogens, the increase in the formation of disinfection by-products, customer complaints over the aesthetic quality of drinking water and operational costs associated with the management of solids deposited within the distribution network. An extensive programme of assessment of water treatment works (WTWs) design in Scottish Water has identified the inadequate washing of granular media filters as a common problem, which is limiting performance and is likely to impact water quality compliance. A desk-top review indicated that 28 out of 41 WTWs assessed would be suitable for media replacement using low density aluminosilicate media to improve filter washing. The low-density media used in this analysis was an expanded aluminosilicate material branded as Filtralite. Scottish Water can exploit the physical properties of the material to mitigate widespread design constraints across the filtration asset base and economically deliver a step-change in filtration performance across the relevant treatment works. The material has been tested at pilot and full scale (see chapter 4) and understanding of its application is now approaching a stage where it can be applied in a structured programme of work. Upgrading the wash systems in these treatment plants is likely to cost in excess of £ 30.79 million. This document illustrates how Scottish Water can avoid such a large investment in assets which are typically between 20 to 50 years old. By replacing the existing media at the end of its operational life with low-density media, costly and complicated upgrades to the backwash systems can be avoided. Replacement of existing

media with alternative materials across the 28 sites was estimated to cost in the region of £ 6.43 million compared to £ 5.79 million for like-for-like media replacement only. However, the lower density media will avoid the projected requirement for £ 30.79 million investment in upgrading the wash systems which would be required to achieve the equivalent performance from the current conventional media design. Low-density media replacement projects are relatively simple and low risk interventions which can make big improvements to the performance of filters as demonstrated at pilot and full-scale trials WTW (Chapter 4). This work does not claim to deliver fully developed designs for media upgrade projects but rather takes a high-level view of the likely interventions and indicative costs for each site identified from the capability assessment data as being appropriate for this kind of intervention. This current analysis covers ~ 40% of the relevant asset base indicating that the potential scope of the application of low-density media is likely to be larger than that indicated in this document.

5.2 Materials and methods

The raw data used in this report was collected as part of a programme of surveys and design assessments of Scottish Water WTWs conducted by the Scottish Water asset capability team. A series of design and cost calculations were applied to the collated raw data from the surveys in order to assess the strategic application of low density media to overcome the issue of poor RGF bed expansion.

5.2.1 Key design calculations

The analysis relied on some standard hydraulic design calculations for media. Clean bed head loss was estimated using the Ergun method in Equation 35 (Ergun & Orning, 1949 in Crittenden *et al.*, 2012). The bed expansion achieved for a specific backwash rate was calculated using an adaptation of the Ergun equation in Equation 36 (Akgiray and Saatçi, 2001). Clean bed head loss and bed expansion estimates used the media effective size modelled at 4°C and 15°C.

Equation 35 Ergun equation for head loss

$$h_L = k_V \frac{(1-\Phi)^2}{\Phi^3} \frac{\mu L v}{\rho_w g d^2} + k_I \frac{1-\Phi}{\Phi^3} \frac{L v^2}{g d}$$

where; h_L = head loss (m) , k_V = head loss coefficient due to viscous forces, Φ = porosity, k_I = head loss coefficient due to inertial forces, v = superficial velocity (m/s), L = depth of filter bed (m), g = acceleration due to gravity (m/s^2), d = grain diameter (m), ρ_w = fluid density (kg/m^3) ; μ = dynamic viscosity (×10-3 kg/m·s).

Equation 36 Backwash bed expansion calculation

$$\varepsilon = \sqrt[3]{X + (X^2 + Y^3)^{\frac{1}{2}}} + \sqrt[3]{X - (X^2 + Y^3)^{1/2}}$$

$$X = \frac{\mu v}{2g(\rho_p - \rho_w)d^2} \left(k_V = \frac{k_I \rho_w v d}{\mu} \right)$$

$$Y = \frac{k_V \mu v}{3g(\rho_p - \rho_w)d^2}$$

Where: X = backwash calculation factor, dimensionless, Y = backwash calculation factor, dimensionless, ρ_p = particle density kg/m3

5.2.2 Media properties

Design calculations require assumptions about the properties of the media material and the size distribution within a given grade of filter media. Assumptions used for the different media properties included in this analysis are shown in Table 15. Viscous and inertial head loss coefficients were estimated to minimise the sum of squared error between predicted expansion and observed expansion as reported by supplier's information. Values for the Ergun coefficients are presented in Table 16.

Table 15 Media material properties

						Diameter (mm)					Supplier reported CBHL (m/m at 15°C)		Backwash velocity for expansion (m/hr at 15°C)		
Material	**Density ***	**Porosity ***	**Sphericity ***	**Size range (mm)***	**Grade***	**D5***	**D10***	**D60 ****	**D90***	**D95 ***	**5 m/hr***	**10 m/hr***	**20%***	**5%***	**0***
Sand	2650	0.43	0.89	0.5-1	16/30	0.5	0.63	0.76	0.95	1	0.23	0.46	42	25	20
Sand	2650	0.43	0.89	0.6-1.2	14/25	0.6	0.74	1	1.1	1.18	0.19	0.36	45	26	20
Sand	2650	0.43	0.89	0.85-1.7	10/18	0.85	0.9	1.2	1.6	1.7	0.1	0.2	76	48	37
Sand	2650	0.43	0.89	1.0-2.0	8/16	1	1.16	1.6	1.9	2	0.08	0.16	84	53	40
Sand	2650	0.43	0.89	1.2-2.8	6/14	1.18	1.425	1.9	2.7	2.8	0.04	0.08	124	83	59
Filtralite HC	1800	0.55	0.78	0.5-1	0.5-1	0.4	0.52	0.76	0.95	1	0.275	0.55	23	13	8
Filtralite HC	1800	0.55	0.55	0.8-1.6	0.8-1.6	0.8	0.98	1.31	1.46	1.6	0.15	0.28	42	23	12
Filtralite NC	1260	0.6	0.78	0.8-1.6	0.8-1.6	0.8	0.98	1.31	1.46	1.6	0.1	0.2	26	15	7
Filtralite NC	1200	0.61	0.78	1.5-2.5	1.5-2.5	1.5	1.525	2.1	1.85	2.5	0.05	0.1	43	26	17
Filtralite MC	1400	0.55	0.78	0.8-1.6	0.8-1.6	0.8	0.98	1.31	1.46	1.6	0.11	0.22	38	23	15
Anthracite	1400	0.5	0.78	0.60 - 1.18	11	0.6	0.7	1.1	0.8	1.18	0.15	0.32	21	14	11
Anthracite	1400	0.5	0.78	0.60 - 1.40	12	0.6	0.725	1.2	0.875	1.4	0.11	0.25	24	15	13
Anthracite	1400	0.5	0.78	0.80 - 1.60	14	0.8	0.925	1.4	1.15	1.6	0.06	0.12	37	24	19
Anthracite	1400	0.5	0.78	0.85 - 1.60	15	0.85	0.975	1.4	1.175	1.6	0.05	0.09	44	29	23
Anthracite	1400	0.5	0.78	1.18 - 2.50	21	1.18	1.36	2	1.7	2.5	0.035	0.07	55	36	28
Anthracite	1400	0.5	0.78	1.40 - 2.50	22	1.4	1.525	2.1	1.85	2.5	0.015	0.03	76	49	38

***Information from supplier** (SAINT GOBAIN, 2021; WESTERN CARBONS, 2010)
****sieve tests**

Table 16 Fitted values for viscous and inertial coefficients

Material	Size range (mm)	k_v	K_i
Sand	0.5-1	140	0.5
Sand	0.6-1.2	190	0.1
Sand	0.85-1.7	135	0.9
Sand	1.0-2.0	205	0.9
Sand	1.2-2.8	175	0.9
Filtralite HC	0.5-1	200	0.1
Filtralite HC	0.8-1.6	390	0.1
Filtralite NC	0.8-1.6	280	0.1
Filtralite NC	1.5-2.5	335	0.1
Filtralite MC	0.8-1.6	210	0.1
Anthracite	0.60 - 1.18	120	2.2
Anthracite	0.60 - 1.40	130	0.1
Anthracite	0.80 - 1.60	130	0.4
Anthracite	0.85 - 1.60	115	0.5
Anthracite	1.18 - 2.50	185	0.3
Anthracite	1.40 - 2.50	175	0.1

5.2.3 Cost estimation

Scottish Water purchases capital maintenance services through a supply framework where contractors have to apply to become a contractor providing a certain type of service. As part of this application unit cost data for different services need to be submitted. This data includes detail such as the price £/m^3 of filter media supply and installation based on various sizes of WTW (Table 17). It also includes prices per £/m2 for repairs and modifications to filter floors and a £/m price for repairs and modifications to pipework, these costs are summarised in Table 18. Using dimension data for the filters at each WTW, collected during the design assessments, and multiplying it by the unit cost for a given refurbishment or media, costs for most of the elements were estimated. Additional costs associated with building backwash tanks and replacing pumps were estimated by building simple cost curves between the size of tanks and pumps and the line item cost from previous backwash upgrade projects (Equation 37, Equation 38). Replacement pumps were sized to deliver the required wash rate to achieve 10% bed expansion for mono-media filters and 15% for dual media filters.

New backwash tanks were sized to hold 10 empty bed volumes (EBVs) to allow for two consecutive washes.

Equation 37 Backwash pump replacement cost curve used for estimation

$$£_{pump} = 72258 + 259324 * Kw_{pump} + 41922 * Kw_{pump}^2$$

Where: $£_{pump}$= pump cost (£), Kw_{pump} = power output of pump

Equation 38 Backwash tank construction cost curve used for estimation

$$£_{tank} = 100092 + 76124 * ML_{tank} + 63744 * ML_{tank}^2$$

Where: $£_{tank}$ = tank construction cost (£), ML_{tank} = volume of tank required (Ml)

Table 17 Unit costs for media replacement used for cost estimation

MediaType	WTW size (Ml/d >)	Cost supply and install new (£/m³)	Cost dispose old (£/m³)
Anthracite	0	502	42
Sand	0	564	42
Support	0	472	42
Anthracite	1	425	42
Sand	1	356	42
Support	1	266	42
Anthracite	5	409	36
Sand	5	326	36
Support	5	236	36
Anthracite	10	392	36
Sand	10	310	36
Support	10	220	36
Anthracite	25	380	36
Sand	25	288	36
Support	25	198	36
Anthracite	50	380	36
Sand	50	288	36
Support	50	198	36

Table 18 Unit prices for filter refurbishment cost estimation

WTW size (Ml/d >)	Replace nozzles (£/m^3)	Repair/replace pipework (£/m)	Repair floor (£/m^2)	Replace floor (£/m^2)
0	122	1780	96	1340
1	120	1780	96	1340
5	120	1780	96	1319
10	120	1780	96	1319
25	120	1780	96	1118
50	120	1780	96	1118

5.3 Overview of filtration systems within Scottish Water

Design assessment data for 41 conventional WTWs were analysed and grouped according to physical treatment stage (Table 19). Primary filters were defined as those which constitute the first stage of filtration and are used to remove particles from flocculated or clarified water. Of the sites 44% of primary filters were preceded by dissolved air flotation, 14% were direct filtration sites and the remainder used a settlement process before filtration. A range of sand and anthracite media were used in primary filters in Scottish Water with bed depths between 0.5 and 2 m (Figure 31). Approximately half of the sites were using a 0.5-1 mm sand, 15% were using 0.6-1.2 mm sand with the remainder using larger. A quarter of sites were using an anthracite layer in combination with sand.

Table 19 Tabulated count of WTWs by filtration and clarification types across assessed sites.

Filter	Actiflo	DAF$_1$	Flat bottom clarifier	Hopper bottom clarifier	Direct filtration (no clarification)
Rapid gravity filter (RGF)$_1$	2	16	9	4	5
Pressure filter		1	1	2	1
1 Includes CoCo DAF systems					

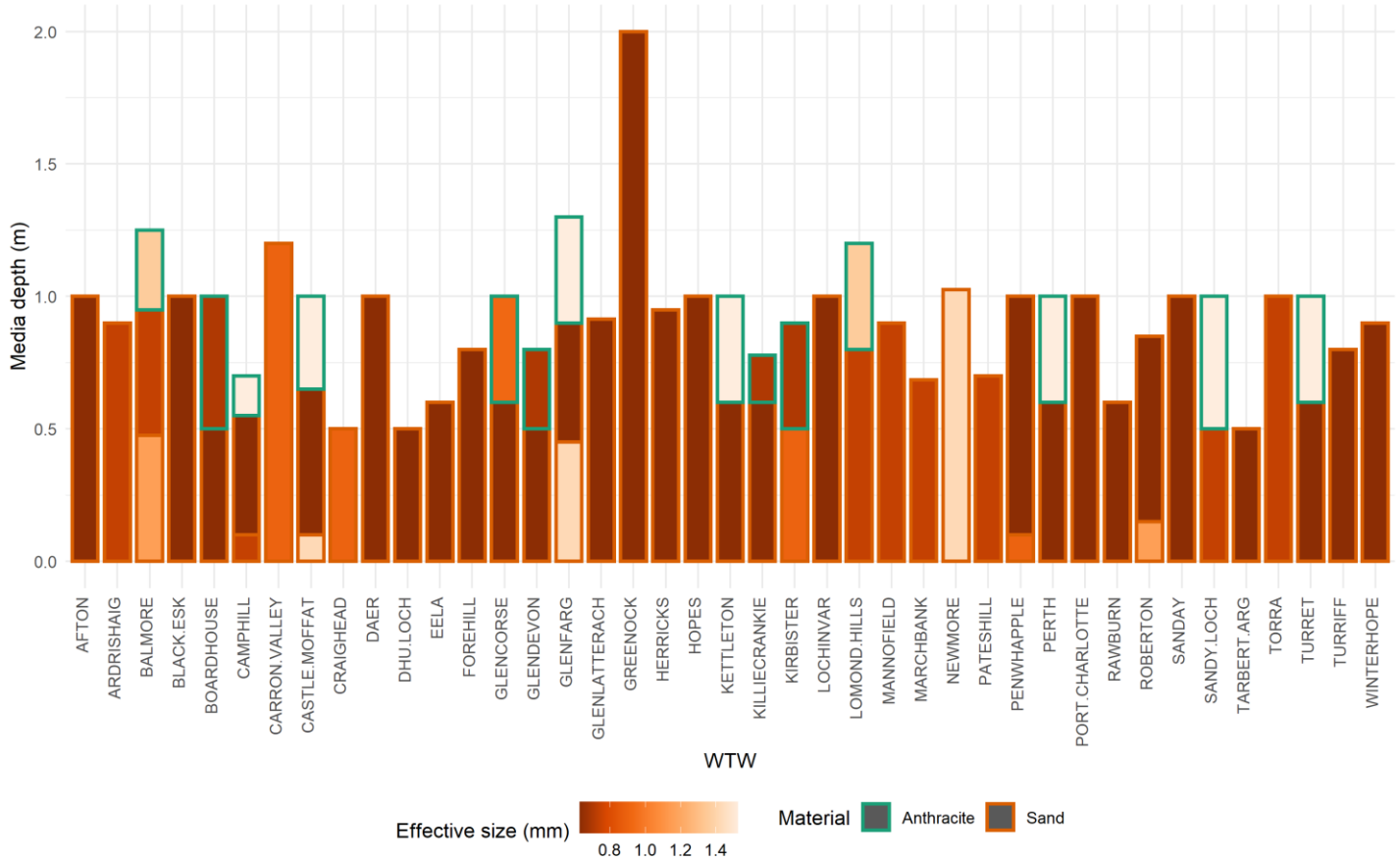

Figure 31 Filter media material profiles for assessed filters.

5.4 Filter backwash systems

When considering the backwash rates achieved for primary filters at each of the assessed WTWs, at 20 of the WTWs filters were washed at rates between 20 - 30 m/hr and 10 were washed between 10 - 20 m/hr (Table 20). Two sites did not achieve an upwash rate of more than 10 m/hr. For conventional media these wash rates are very low and are frequently insufficient to expand a sand filter bed or re-grade a multimedia filter. The volume of wash water used, normalised to the volume of the media bed, is an important factor affecting the performance of filter washes and is illustrated in Table 20. Here, 11 sites used less than two empty bed volumes of water during a filter wash.

Table 20 Tabulated count of WTWs by back-wash rates and volumes

Wash Type	High-rate wash (m/hr)	Wash volume (EBVs)			
		<2	2-3	3-5	5+
Combined A&W	10-20	2	0	3	2
	20-30	0	0	0	1
	30+	0	1	1	3
Separate A&W	<10	2	0	0	0
	10-20	2	0	1	0
	20-30	4	9	6	0
	30+	1	0	2	1

Insufficient backwash volume can be either an operational issue or a design constraint. For some systems the volume of water used in the wash exceeds the volume of the available storage. This indicates that the backwash tank is being re-filled during the backwash and the wash volume limiting factor is the flow balance between the water pumped out and the rate at which the tank is filled from the backwash water channel. Given that the volume of the backwash tank is not always the limiting factor for the availability of wash water, some broad assumptions, detailed below, were made in order to inform on a flow balance from which an estimate of the potential volume of water available to backwash a filter could be made. The water treatment design assessments collected data on the chemical dosing of the backwash water. This information was used to inform assumptions regarding the proportion of the filtered water flow which could be diverted to the backwash pumps.

- For sites which drew water prior to the dosing of chlorine for disinfection it was assumed that 30% of the flow could be diverted to feed the backwash tank or pumps and this was proposed to limit the impact of large flow changes on disinfection control.
- If the flow to the backwash tank was diverted between the chlorine dosing point and the pH correction dosing point it was assumed that 60% of the flow could be diverted to fill the backwash tank or pumps. This larger variation is acceptable as some instability in pH control can be buffered out in the clear water tank. If the wash-water was drawn after pH correction it was assumed that all of the flow could be diverted to the backwash pumps as there would be no likely impact on final water quality.

To better show the design constraints limiting wash water volume the number of WTWs with different stored and available wash water volumes (normalised to EBV) are summarised in Table 21. Six sites had serious constraints on the availability of wash water under normal operating conditions having less than three bed volumes of water available for backwashing. A further four sites were at risk of having insufficient water available water for backwashing with between three and six bed volumes of water available for backwashing under normal operation.

Table 21 Tabulated count of WTWs by wash water storage volumes and estimated available volumes based on flow balance.

Tank volume (EBVs)	Available wash volume based on observed flow balance (EBVs)		
	<3	3-6	6+
<3	6	1	3
3-6	NA	3	5
6+	NA	NA	23

Based on the recorded values for upwash rates and using Equation 36, estimates for bed expansion for the D10 (10^{th} percentile by diameter) media grain size at each of the assessed sites were calculated using Equation 36 and summarised in Table 22. At 15°C 12 were estimated to expand less than 1% and a further 10 had an estimated expansion between 1 and 5%.

Table 22 Summary of bed expansion during high-rate rinse for different filter types

Wash Type	Bed Type	Bed expansion during high-rate wash at 15°C					
		<1 %	1-5 %	5-10 %	10-15 %	15-20 %	20+ %
Combined A&W	Dual Media	0	1	3	0	0	2
	Mono Media	7	0	0	0	0	0
Separate A&W	Dual Media	4	1	1	0	1	1
	Mono Media	5	8	5	2	0	0

5.5 Potential solutions to design constraints

Based on the review of the engineering constraints from design reviews, three main design constraints with potential water quality risk relevant to the effective application of low-density media were observed:

• *Expansion: if bed expansion of >5% was not achieved at 15 °C*. Effective expansion of a media bed is required to consistently remove deposits from the media during the wash and maintain consistently high performance from a filter and avoid the risk of breakthrough. Replacing sand with a material of a lower density improves the bed expansion for a given backwash flow improving the removal of solids from the bed and reducing water quality risk.

• *Re-grade: for dual media filters if the bed expansion did not exceed at 10% at 15°C*. Where dual medias were not effectively expanded the re-grading of the 2 layers of media becomes less effective This results in higher head losses and lower solids handling capacity of these media. Replacing sand with a material of a lower density improves the bed expansion for a given backwash flow improving the re-grade of the media layers.

• *Backwash volume: if less than 4 empty bed volumes of backwash water were available for backwashing.* In cases where the balance of flows and wash water storage constrain the volume of water available to back wash filters, reducing media density can reduce the flow of backwash water required increasing the total volume available. This allows for more effective transport of deposits from the bed into the dirty wash water collection systems. Furthermore, in many instances the greater expansion of the low density media results in a more efficient wash and requires a lower volume of water in total.

5.5.1 Modelling wash-system upgrade scenarios

The conventional approach used to consistently achieve good filtration performance where the backwash system is inadequate is to upgrade the backwash system. It is possible to increase the rate at which water is delivered to wash the media by replacing the backwash pumps and, if necessary, pipework. It is also possible to construct new larger tanks in which to store backwash water allowing sufficient volumes of water to be passed through the bed during a wash. The upgrades required in order to achieve effective washing of the existing media were modelled in order to provide a baseline to compare the application of low-density media. Sites were identified for potential investment if they exhibited one or more of the design constraints detailed in sections 5.5 .

Several WTWs in the Scottish Water region were built without provision for dedicated backwash water tanks. In these cases wash water is provided from the filtered water channel or tank configuration which preferentially draws in filtered water. Depending on the number and size of the filters the flow of backwash water can exceed the flow of water through the plant constraining the volume of wash water that can be delivered. Any increase in the flow of water delivered during the backwash would in-these circumstances reduce the available volume of wash water. In order to model the costs associated with upgrading the wash the following assumptions were applied:

1. Where an increase in backwash rate was required, this would necessitate the purchase of new pumps. Given the age of most of the backwash pumps and the requirement to maintain a duty duty standby configuration it was considered that replacement of the existing pumps was most likely in most cases.
2. If upwash rate increases > 50% new wash water pipework and valves will be required to deliver and drain the backwash water and extensive changes to the filter floor will be required. Larger increases in wash rate would result in the hydraulic overloading of the existing pipe work and underdrain system which could lead to an unacceptable risk of serious damage to the filter. Damage to the filter under such circumstances could increase water supply risk.

3. If the available wash water volume at the increased backwash flow is < 4 empty bed volumes a new backwash tank was considered to be needed. Where the additional upgrade was likely to limit the available wash water it was assessed that additional storage would be required.

According to these broad rules the numbers of sites which would require different levels of upgrade are as follows: 7 sites were anticipated to require a new backwash water storage tank, 12 sites needed new wash-water pipework and 24 sites needed new backwash pumps. These outcomes, based on the assumptions above, were then fed into the indicative cost models described in section 5.2.3 to estimate the cost for each upgrade option.

Table 23 Tabulated numbers of WTWs identified for backwash upgrade

Bed expansion	Re-grade	Extra clean BW storage required (< 4 EBVs available)	Clean BW storage adequate (> 4 EBVs available)
< 5%	Dual media (ineffective re-grade at < 10 %)	2	4
< 5%	Mono-media	3	17
> 5%	Dual media (ineffective re-grade at 5-10 % expansion)	0	4
>5%	Mono-media or effective re-grade (no backwash rate increase required)	2	0

5.5.2 Use of low-density media

The alternative to the cost, complication and disruption of upgrading backwash tanks proposed in this chapter is to select a size and grade of media which is appropriate to the backwash system currently in place. Expanded aluminosilicate has a lower density than sand meaning that the equivalent sized grain can be backwashed at a lower wash rate as demonstrated through pilot trials documented in chapter 4. Anthracite, pumice and carbon media also have a low density but are more friable (Humby and Fitzpatrick, 1996). Filtralite exhibits low density, friability and some advantageous surface and shape characteristics which lead to higher porosity (Davies and Wheatley, 2012). The mechanisms driving potential performance gains from using Filtralite are discussed in more detail in chapter 4. But in summary the benefits are:

- Filtralite of with a particle size of 0.8-1.6 mm or greater exhibit improved solids handling capacity and lower head loss compared to equivalent graded sand due to increases in porosity relative to comparable grades of sand (Cescon *et al.*, 2016; Davies and Wheatley, 2012; Eikebrokk and Saltnes, 2001; Mikol *et al.*, 2007). Filtralite grades 0.5-1 mm (only the high density 1700 kg/m^3 type is available at this size) were observed in pilot trials not to exhibit this benefit.
- Due to its lower density, a Filtralite media bed will exhibit greater bed expansion than the equivalent sized bed of sand for a given wash rate. This allows deposited material to be more effectively and efficiently transported from the bed (Bayley *et al.*, 2006).

Most of the filters used by Scottish Water have a bed depth of 1m or less (Figure 31). Bed depths of a metre or less, when used as a final particle barrier, typically require a relatively fine media for consistently effective particle capture. Converting to a media of larger size while retaining the same depth of media, would likely decrease the efficiency of particle capture and be associated with an increased water quality risk. As most of the filters in Scottish Water use a filter media with an effective size of 0.64 mm at a depth of 1m or less, the appropriate replacement Filtralite bed is likely, in most cases to include the use of the finer grade Filtralite (HC 0.5-1 mm) material. Pilot trials of Filtralite HC 0.5-1 mm (Chapter 4) have demonstrated higher head loss from this material than an equivalent grade of sand. It is likely, therefore, that in most cases that the benefits of using Filtralite will be gained by the improvement to filter backwashing when using a lower density media for most Scottish Water filters.

The availability of a greater range of grades of sand, anthracite and expanded aluminosilicate has increased the number of available media options for any replacement project. The estimated backwash velocities required to achieve 5 and 25% bed expansion for different filter media materials and potential combinations in dual media filters are presented in the supplementary materials (Table_Apx 5). Variation in the relative depths of the different media layers can be used to manage the hydraulic properties of the bed. A greater depth of the finer media will increase surface area for particle collection whereas a greater depth of the larger media on top will increase the solids handling capacity.

The application of all potential candidate media and all plausible dual media combinations was modelled for all the sites requiring upgrade. The candidate media solution which is most likely to be appropriate was identified using Equation 35 and Equation 36 considering the varying physical properties of the different media materials and grades. Data gathered during site capability assessments was used as input data for these models. In order to contain the greater bed expansion of low-density media and the greater surface area of dual media filters using the same filter box, options to change the bed depth by factors of 0.4, 0.6, 0.8, 1 &1.2 of the original depth were considered. For each of the candidate media replacement solutions, bed expansion head loss and bed depth to grain diameter ratio (L/d ratio) was calculated.

Not all of the candidate media interventions were acceptable and the following criteria were used to classify the candidate media solutions into those which should be discounted and those which could be considered further.

- For mono media beds, the minimum bed expansion at the maximum temperature should be greater than 10%. Expansion less than this would not likely deliver the expected performance improvements.
- For dual media filters, both media layers should be expanded by > 15% at 15 °C to achieve re-grade all year round.
- The L/d ratio should be greater than 1000 to provide adequate surface area for particle collection and less than 1800 to avoid excessive head loss. L/d ratios smaller or larger than this range are unlikely to provide acceptable water quality or hydraulic performance.

Based on these criteria there were 4 sites where the backwash rate was so low that replacement of the media alone would probably not provide sufficient performance improvement. However, for the remaining 28 sites identified as having inadequate backwash systems it was possible to identify a low-density media replacement solution which will improve filtration performance and avoid the cost and complexity of a major upgrade project. Of all the viable alternatives, the most promising media replacement scenario was selected for indicative costing purposes on the basis of the data available and in the absence of a detailed assessment for each site by applying the following rules sequentially:

- If a dual media option is possible it is preferable unless there is a backwash availability constraint to be considered.

- Where there is a backwash availability reason to invest, the upwash rate required for expansion should be less than the current backwash rate. This limits solutions to those filters which do not require the provision of additional back wash water storage.
- For each potential media combination and bed depth, the ratio of layer depths is selected to give a L/d ratio as close to 1200 as possible. This rule of thumb is commonly used to balance particle capture performance and head loss.
- Media solutions increasing estimated clean bed head loss by more than 20% were excluded except for the special case of Newmore, at which a retrofitted pre-treatment stage means that a much smaller grade of media than is currently used is now appropriate. The driving head available is limited which excludes potential solutions that may result in reduced run times due to the limited availability of driving head.
- Where possible, the media bed depth should be kept as close to the current depth as possible. Large changes in media depth are likely to result in additional cost and complexity, adapting the hydraulic arrangement of the filter which have not been included in this analysis.
- The solution incorporating media with smallest effective size was preferable in order to maximise surface area for collection and provide the highest quality filtered water.
- Where wash volume availability is a reason to invest, the media offering the greatest reduction in effective backwash flow was assumed to be preferable.
- The solution with lowest clean bed head loss was selected.

Indicative alternative media replacement solutions identified for each site according to these rules are illustrated in Figure 32 which shows that 12 sites with mono-media sand filters could be up-graded to dual media filters and more effective re-grading is likely to occur in 11 existing dual media filters. There are 5 further filters where it was anticipated that the backwash rate would not be sufficient to re-grade even a low-density dual media filter but that a mono media design with improved wash performance could be identified.

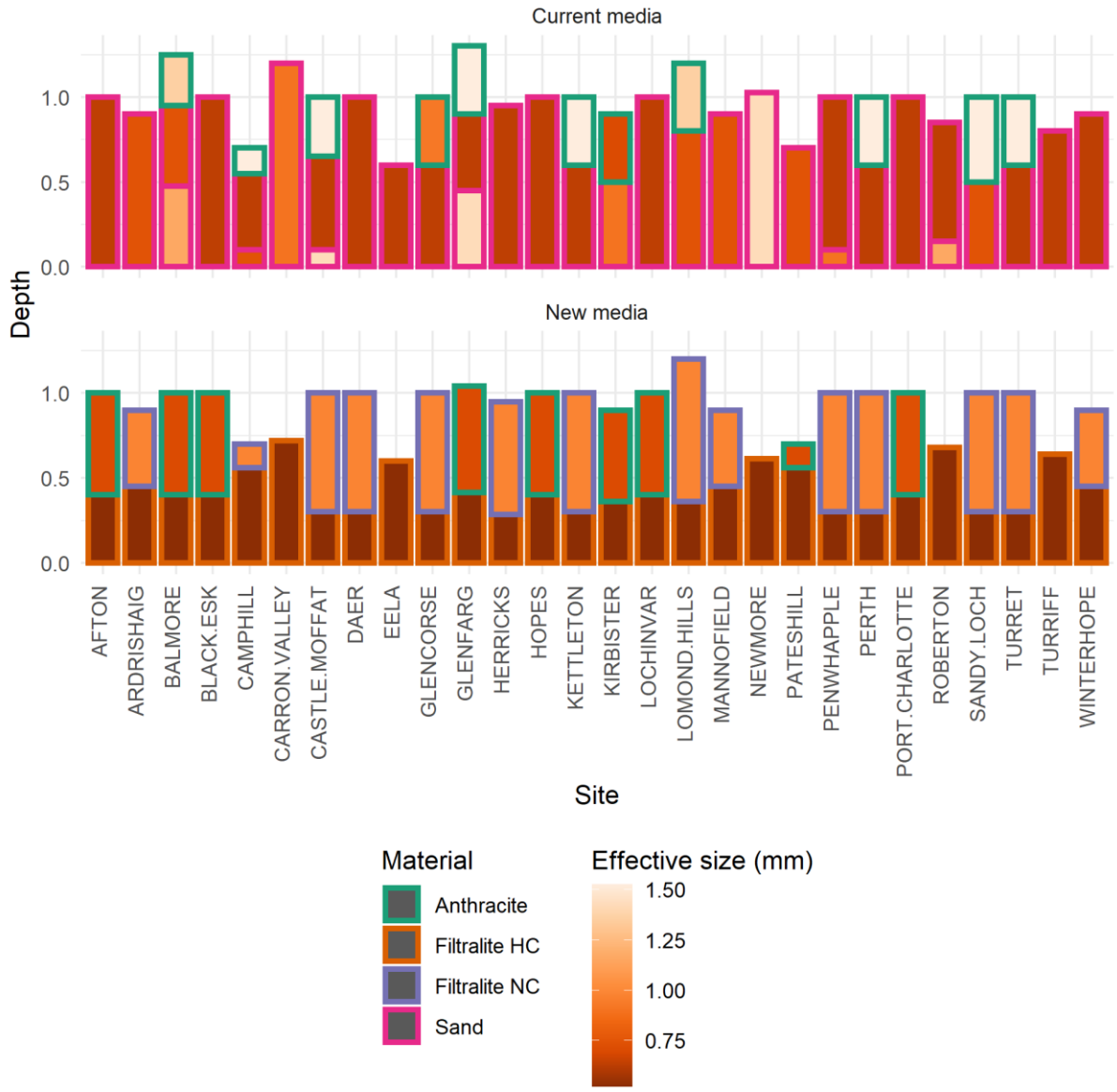

Figure 32 Current and likely replacement media designs based on selection process

5.5.3 Cost modelling

High level cost estimates have been calculated for the alternative solutions to the filtration design constraints observed across the filtration asset base. Conventional media replacement costs can be estimated from framework cost information produced by suppliers in the application process to join the Scottish water purchasing framework. Based on comparative quotes for conventional and low-density media proposed as part of the Rosebery (WTW A) upgrade (Chapter 4), the additional costs

associated with alternative materials can be factored in. Filtralite NC costs £16 more than anthracite per m^3 of media and Filtralite HC costs £166.21 more than sand per m^3 (Figure 32). Alternative media on average is estimated to cost in the region of 21% more than like for like media replacement only.

The data upon which to base estimates of the costs of upgrading the wash systems are limited. However, based on project cost summaries from previous capital schemes upgrading water treatment works at Scottish Water it has been possible to generate cost curves for pumps and tanks. Wash water pipework replacement costs were estimated on a £1780 per m framework price for pipework and valve repair (Filtec, 2014). Filter floor and nozzle replacement costs per m^2 were also included. These costs are aggregated with framework contractor prices for testing, commissioning and handover. Three levels of wash system upgrade were estimated:

- Pump replacement costs were estimated for sites requiring > 10% increase in backwash flow.
- Pipework and valve replacement costs were added for sites requiring > 50% increase in backwash flow.
- Tank construction costs were added for sites where the upwash rate increases were projected to leave < 4 empty bed volumes of usable backwash water storage.

Additional costs such as control integration, MCC replacement, pump lifting equipment were not included in the cost estimates and, as such, cost estimates are conservative.

A comparison of the projected costs of media replacement and wash system replacement show that replacement of media with a lower density alternative is likely to be a lower cost alternative than upgrading wash systems at 27 out of 28 sites (Figure 33, Table 24). Like-for-like media replacement projects are estimated to be between £21,000 and £2,000,000 depending on the size of the site. Wash system upgrades are projected to cost between £75,000 and £12M based on the cost models.

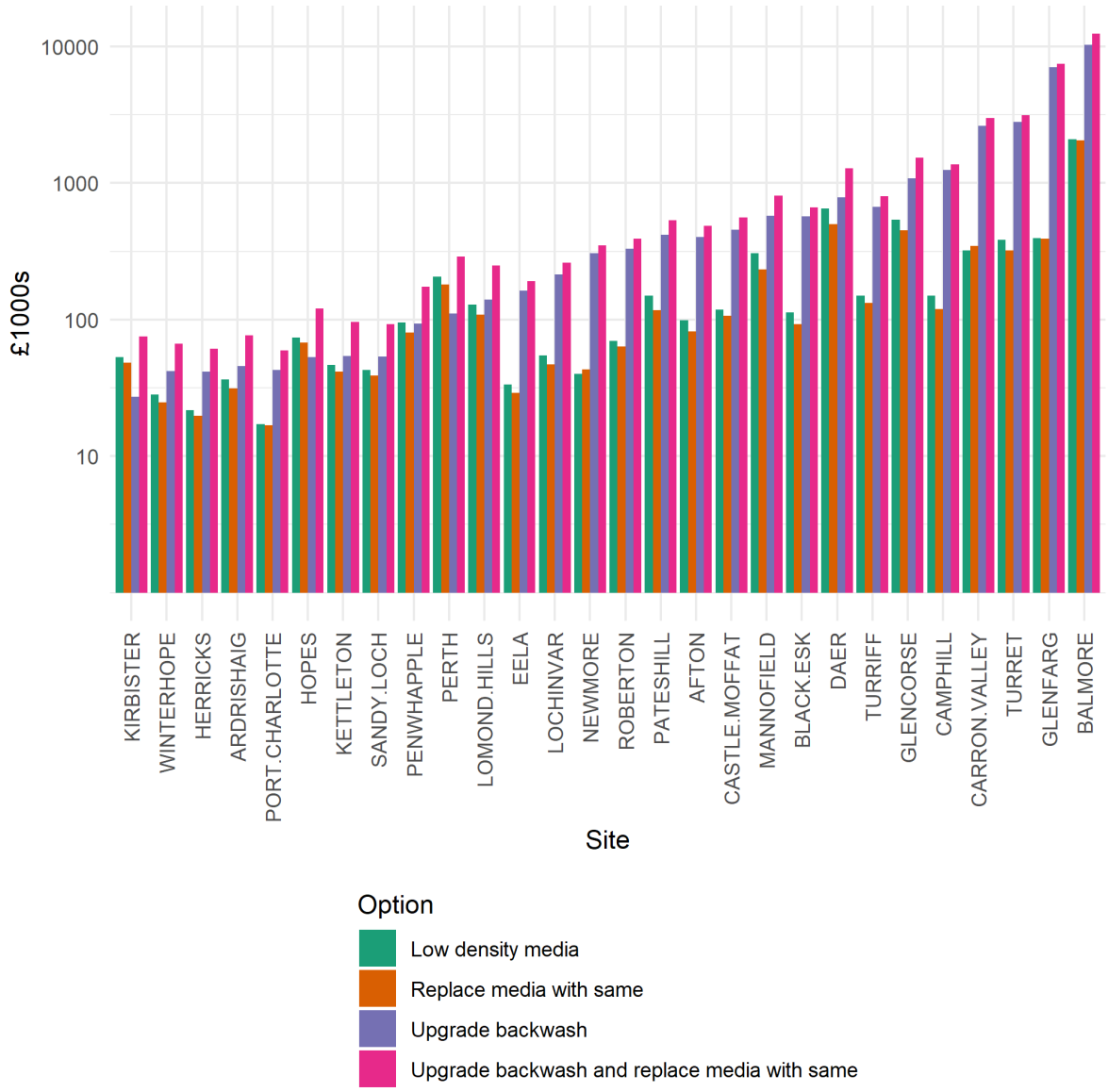

Figure 33 Comparison of modelled costs for the upgrade scenarios at selected WTWs.

Table 24 Summary of cost modelling outputs by site

Site	Replace media with same (£)	Upgrade backwash (£)	Upgrade backwash and replace media with same (£)	Low density media (£)	Saving (£)
BALMORE	2,049,070	10,346,697	12,395,767	2,101,040	10,294,727
GLENFARG	392,253	7,058,778	7,451,030	396,106	7,054,924
TURRET	322,489	2,808,806	3,131,295	385,572	2,745,723
CARRON.VALLEY	346,400	2,638,892	2,985,293	321,134	2,664,159
CAMPHILL	119,133	1,251,064	1,370,197	149,711	1,220,486
GLENCORSE	451,896	1,087,368	1,539,264	540,741	998,523
TURRIFF	132,797	671,899	804,696	149,485	655,211
DAER	498,980	787,964	1,286,944	649,754	637,190
BLACK.ESK	92,783	570,618	663,401	112,773	550,628
MANNOFIELD	233,705	577,175	810,880	307,610	503,270
CASTLE.MOFFAT	106,350	454,067	560,417	118,438	441,978
AFTON	81,597	403,927	485,524	99,354	386,170
PATESHILL	117,723	417,067	534,790	150,250	384,540
ROBERTON	63,489	329,279	392,768	69,812	322,957
NEWMORE	43,168	305,815	348,983	40,211	308,772
LOCHINVAR	46,871	214,833	261,704	54,604	207,100
EELA	28,989	163,020	192,008	33,429	158,580
LOMOND.HILLS	108,988	139,908	248,896	128,301	120,596
PERTH	180,357	110,471	290,828	207,243	83,584
PENWHAPPLE	80,403	93,388	173,791	95,476	78,315
SANDY.LOCH	38,981	53,821	92,802	42,935	49,867
KETTLETON	41,543	54,351	95,894	46,470	49,423
HOPES	67,620	53,182	120,801	73,769	47,032
PORT.CHARLOTTE	16,898	42,664	59,563	17,109	42,454
ARDRISHAIG	31,314	45,618	76,932	36,406	40,526
HERRICKS	19,752	41,516	61,268	21,594	39,674
WINTERHOPE	24,768	41,971	66,739	28,162	38,577
KIRBISTER	48,285	27,317	75,602	53,288	22,314

5.6 Discussion

Inadequate bed expansion during the backwash has been shown to be a particular challenge for Scottish WTWs. The inability to effectively remove dirt from the filter bed can result in a vicious cycle of performance decline. Dirt retained within the media causes excessive head loss and premature breakthrough of turbidity, resulting in a reduction in filter run times. Shorter run times result in higher hydraulic loading on sludge treatment systems which in turn can reduce the solids removal performance potentially leading to higher loads of solids in the return water. Pilot and full-scale trials shown have demonstrated that the additional bed expansion that can be achieved by low density media leaves the bed cleaner (Chapter 4).

The high level WTW design analysis and high-level cost modelling demonstrate a clear case for an extensive programme of filter media changes to mitigate the design constraints of existing filter backwash systems. Achieving improvements to filter performance through wash system upgrades is inherently complicated and risky. Head loss within pipework increases in proportion to the velocity squared, therefore increases in rise rate within the filter box will be associated with large increases in head loss across the filter nozzles, under drain and pipework. This increase in head loss can have implications beyond the sizing of the backwash pump required. The backwash pumps typically represent the largest draw of power on conventional filtration works in Scotland. Significant upgrading of the backwash pumps may require a new power supply. In remote areas this may mean considerable costs in upgrading the power supply system. This increased demand for power may mean that the emergency generator is insufficient. Increased head losses in the under-drain will increase stress on the filter floor potentially reducing operational life through failure of the filter floor. The ability to source sufficient backwash water is also a constraint. If insufficient storage of backwash water is provided, such as where the backwash is sourced from (such as the filtered water channel or chlorine contact tank), increasing the backwash flow increases the disruption to the disinfection process. Such circumstances can create a chlorine or base dosing control challenge leading to instability in the chlorine contact time that can be achieved in disinfection.

Switching media is not without risk. However, this risk is primarily associated with the replacement rate of the filtration material. There is an initial risk associated with loss of the lowest density expanded clay (Filtralite NC) during the first backwash. When dry, Filtralite NC has a buoyant fraction. With soaking, this fraction is much reduced, however, it will not be eliminated entirely and strategies to collect and manage this material need to be developed (Chapter 4). In some instances, this may mean that media retention plates need to be fitted in order to prevent carry-over of media during the rinse or additional flow control measures to limit the expansion of media during the winter. This will need to be assessed on an individual site-by-site basis. However, with careful design and validation of flow rates and expansion curves it is relatively simple and cheap to understand and manage this risk.

In order to present a relatively clear high-level view, over a heterogeneous asset base, this report has presented low density media and backwash upgrades as a dichotomous choice. In reality, for some sites, the best solution may be low density media replacement in combination with relatively minor upgrades to the pumping and control of backwash water. This choice will depend on design constraints which are specific to the individual site.

5.7 Conclusions

- The high-rate filter backwash at 22 of 41 conventional WTWs was insufficient to expand the media by 5% at 15°C, a further two sites would achieve expansion of between 5-10%.
- Six sites had less than 3 empty bed volumes of water available for filter backwashing.
- Design constraints in the filters or backwash systems likely to impact treatment performance could be over were identified at 28 of 41 WTWs surveyed.
- Replacing sand with lower density Filtralite media provides a comparatively low-cost solution for Scottish Water to overcome legacy design constraints at 27 WTWs out of the 41 surveyed.
- The backwash rate at a further 4 WTWs is below a rate at which Filtralite would be consistently expanded at 15°C.

- Use of lower density media has the potential to avoid a large number of high risk, expensive and disruptive backwash improvement projects and may contribute to the realisation of the full design life of up to 2/3 of existing rapid gravity filtration assets in Scottish Water.

5.8 References

Akgiray, Ö., & Saatçı, A. M. (2001). A new look at filter backwash hydraulics. *Water Science and Technology: Water Supply*, *1*(2), 65-72.

Bayley, R. G. W., Chipps, M. J., Steele, M. E., White, R., Mikol, A., & Fitzpatrick, C. S. B. (2006). 'Alternative low density media for use in biological roughing filtration prior to slow sand filtration'. In Gimbel, R., Graham, NJD and Collins, MR (Ed.s), *Recent Progress in Slow Sand and Alternative Biofiltration Processes,* London: IWA Publishing, 460-464.

Cescon, A., Jiang, J. Q., Haffey, M., Moore, G., & Callaghan, K. (2016). Assessment of recycled glass and expanded clay in a dual media configuration for drinking water treatment. *Separation Science and Technology*, *51*(14), 2455-2464.

Crittenden, J. C., Trussell, R. R., Hand, D. W., Howe, K., & Tchobanoglous, G. (2012). *MWH's water treatment: principles and design*. Hoboken, New Jersey: John Wiley & Sons.

Davies, P. D., & Wheatley, A. D. (2012). Pilot plant study of alternative filter media for rapid gravity filtration. *Water Science and Technology*, *66*(12), 2779-2784.

Eikebrokk, B., Vogt, R. D., & Liltved, H. (2004). NOM increase in Northern European source waters: discussion of possible causes and impacts on coagulation/contact filtration processes. *Water Science and Technology: Water Supply*, *4*(4), 47-54.

Ergun, S., & Orning, A. A. (1949). Fluid flow through randomly packed columns and fluidized beds. *Industrial & Engineering Chemistry*, *41*(6), 1179-1184.

Filtec. (2014) *Capital maintenance of filters submission*.

Humby, M. S., & Fitzpatrick, C. S. (1996). Attrition of granular filter media during backwashing with combined air and water. *Water Research*, *30*(2), 291-294.

Mikol, A., Fitzpatrick, C. S. B., Chipps, M. J., Steele, M. E. J., & Bayley, R. G. W. (2007). Novel dual media combination for drinking water treatment. *Water Science and Technology: Water Supply*, *7*(5-6), 131-139.

Western Carbons. (2010) *Western Carbons*. Available at: http://www.westerncarbons.co.uk/ (Accessed: 24 April 2021).

6 Discussion

The initial aim of this research was to identify how Scottish Water could achieve a filtered water turbidity target of <0.1 NTU. In some ways the technical means to achieve this aim already existed, and this area of the research can be viewed as an implementation gap rather than a knowledge gap. This is because the available body of research and practice demonstrates that with: effective pre-treatment; appropriate solids loading; good practice in process unit design; monitoring with sufficiently sensitive turbidity meters and particle counters; timely and appropriate maintenance; and effective operation, delivering filtered water turbidity of less than 0.1 NTU is readily achievable. This would, however, ignore the constraints within which Scottish Water and other municipal water suppliers operate. Municipal water suppliers need to provide safe and acceptable drinking water at a cost which is affordable and perceived to represent good value. This means that water companies are, to a certain extent, constrained by the value of the existing assets used to supply water.

This research is focussed on the implicit rather than explicit elements of the research question and could, more clearly be stated as: How can Scottish Water efficiently deliver filtered water turbidity of <0.1NTU within the constraints of existing assets? To that end this investigation has developed the application of a suite of approaches to improve performance from existing depth filtration assets, these include metrics, algorithms, methods, measurements and materials.

With filters of different design that have different pre-treatment processes and face different water quality challenges, it was evident that no one solution would deliver on the project aims within the implicit constraints. Neither was it appropriate to exhaustively address all aspects of filter design, operation, and maintenance. Instead, the project required focus on research areas which both provided opportunity to both develop new knowledge and the potential to improve performance across many diverse filter assets.

From a practical perspective, the knowledge generated in this thesis could be applied to improve seven categories of filter operation (Figure 34). Initial work

described in chapter 2 focussed on improving the efficiency of assessment and diagnosis of filtration performance using operational online monitoring data through the development of effective metrics and efficient diagnostic modelling methods. These metrics can help determine and identify the cause of filtration issues. Once identified, the solutions to the issue are commonly well developed. For example, operational and maintenance practice for the majority of issues are well established (Logsdon *et al.*, 2002). Modern design practice has solutions which minimise risk from interacting issues of hydraulic loading and shocking, while the effects of ineffective backwashing and optimal conditions for backwashing are also well described in the literature (Ambergey *et al.*, 2003; Amburgey, 2005; Crittenden *et al.*, 2012; Glasgow and Wheatley, 1998; Han *et al.*, 2009a; Hendricks, 2006). However, these improvements can be complicated and disruptive to retrofit into existing treatment processes and may not provide good value for money for assets with limited remaining life.

There were two key areas in which there was a lack of consensus both in practice and in academic opinion which provided opportunity for a novel contribution. Specifically, design for a backwash rinse rate that expanded the media has not been consistently practiced, and reported values for the optimal zeta potential window for charge-neutralisation coagulation vary (Bratby, 2016; Hendricks, 2006; Jefferson *et al.*, 2004; O'Melia, 1969). In addition, newly available technologies or products have become available that had the potential to resolve filtration challenges in ways that have not been previously possible. The main contributions to knowledge have been focused on three areas: filtration performance assessment and diagnosis; the use of novel online particle charge measurement technologies for optimising the preparation of water prior to filtration; and the application of newly available grades of low-density media materials to mitigate legacy filter design constraints.

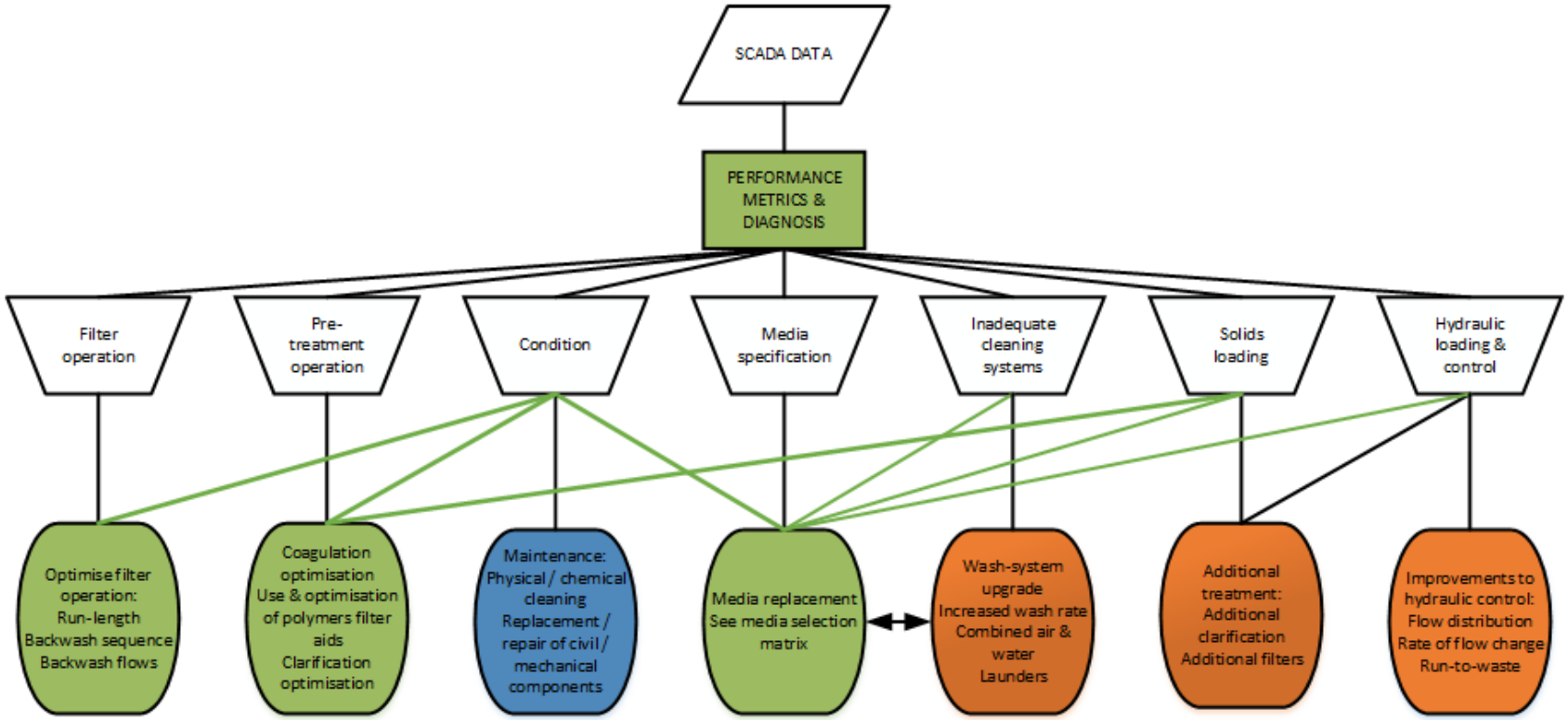

Figure 34 Overview of filtration performance issue types and solutions. Blue boxes indicate operation and maintenance activities and costs. Orange indicates potentially costly upgrades to civil and mechanical components. Green boxes indicate where this project has developed potential opportunities to mitigate risks with lower cost interventions. Green lines indicate areas in which there are potential opportunities to improve

6.1 Filtration performance metrics and diagnostics

A water treatment plant consists of multiple barriers, each potentially made up of several unit processes. A water utility may have hundreds of water treatment plants and assets to manage. The automation of many water treatment processes has reduced the labour force available for operation but has hugely increased the amount of available data describing process performance. As such, there is often insufficient operator time to review all of the operational data produced. Appropriate systems and methods are required to efficiently convert this data into actionable information to aid process operation and management. Chapter 2 of this thesis presents a justifiable and efficient methodology for the assessment and diagnosis of rapid gravity filtration performance issues. By making it simpler and easier to identify and diagnose performance, relatively minor issues within individual process units can be identified, prioritised and managed. This reduces the risk of a compound failure of microbiological barriers that could lead to harm to public health.

6.1.1 Context of work

Investigators have previously described the application of systematic methods for collecting and analysing filter performance data using traditional summary statistics (Logsdon *et al.*, 2002). Previous investigators have sought to move beyond the use of traditional summary statistics and develop specific metrics for the managing the performance of filters using turbidity trends (Hartshorn *et al.*, 2014; Huck and Coffey, 2004; Li and Huck, 2008). Systematic trials of these approaches, shown in chapter 2, identified inconsistent and counter-productive results driven by inconsistently shaped distributions of turbidity data.

In order to effectively manage filtration performance, an understanding of the causes of poor performance is required. Diagnosis of filtration issues are traditionally achieved through time consuming and subjective manual interpretation of turbidity trends (Logsdon *et al.*, 2002). Framing the diagnosis of filtration issues as a classification problem was used in this thesis to increase the

efficiency of the process such that it can be applied more extensively to understand marginal treatment performance concerns. This enables the management of occasional small spikes in filtered water turbidity, rather than retrospectively identify the cause of a water quality failure. The classification and regression tree (CART) algorithm, when used with calculated variables generated from other relevant and meaningful online measurements (describing water quality & physical conditions summarised in Table 2), was demonstrated to facilitate fitting of simple and interpretable classification tree models to operation of filtration. Better understanding and management of marginal performance issues in individual process stages can reduce the likelihood of acute compound failures (Venkatasubramanian *et al.*, 2003a).

6.1.2 Contribution to knowledge and practice

In the absence of a consistent function relating turbidity to risk, using turbidity as an indicator rather than a quantitative measure of filtration performance is a more reliable approach when the limitations of the measurement and its relationship with risk are considered. Turbidity observations above a limit of 0.1 NTU can be considered as “failure” of the filter. The failure rate against a goal of 0.1 NTU was deemed to be a good metric for filtration performance as it is understandable, comparable, insensitive to measurement error and easily applied. The reliability of a filtration process can be compared by contrasting the average time between turbidity spikes. The performance of filters spiking more frequently can be described as less reliable. The resilience of the performance of a filter can be compared by contrasting the average duration of turbidity spikes. Filters which on average return to acceptable performance in a shorter time period can be considered more resilient.

The alternative measures of filtration performance developed and described in Chapter 2 offer a sensible and intuitive approach to characterising the aspects of performance which are effectively measured using turbidity. Furthermore, when applying the failure rate, Mean Time Between Failures (MTBF) and Mean Time To Recovery (MTTR) there is no reliance on an implicit assumption that risk is a consistent linear function of turbidity. There is merely an assumption that turbidity

above 0.1 NTU is consistently indicative of a greater risk than turbidity less than 0.1 NTU. Assessment of filter performance on the basis of turbidity could be further improved by a process for the effective definition of a risk function for turbidity. Recent investigations have demonstrated that the impact of elevated turbidity on disinfection performance is subject to the type of turbidity causing materials present (Farrell *et al.*, 2018; Léziart *et al.*, 2019).

The operational performance and diagnosis methodology demonstrated in Chapter 2 has been shown to identify a range of operational issues related to poor performance. It can condense several years of process data into an interpretable tree diagram. These diagnostic models can be used as evidence during the review of operational set points, alarm and limit values, as well as for adjusting set-points or for focussing further investigations required to support additional maintenance or investment.

The novel methods developed in this research were incorporated into demonstration software which supported the management of performance and diagnosis of filtration issues at a case study WTW. Development of this software was demonstrated at the American Water Works Water Quality & Technology Conference 2015; the International Water Association particle separation conference 2016 and in a Chemical Engineering Journal paper (Upton, Jarvis and Jefferson, 2015, 2016; Upton *et al.*, 2017).

6.1.3 Limitations

Whilst the described approach was useful, it was limited to the management of filtration issues for those factors where useful data was collected and stored. The approach is less effective for longer term issues affecting the condition of filters. For example, in the case of a blocked lateral, the approach described would identify if a particular filter was more likely to produce high turbidity water than others, suggesting a condition issue, but would not identify the specific fault. In addition, design constraints are less likely to be effectively captured by using operational data. It is also comparatively simple and cheap to demonstrate a concept using a case-study set of data. The implementation of a stable system

which takes inconsistent and incomplete data from hundreds of different inconsistent systems will be a significant challenge to address.

To implement such monitoring and diagnostic system outside of a proprietary SCADA system is challenging. Interaction with existing proprietary control systems is awkward or costly by design. Typically, only relatively few key performance trends are communicated to corporate telemetry systems. Large scale uptake of such methods are only likely to be implementable when large amounts of process monitoring data are routinely extracted from local control systems and stored accessibly in a standardised format. With growing security concerns associated with control systems for critical infrastructure, the appetite for innovation in this area became more constrained over the course of this project. However, when the security concerns are resolved the application of such systems will become easier and more likely. Realistically this is likely to require the separation of monitoring and control.

6.2 On-line zeta potential measurement for coagulation optimisation

The sub-optimal preparation of water for filtration is a key cause of poor process performance (Huck *et al.*, 2001; Logsdon *et al.*, 2002). On-line monitoring of zeta potential has only been available in the last few years and provides a unique opportunity to improve operation of clarification and filtration processes (Smith *et al.*, 2019). Research presented in Chapter 3 developed methods for analysing online zeta potential data to improve understanding of how to optimally operate non-ideal coagulation-flocculation processes for the treatment of low turbidity water. This enabled optimal preparation of water for filtration, reducing the risks of turbidity breakthrough into final treated water.

6.2.1 Context of work

Electro-kinetic measurements of dosed water have long been established for describing the success of colloidal destabilisation (Pilipovich *et al.*, 1958; Black *et al.*, 1961; Jefferson *et al.*, 2004; Sharp *et al.*, 2005). More recent investigations have extended these observations to on-line measurement at full scale WTWs

(Black and Willems, 1961; Jefferson *et al.*, 2004; Pilipovich *et al.*, 1958; Sharp *et al.*, 2005; Smith *et al.*, 2019). However, concerns with the application of zeta potential centre around questions of consistency between systems and over time (Bratby, 2016; Hendricks, 2006; O'Melia, 1969). For zeta potential measurements to be of value for informing and optimising coagulation performance the charge neutralisation mechanism must be predominant (Bratby, 2016). Previous investigations at bench and pilot scale have identified optimal windows for zeta potential within which performance variation is independent of variation in charge, but the location and size of these windows are system dependent (Jeffereson *et al.*, 2004). It is known that the range of effective coagulant dose comprising the destabilisation zone reduces with lower colloid concentrations (Stumm and Morgan, 1996), making application of zeta potential to low turbidity water sources more challenging.

There is an inherent sensitivity challenge in optimising coagulation using electrophoretic measurements, particularly with systems with lower colloid concentrations. Zeta potential is derived from measurements of the electrophoretic mobility which is a function of particle charge. Particle systems that approach net neutral surface charge will therefore exhibit reduced electrophoretic mobility relative to random movement. Where the objective of coagulation is to neutralise the charge of colloidal particles to minimise inhibition of particle interaction then measurements in this region will have relatively large error and be less sensitive than measurements of a particle system with a strong charge. Online measurement of zeta potential provides a new opportunity, by taking the average of numerous measurements, to increasing measurement sensitivity within the region for charge-neutralisation coagulation.

6.2.2 Contribution to knowledge and practice

By combining online measurement of zeta potential with appropriate statistical modelling and supplementary jar testing this investigation was able to identify variations in treatment performance within zeta potential ranges of between -5 & 0 mV. To the author's knowledge, this is the first time that changes in treatment performance related to zeta potential have been seen within a region where

performance was considered independent of zeta potential. Though the mechanism driving this performance change could not be proven, modelling of full scale and jar test data indicated that, depending on prevailing conditions, likely performance benefits resulted from increased collision rate, increased adsorption and/or improved floc strength. This has improved understanding of how coagulation-flocculation systems challenged by multiple process constraints and changing raw water quality can be most effectively operated and optimised.

The use of online zeta potential simplifies the modelling and optimisation of coagulation in isolation from other sources of variance. This opens up greater opportunities for understanding and optimising treatment systems which are characterised by autocorrelated processes, multicollinearity in process variables and constraints on experimental manipulation (from monitoring of an operational WTWs). However, investigations have confirmed that neutralisation of charge alone does not always guarantee optimisation of a treatment process and further measurements of particle systems are required in order to ensure optimal floc aggregation.

The approaches demonstrated can enable specification of the effective operational zeta potential window for the prevailing conditions within a specific treatment system. This was shown to be of particular use for collision-, adsorption- or shear-limited systems. Where floc size is constrained by too low a concentration of particles resulting in too few opportunities for the agglomeration of particles within the available retention time of the flocculator, the methods presented indicated how coagulation conditions could be optimised to improve the collision rate without triggering re-stabilisation. Similarly, for systems in which floc formation is limited by a low coagulant to NOM ratio, modelling of online zeta potential data appeared to enable the optimisation of floc strength and or adsorption with additional coagulant dose whilst avoiding re-stabilisation.

6.2.3 Limitations

Lack of independent pH control in coagulation, and conducting trials within an operational WTWs, prevented the use of controlled experiments to demonstrate the application of online zeta potential and therefore limited the confidence with

which observations could be attributed to specific mechanisms. While the investigation demonstrated how the dose of coagulant could be optimised using online zeta potential, other approaches to improve the performance of coagulation-flocculation in non-ideal reactors were not explored. It is possible that the use of flocculation aids, including nucleating particles and/or polymers would result in more consistently effective performance over the range of treatment issues observed.

6.3 Expanded aluminosilicate in shallow RGFs

Most of the filters operating in Scotland today were constructed more than 30 years ago during which time raw water quality, performance expectations and design best practice have changed. The concrete components of an RGF have a typical asset life of 60 years whilst the filtration media is normally replaced within 20 years, meaning that there are likely to be at least two opportunities in the life of any filter to re-consider if the media in use is the most appropriate.

6.3.1 Context of work

Several investigations in the last 50 years have developed knowledge of, and practice for, the backwashing of granular media filters (Ambergey *et al.*, 2003; Amirtharajah, 1971, 1984, 1993; Chipps *et al.*, 1995; Fitzpatrick 1993; Ginn and Amirtharajah, 1992; Logsdon *et al.*, 2002). These investigations have developed understanding of the key requirements of an effective backwash. These are to impart sufficient turbulence to detach deposits from media grains and effective transport of the detached grains from the filter into the wash water system. Best practice for filter washing involves the expansion of the media by more than 10% (Ambergey *et al.*, 2003). However, many filters in the UK have been designed with a rinse rate which is at a fluidisation or sub-fluidisation rate that does not enable this level of expansion (Beverly, 2005; Brandt *et al.*, 2016; Hendricks, 2006). Several previous investigations have exploited media with lower density to improve performance of filters with sub-optimal backwashing (Bayley *et al.*, 2006; Mörgeli and Ives, 1979). In addition, the concentration of natural organic matter (NOM) in surface waters has increased in northern Europe and America over recent decades, further challenging the performance of filters which were

designed and built before the water quality had changed (Eikebrokk *et al.*, 2004; Jarvis *et al.*, 2005a; Pagano *et al.*, 2014).

Previous investigations and several case studies have documented successful applications of coarser low density Filtralite media in deep bed filters ≥1m (Eikebrokk and Saltnes, 2001; Mikol *et al.*, 2007). However, investigators have observed treated water quality concerns for its use as a media replacement in fine sand filters with shallower bed depth (Davies and Wheatley, 2012; Saltnes *et al.*, 2002). Where treatment benefits have been observed using Filtralite for depth filtration in drinking water, the performance gains have been associated with the media's additional porosity, surface and shape characteristics (Cescon *et al.*, 2016; Davies and Wheatley, 2012).

6.3.2 Contribution to knowledge and practice

This investigation demonstrated the effective application of 0.5-1 mm expanded aluminosilicate (Filtralite HC) and 0.8-1.6 mm expanded aluminosilicate Filtralite (NC) or Anthracite media within a 1m deep filter as a replacement for a fine sand (0.5-1 mm) and anthracite (0.8-1.6 mm) media which was not effectively expanded during the backwash. To the author's knowledge, this is the first time that such a configuration has been researched and applied at pilot and full scale. This work showed that the use of the lower density media delayed breakthrough and reduced clean bed head loss when compared to sand-anthracite filters of equivalent size at backwash rates typical of those used in many UK filtration plants. This showed that design constraints leading to increased solids loading and poor backwash performance could be effectively mitigated by replacing fine sand with Filtralite, addressing an issue common to many filters in the UK. Similar outcomes could be achieved with comparatively costly upgrades to the backwash system.

Pilot trials showed that, when comparing dual media Filtralite beds (0.5-1 mm & 0.8-1.6 mm), after normalising for the minimum fluidisation velocity, there was no residual performance advantage in terms of delayed breakthrough or clean bed-head loss associated with using Filtralite. This suggests that in finer-media configurations, the mechanism leading to benefits from the use of Filtralite is

different to those previously attributed for the coarse media. Previous investigators have identified increased surface roughness and porosity as likely causes for the improved performance (Mikol *et al.*, 2007; Mitrouli *et al.*, 2009). In finer media applications, the performance advantage arises from the lower density material achieving additional bed expansion at rinse rates which are sufficient only to fluidise sand. In other words, the Filtralite filters are more effectively cleaned during the backwash.

The evidence presented in Chapter 4 has now been exploited to improve water quality in Scottish Water at three WTWs, where the sand media has been replaced by Filtralite. Improved understanding of the mechanisms that drive performance gains from low density media has enabled its application to a greater range of scenarios. From the research presented here, expanded aluminosilicate is worth considering when mono media sand filters are overloaded with solids, inadequate backwash bed expansion is limiting recovery of media void space or short filter run times are resulting in poor performance from backwash systems. Based on the experience gained through this and previous investigations a summary of the likely media options for a range of scenarios are summarised in Table 25.

Table 25 Matrix of potential Filtralite media replacement options for given situations.

<table>
<tr><td></td><td colspan="4">High rate backwash, $m^3/m^2/hr$</td></tr>
<tr><td>Current media</td><td>15-21</td><td>21-27</td><td>27-35</td><td>35+</td></tr>
<tr><td rowspan="2">Coarse sand (D10 >0.8 mm)</td><td rowspan="2">Filtralite NC 0.8-1.6 mm</td><td>Filtralite NC 0.8-1.6 mm</td><td>Filtralite MC (Medium Density) 0.8-1.6 mm**</td><td>Filtralite mono-multi (HC 0.8-1.6 mm & NC 1.5-2.5 mm)**</td></tr>
<tr><td colspan="2">Filtralite mono-multi fine (HC 0.5-1 mm & NC 0.8-1.6 mm).
Or Filtralite – Anthracite (HC 0.5-1 mm & Anthracite 0.8-1.6 mm).</td><td>Filtralite HC 0.8-1.6 mm**</td></tr>
<tr><td>Fine sand (D10 <0.6 mm)</td><td>Filtralite HC 0.5-1 mm</td><td colspan="2" rowspan="2">Filtralite mono-multi fine (HC 0.5-1 mm & NC 0.8-1.6 mm)</td><td rowspan="2">Not tested</td></tr>
<tr><td>Fine sand - anthracite</td><td>Filtralite mono-multi fine (HC 0.5-1 mm & NC 0.8-1.6 mm) *</td></tr>
<tr><td colspan="5">* Longer term performance needs testing
** not trialled in this investigation
HC = High density Crushed, NC = Normal density Crushed</td></tr>
</table>

6.3.3 Limitations

The primary limitation of this research was that during the main pilot trials at WTWA, backwash rate was adjusted, and the backwash time was kept constant this meant that the total volume of backwash water used was not constant across backwash rates. The transport of solids from the filter during the backwash rinse is critical for an effective backwash. Failure to adequately control for backwash volumes whilst changing other backwash conditions could result in misunderstanding due to the misattribution of an effect. This failure to keep equal wash volumes does not affect the comparison between the media at absolute wash rates because during these trials the same backwash protocol was applied

to both media at the same time. However, during a subsequent re-analysis of the data, performance of two media were compared after normalising wash rate for the minimum-fluidisation velocity and were found to operate similarly. In this comparison, it was possible that the lack of a significant difference between the performance of Filtralite-anthracite and sand-anthracite filters could have been attributed to the additional volume of water used to rinse the sand-anthracite or the fact that expansion was roughly equivalent.

6.4 Summary

The metrics, algorithms, methods, instruments and materials developed and investigated in this research are summarised in Table 26. These approaches have been developed to support the delivery of consistently low turbidity in filtered water.

Table 26 Summary of approaches developed in this project to help achieve filtered water turbidity of less than 0.1 NTU.

Approach	Objective met	Application for improving filtered water quality	How this could be of benefit to the broader water industry
Turbidity performance metrics Failure rate, Mean Time Between Failures (MTBF), Mean Time To Recovery (MTTR) relative to a target of 0.1 NTU (Chapter 2)	1. Develop novel methods for assessment of filtration performance and diagnosis of the potential causes of operational issues associated with rapid gravity filters using online data to improve the management of preventative maintenance activities.	Chapter 2 presents robust and simple assessments of filtration performance which avoids pitfalls associated with comparing average or percentile values, which require the inherent assumption that risk is a consistent function of turbidity. The metrics developed enable the management of individual process units within a multiple barrier system. The failure rate will identify filter systems which most commonly supply water with turbidity >0.1 NTU. MTTF will detect systems which produce water > 0.1 NTU frequently, even if only for a relatively short period. MTTR will detect systems which continue to operate at turbidity >0.1 NTU for extended periods, even if relatively infrequently.	These approaches could be used by the broader water industry to improve the quality of water supplied to customers and deliver increasingly challenging improvements in water quality compliance. By improving the efficiency with which slight or short periods of deterioration in water quality from individual process units are managed the risk of failure of can be reduced.
CART algorithm for efficient filtration diagnostics (Chapter 2)		The application of relatively intuitive statistical learning models capable of rapidly and simply identifying and characterising operational conditions most likely to be associated with elevated filter turbidity has been developed. This speeds up the identification and exclusion of potential root causes of filtration issues. This can	

		enable investigation of sub-optimal performance to be carried out for more marginal performance issues. Efficiently identifying and resolving marginal issues enables management of individual treatment units within a multiple barrier system, reducing the risk of compound failures.	
Online measurement of Zeta potential and modelling of the performance window (Chapter 3)	2. Develop methods for modelling and optimising upstream coagulation using online zeta potential measurement.	By combining comparatively high frequency measurement of charge conditions afforded by online instrumentation, and appropriate statistical techniques, treatment sensitivity to slight variations in coagulation conditions can be resolved and modelled. The approach demonstrated allows the specification of an effective operational window for zeta potential within a treatment system for a given set of prevailing water quality conditions. This approach will enable the optimisation of treatment systems with design limitations or challenging raw water conditions. In turn, this allows for secondary mechanisms to occur within the charge neutralisation zone. This tool will enable more consistent preparation of water for filtration, reducing the risk of producing water with elevated turbidity.	This approach can be used by the water industry to optimise the preparation of water for filtration and disinfection within the constraints of existing assets. This could inform operational changes to meet increasing performance expectations and increasing water quality challenges.
Alternative low-density media for fine sand filters. Chapter 4.	3.Understand the potential application of novel filter media within Scottish Water.	Filtralite has been used extensively and successfully in coarse deep-bed filter applications. Pilot and full-scale trials of Filtralite media at grades smaller than those previously researched have demonstrated the effective application of the	This understanding enables mitigation of water quality risks in hundreds of filters with legacy backwash design constraints at a fraction of

		alternative media in fine sand filters with ineffective backwash systems. Pilot trials showed that for fine media (0.5-1 mm), backwashed at rates commonly used in the UK, the benefit of using Filtralite was primarily associated with improved backwash performance in conditions which did not clean sand effectively. It was also demonstrated that it is possible to convert many of these currently mono-media filters to dual media filters, improving the solids handling capacity.	the cost of upgrading the backwash systems to meet design best practice. This approach will enable the improved operation of existing filters across the UK and reduce water quality risk. This may potentially allow existing treatment assets to meet higher performance expectations and realise their original design life, improving value for customers.

6.5 References

Amburgey, J. E. (2005). Optimization of the extended terminal subfluidization wash (ETSW) filter backwashing procedure. *Water Research*, *39*(2-3), 314-330.

Amburgey, J. E., Amirtharajah, A., Brouckaert, B. M., & Spivey, N. C. (2003). An enhanced backwashing technique for improved filter ripening. *Journal of the American Water Works Association*, *95*(12), 81-94.

Amirtharajah, A. (1971). *Optimum expansion of sand filters during backwash*. Iowa State University.

Amirtharajah, A. (1984). Fundamentals and theory of air scour. *Journal of Environmental Engineering*, *110*(3), 573-590.

Amirtharajah, A. (1993). Optimum backwashing of filters with air scour: a review. *Water Science and Technology*, *27*(10), 195-211.

Bayley, R. G. W., Chipps, M. J., Steele, M. E., White, R., Mikol, A., & Fitzpatrick, C. S. B. (2006). 'Alternative low density media for use in biological roughing filtration prior to slow sand filtration'. In Gimbel, R., Graham, NJD and Collins, MR (Ed.s), *Recent Progress in Slow Sand and Alternative Biofiltration Processes,* London: IWA Publishing, 460-464.

Beverly, R. P. (2011). *Filter troubleshooting and design handbook*. Denver: American Water Works Association.

Black, A. P., & Willems, D. G. (1961). Electrophoretic studies of coagulation for removal of organic color. *Journal of the American Water Works Association*, *53*(5), 589-604.

Brandt, M. J., Johnson, K. M., Elphinston, A. J., & Ratnayaka, D. D. (2016). *Twort's water supply*. Oxford: Butterworth-Heinemann.

Bratby, J. (2016). *Coagulation and Flocculation in Water and Wastewater Treatment*–3rd edn. London: IWA Publishing.

Cescon, A., Jiang, J. Q., Haffey, M., Moore, G., & Callaghan, K. (2016). Assessment of recycled glass and expanded clay in a dual media configuration for drinking water treatment. *Separation Science and Technology*, *51*(14), 2455-2464.

Chipps, M. J., Bauer, M. J., & Bayley, R. G. (1995). Achieving enhanced filter backwashing with combined air scour and sub-fluidising water at pilot and operational scale. *Filtration & Separation*, *32*(1), 55-63.

Crittenden, J. C., Trussell, R. R., Hand, D. W., Howe, K., & Tchobanoglous, G. (2012). *MWH's water treatment: principles and design*. Hoboken, New Jersey: John Wiley & Sons.

Davies, P. D., & Wheatley, A. D. (2012). Pilot plant study of alternative filter media for rapid gravity filtration. *Water Science and Technology*, *66*(12), 2779-2784.

Eikebrokk, B., & Saltnes, T. (2001). Removal of natural organic matter (NOM) using different coagulants and lightweight expanded clay aggregate filters. *Water Science and Technology: Water Supply*, *1*(2), 131-140.

Eikebrokk, B., Vogt, R. D., & Liltved, H. (2004). NOM increase in Northern European source waters: discussion of possible causes and impacts on coagulation/contact filtration processes. *Water Science and Technology: Water Supply*, *4*(4), 47-54.

Farrell, C., Hassard, F., Jefferson, B., Leziart, T., Nocker, A., & Jarvis, P. (2018). Turbidity composition and the relationship with microbial attachment and UV inactivation efficacy. *Science of the Total Environment*, *624*, 638-647.

Fitzpatrick, C. S. B. (1993). Observations of particle detachment during filter backwashing. *Water Science and Technology*, *27*(10), 213-221.

Ginn Jr, T. M., Amirtharajah, A., & Karr, P. R. (1992). Effects of particle detachment in granular-media filtration. *Journal of the American Water Works Association*, *84*(2), 66-76.

Glasgow, G. D., & Wheatley, A. D. (1998). The effect of surges on the performance of rapid gravity filtration. *Water Science and Technology*, *37*(2), 75-81.

Han, S., Fitzpatrick, C. S., & Wetherill, A. (2009). The impact of flow surges on rapid gravity filtration. *Water Research*, *43*(5), 1171-1178.

Hartshorn, A. J., Prpich, G., Upton, A., Macadam, J., Jefferson, B., & Jarvis, P. (2015). Assessing filter robustness at drinking water treatment plants. *Water and Environment Journal*, *29*(1), 16-26.

Hendricks, D. W. (2006). *Water Treatment Unit Processes Physical and Chemical*; Boca Raton, Florida. CRC Press.

Huck, P.M., Emelko, M.B., Coffee, B.M.M, Maurizio, D.D. and O'Melia, C.R. (2001). *Filter operation effects on pathogen passage*. Denver: AWWA Research Foundation and American Water Works Association.

Huck, P. M., & Coffey, B. M. (2004). The importance of robustness in drinking-water systems. *Journal of Toxicology and Environmental Health, Part A*, *67*(20-22), 1581-1590.

Jarvis, P., Jefferson, B., & Parsons, S. A. (2005). How the natural organic matter to coagulant ratio impacts on floc structural properties. *Environmental Science & Technology*, *39*(22), 8919-8924.

Jefferson, B., Sharp, E. L., Goslan, E., Henderson, R., & Parsons, S. A. (2004). Application of charge measurement to water treatment processes. *Water Science and Technology: Water Supply*, *4*(5-6), 49-56.

Léziart, T., Dutheil de la Rochere, P. M., Cheswick, R., Jarvis, P., & Nocker, A. (2019). Effect of turbidity on water disinfection by chlorination with the emphasis on humic acids and chalk. *Environmental Technology*, *40*(13), 1734-1743.

Li, T., & Huck, P. M. (2008). Improving the evaluation of filtration robustness. *Journal of Environmental Engineering and Science*, *7*(1), 29-37.

Logsdon, G., Hess, A., Chipps, M. J., & Rachwal, A. (2002). *Filter maintenance and operations guidance manual*. Denver: Awwa Research Foundation and American Water Works Association.

Mikol, A., Fitzpatrick, C. S. B., Chipps, M. J., Steele, M. E. J., & Bayley, R. G. W. (2007). Novel dual media combination for drinking water treatment. *Water Science and Technology: Water Supply*, *7*(5-6), 131-139.

Mitrouli, S. T., Karabelas, A. J., Yiantsios, S. G., & Kjølseth, P. A. (2009). New granular materials for dual-media filtration of seawater: Pilot testing. *Separation and Purification Technology*, *65*(2), 147-155.

Mörgeli, B., & Ives, K. J. (1979). New media for effluent filtration. *Water Research*, *13*(10), 1001-1007.

O'Melia, C. R. (1969). A review of the coagulation process. *Public works*, *100*(5), 87-98.

Pagano, T., Bida, M., & Kenny, J. E. (2014). Trends in levels of allochthonous dissolved organic carbon in natural water: a review of potential mechanisms under a changing climate. *Water*, *6*(10), 2862-2897.

Pilipovich, J. B., Black, A. P., Eidsness, F. A., & Stearns, T. W. (1958). Electrophoretic studies of water coagulation. *Journal of the American Water Works Association*, *50*(11), 1467-1482.

Saltnes, T., Eikebrokk, B., & Ødegaard, H. (2002). Contact filtration of humic waters: performance of an expanded clay aggregate filter (Filtralite) compared to a dual anthracite/sand filter. *Water Science and Technology: Water Supply*, *2*(5-6), 17-23.

Sharp, E. L., Banks, J., Billica, J. A., Gertig, K. R., Henderson, R., Parsons, S. A., ... & Jefferson, B. (2005). Application of zeta potential measurements for coagulation control: pilot-plant experiences from UK and US waters with elevated organics. *Water Science and Technology: Water Supply*, *5*(5), 49-56.

Smith, R., Hassard, F., Sharp, E., Jarvis, P., Montalban, L., Worley, T., Liu, P. and Jefferson, B. (2019), Coagulation Control Using On-Line Zeta Potential Measurements: Can It Save Money and Improve Performance? *Institute of Water Journal*, 3(Spring 2019): 6–7.

Stumm, W. and Morgan, J.J. (1996) *Aquatic chemistry: Chemical equilibria and rates in natural waters*. 3rd edn. Chichester, UK: Wiley.

Upton, A., Jarvis, P. and Jefferson, B. (2015), 'An Expert System for RGF Operation'. *Proceedings of the AWWA Water Quality Technology Conference and Exposition (WQTC)*, Salt Lake City, UT, USA.

Upton, A., Jarvis, P. and Jefferson, B. (2016), Effective Assessment of Filtration Performance with On-Line Turbidity Data, In *Proceedings IWA Conference on Particle Separation 2016*, Oslo, Norway. IWA Publishing.

Upton, A., Jefferson, B., Moore, G., & Jarvis, P. (2017). Rapid gravity filtration operational performance assessment and diagnosis for preventative maintenance from on-line data. *Chemical Engineering Journal*, *313*, 250-260.

Venkatasubramanian, V., Rengaswamy, R., Yin, K., & Kavuri, S. N. (2003a). A review of process fault detection and diagnosis: Part I: Quantitative model-based methods. *Computers & Chemical Engineering*, *27*(3), 293-311.

7 Conclusions

The key conclusions with regards to objective 1, the development of novel methods for the performance assessment and diagnosis of filter operation from online data are:

1. As there is no clear consistent relationship between turbidity and risk or solids concentration in the region of interest below 1 NTU simple performance metrics which describe the frequency and duration of turbidity spikes using compliance rate, mean time between failures and mean time to recovery provide a more appropriate and effective indication of filter performance, avoiding spurious scoring and comparisons arising from current methods.
2. The diagnosis of operational causes of elevated filtrate turbidity can be framed as a machine learning classification problem for a more efficient and scalable approach to performance investigation than traditional manual interpretation of turbidity time series. The CART algorithm was demonstrated to be an effective and interpretable diagnostic method generating highly accurate and communicable models describing conditions associated with elevated filtrate turbidity and can applied to inform operational and preventative maintenance decisions. This is particularly useful for showing the interaction of filtration challenges such as low temperature, solids overloading from floc-carry-over and hydraulic surging that have been shown in combination to cause poor filtered water quality.

The key conclusions with regards to the development of methods for the modelling and optimising coagulation using online zeta potential measurement

3. Online zeta potential can be a valuable measurement for understanding and maintaining optimal coagulation conditions in the face of changing raw water conditions. The additional sensitivity, gained by multiple measurements enables online monitoring of zeta potential to show that even a small residual charge of a few mV can have a significant impact on the performance of downstream

processes in a low turbidity treatment system which does not use an additional polymer as a flocculant aid.

4. WTWs with shorter process contact times, colder waters and relatively low raw water particle concentration are likely to exhibit performance which is less robust in response to variation in zeta potential achieved in coagulation and are therefore likely to benefit from investment in online zeta potential.
5. The sensitivity to zeta potential and the effective operational window for treatment and coagulant dose appears contingent upon collision rate. It is likely that this will have implications on the relative costs and benefits associated with using different charge measurements for optimising treatment. In more robust systems streaming current is likely to be adequate, whereas in more sensitive systems the greater precision and interpretability of online zeta potential measurements are likely to provide an additional benefit.
6. Using a PCA-GAMM model to relate online zeta potential measurements with other online quality and operational control measurements can enable the identification of the effective operational zeta potential window for a treatment system with a given prevailing water quality, operational constraints and treatment goals. This is particularly the case where conditions and constraints vary such that the optimal treatment strategy may change between charge-neutralisation and sweep-flocculation.
7. Where this additional control provides the opportunity to consistently operate WTWs treating low turbidity water in a charge-neutralisation, rather than sweep flocculation, regime there is potential for reduced chemical use and metal sludge production.

The key conclusions regarding the application of aluminosilicate filter media within Scottish Water are:

8. The improved media cleaning achieved through additional expansion of a lower density aluminosilicate media (Filtralite) relative to sand for a given grain size and wash rate enables the media to more effectively

recover its primary porosity. This contributes to additional solids loading capacity, delaying the breakthrough of turbidity. Switching to an appropriate grade of Filtralite can allow poorly expanded sand filters to maintain good performance in the face of increasing raw water solids load.

9. The improved wash performance achieved by switching to Filtralite media was shown to mitigate the water quality risk associated with sub-optimal hydraulic control of a rapid gravity filter and the premature breakthrough of weak NOM floc.
10. This improved understanding of the mechanisms driving the comparative performance advantage associated with using Filtralite can allow municipal water suppliers to more effectively exploit the material to economically improve the filtration performance of filters with outmoded design.
11. Mono-media 0.5-1 mm or 0.6-1.2 mm sand filters backwashed at >22 m/hr in order to achieve <5% bed expansion can be successfully converted to dual media filters with extended run times by using the combination of Filtralite HC (0.5-1 mm) and either Filtralite NC or Anthracite (0.8-1.6 mm) without requirement for upgrades to backwash provision.
12. Deep-bed coarse non-fluidising 10/18 sand (0.85-1.7 mm) filters with rinse rates in the region of 15-18 m/hr can be converted to fluidising mono-media filters with greater solids handling capacity using Filtralite NC (0.8-1.6 mm). This is particularly advantageous if there is no surface (or cross) wash facility.

7.1 Further work

This investigation has developed knowledge of particle aggregation and filtration systems which, with further investigation, may provide opportunities to improve the performance of conventional coagulation–clarification–filtration processes.

- It was evident that particle charge is only part of the story in determining the performance of aggregation and separation processes. Improvements to the techniques available for monitoring and measuring the size and shape of water treatment flocs in situ are required to capture and manage the influence of mixing shear rate and collision rate effects in order to maintain optimal process performance.
- Application of the zeta potential modelling approach described in Chapter 3 to a broader range of controlled conditions at pilot scale would test the generalisability of the approach and provide greater evidence as to the mechanisms involved.
- Previous investigations have demonstrated the benefit of using larger and more porous Filtralite media of sufficient depth to improve the solids handling capacity of filters. This investigation has shown the benefit of using Filtralite to achieve filter performance in shallower filter systems where sand is not adequately expanded. There is a further class of filters (sand or sand-anthracite) which are currently washed effectively but that may have insufficient depth or receive inappropriate floc characteristics to enable conversion to a Filtralite of a larger size grade. In such situations, pilot testing the combination of fine sand (0.5-1 or 0.6-1.2 mm) with Filtralite HC (0.8-1.6 mm) and Filtralite NC (1.5-2.5 mm) may provide a means to increase solids handling capacity whilst maintaining the resilience of particle capture.
- Pilot-scale trials of filtration have allowed the more effective gathering of evidence to support the application of alternative media to overcome process constraints in existing filters allowing a step-change in performance across many WTWs. It is possible that a pilot-scale coagulation-flocculation system with variable coagulant, pH, polymer, rapid mixing, flocculant mixing, and process time would enable the development of interventions to overcome limitations in the performance of existing coagulation–flocculation assets. Instrumentation allowing the measurement of floc size would allow more effective optimisation of existing coagulation systems than that

which can realistically be achieved online or with jar testing alone. The solutions identified would likely be lower cost than building additional process units to achieve improvements in treatment performance. Furthermore, fitting such a pilot-plant with online zeta potential instrumentation, streaming current monitors and UV absorbance instrumentation would allow a useful assessment and development of the most appropriate coagulation control solutions for different water types and dynamic challenges.

- Deep bed-coarse media filters are capable of high filtration rates. There is an inherent trade-off in the washing of these deep bed filters between expansion for particle removal during backwash and in maintaining the hydraulic efficiency of the bed by preventing size sorting of media grains. Unquantified observations during this investigation suggested that variation in density between Filtralite media grains may act to prevent size sorting during fluidisation. Further testing of this observation may identify if deliberate exploitation of variation in density between media grains of equal size can be used to engineer more ideal media distribution in filters that might potentially enable higher filtration rates.

APPENDICES

Appendix A Supplementary materials for chapter 2

A.1 Data flow diagram

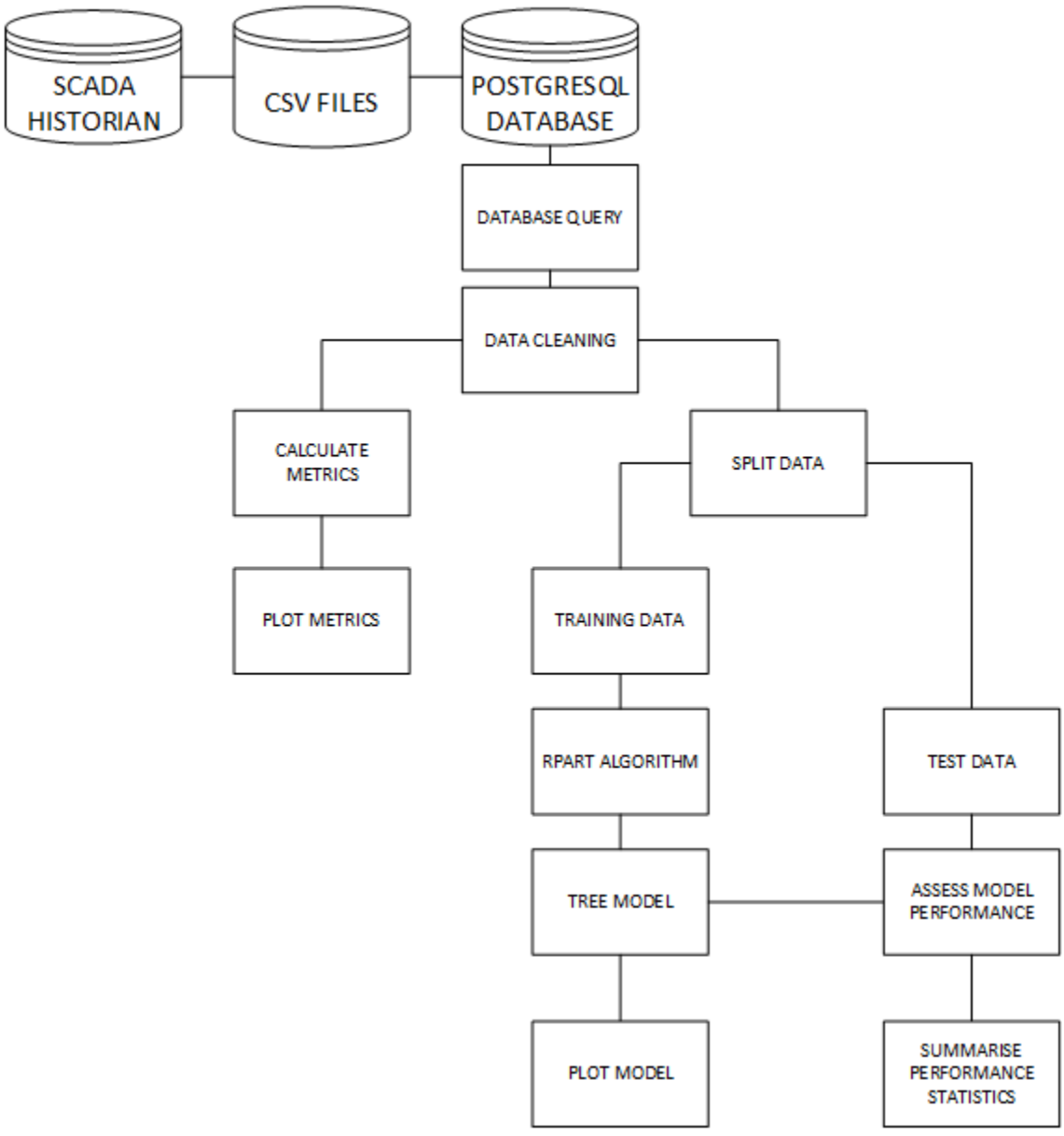

Figure_Apx 1 Data flow diagram for Chapter 2

A.2 Turbidity time series

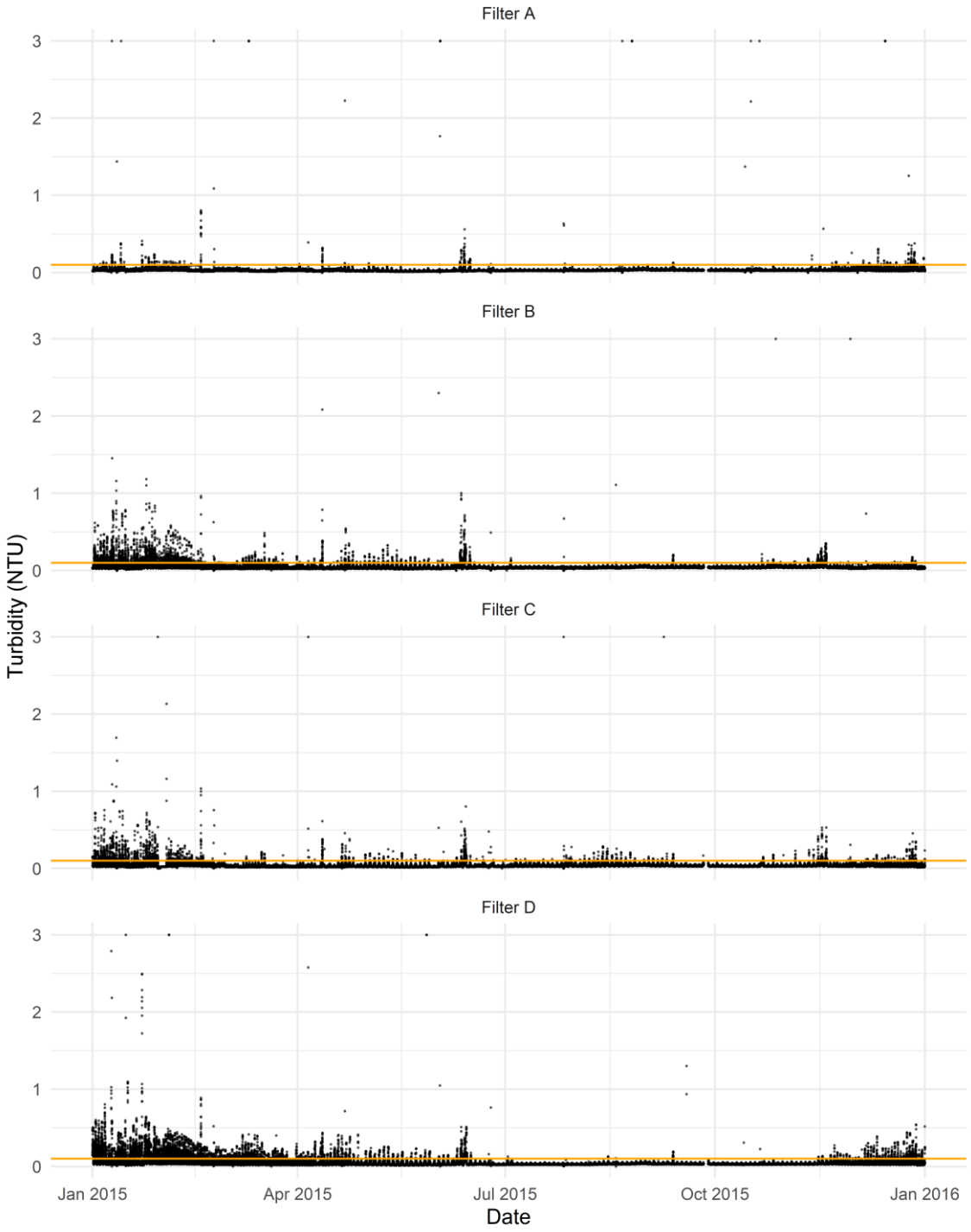

Figure_Apx 2 Turbidity time series for individual filters in 2015

A.3 Filter performance metrics

Below the sub-plots of Figure 8 are reproduced at larger scale

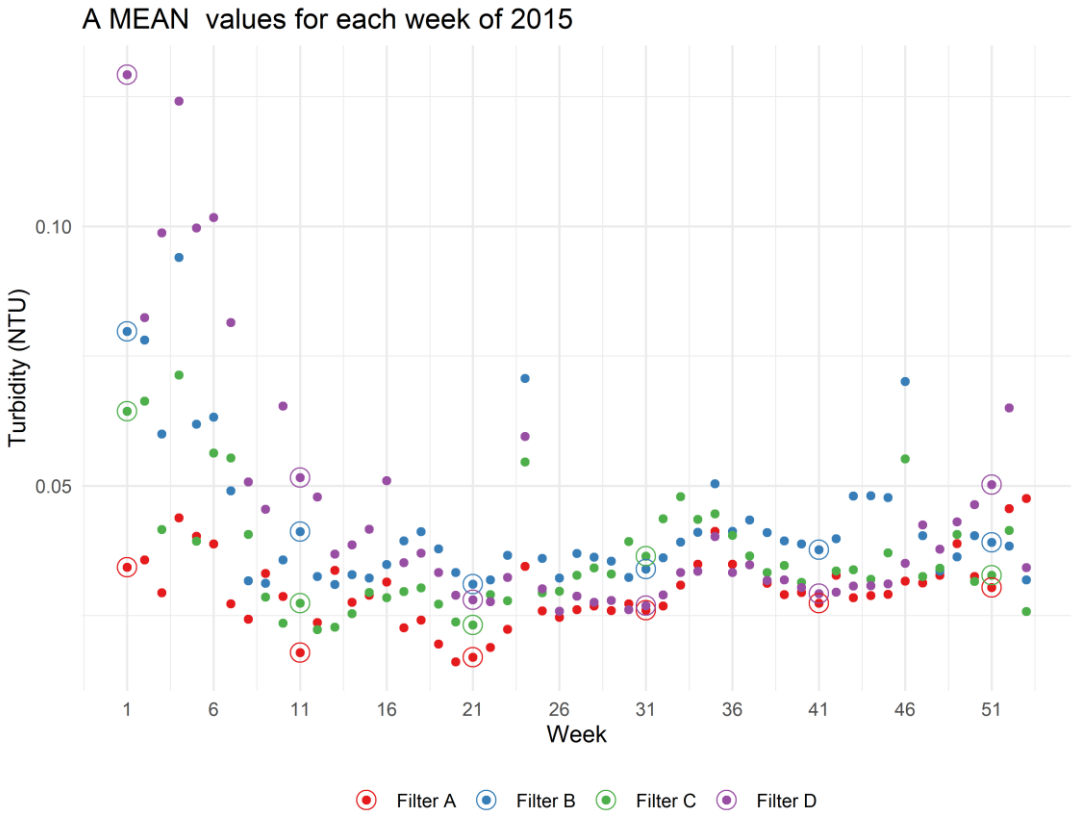

Figure_Apx 3 Enlargement of figure Figure 8 A weekly turbidity mean values

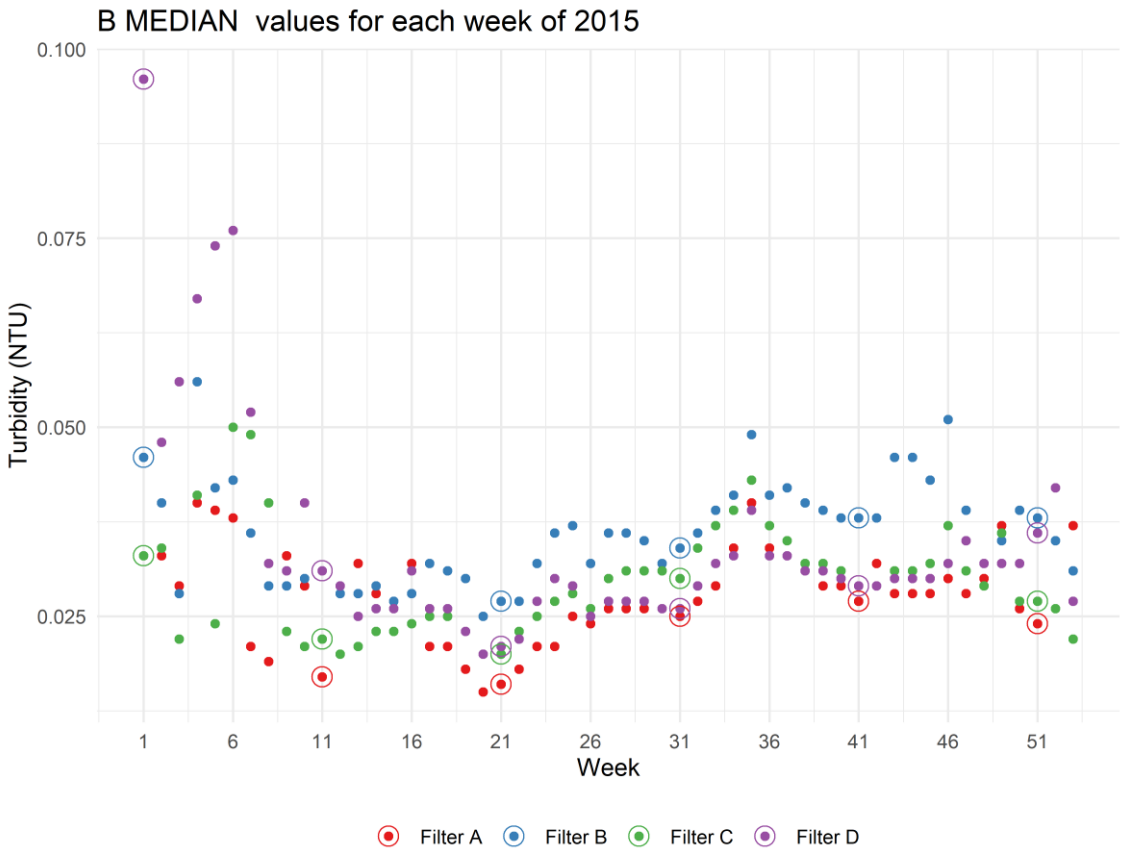

Figure_Apx 4 Enlargement of figure Figure 8 B weekly turbidity median values

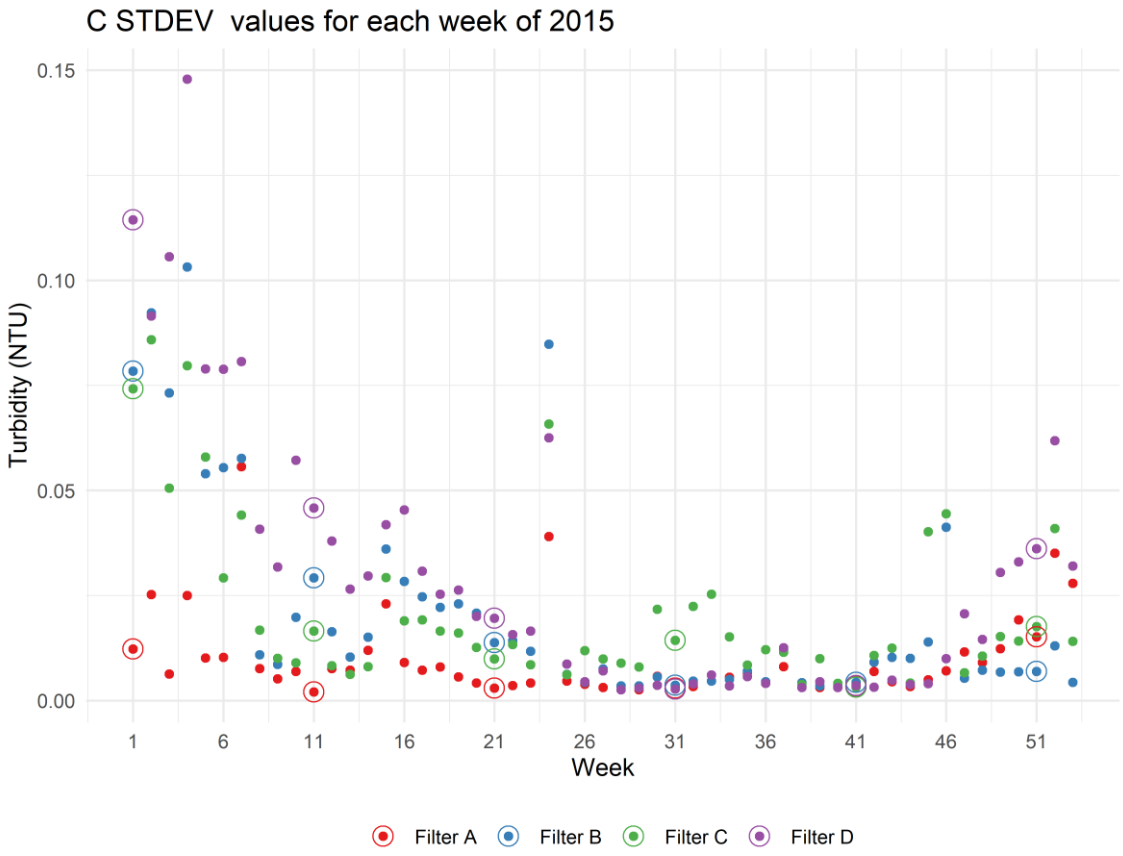

Figure_Apx 5 Enlargement of figure Figure 8 C weekly turbidity standard deviation

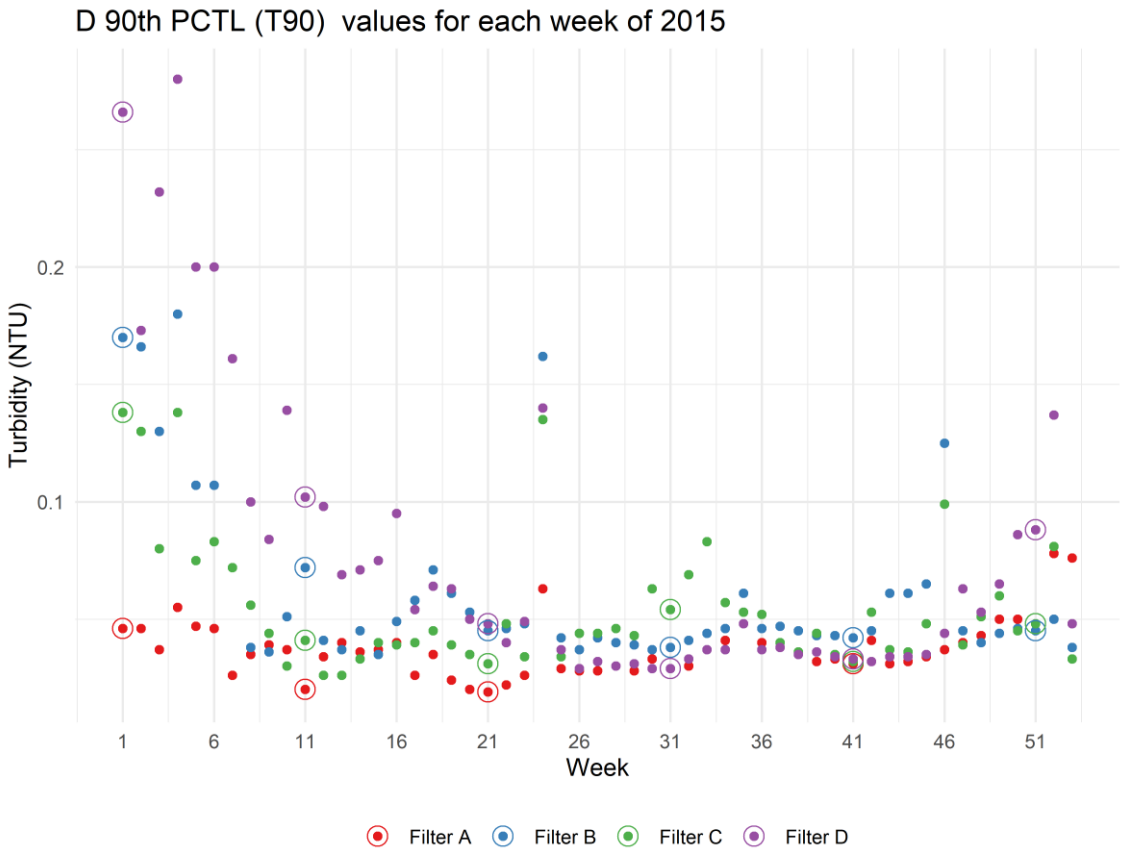

Figure_Apx 6 Enlargement of figure Figure 8 D weekly turbidity 90th percentile values

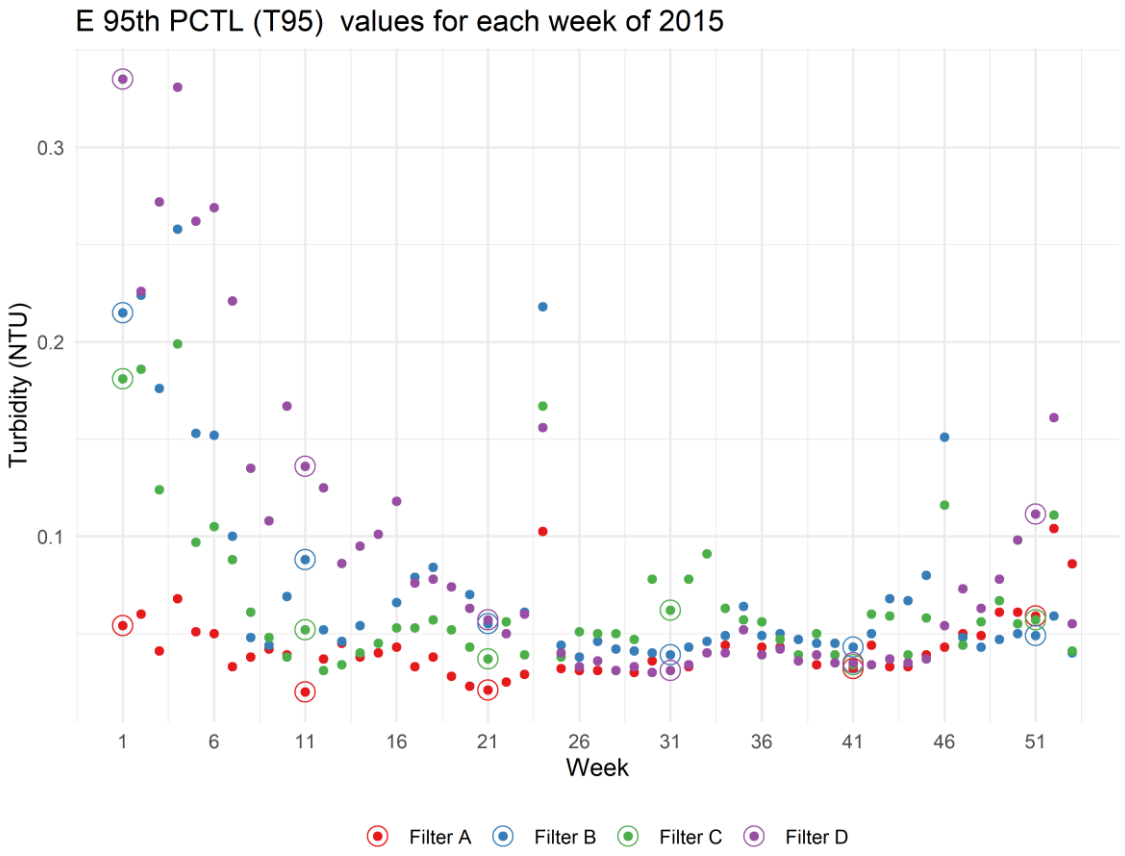

Figure_Apx 7 Enlargement of figure Figure 8 E weekly turbidity 95th percentile values

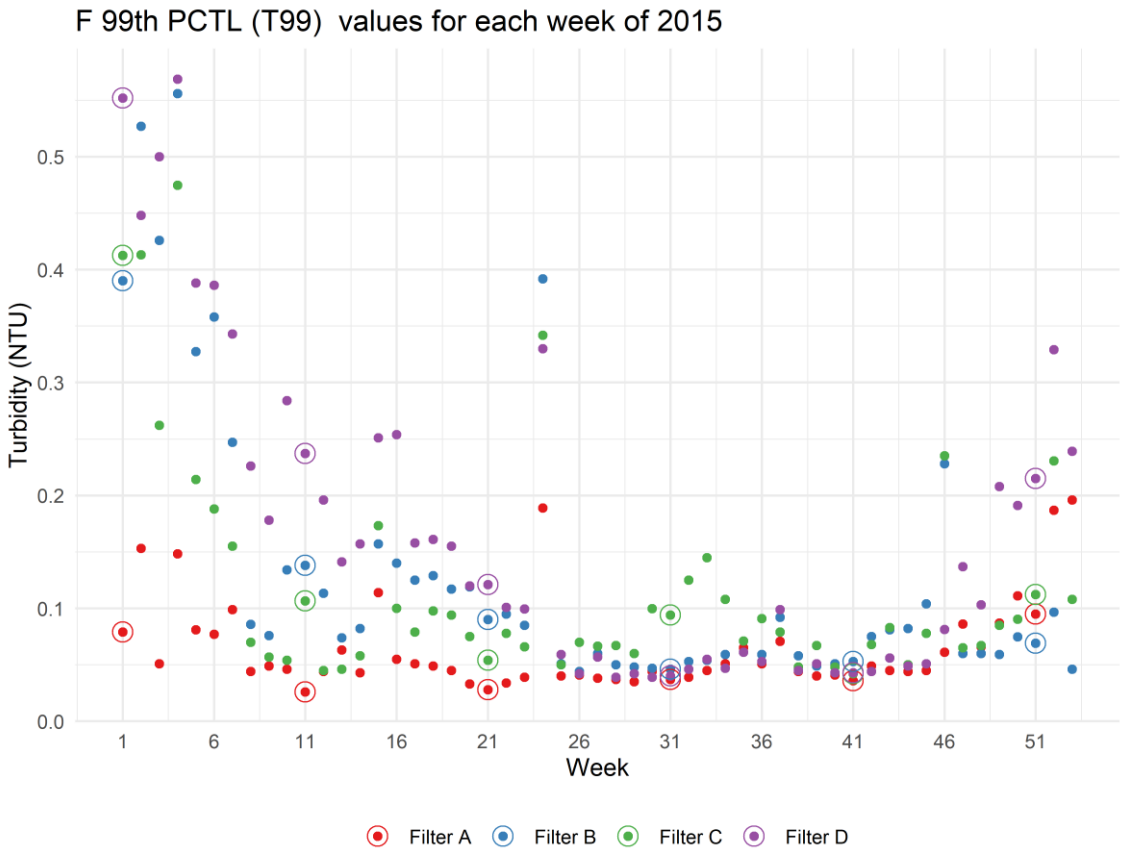

Figure_Apx 8 Enlargement of figure Figure 8 F weekly turbidity 99th percentile values

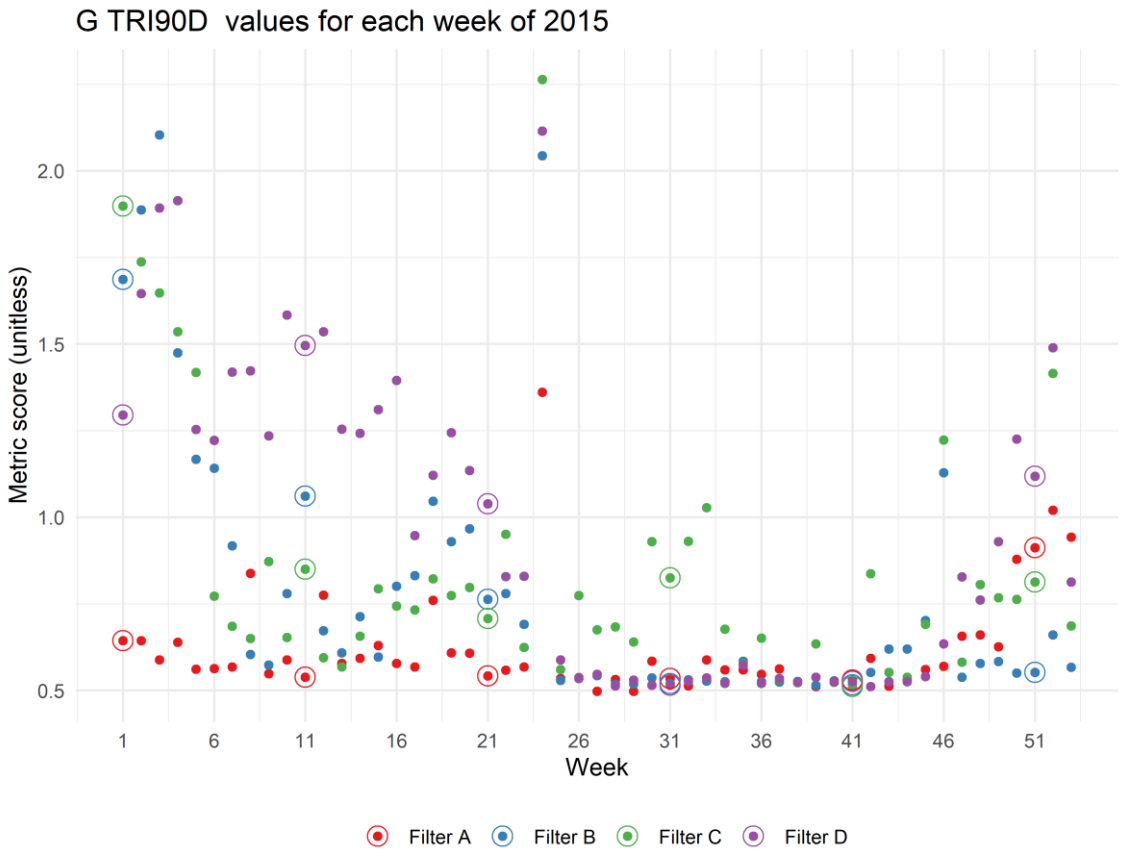

Figure_Apx 9 Enlargement of figure Figure 8 G weekly turbidity $TRI_{90}D$ values

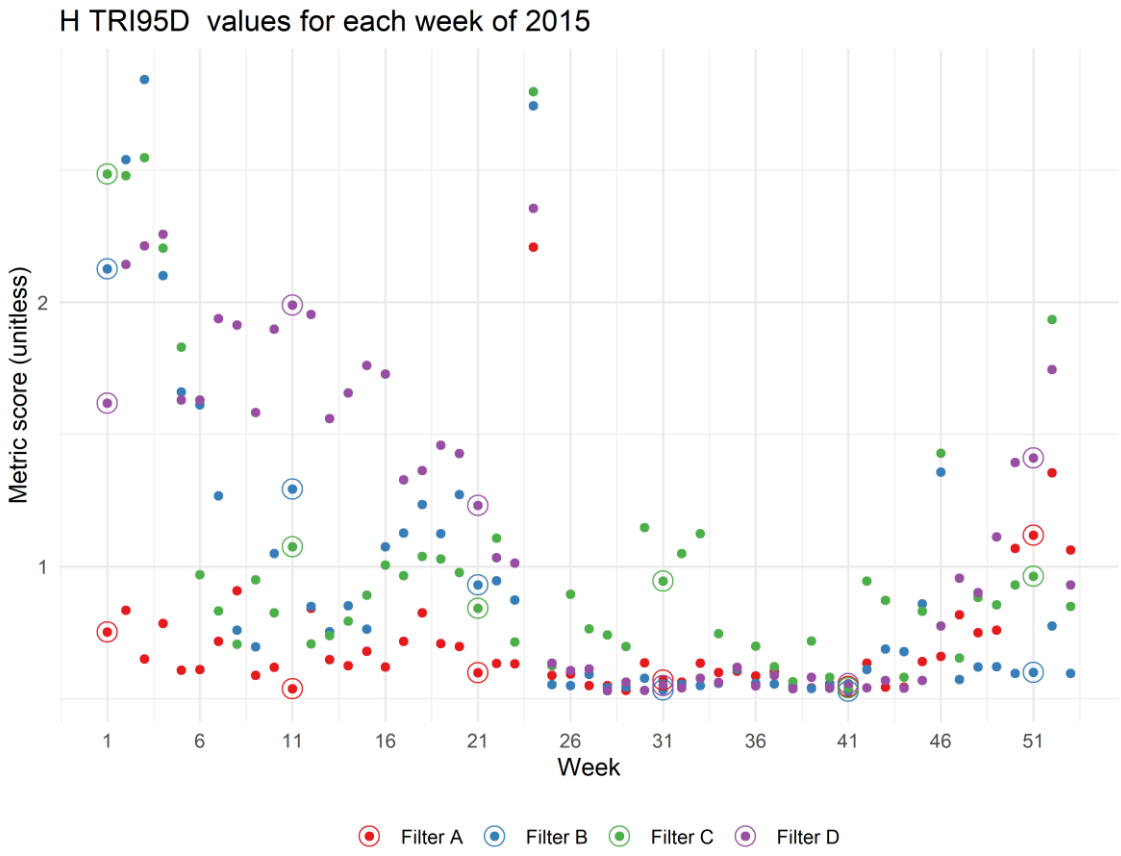

Figure_Apx 10 Enlargement of figure Figure 8 H weekly turbidity $TRI_{95}D$ values

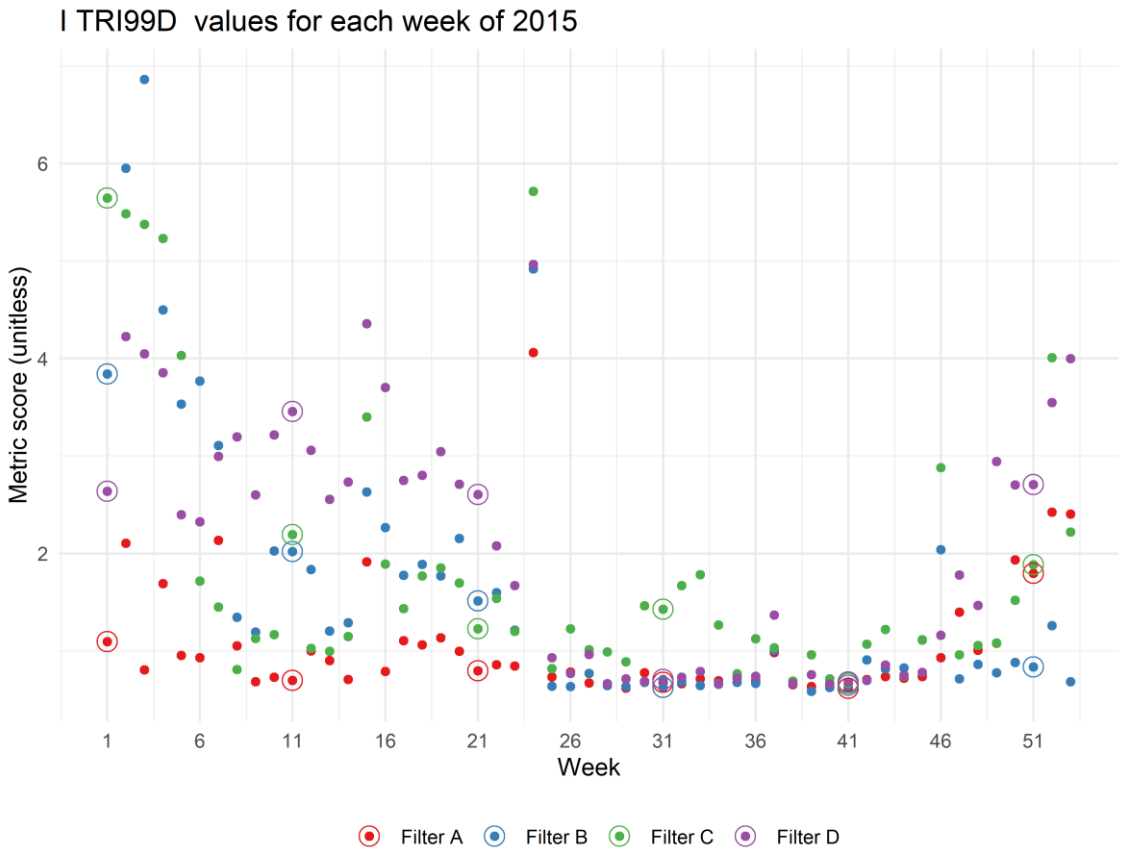

Figure_Apx 11 Enlargement of figure Figure 8 I weekly turbidity $TRI_{99}D$ values

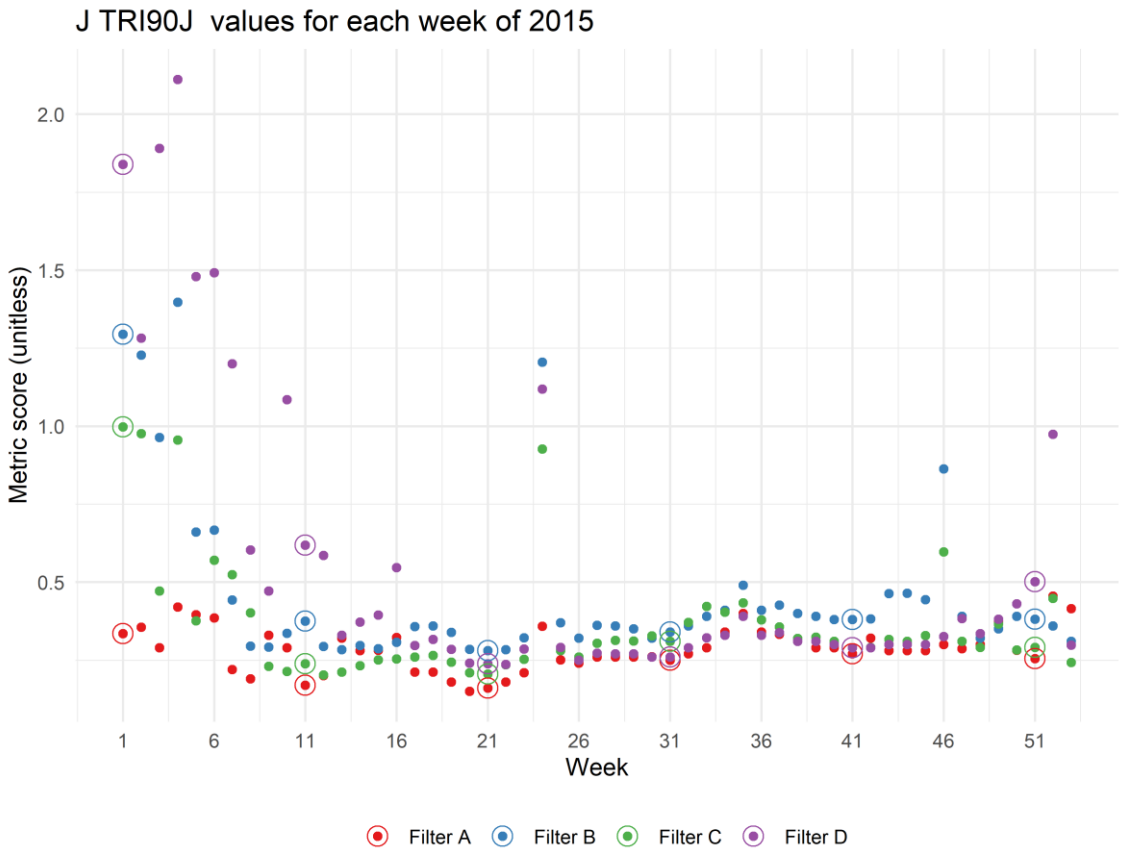

Figure_Apx 12 Enlargement of figure Figure 8 J weekly turbidity $TRI_{90}J$ values

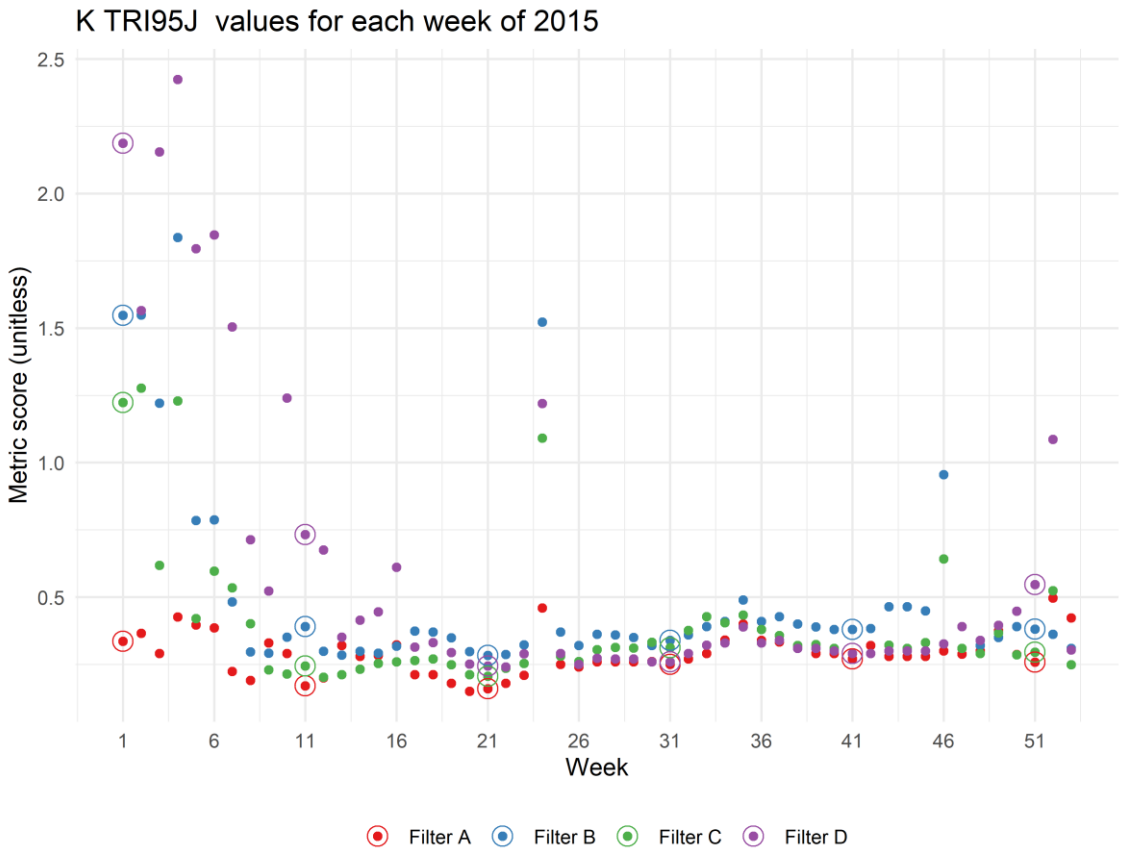

Figure_Apx 13 Enlargement of figure Figure 8 K weekly turbidity $TRI_{95}J$ values

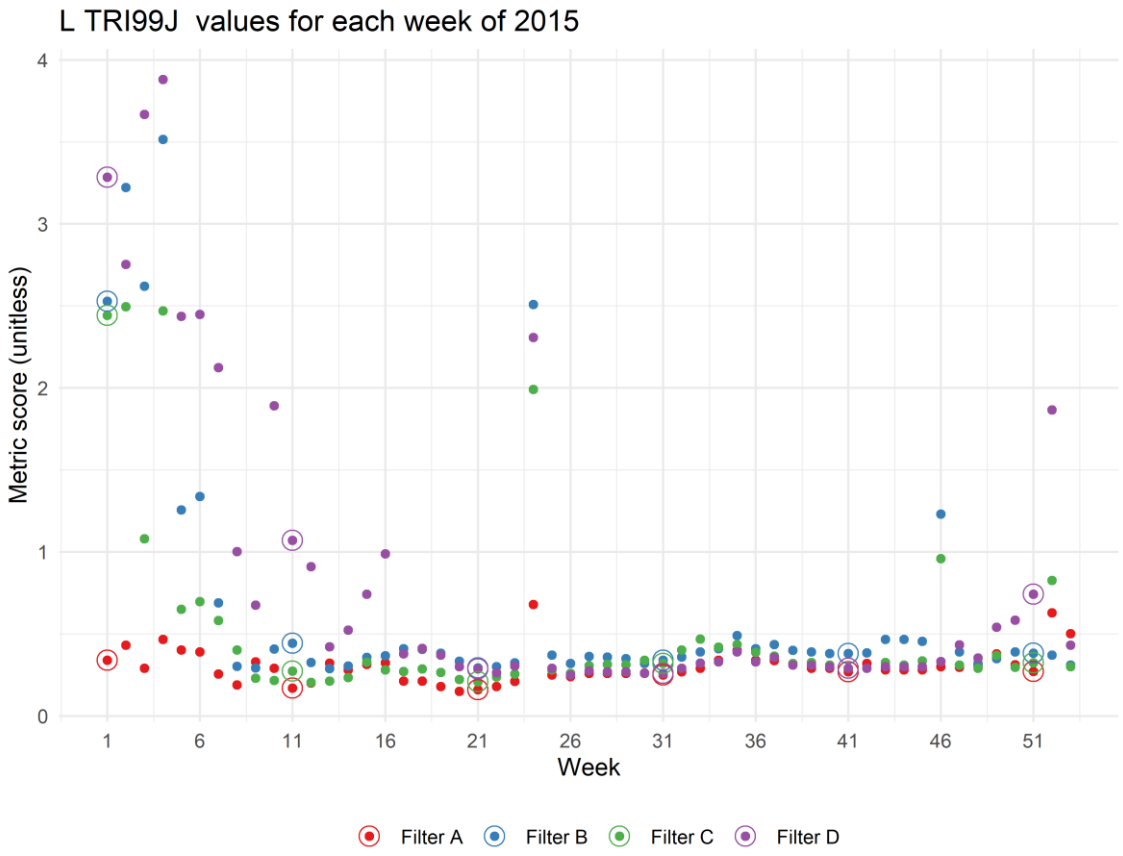

Figure_Apx 14 Enlargement of figure Figure 8 L weekly turbidity $TRI_{99}J$ values

Appendix B Supplementary materials for chapter 3

B.1 Data processing & modelling diagrams

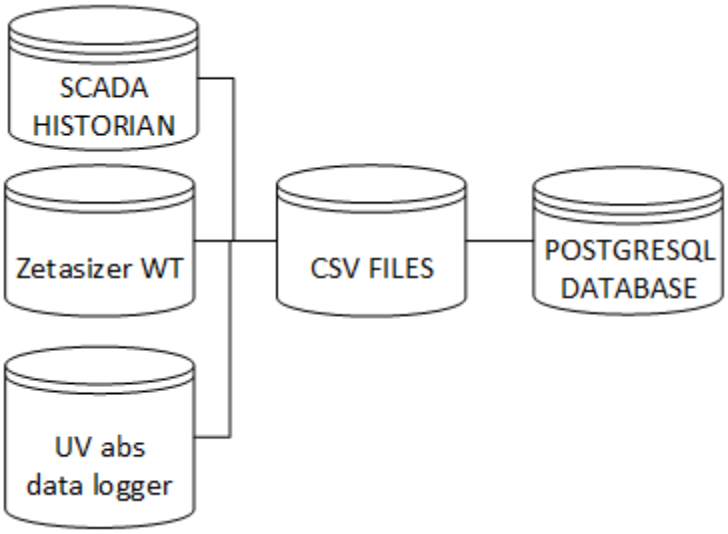

Figure_Apx 15 Data processing diagram for on-line data from case study WTW

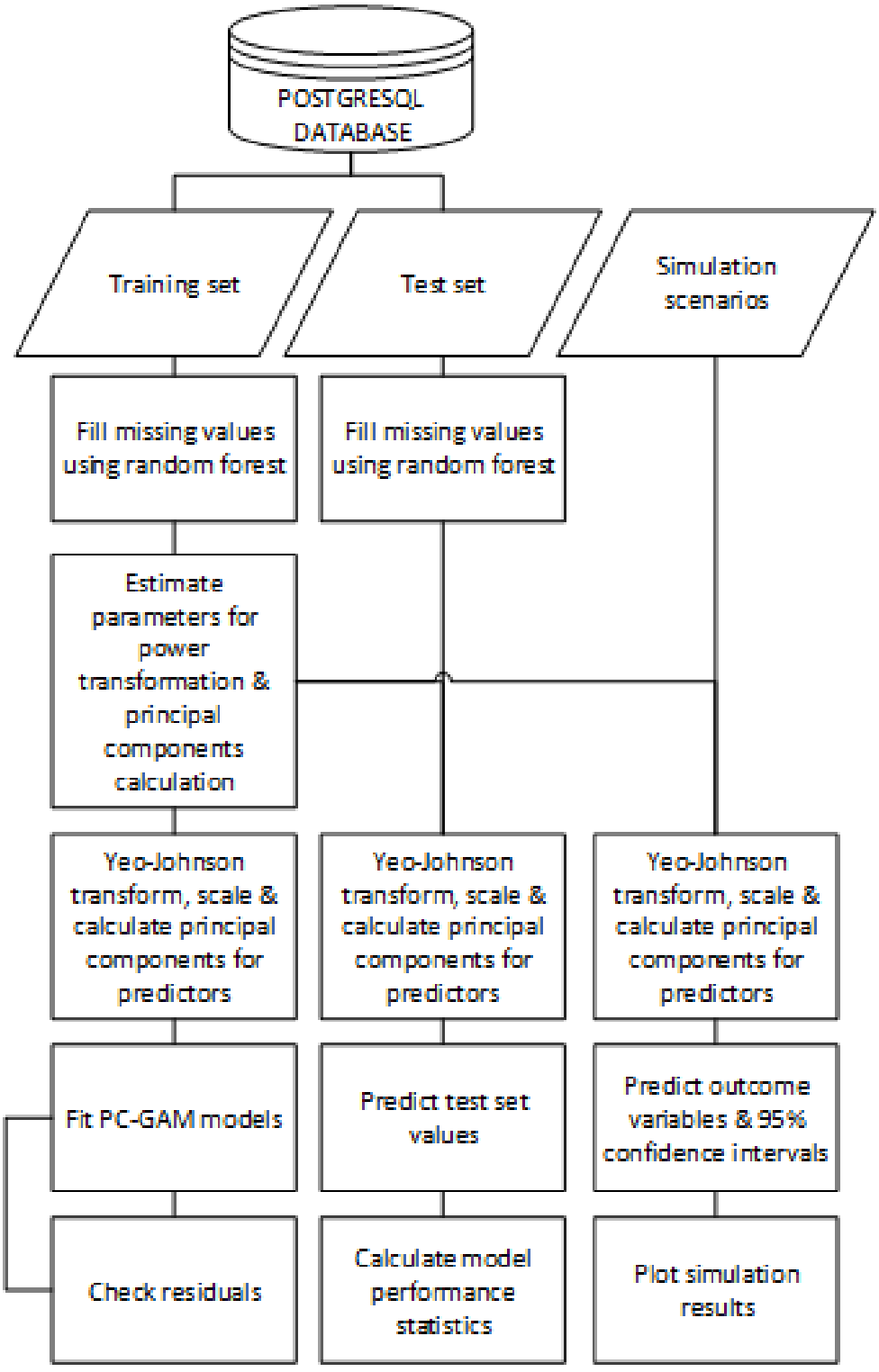

Figure_Apx 16 Data modelling and analysis process for PC-GAMM models and simulations

B.2 Raw water quality

Table_Apx 1 Summary of raw water quality data

Source	Determinand	mean	5th %ile	25th %ile	75th %ile	95th %ile	n
Source A	Absorbance UV/cm	0.17	0.15	0.15	0.18	0.2	74
Source B	Absorbance UV/cm	0.29	0.23	0.26	0.33	0.35	74
Source A	Colour mg/l Pt/Co	24.5	20	22	26	30	74
Source B	Colour mg/l Pt/Co	41.54	28.65	37	48	54.35	74
Source A	Hydrogen Ion pH value	7.28	6.98	7.2	7.4	7.62	17
Source B	Hydrogen Ion pH value	7.51	7.3	7.5	7.6	7.64	17
Source A	SUVA L/mg/m	4.81	3.94	4.5	5.08	5.68	74
Source B	SUVA L/mg/m	4.7	3.35	4.2	4.79	5.28	74
Source A	Total Organic Carbon mgC/l	3.57	3	3.3	3.88	4.17	74
Source B	Total Organic Carbon mgC/l	6.6	5.1	5.8	7.3	8.2	74
Source A	Turbidity NTU	0.9	0.4	0.5	0.9	2.86	65
Source B	Turbidity NTU	1.55	0.9	1.1	1.8	2.76	65

B.3 Individual water quality trends

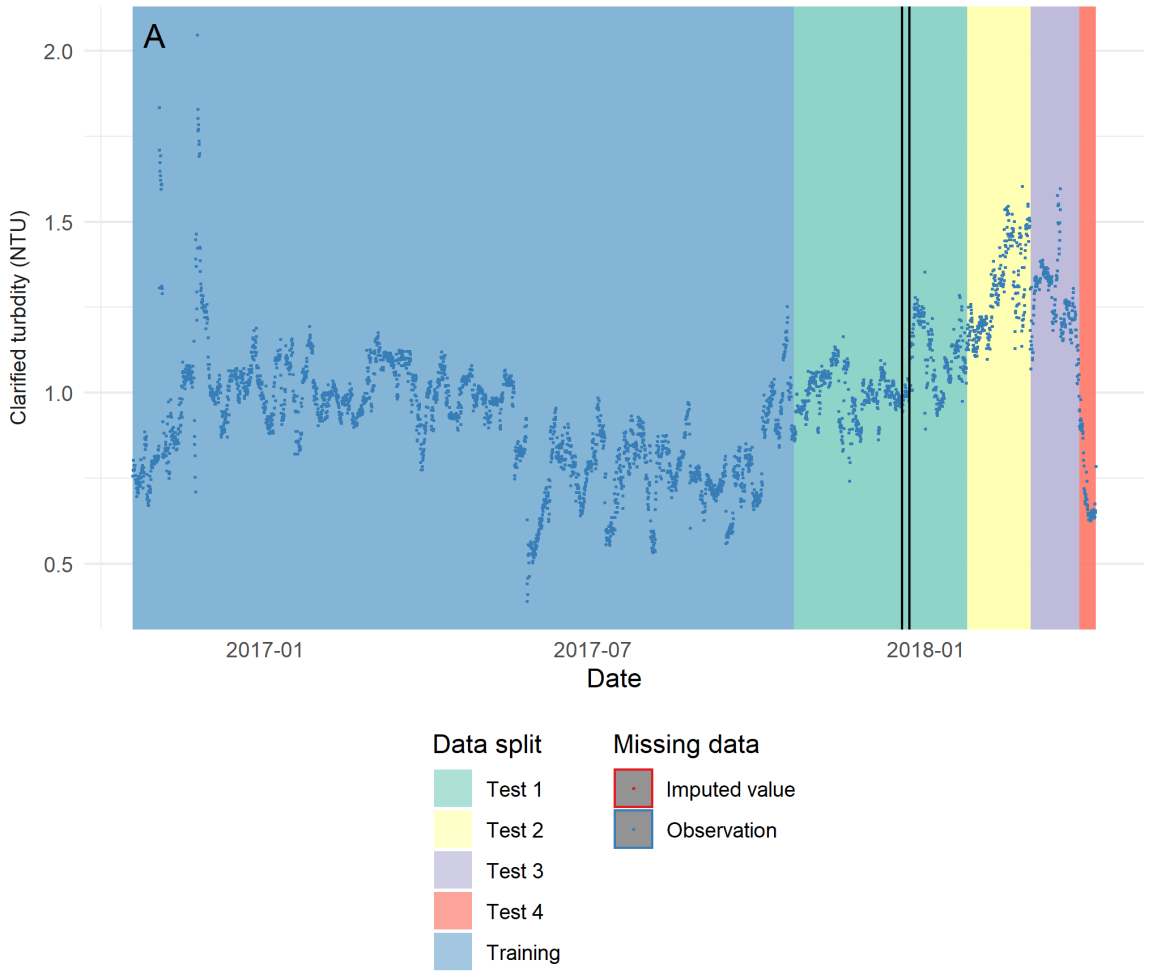

Figure_Apx 17 Enlargement of figure Figure 12 A three-hourly mean turbidity in clarified water

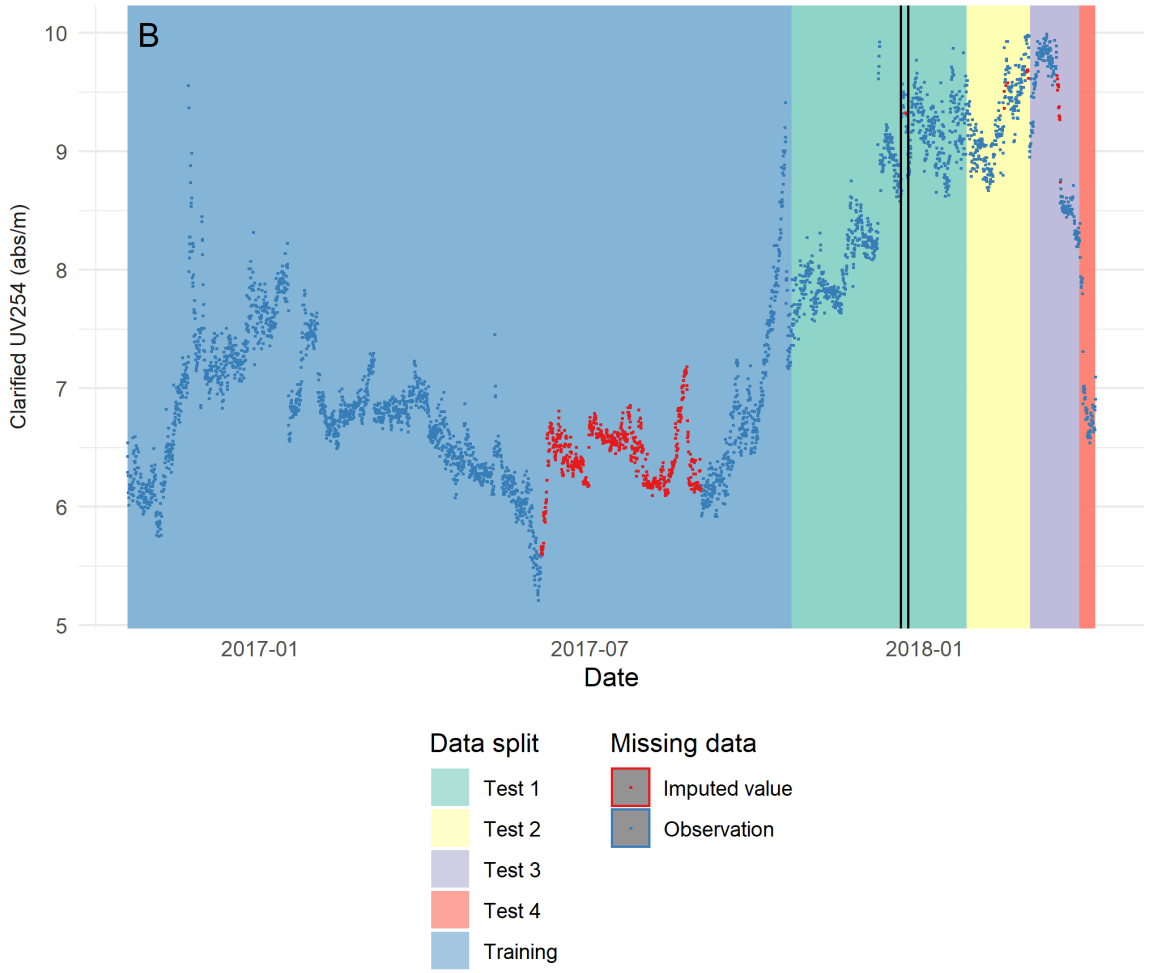

Figure_Apx 18 Enlargement of figure Figure 12 B three-hourly mean UV254 absorbance in clarified water

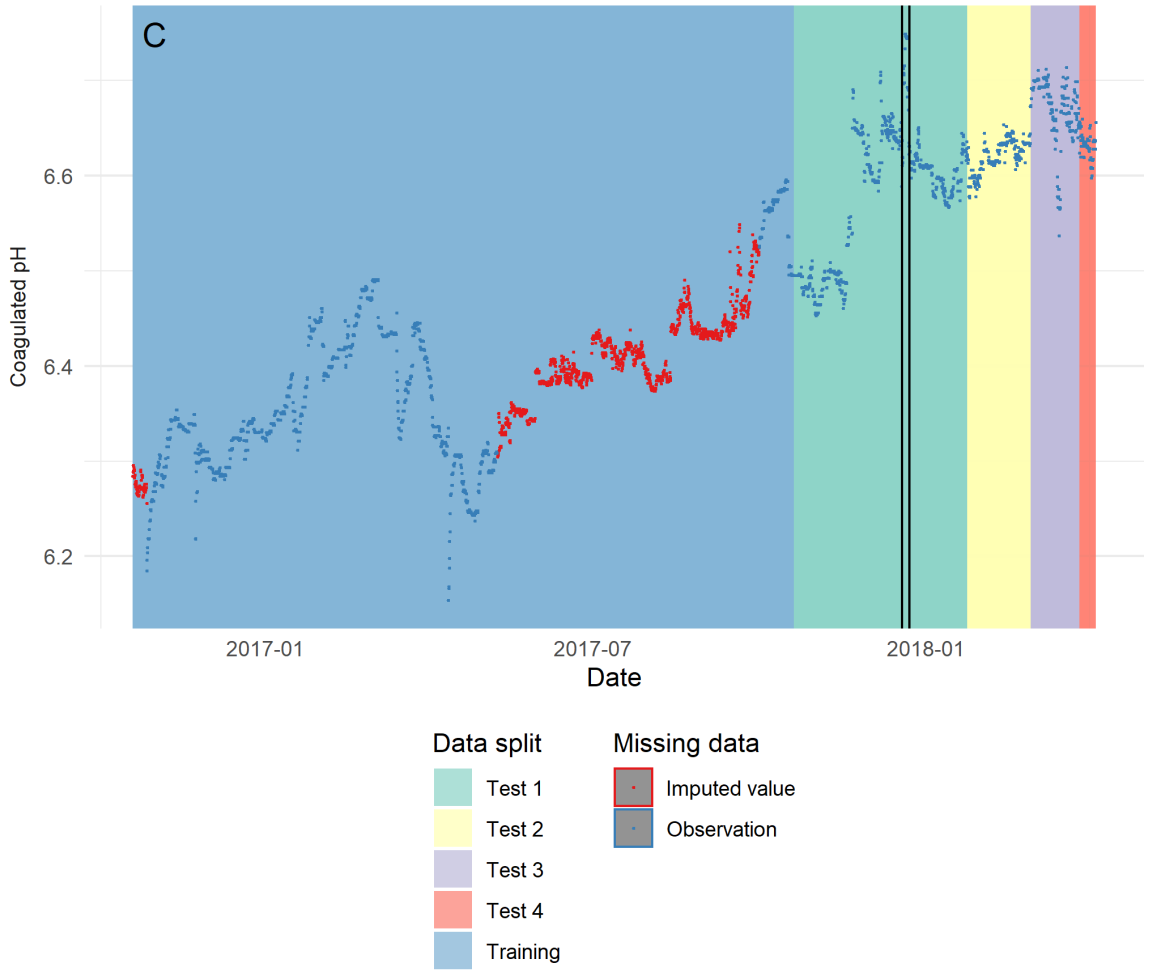

Figure_Apx 19 Enlargement of figure Figure 12 C three-hourly mean pH in coagulated water

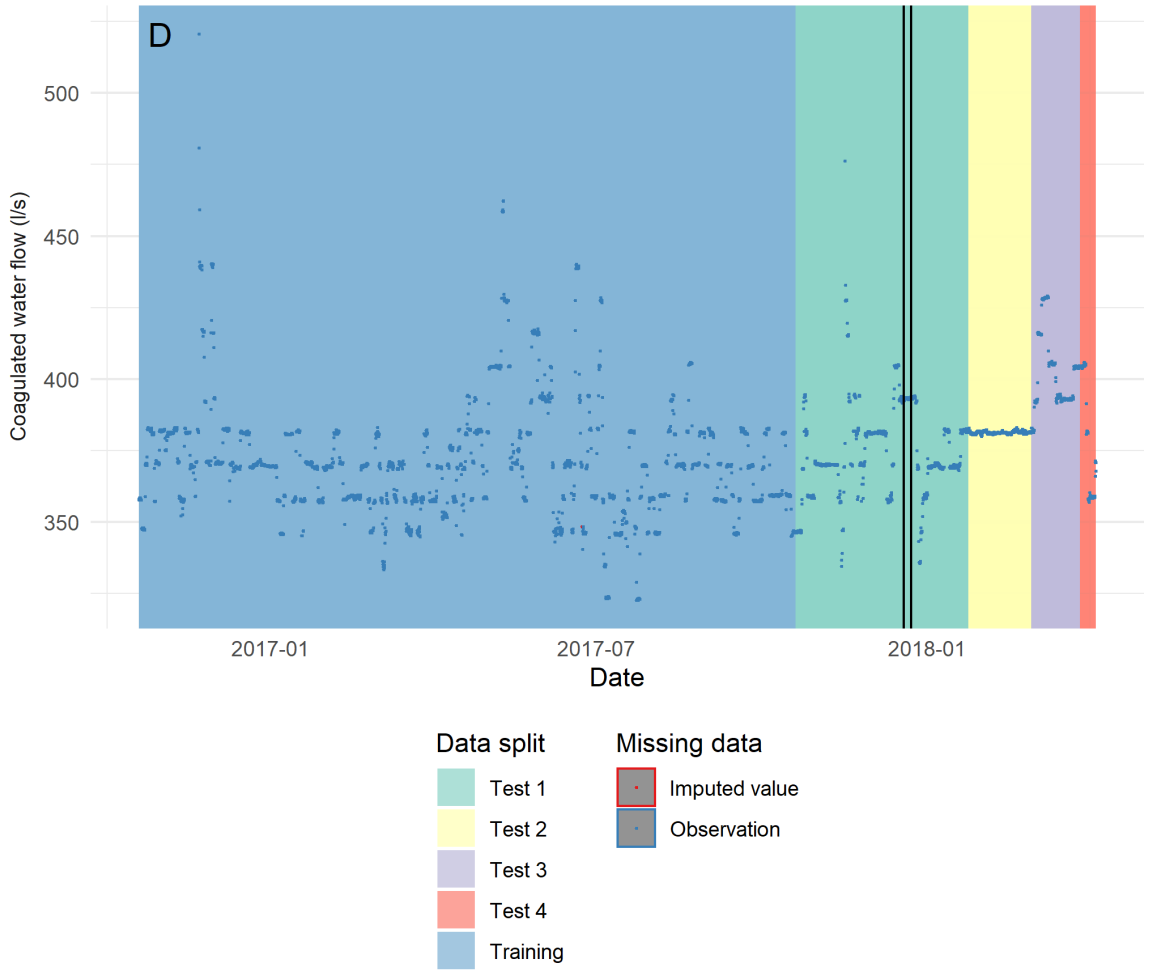

Figure_Apx 20 Enlargement of figure Figure 12 D three-hourly flow of coagulated water

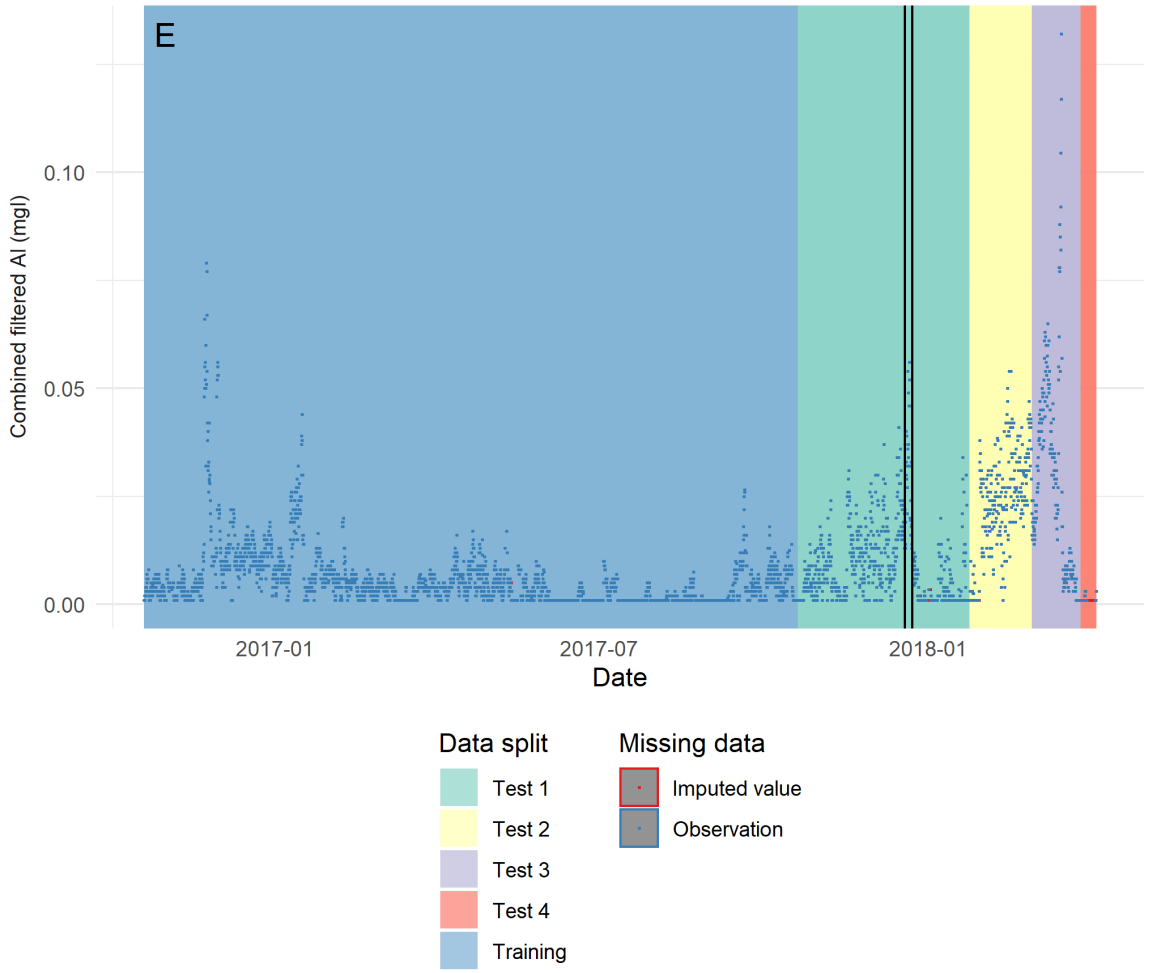

Figure_Apx 21 Enlargement of figure Figure 12 E three-hourly mean Aluminium in filtered water

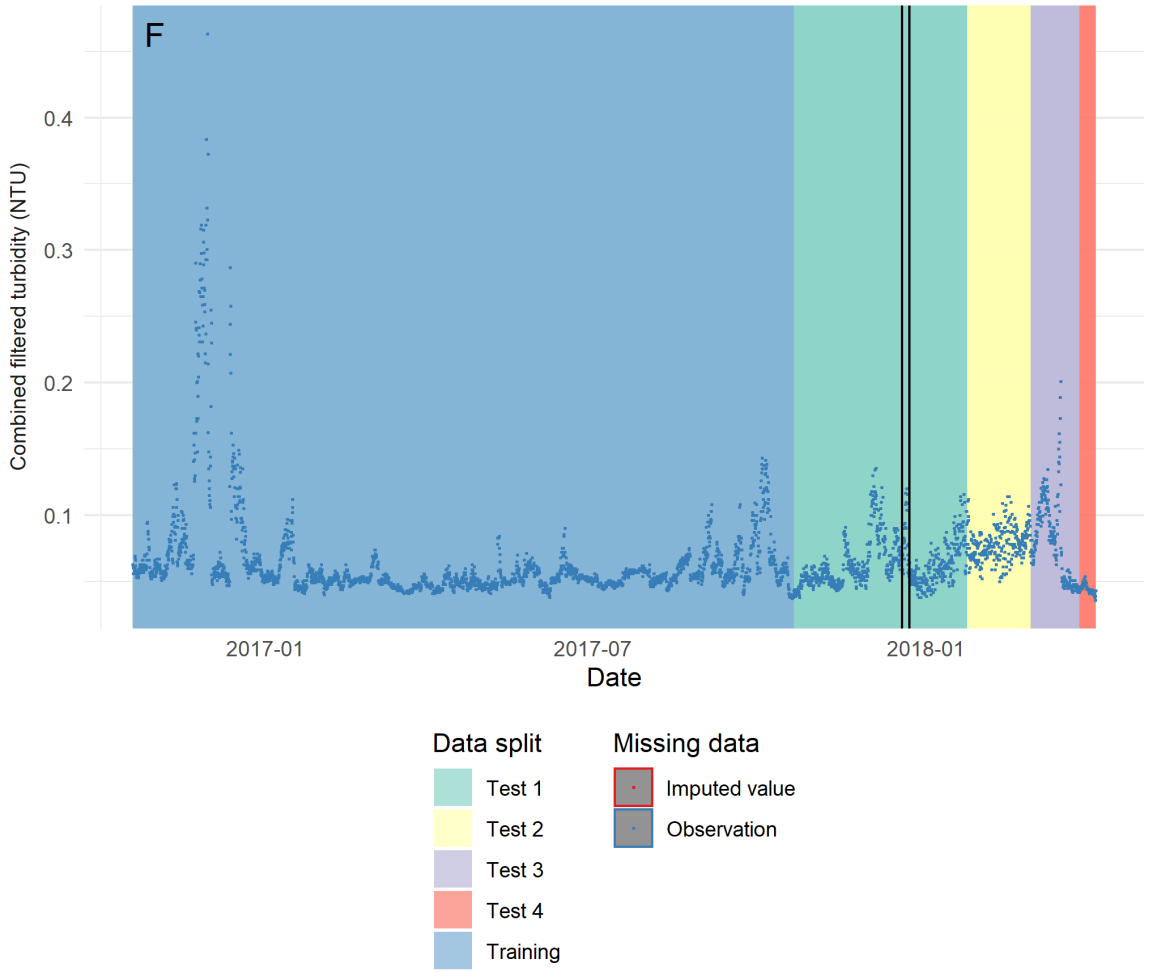

Figure_Apx 22 Enlargement of figure Figure 12 F three-hourly mean turbidity in filtered water

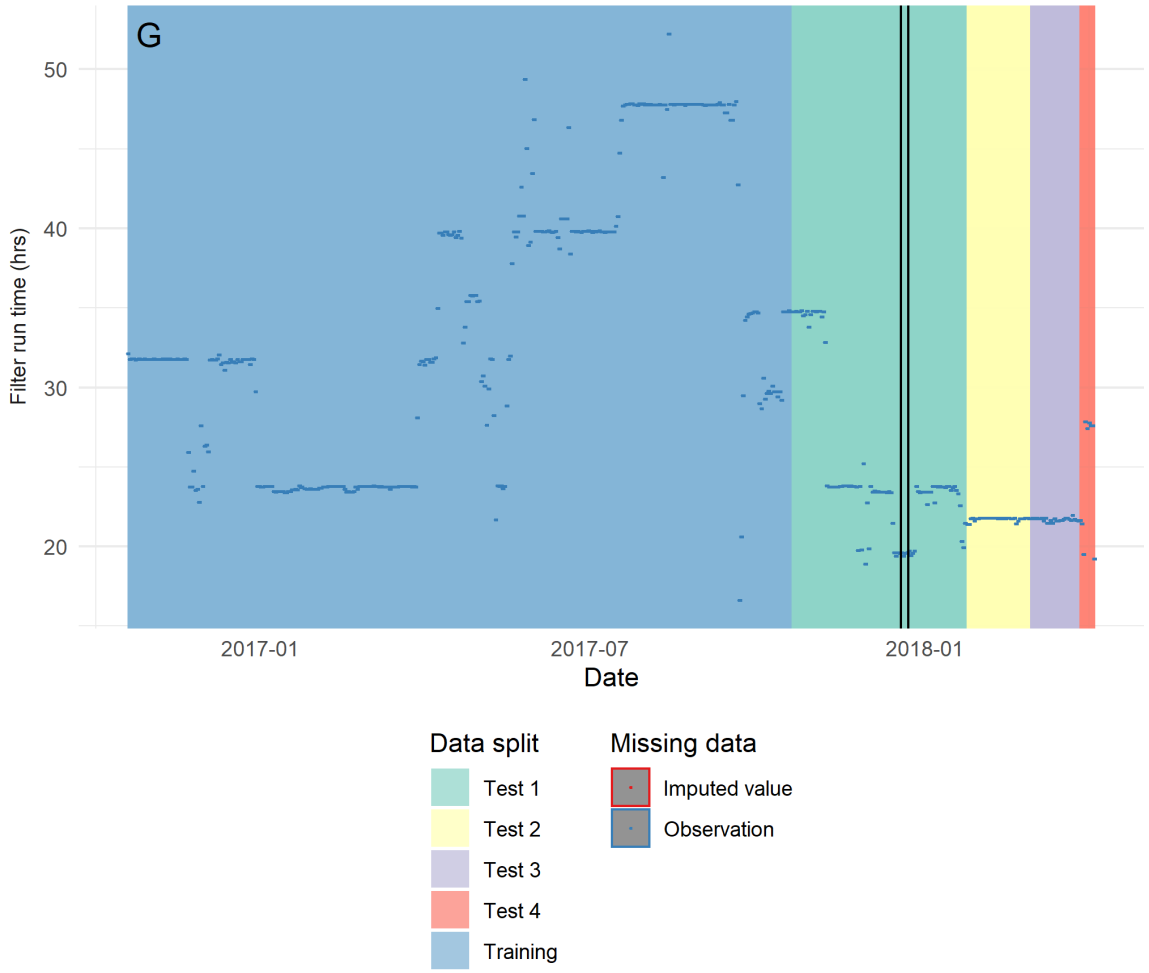

Figure_Apx 23 Enlargement of figure Figure 12 G three-hourly mean filter run time

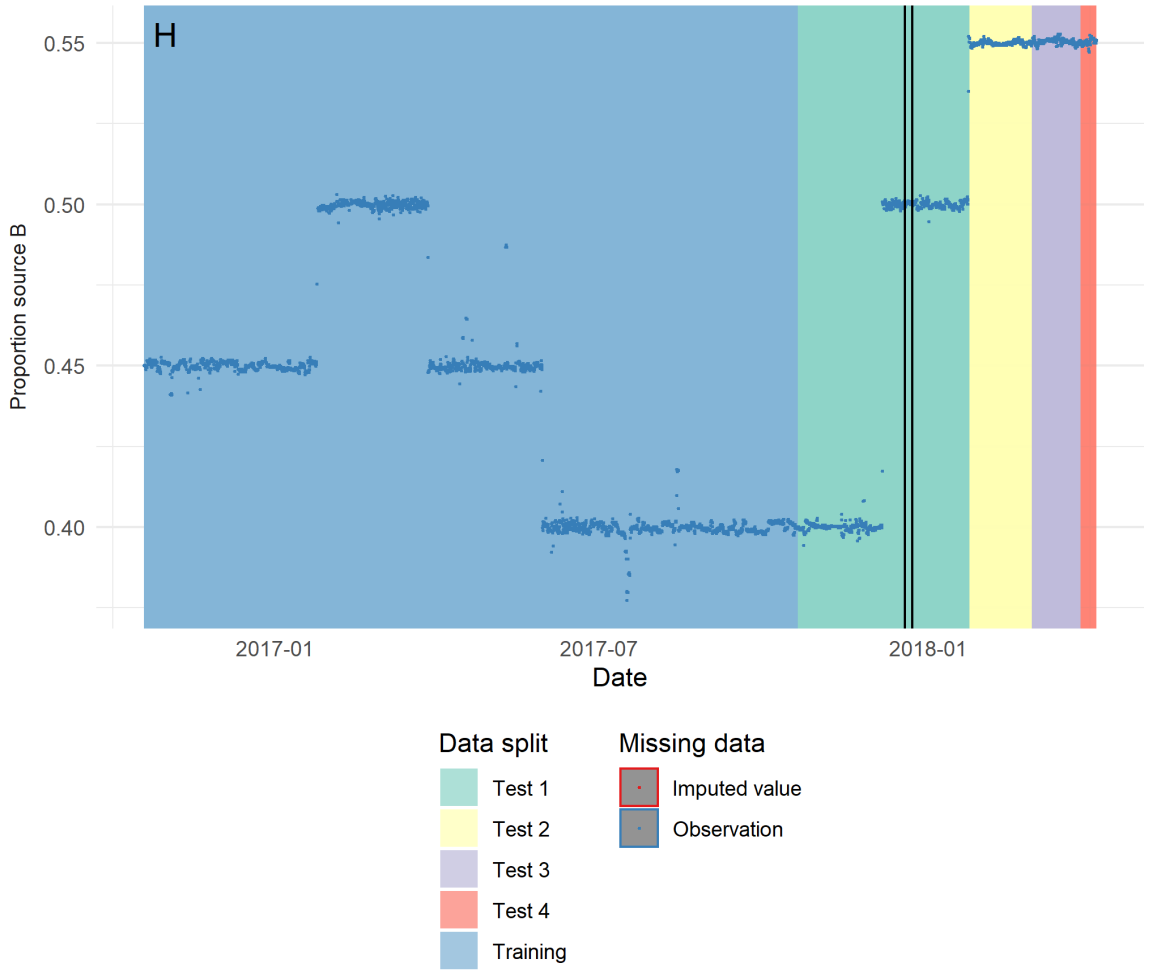

Figure_Apx 24 Enlargement of figure Figure 12 H three-hourly mean proportion flow from source B

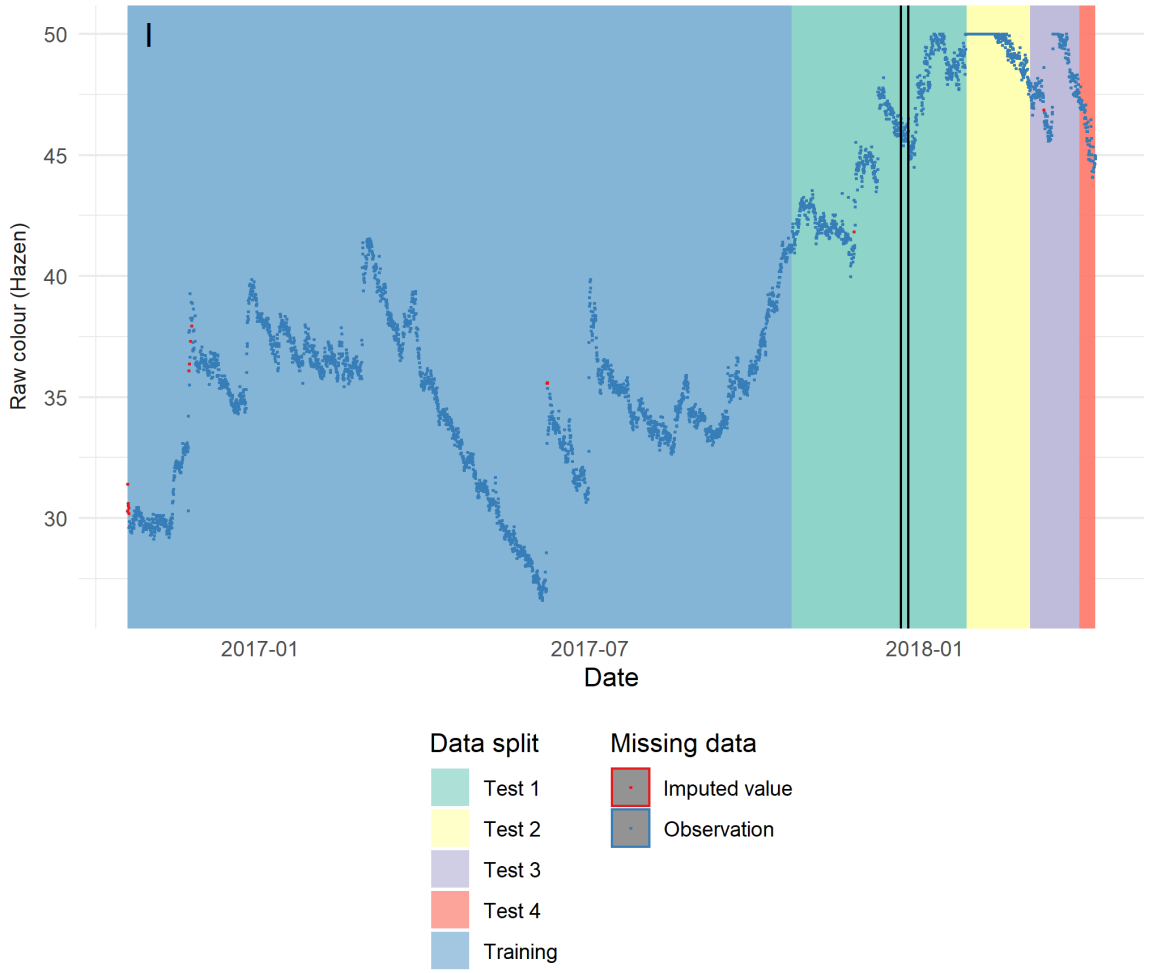

Figure_Apx 25 Enlargement of figure Figure 12 I three-hourly mean colour in raw water

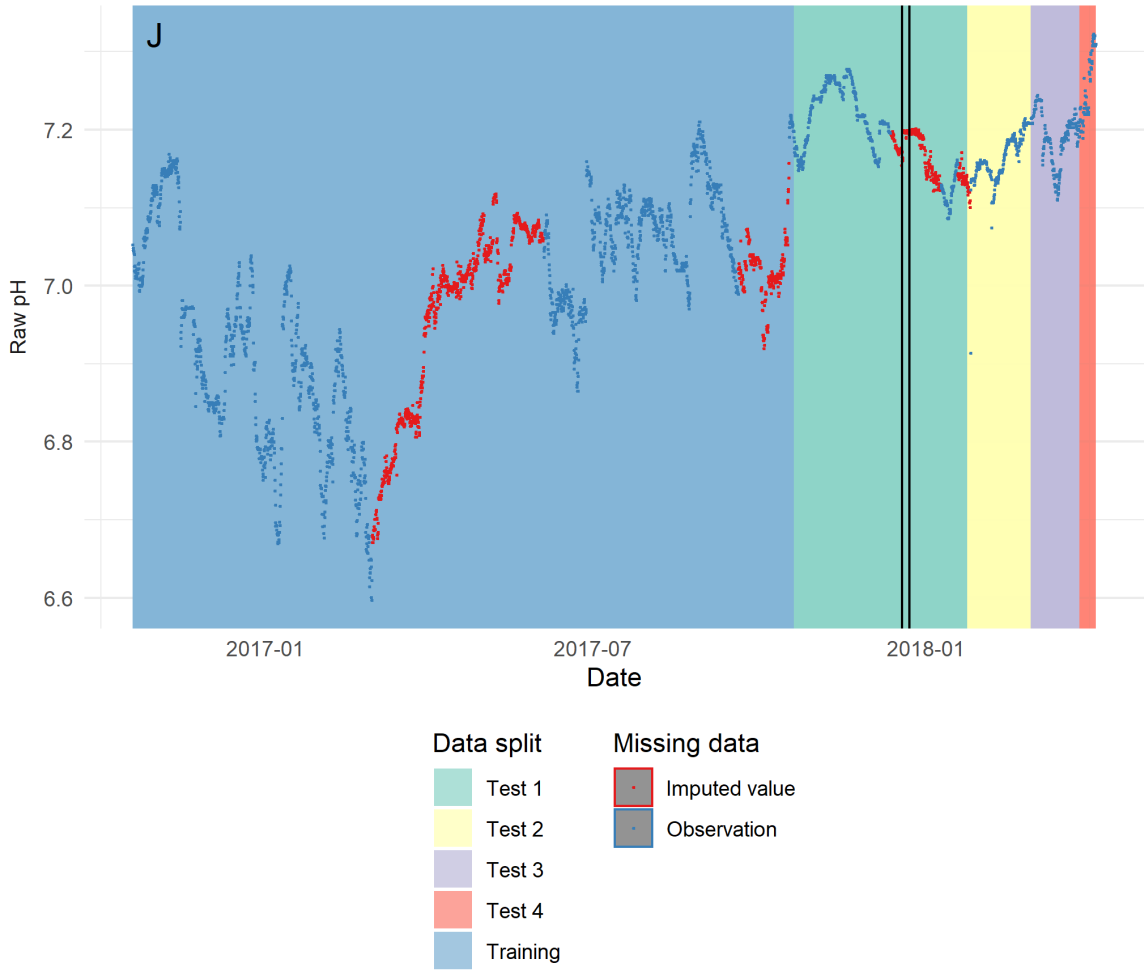

Figure_Apx 26 Enlargement of figure Figure 12 J three-hourly mean pH in raw water

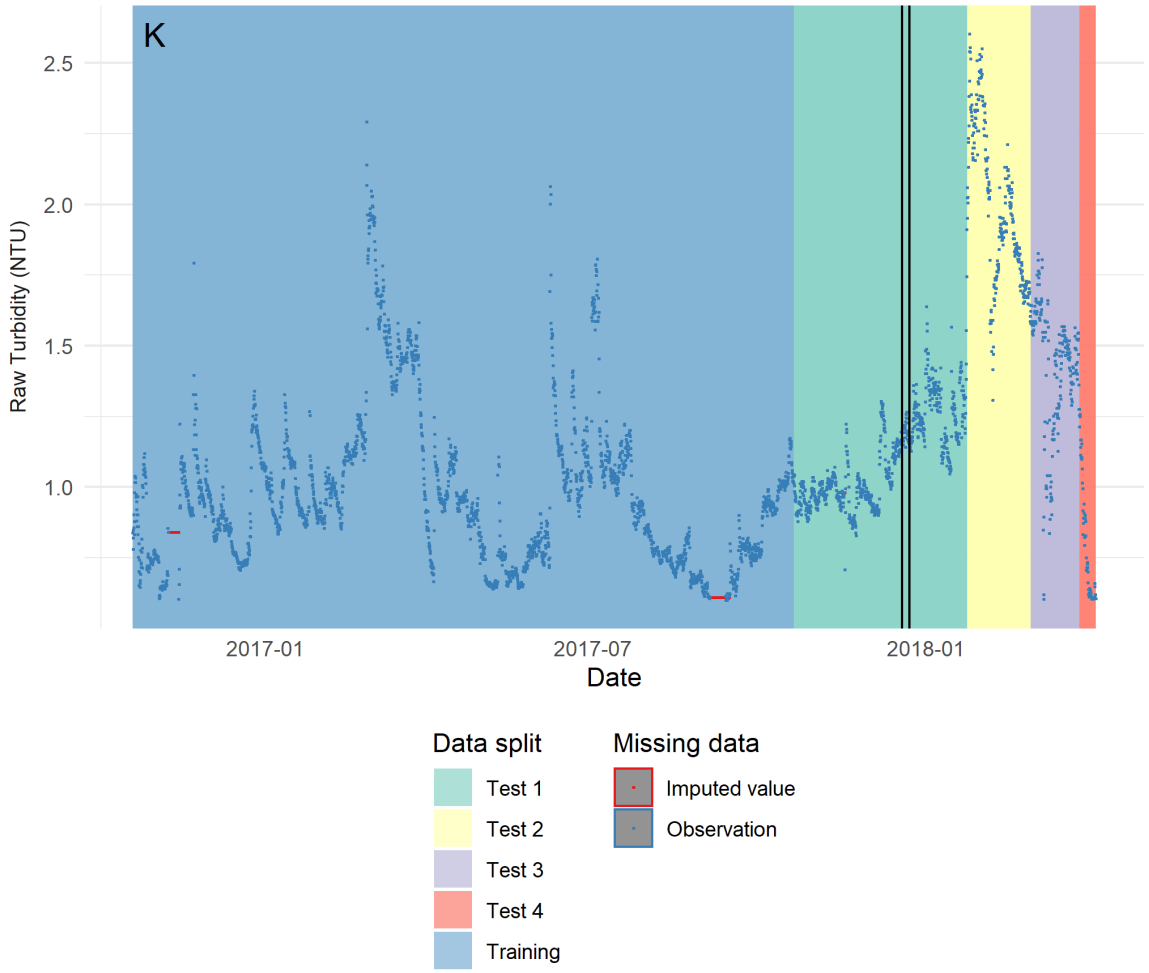

Figure_Apx 27 Enlargement of figure Figure 12 K three-hourly mean turbidity in raw water

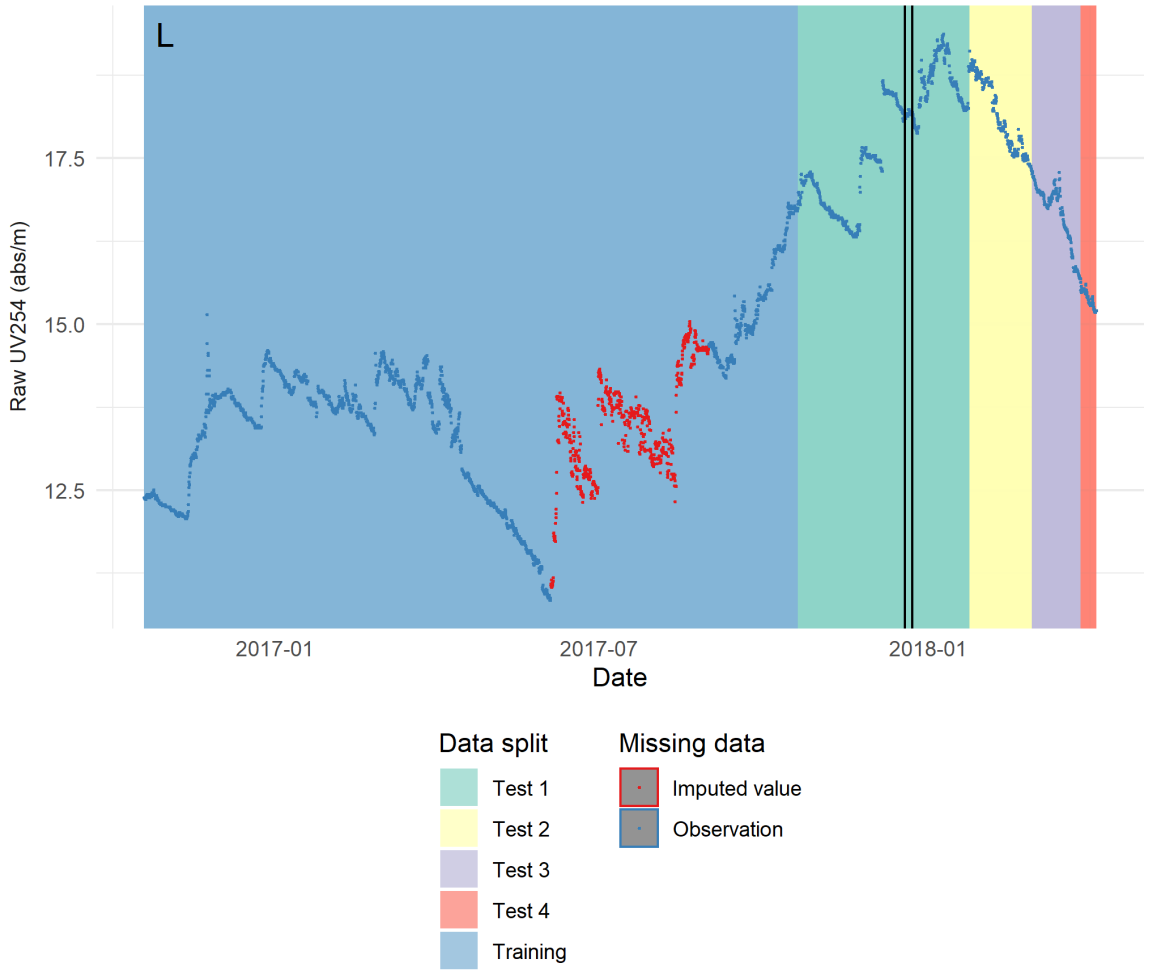

Figure_Apx 28 Enlargement of figure Figure 12 L three-hourly mean UV254 absorbance in raw water

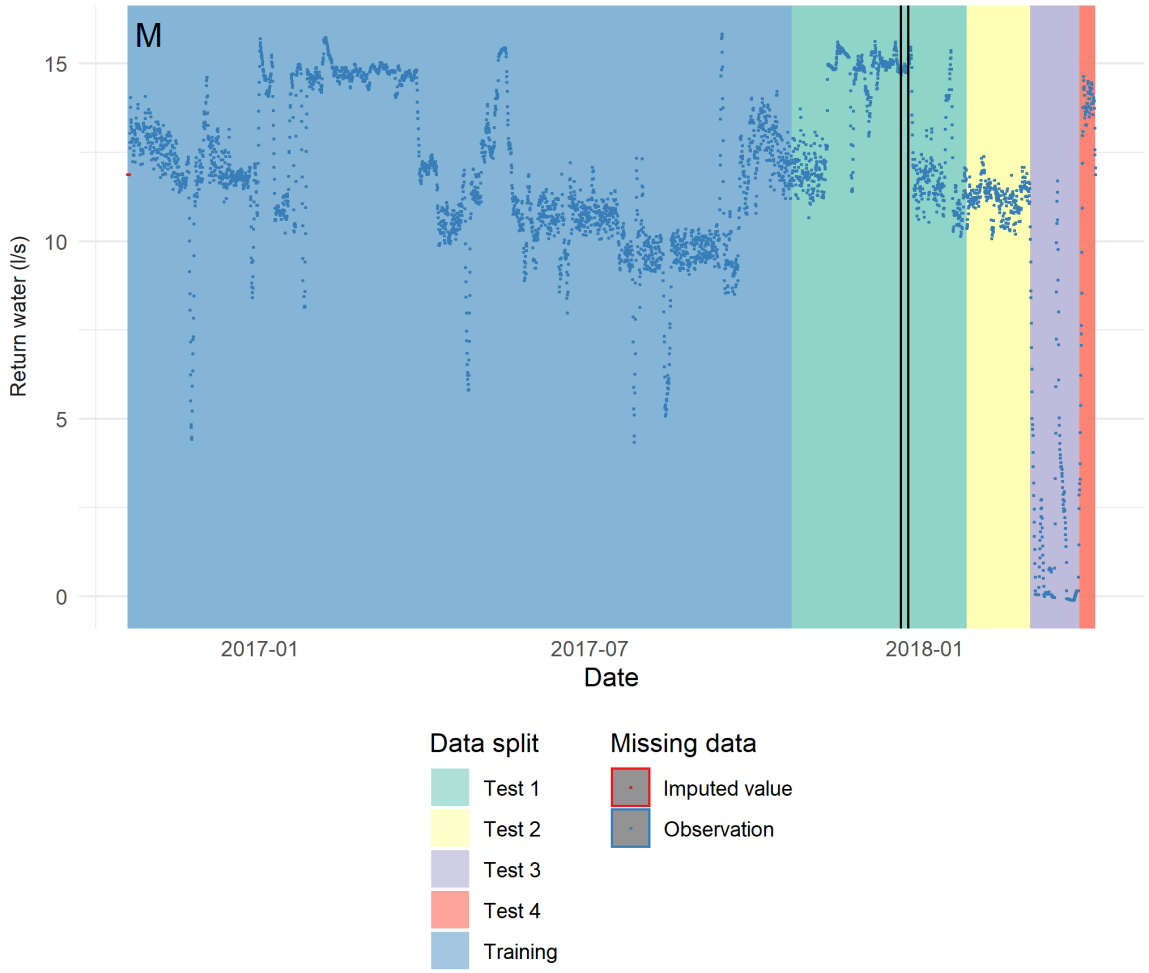

Figure_Apx 29 Enlargement of figure Figure 12 M three-hourly mean flow of recycled water

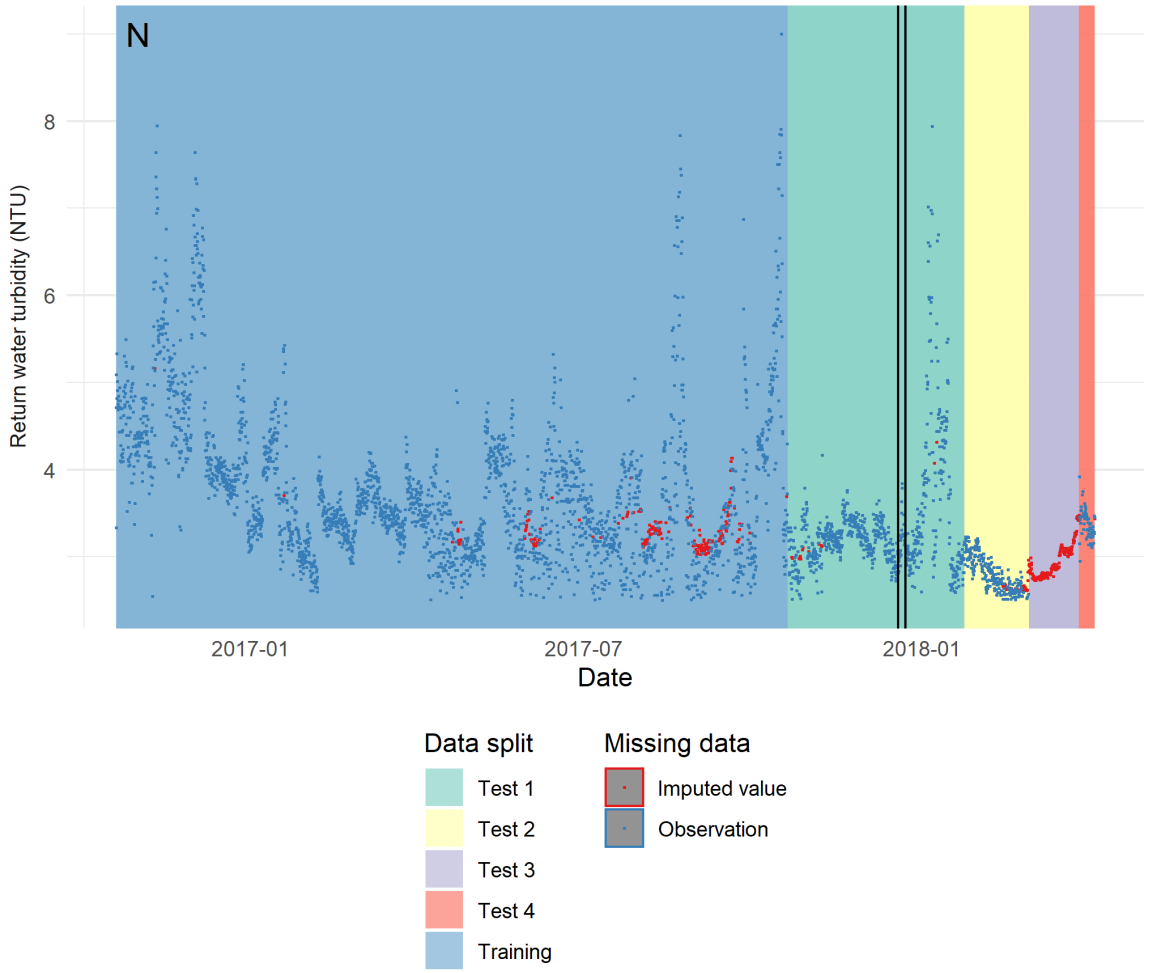

Figure_Apx 30 Enlargement of figure Figure 12 N three-hourly mean turbidity in recycled water

Figure_Apx 31 Enlargement of figure Figure 12 O three-hourly mean zeta potential of coagulated water

B.4 Relative variance of zeta potential measurements approaching 0mV|

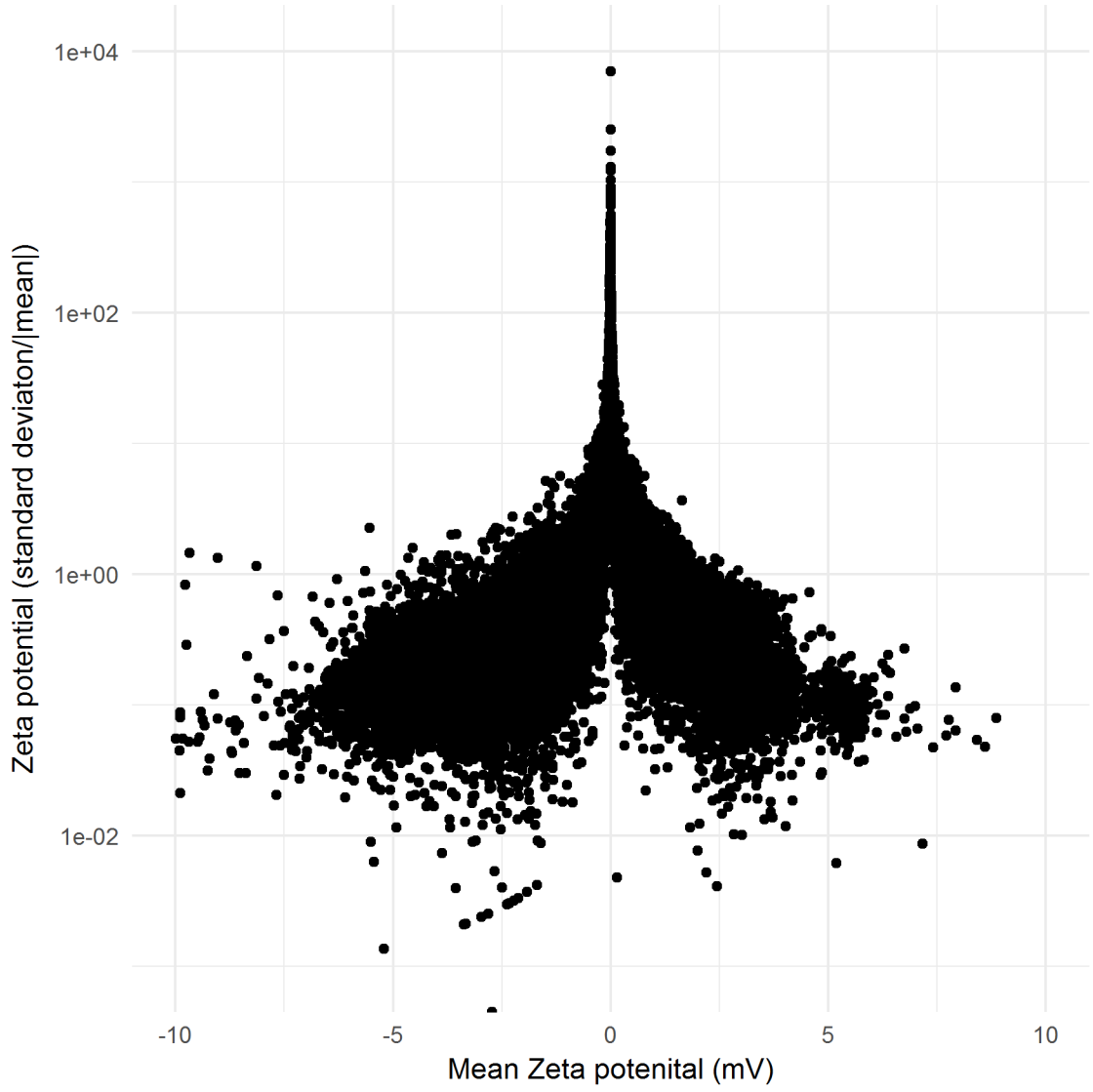

Figure_Apx 32 Relative variance of zeta potential measurements is shown to increase approaching zero. Online zeta potential takes repeated measurements of a single physical sample to reduce measurement error. This plot illustrates the increase in the standard deviation of repeat measurements for a single sample as the mean zeta potential approaches zero.

B.5 Treated water quality over the range of zeta potentials observed

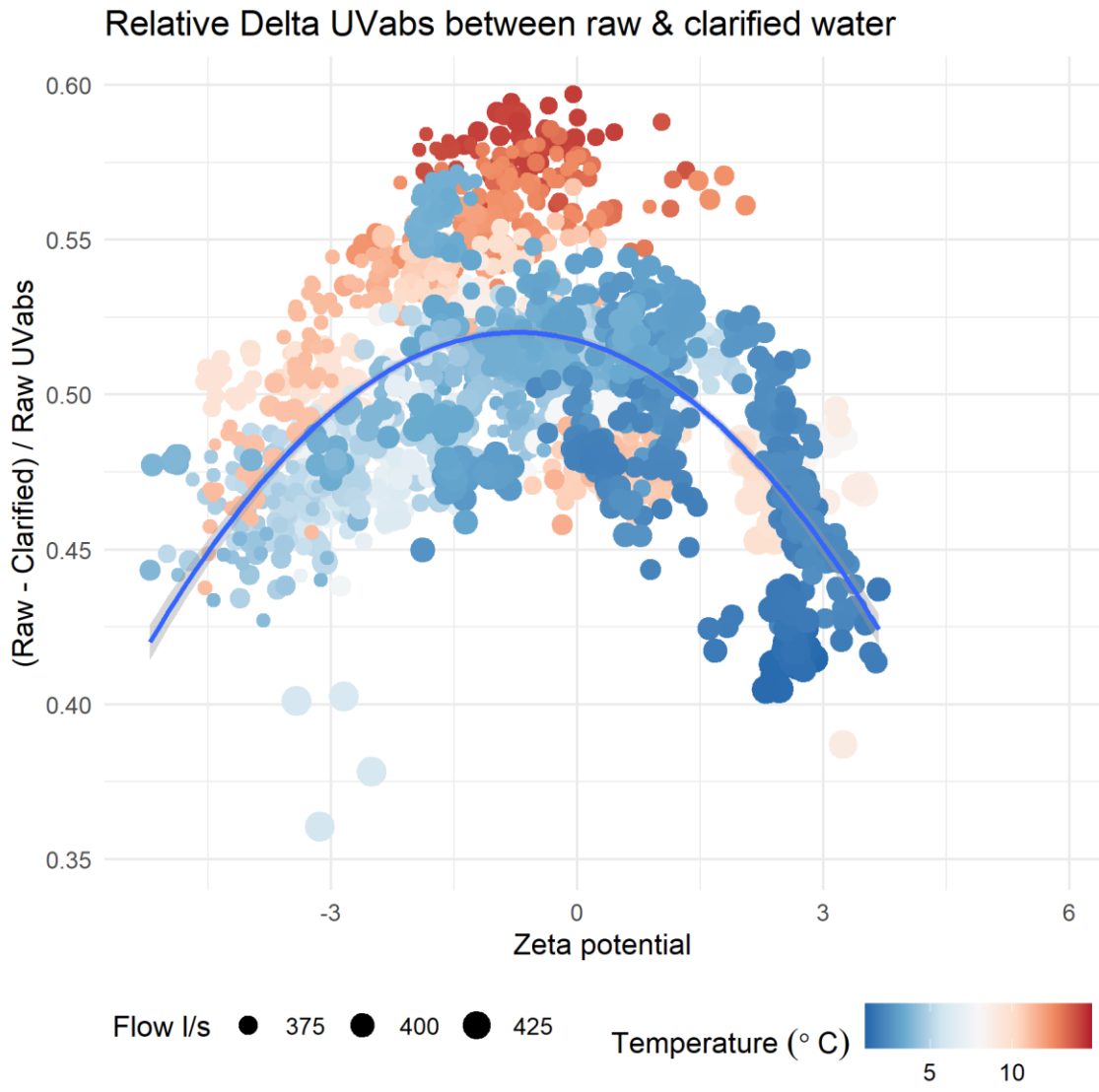

Figure_Apx 33 Relative change in UV absorbance between raw and clarified water over the range of zeta potentials observed. Temperature is indicated by colour and plant flow is indicated by point size.

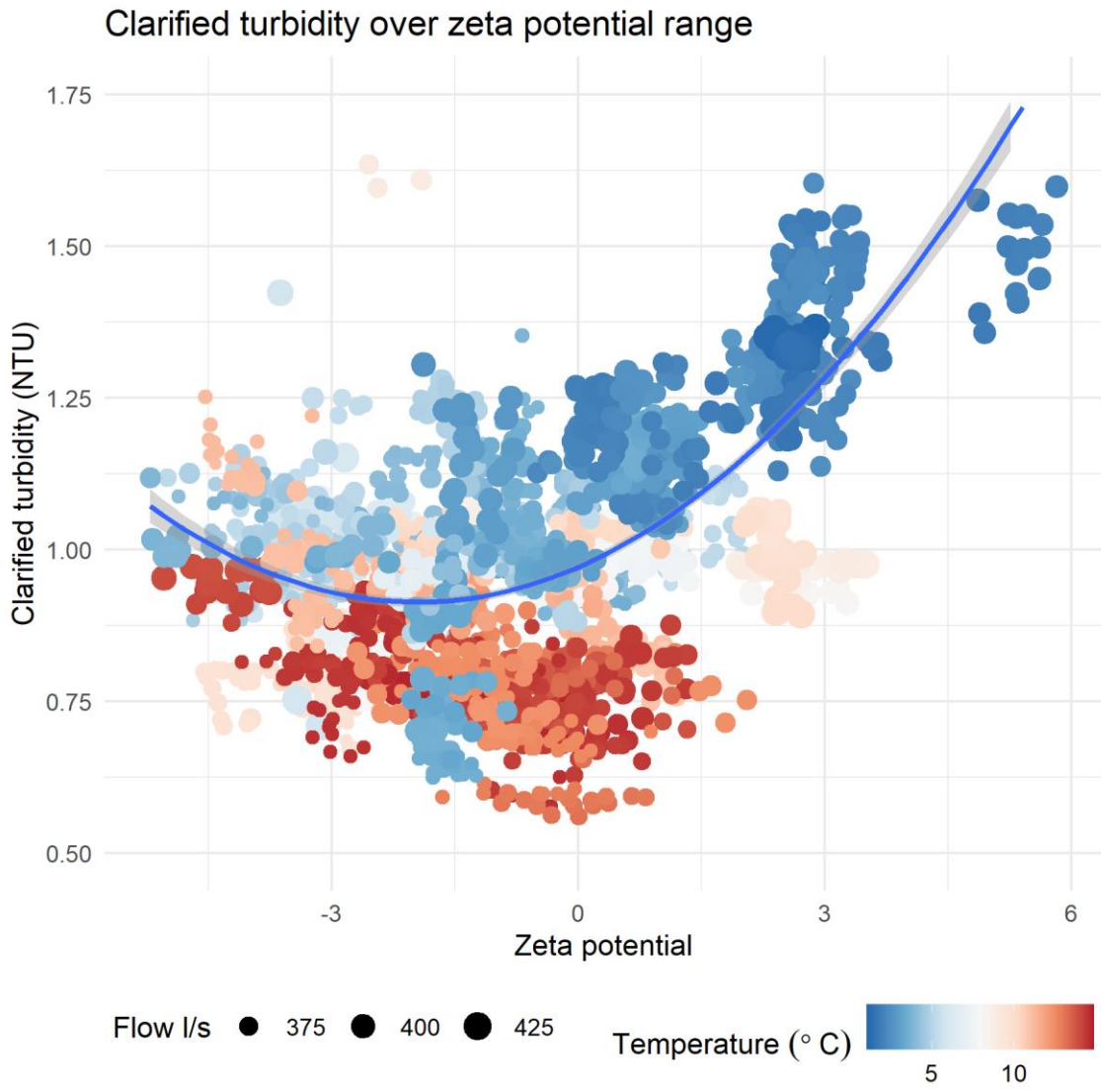

Figure_Apx 34 Clarified water turbidity over the range of zeta potentials observed. Temperature is indicated by colour and plant flow is indicated by point size.

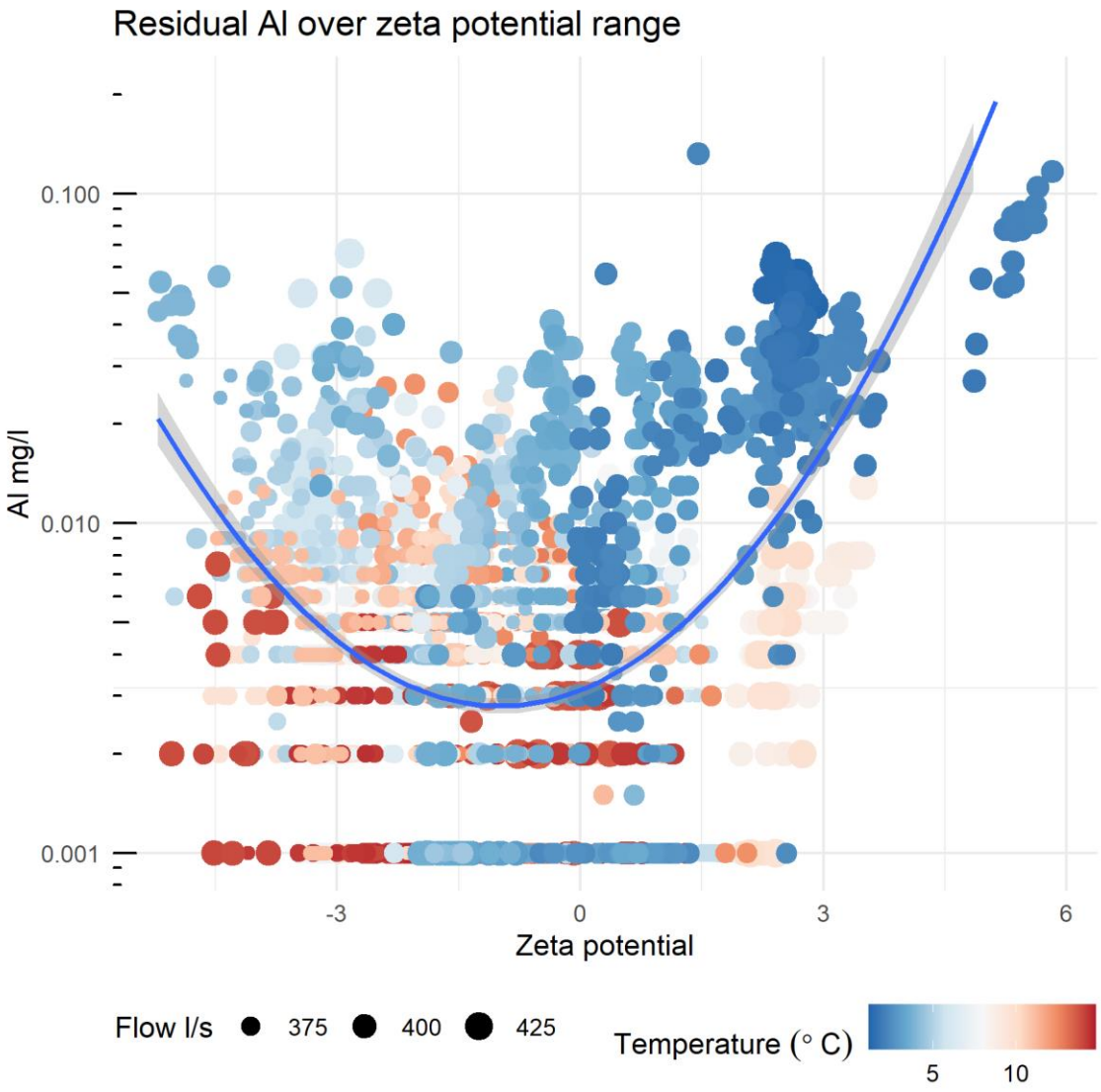

Figure_Apx 35 Filtered water aluminium residual over the range of zeta potentials observed. Temperature is indicated by colour and plant flow is indicated by point size.

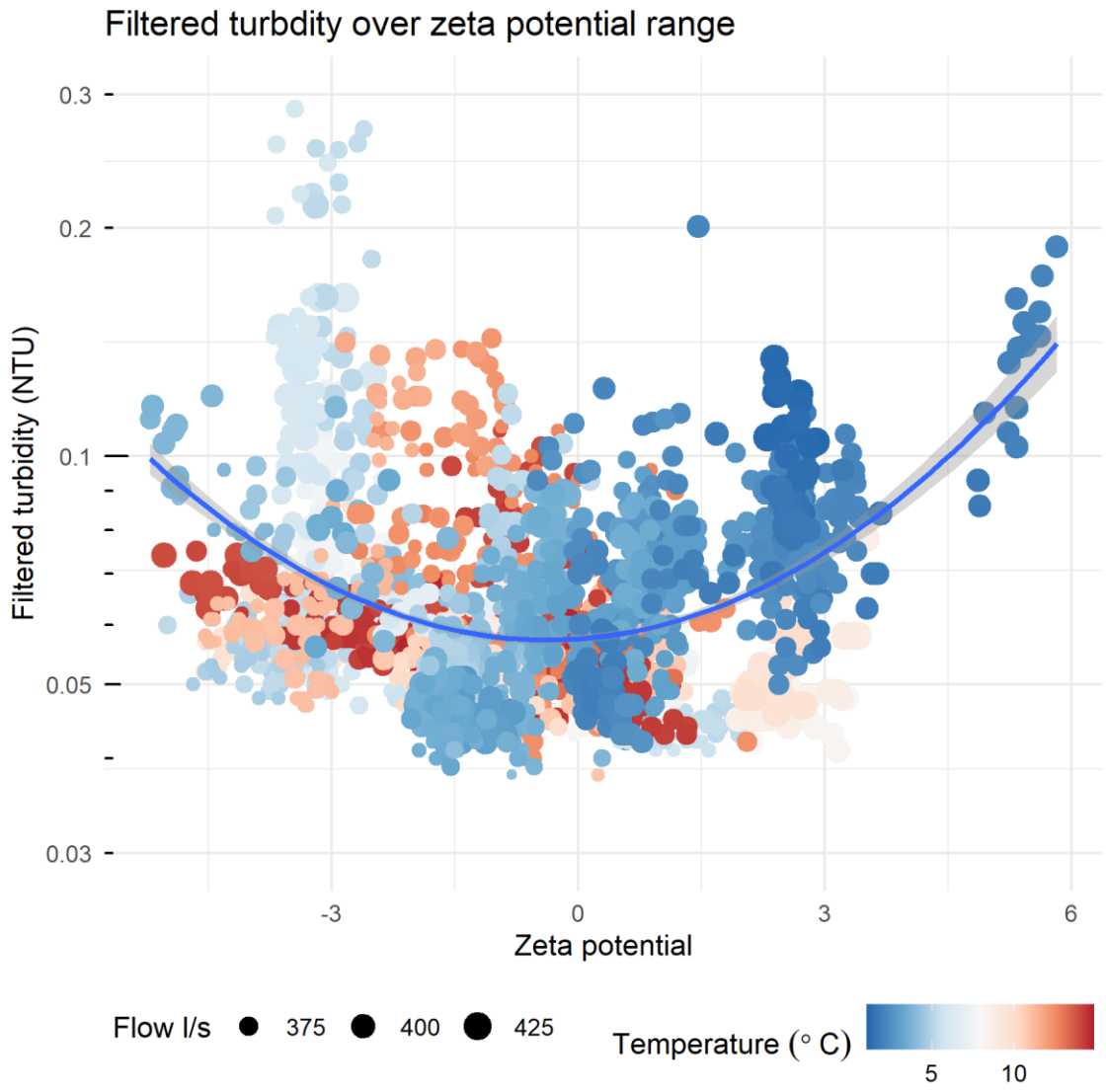

Figure_Apx 36 Filtered water turbidity over the range of zeta potentials observed. Temperature is indicated by colour and plant flow is indicated by point size.

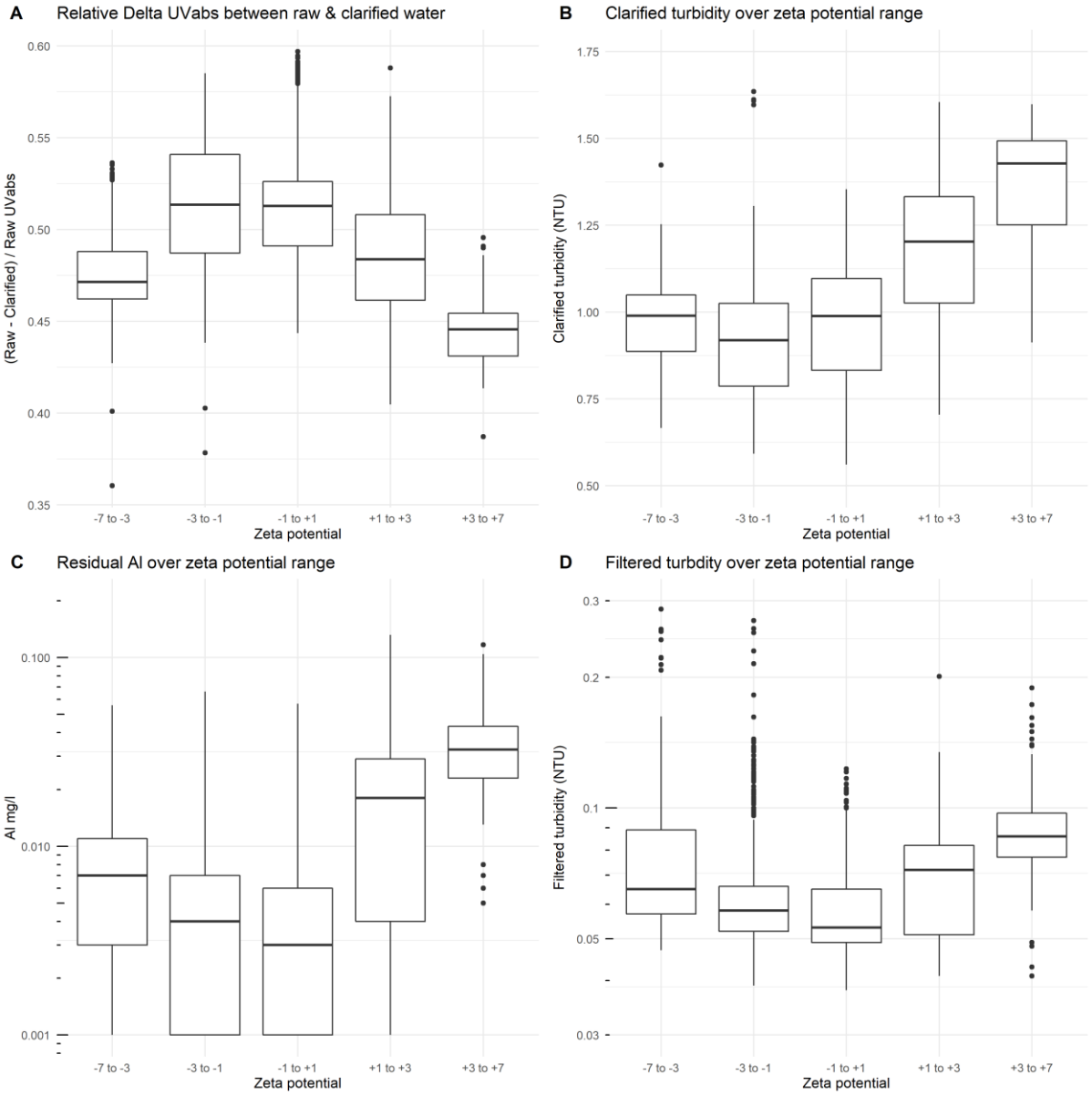

Figure_Apx 37 Downstream water quality observed over the zeta potential range seen in this study presented as boxplots for clarity. Panel A shows the relative removal of UV254 absorbing material; B shows the clarified turbidity; C shows the residual aluminium in the filtered water, and; D shows the filtered water turbidity.

B.6 Relationships between predictor variables used in modelling of online data

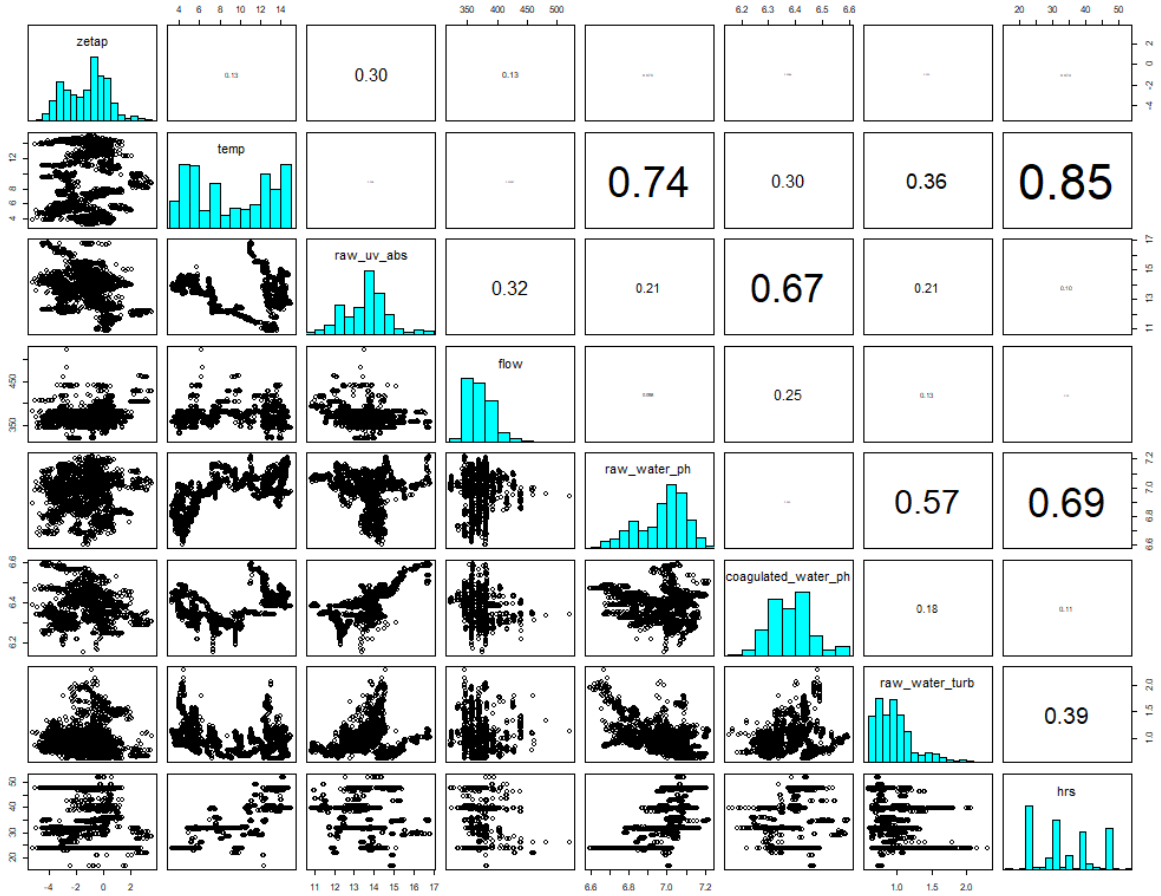

Figure_Apx 38 Pairwise dot plots & correlation coefficients between predictor variables in training data

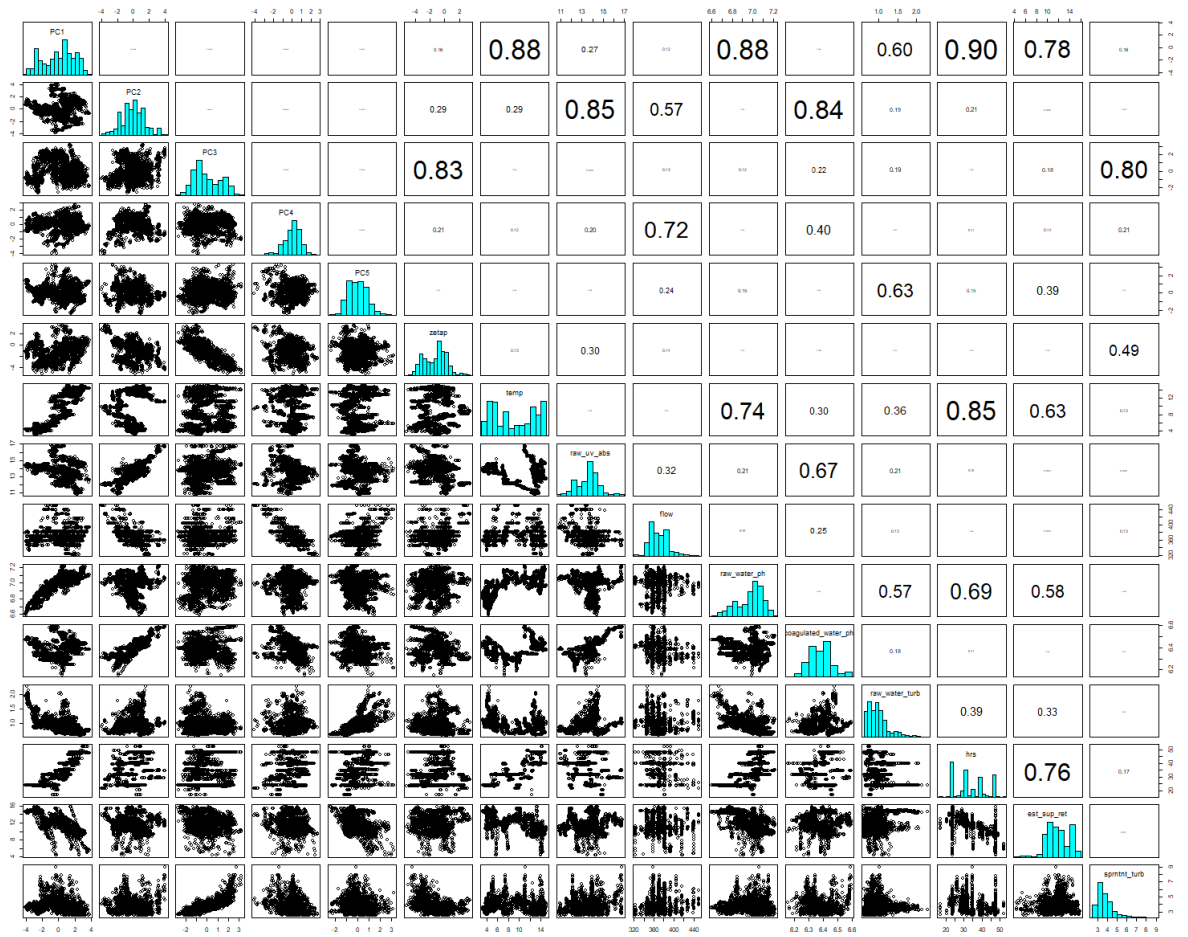

Figure_Apx 39 Pairwise dot plots and correlation coefficients between predictor variables and principal components

B.7 Presentation of PC-GAMMs

Plots included in this section are shown to illustrate the shape of the principal component smoothers identified in Table 6 PC GAMM regression table. They are presented to visualise the shape of the model and for confirming model validity, the scale in this instance is not directly meaningful but is consistent across all plots of the same model. These are not intended to allow the reader to interpret the key relationships between dependent and independent variables. Simulations from the model are shown in section 3.4.5 to aid interpretation of the key phenomena of interest.

Each of the PC-GAMMs has 21 smooth functions which to save paper have been plotted on a single page. Two types of plot are included in the presentation of each model:

1. The main effect smooths are plotted with the principal component on the x axis and the scaled independent variable on the y axis, the solid line shows the shape of the estimated smooth function with standard errors indicated by the dashed lines. The y axis label identifies the smooth and the estimated degrees of freedom. Smooths which are insufficiently explanatory of the dependent variable are penalised to a flat line. On the two dimensional plots points show residuals (which can be checked for patterns to identify poor model specification).
2. For the interactions between smooths the smooth is identified above the plot and the relevant principal components are labelled on the x & y axis. The scaled dependent variable surface is projected in two dimensions onto the shaded and contoured area red is high yellow is low.

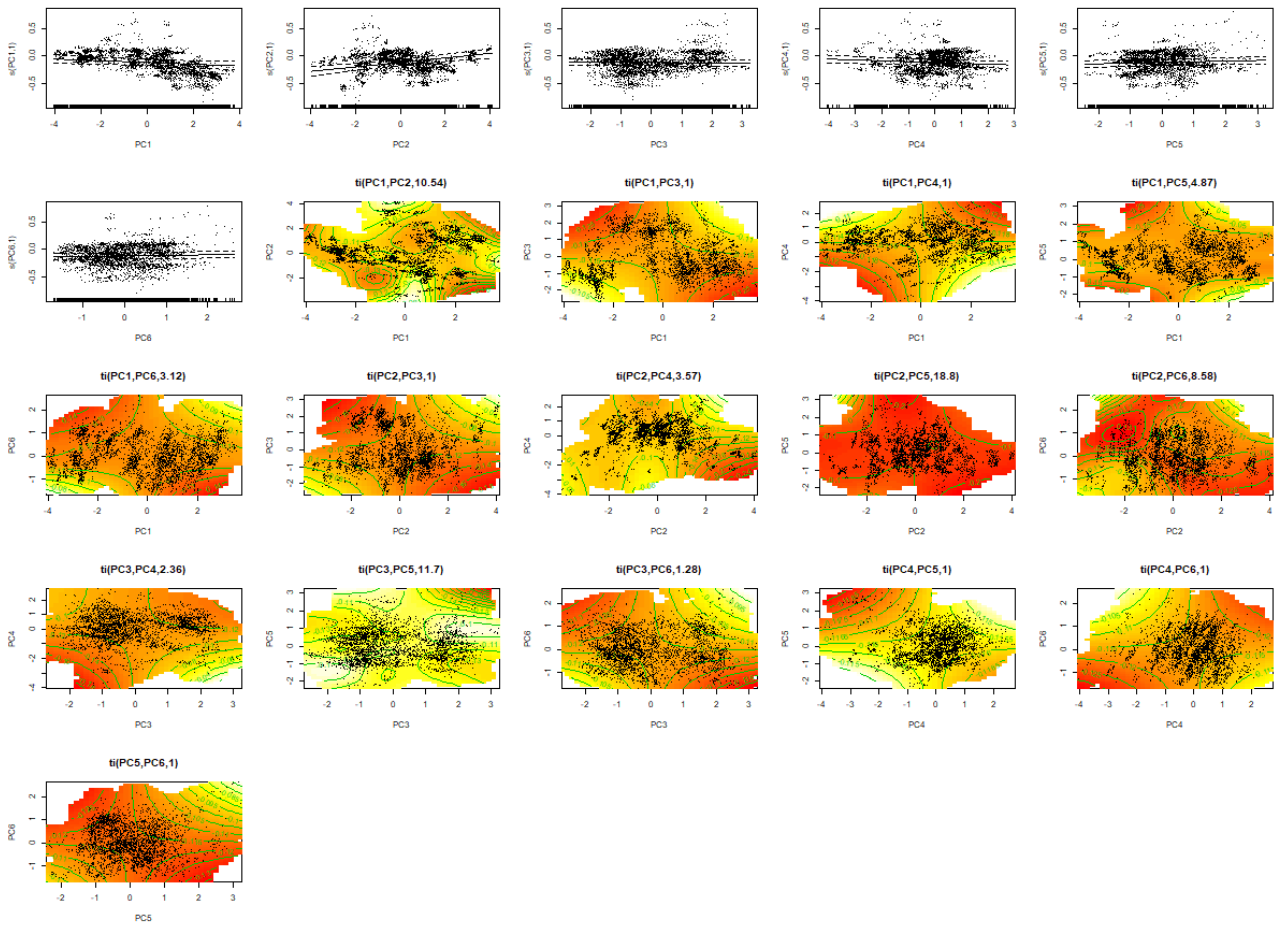

Figure_Apx 40 Presentation of GAMM smooth effects showing the marginal contribution of principal components to the additive linear predictor of clarified water turbidity over the training period 2016/10/20 to 2017/10/20.

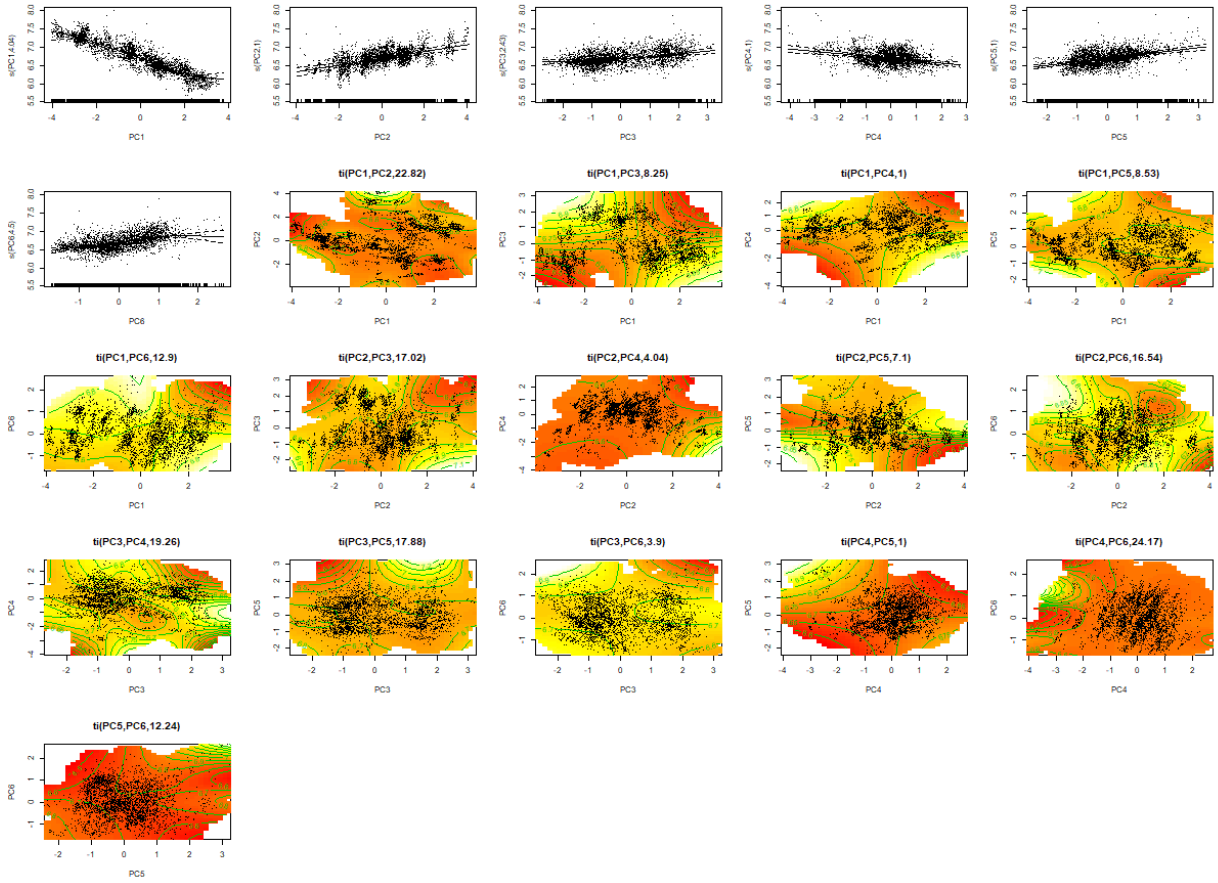

Figure_Apx 41 Presentation of GAMM smooth effects showing the marginal contribution of principal components to the additive linear predictor of clarified water UV absorbance over the training period 2016/10/20 to 2017/10/20.

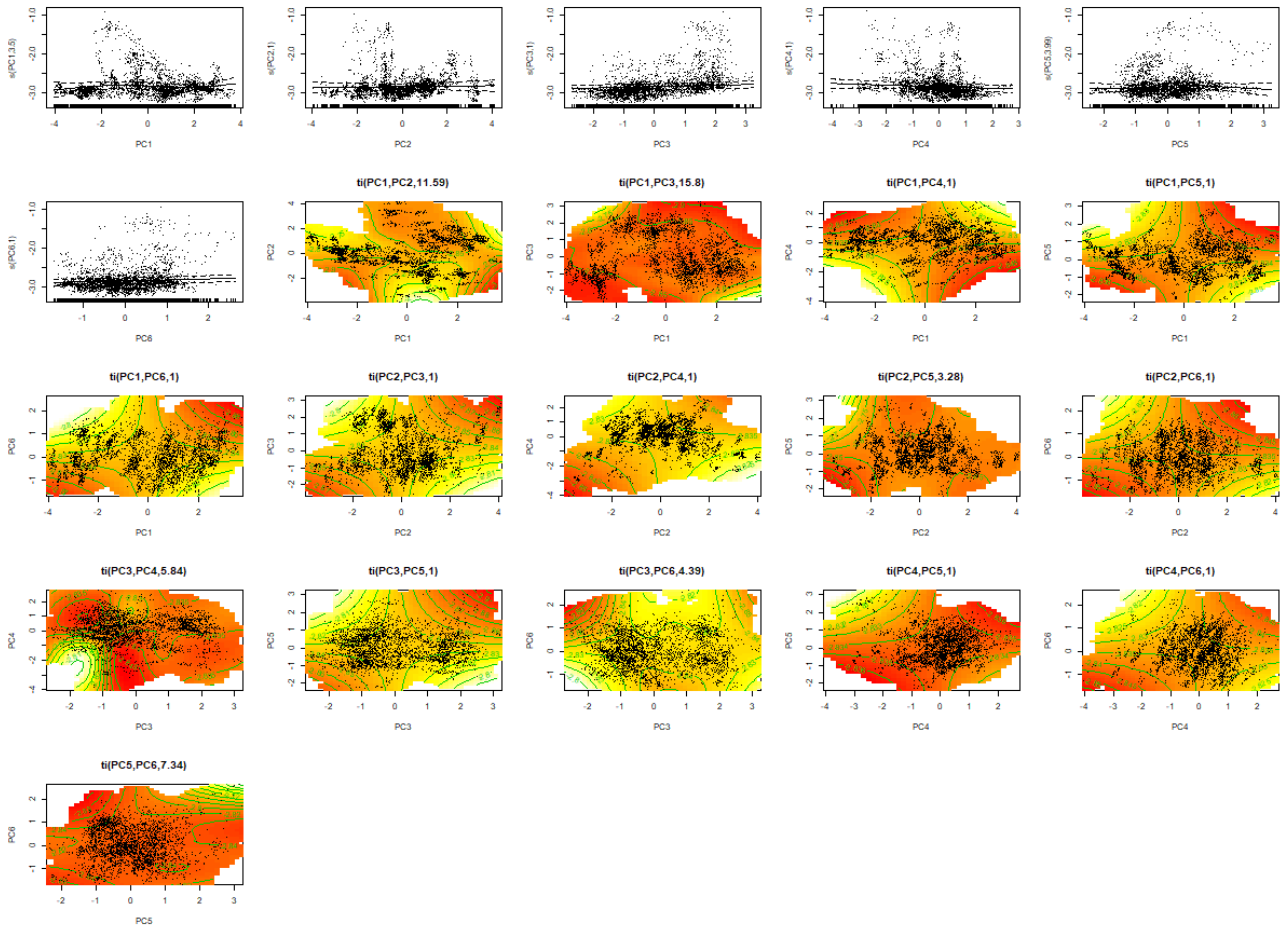

Figure_Apx 42Presentation of GAMM smooth effects showing the marginal contribution of principal components to the additive linear predictor of filtered water turbidity over the training period 2016/10/20 to 2017/10/20.

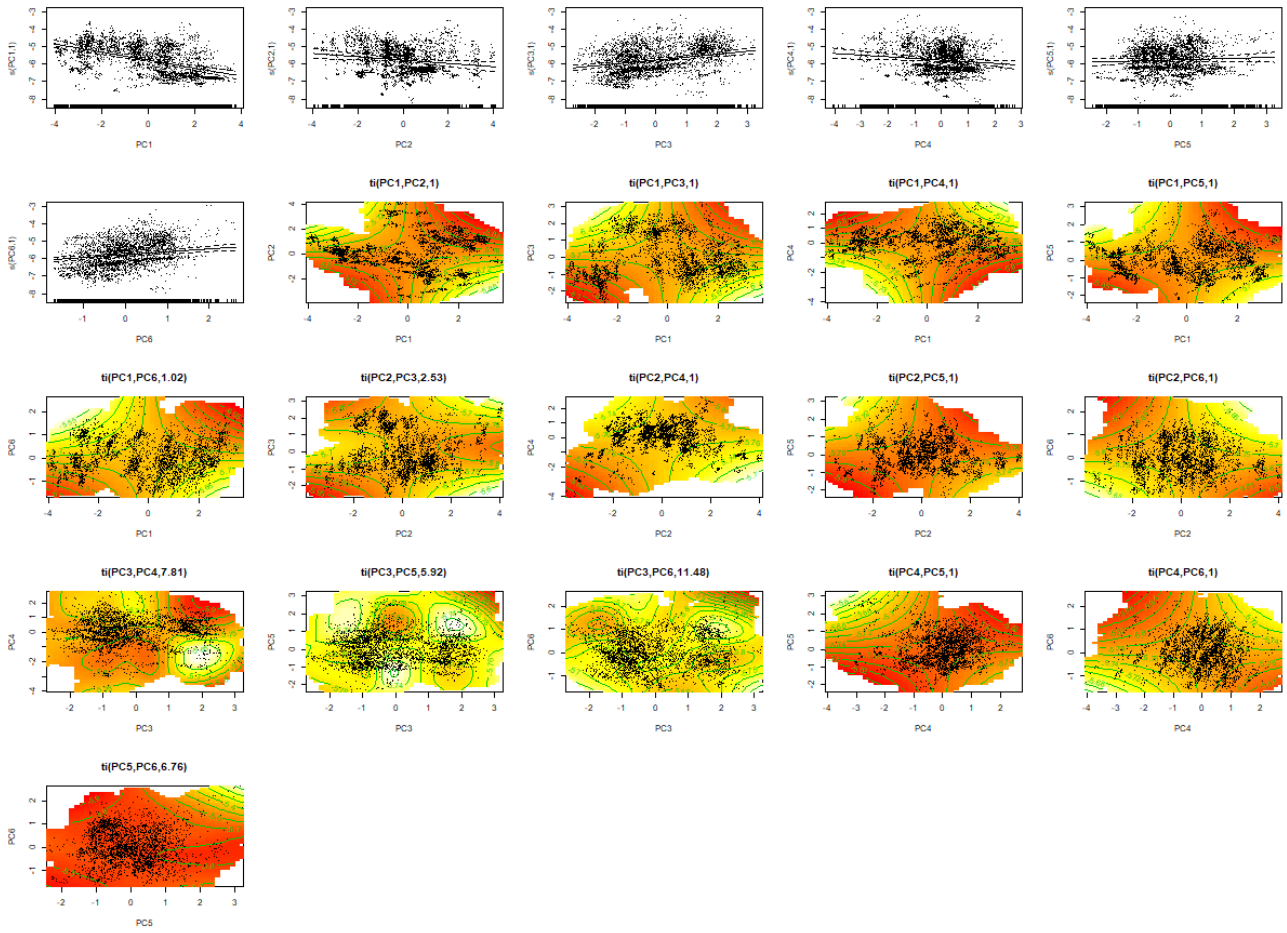

Figure_Apx 43 Presentation of GAMM smooth effects showing the marginal contribution of principal components to the additive linear predictor of filtered water aluminium over the training period 2016/10/20 to 2017/10/20.

B.8 Additional diagnostic plots for GAMMs

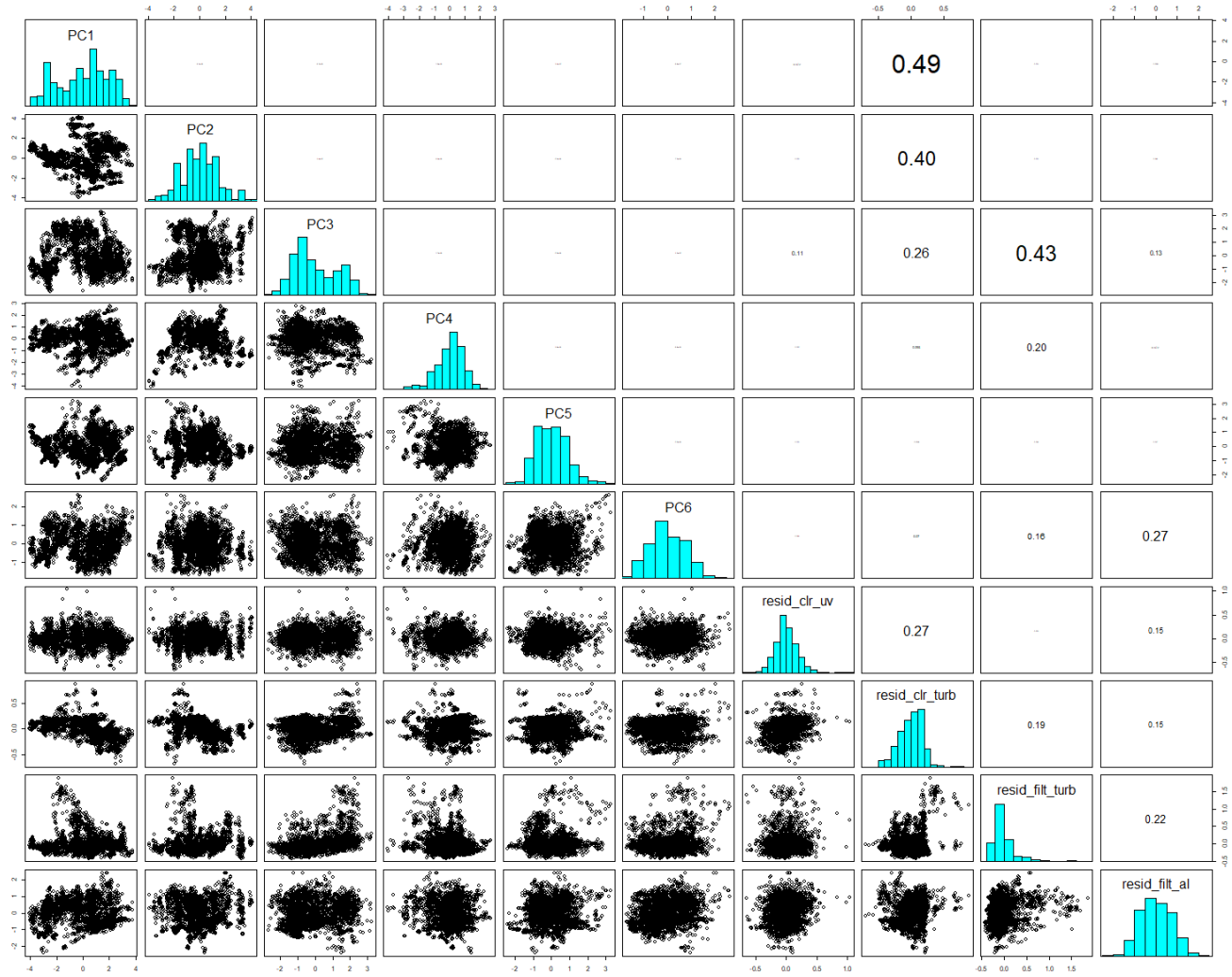

Figure_Apx 44 Plot relating principal components to PC-GAMM residuals to identify relationships

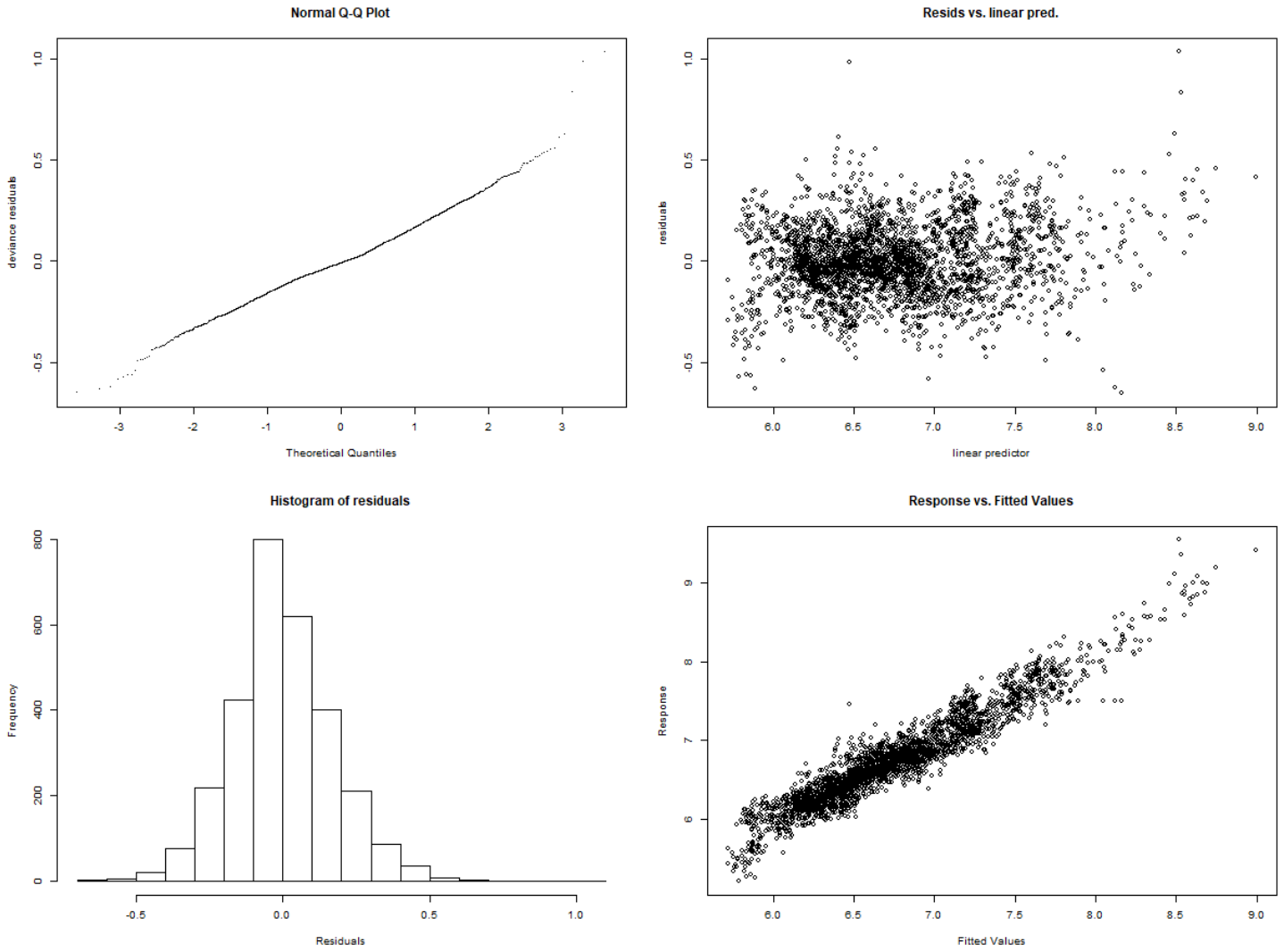

Figure_Apx 45 Model diagnostic plots for PC-GAMM model of clarified UV absorbance

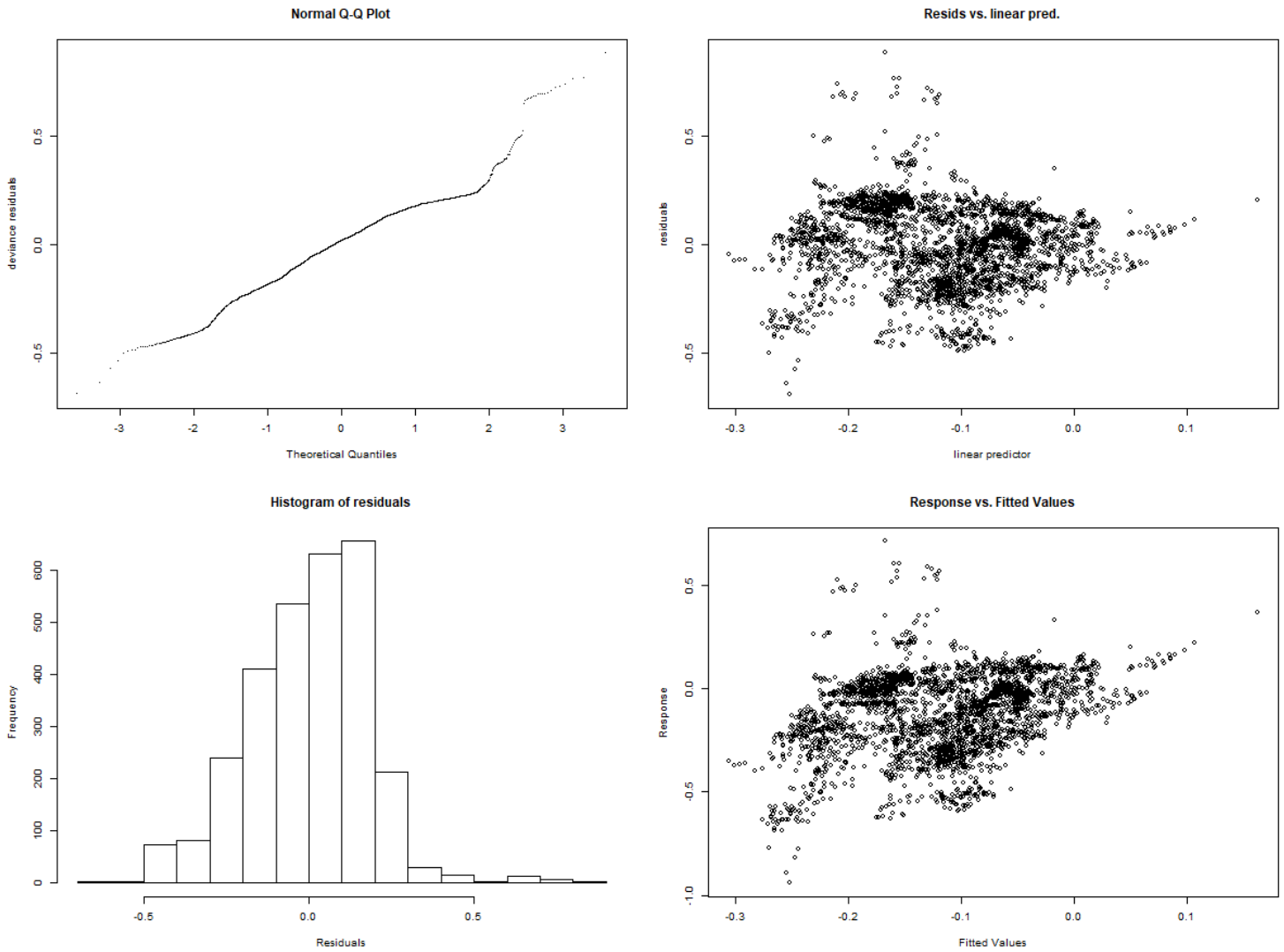

Figure_Apx 46 Model diagnostic plots for PC-GAMM model of clarified turbidity

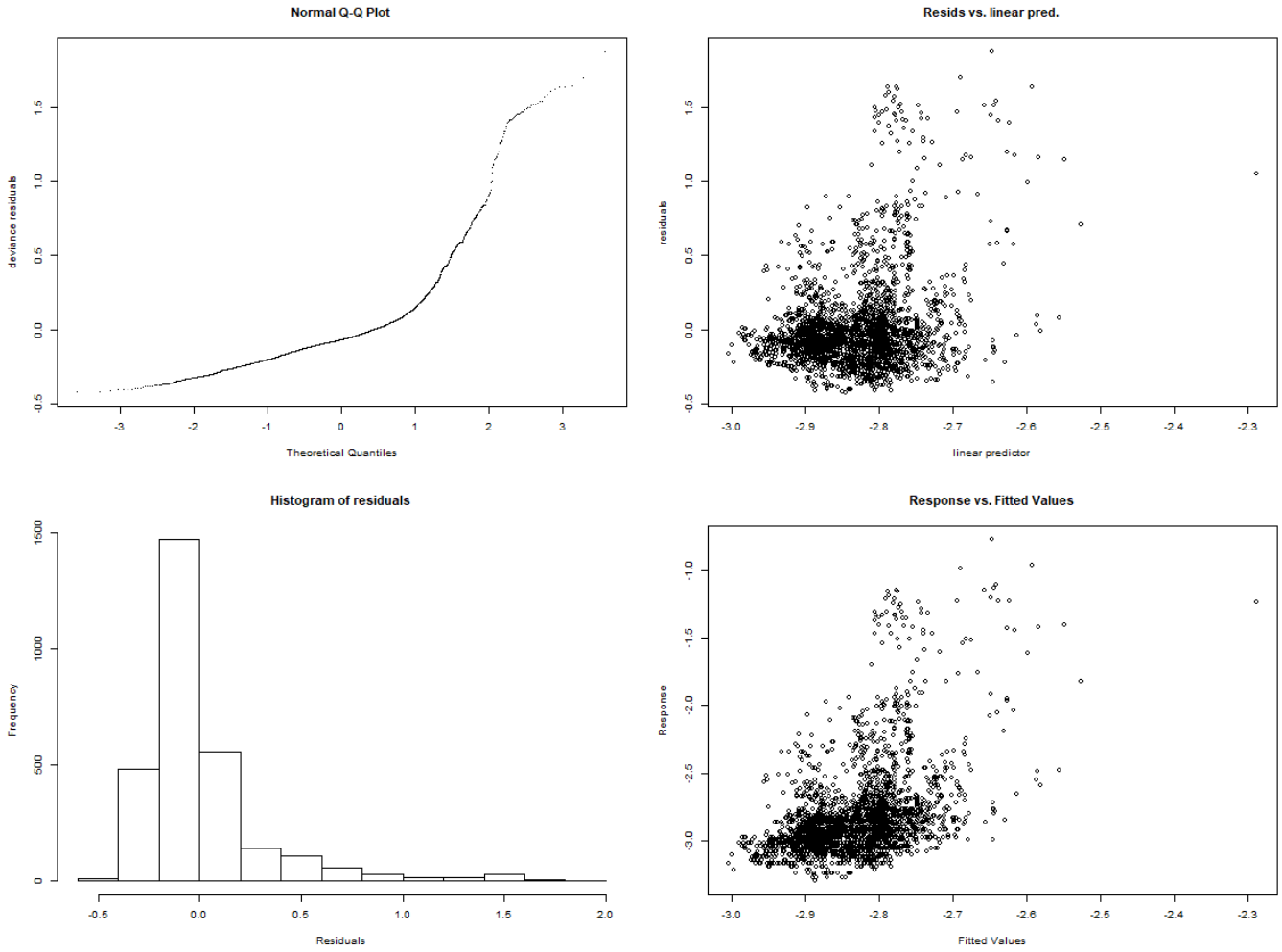

Figure_Apx 47 Model diagnostic plots for PC-GAMM model of filtered water turbidity

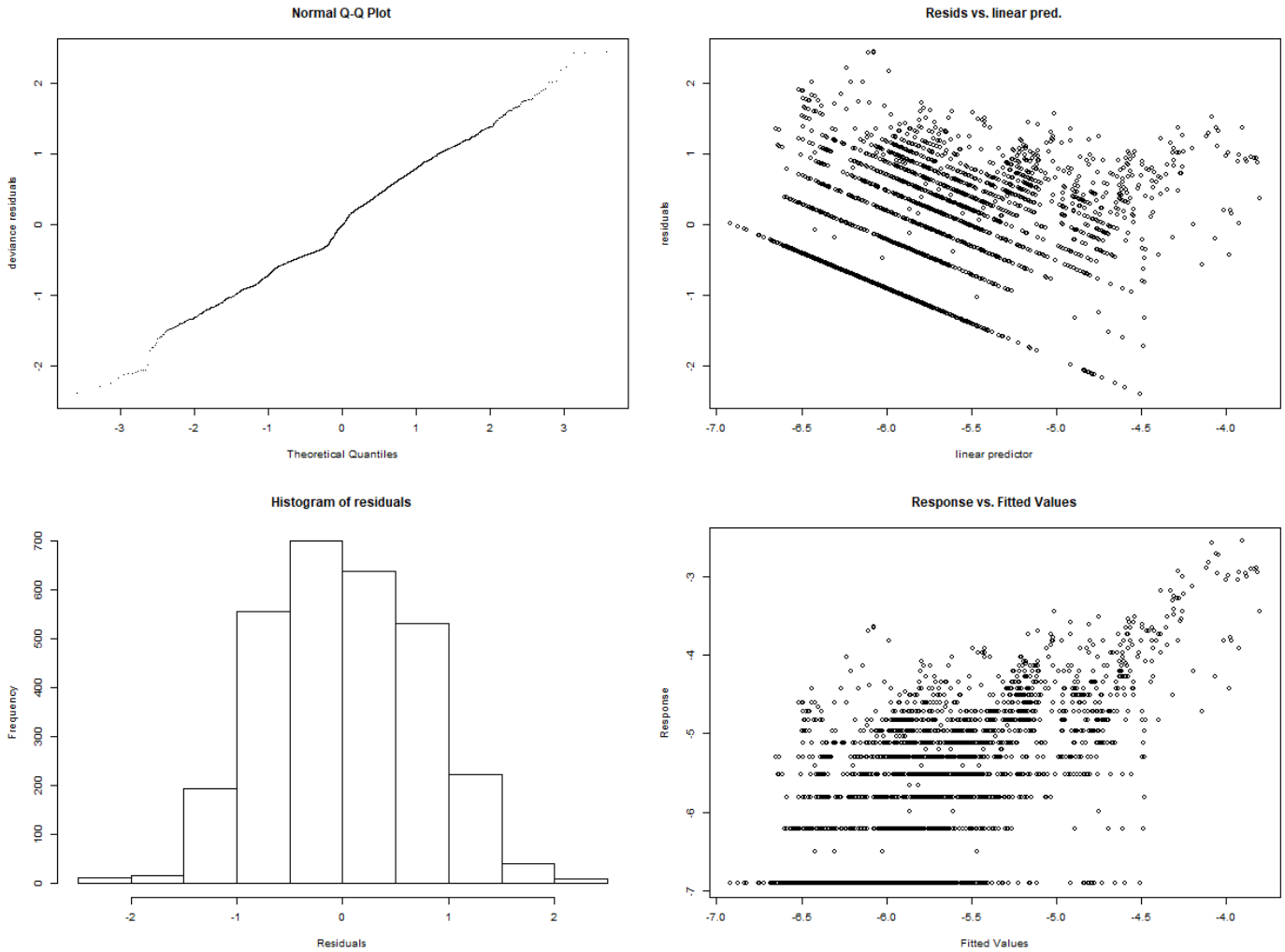

Figure_Apx 48 Model diagnostic plots for PC-GAMM model of filtered water aluminium residual

B.9 Additional simulation plots for models treated water turbidity.

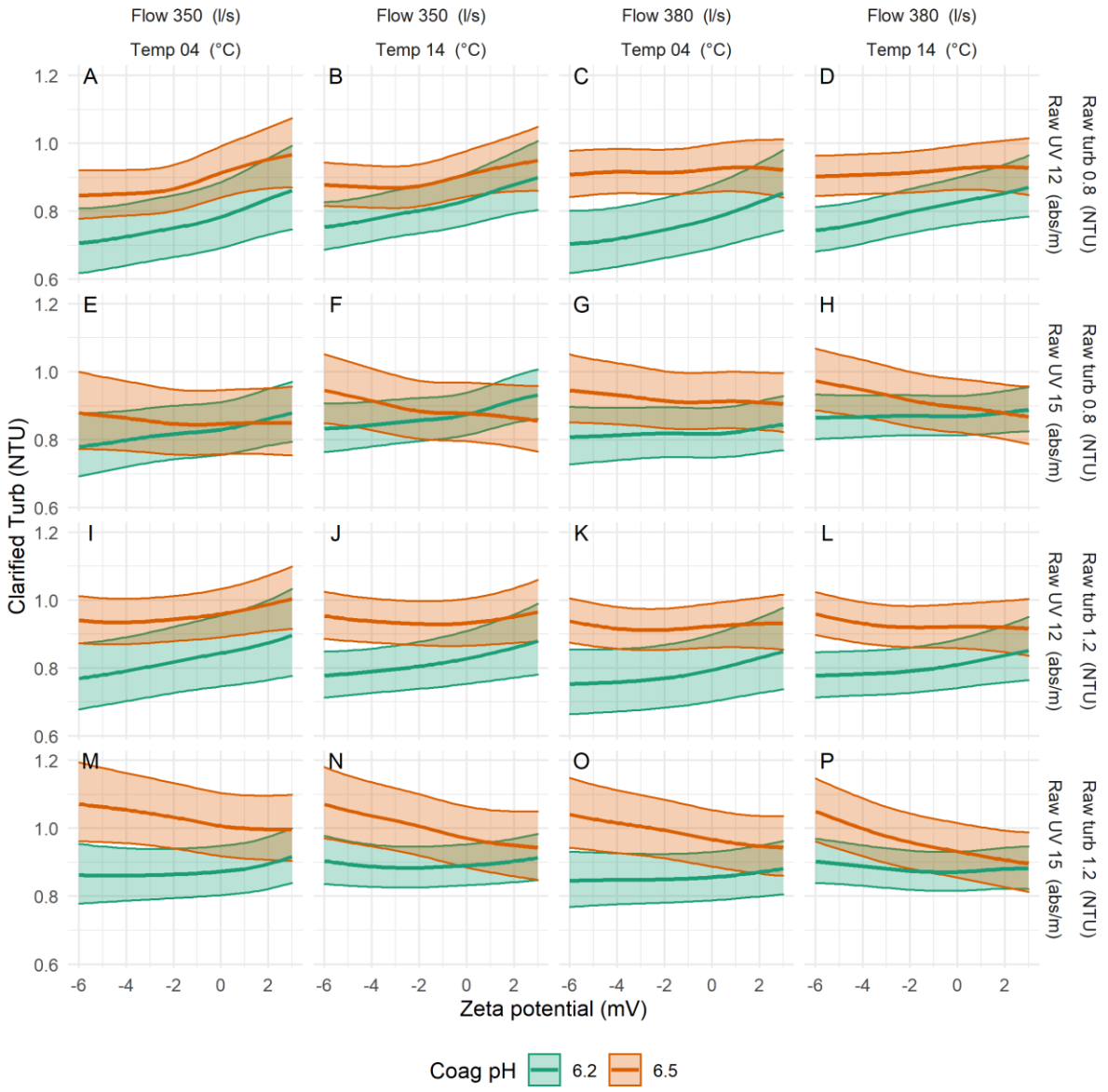

Figure_Apx 49 Simulation results from PC-GAMM model showing mean and 95% confidence interval predictions for clarified water turbidity (NTU) over a range of zeta potentials (-6 to +3) at pH 6.2 & 6.5 at different temperature (4°C & 14°C), flow (350 & 380 l/s), raw UV (12 & 15 abs/m) turbidity (0.8 & 1.2 NTU) other variables were held constant supernatant return flow (15 l/s) supernatant turbidity (3.5 NTU) filter run time (30 hrs).

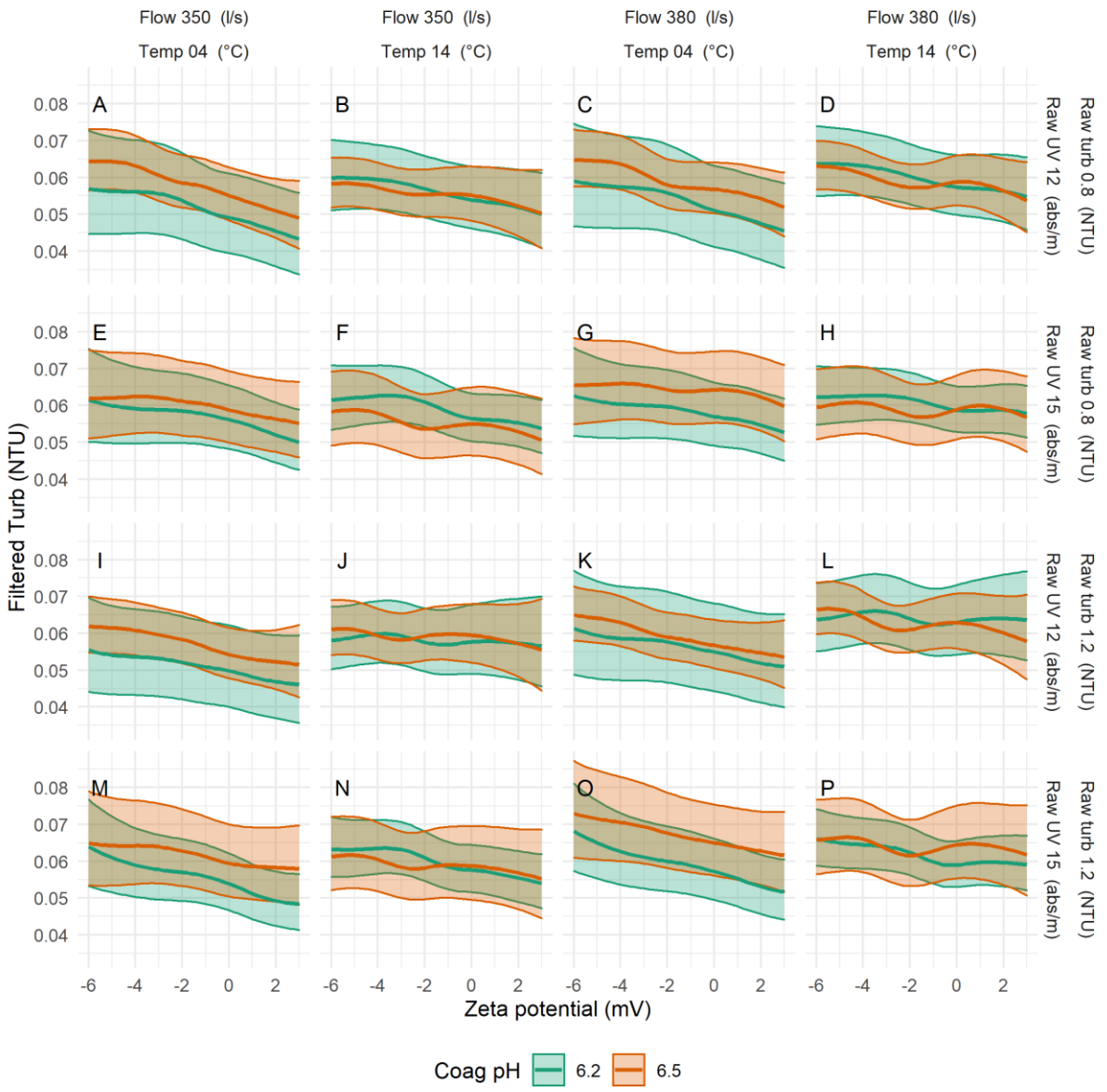

Figure_Apx 50 Simulation results from PC-GAMM model showing mean and 95% confidence interval predictions for filtered water turbidity (NTU) over a range of zeta potentials (-6 to +3) at pH 6.2 & 6.5 at different temperature (4°C & 14°C), flow (350 & 380 l/s), raw UV (12 & 15 abs/m) turbidity (0.8 & 1.2 NTU) other variables were held constant supernatant return flow (15 l/s) supernatant turbidity (3.5 NTU) filter run time (30 hrs).

B.10 Floc growth curves in jar tests

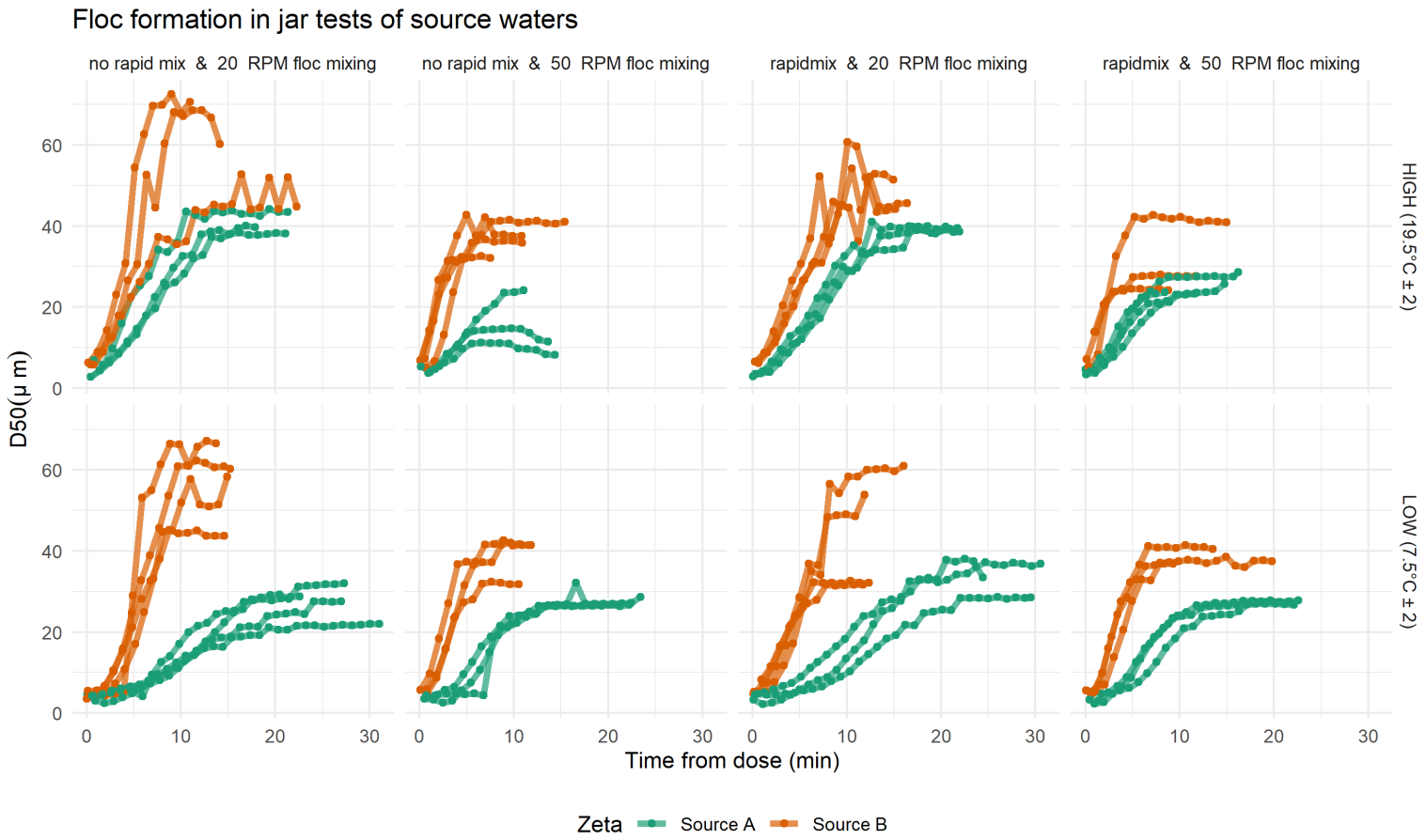

Figure_Apx 51 Floc size over time during jar tests of Source A & Source B waters under different temperature and mixing conditions

Appendix C Supplementary materials for chapter 4

C.1 Data flow diagram for Chapter 4

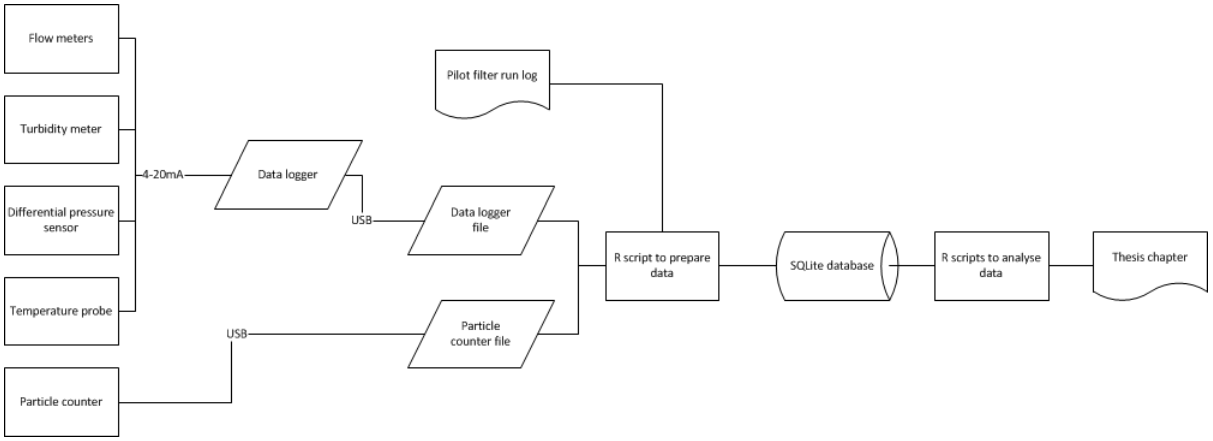

Figure_Apx 52 Data flow diagram for Chapter 4

C.2 Media properties

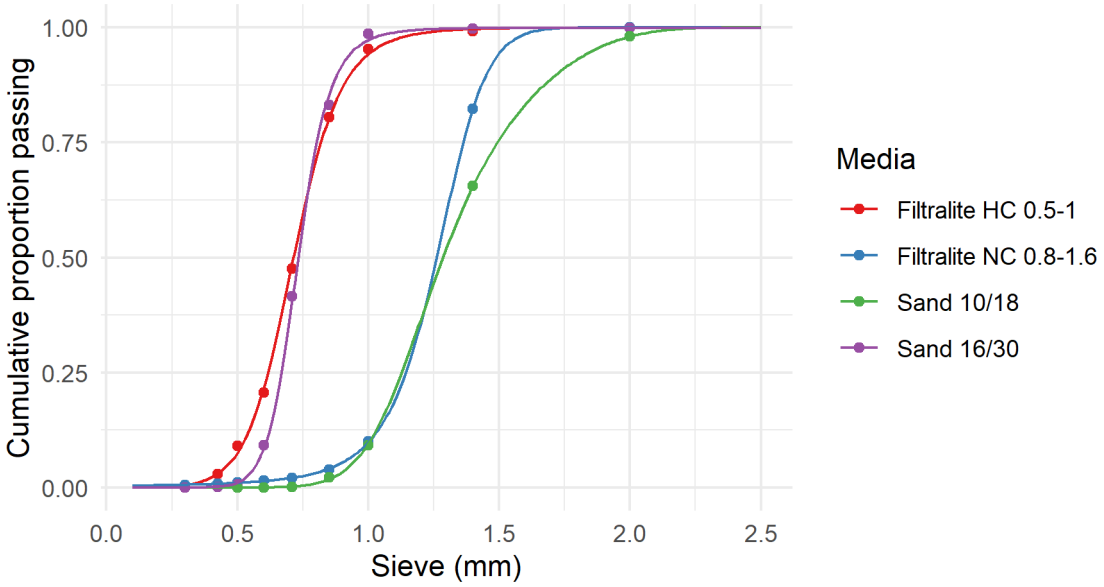

Figure_Apx 53 Particle size distributions from sieve analysis for media used in pilot trials. Sieve testing conducted as per British standard 1796:1 (British Standards Institution, 1989).

C.3 Summary tables of pilot run data

Table_Apx 2 Aggregated summary statistics for pilot filter run conditions.

Table shows the aggregated results for pilot runs by condition. Unit filter run volume (UFRV) is the empty bed volume of water treated during the trial run. Breakthrough (BT) is the volume of water treated in empty bed volumes (EBV) at particle breakthrough (counts consistently increased by more than 10% in a 4 hour period). Normalised clean bed head loss (NCBHL) is the flow and temperature normalised starting head loss. Volume normalised head loss is the average rate of head loss accumulation (mm/EBV). The number of replicate runs under each condition are recorded and well as the number of runs which are censored in that they are ended before breakthrough is observed.

Media Blend	Upwash rate (m/hr)	UFRV (EBV) mean (min – max)	BT (EBV) Mean (min – max)	NCBHL (m) Mean (min – max)	VNHL (mm/EBV) Mean (min – max)	No. Runs	Censored
A - SA Spring	17	255.51 (235.98 - 270.45)	162.09 (107.54 - 235.98)	0.39 (0.36 - 0.42)	3.63 (2.63 - 4.8)	3	1
B - FL Spring	17	262.73 (243.02 - 279.31)	208.25 (104.81 - 279.31)	0.4 (0.36 - 0.47)	6.99 (5.28 - 9.15)	3	1
A - SA Spring	23	276.61 (173.51 - 357.98)	164.2 (76.6 - 318.49)	0.34 (0.32 - 0.36)	2.58 (2.33 - 3.38)	5	1
B - FL Spring	23	271.55 (174.81 - 359.26)	222.88 (148.6 - 312.3)	0.32 (0.28 - 0.35)	5.81 (4.89 - 8.03)	5	3
A - SA Spring	28	249.94 (156.96 - 391.16)	98.7 (96.88 - 100.62)	0.32 (0.32 - 0.33)	2.75 (2.09 - 3.45)	4	0
B - FL Spring	28	257.94 (165.39 - 404.31)	198.32 (165.39 - 215.08)	0.31 (0.27 - 0.36)	5.25 (4.34 - 6.21)	4	2
A - SA Spring	34	381.93 (381.93 - 381.93)	263.93 (263.93 - 263.93)	0.3 (0.3 - 0.3)	4.5 (4.5 - 4.5)	1	0
B - FL Spring	34	401.26 (401.26 - 401.26)	401.26 (401.26 - 401.26)	0.26 (0.26 - 0.26)	7.06 (7.06 - 7.06)	1	1
A - SA Summer	17	342.62 (279.52 - 419.83)	279.07 (153.68 - 419.83)	0.42 (0.39 - 0.49)	3.49 (3.02 - 4.08)	5	1
B - FL Summer	17	343.65 (288.14 - 410.9)	339.4 (288.14 - 410.9)	0.35 (0.31 - 0.39)	7.11 (5.6 - 8.99)	6	5
A - SA Summer	20	391.07 (391.07 - 391.07)	309.78 (309.78 - 309.78)	0.36 (0.36 - 0.36)	3.76 (3.76 - 3.76)	1	0
B - FL Summer	20	394.17 (394.17 - 394.17)	394.17 (394.17 - 394.17)	0.33 (0.33 - 0.33)	7.55 (7.55 - 7.55)	1	1
A - SA Summer	23	312.1 (191.04 - 396.07)	263.17 (133.96 - 390.66)	0.36 (0.34 - 0.39)	3.2 (2.53 - 4.02)	13	6
B - FL Summer	23	312.17 (197.53 - 395.81)	312.17 (197.53 - 395.81)	0.34 (0.29 - 0.47)	7.55 (5.27 - 11.01)	13	13
A - SA Summer	28	230.09 (202.85 - 257.33)	230.09 (202.85 - 257.33)	0.32 (0.31 - 0.33)	3.59 (2.99 - 4.2)	2	2

B - FL	Summer	28	233.76 (206.63 - 260.88)	233.76 (206.63 - 260.88)	0.35 (0.34 - 0.36)	9.41 (8.98 - 9.84)	2	2
A - SA	Summer	34	237.14 (237.14 - 237.14)	237.14 (237.14 - 237.14)	0.31 (0.31 - 0.31)	3.64 (3.64 - 3.64)	1	1
B - FL	Summer	34	257.41 (234.06 - 280.76)	257.41 (234.06 - 280.76)	0.28 (0.27 - 0.29)	8.19 (6.9 - 9.49)	2	2
A - SA	Winter	17	218.93 (139.06 - 282.12)	58.85 (55.99 - 60.75)	0.37 (0.36 - 0.38)	2.89 (2.63 - 3.27)	3	0
B - FL	Winter	17	260.37 (242.13 - 278.61)	115.56 (89.2 - 141.92)	0.3 (0.27 - 0.33)	5.54 (4.97 - 6.11)	2	0
A - SA	Winter	23	215.71 (158.78 - 251.51)	125.95 (103.94 - 158.78)	0.32 (0.31 - 0.32)	3.06 (2.7 - 3.7)	4	1
B - FL	Winter	23	212.56 (167.14 - 248.6)	198.06 (167.14 - 221.93)	0.26 (0.25 - 0.27)	6.49 (5.42 - 8.22)	3	2
A - SA	Winter	28	359.02 (359.02 - 359.02)	112.97 (112.97 - 112.97)	0.31 (0.31 - 0.31)	4.4 (4.4 - 4.4)	1	0
B - FL	Winter	28	367.84 (367.84 - 367.84)	210.34 (210.34 - 210.34)	0.28 (0.28 - 0.28)	7.02 (7.02 - 7.02)	1	0
A - SA	Winter	34	275.82 (195.1 - 320.09)	131.4 (97.69 - 195.71)	0.3 (0.28 - 0.31)	3.5 (2.44 - 4.67)	11	0
B - FL	Winter	34	289.36 (268.94 - 331.19)	224.81 (187 - 279.98)	0.24 (0.23 - 0.26)	5.05 (4.24 - 6.05)	10	2

Table_Apx 3 Summary statistics for individual pilot filter runs

Start Date	Run ID	Blend	BW rate (m/hr)	Media	UFRV (EBV)	BT (EBV)	NCBHL (m)	VNHL (m)	Censored
2017-02-06	17_FEBB	Winter	34	A - SA	272	168	0.28	3.97	FALSE
2017-02-06	17_FEBB	Winter	34	B - FL	280	280	0.24	5.51	TRUE
2017-02-08	17_FEBC	Winter	34	A - SA	320	119	0.3	3.37	FALSE
2017-02-08	17_FEBC	Winter	34	B - FL	331	253	0.25	4.72	FALSE
2017-02-11	17_FEBD	Winter	34	A - SA	267	125	0.3	3.22	FALSE
2017-02-11	17_FEBD	Winter	34	B - FL	276	276	0.26	4.7	TRUE
2017-02-13	17_FEBE	Winter	34	A - SA	264	108	0.31	2.75	FALSE
2017-02-13	17_FEBE	Winter	34	B - FL	269	190	0.24	4.3	FALSE

2017-02-15	17_FEBF	Winter	34	A - SA	276	120	0.3	2.77	FALSE
2017-02-15	17_FEBF	Winter	34	B - FL	282	203	0.24	4.24	FALSE
2017-02-22	17_FEBJ	Winter	34	A - SA	300	102	0.3	3.14	FALSE
2017-02-22	17_FEBJ	Winter	34	B - FL	299	187	0.23	4.55	FALSE
2017-02-24	17_FEBK	Winter	34	A - SA	195	101	0.29	2.44	FALSE
2017-02-24	17_FEBK	Winter	34	B - FL	280	188	0.24	4.62	FALSE
2017-03-01	17_MARA	Winter	17	A - SA	139	61	0.38	2.63	FALSE
2017-03-02	17_MARB	Winter	17	A - SA	282	60	0.36	2.78	FALSE
2017-03-02	17_MARB	Winter	17	B - FL	279	142	0.27	4.97	FALSE
2017-03-04	17_MARC	Winter	23	A - SA	252	104	0.32	2.7	FALSE
2017-03-04	17_MARC	Winter	23	B - FL	249	205	0.26	5.42	FALSE
2017-03-06	17_MARD	Winter	34	A - SA	293	196	0.29	4.67	FALSE
2017-03-09	17_MARE	Winter	34	A - SA	265	165	0.3	4.17	FALSE
2017-03-09	17_MARE	Winter	34	B - FL	269	202	0.24	6.05	FALSE
2017-03-11	17_MARF	Winter	23	A - SA	231	121	0.32	3.05	FALSE
2017-03-13	17_MARG	Winter	23	A - SA	221	120	0.31	2.79	FALSE
2017-03-13	17_MARG	Winter	23	B - FL	222	222	0.27	5.84	TRUE
2017-03-15	17_MARH	Winter	34	A - SA	269	98	0.29	3.9	FALSE
2017-03-15	17_MARH	Winter	34	B - FL	281	208	0.24	5.87	FALSE
2017-03-17	17_MARI	Winter	34	A - SA	314	144	0.29	4.15	FALSE
2017-03-17	17_MARI	Winter	34	B - FL	326	260	0.25	5.92	FALSE
2017-03-20	17_MARJ	Winter	28	A - SA	359	113	0.31	4.4	FALSE
2017-03-20	17_MARJ	Winter	28	B - FL	368	210	0.28	7.02	FALSE

2017-03-23	17_MARK	Winter	17	A - SA	236	56	0.38	3.27	FALSE
2017-03-23	17_MARK	Winter	17	B - FL	242	89	0.33	6.11	FALSE
2017-03-25	17_MARL	Winter	23	A - SA	159	159	0.32	3.7	TRUE
2017-03-25	17_MARL	Winter	23	B - FL	167	167	0.25	8.22	TRUE
2017-03-27	17_MARM	Spring	28	A - SA	252	101	0.33	3.21	FALSE
2017-03-27	17_MARM	Spring	28	B - FL	253	215	0.3	6.21	FALSE
2017-03-29	17_MARN	Spring	23	A - SA	174	109	0.34	2.46	FALSE
2017-03-29	17_MARN	Spring	23	B - FL	175	175	0.28	5.12	TRUE
2017-04-04	17_APRA	Spring	17	A - SA	260	108	0.42	3.48	FALSE
2017-04-04	17_APRA	Spring	17	B - FL	266	241	0.37	6.53	FALSE
2017-04-06	17_APRC	Spring	34	A - SA	382	264	0.3	4.5	FALSE
2017-04-06	17_APRC	Spring	34	B - FL	401	401	0.26	7.06	TRUE
2017-04-10	17_APRD	Spring	28	A - SA	157	98	0.32	2.09	FALSE
2017-04-10	17_APRD	Spring	28	B - FL	165	165	0.29	4.34	TRUE
2017-04-11	17_APRE	Spring	28	A - SA	199	97	0.33	2.23	FALSE
2017-04-11	17_APRE	Spring	28	B - FL	209	209	0.27	4.49	TRUE
2017-04-17	17_APRI	Spring	23	A - SA	318	318	0.32	2.35	TRUE
2017-04-17	17_APRI	Spring	23	B - FL	327	149	0.32	4.89	FALSE
2017-04-19	17_APRJ	Spring	17	A - SA	236	236	0.39	2.63	TRUE
2017-04-19	17_APRJ	Spring	17	B - FL	243	105	0.36	5.28	FALSE
2017-05-01	17_MAYA	Spring	28	A - SA	391	99	0.32	3.45	FALSE
2017-05-01	17_MAYA	Spring	28	B - FL	404	204	0.36	5.95	FALSE
2017-05-06	17_MAYC	Spring	17	A - SA	270	143	0.36	4.8	FALSE

2017-05-06	17_MAYC	Spring	17	B - FL	279	279	0.47	9.15	TRUE
2017-05-17	17_MAYG	Spring	23	A - SA	228	82	0.36	2.39	FALSE
2017-05-17	17_MAYG	Spring	23	B - FL	185	230	NA	NaN	TRUE
2017-05-19	17_MAYH	Spring	23	A - SA	358	77	0.34	2.33	FALSE
2017-05-19	17_MAYH	Spring	23	B - FL	359	248	0.33	5.18	FALSE
2017-05-21	17_MAYI	Spring	23	A - SA	305	235	0.33	3.38	FALSE
2017-05-21	17_MAYI	Spring	23	B - FL	312	312	0.35	8.03	TRUE
2017-06-13	17_JUNB	Summer	23	A - SA	191	134	0.34	2.53	FALSE
2017-06-13	17_JUNB	Summer	23	B - FL	198	198	0.47	11.01	TRUE
2017-06-14	17_JUNC	Summer	17	A - SA	280	154	0.41	3.12	FALSE
2017-06-14	17_JUNC	Summer	17	B - FL	288	288	0.33	5.6	TRUE
2017-06-16	17_JUND	Summer	23	A - SA	316	191	0.36	2.77	FALSE
2017-06-16	17_JUND	Summer	23	B - FL	327	327	0.29	5.29	TRUE
2017-06-18	17_JUNE	Summer	34	B - FL	281	281	0.29	6.9	TRUE
2017-06-20	17_JUNF	Summer	17	A - SA	333	290	0.39	3.89	FALSE
2017-06-20	17_JUNF	Summer	17	B - FL	352	326	0.31	7.04	FALSE
2017-06-23	17_JUNG	Summer	17	B - FL	341	341	0.36	8.77	TRUE
2017-06-26	17_JUNH	Summer	28	A - SA	257	257	0.31	2.99	TRUE
2017-06-26	17_JUNH	Summer	28	B - FL	261	261	0.34	8.98	TRUE
2017-06-28	17_JUNI	Summer	20	A - SA	391	310	0.36	3.76	FALSE
2017-06-28	17_JUNI	Summer	20	B - FL	394	394	0.33	7.55	TRUE
2017-07-01	17_JULA	Summer	23	A - SA	304	304	0.37	3.62	TRUE
2017-07-01	17_JULA	Summer	23	B - FL	306	306	0.35	7.25	TRUE

2017-07-07	17_JULC	Summer 28	A - SA	203	203	0.33	4.2	TRUE
2017-07-07	17_JULC	Summer 28	B - FL	207	207	0.36	9.84	TRUE
2017-07-18	17_JULD	Summer 34	A - SA	237	237	0.31	3.64	TRUE
2017-07-18	17_JULD	Summer 34	B - FL	234	234	0.27	9.49	TRUE
2017-07-20	17_JULE	Summer 17	A - SA	420	420	0.4	4.08	TRUE
2017-07-20	17_JULE	Summer 17	B - FL	411	411	0.37	8.99	TRUE
2017-07-23	17_JULF	Summer 23	A - SA	250	250	0.36	3.01	TRUE
2017-07-23	17_JULF	Summer 23	B - FL	248	248	0.34	7.4	TRUE
2017-07-25	17_JULG	Summer 23	A - SA	272	272	0.36	2.8	TRUE
2017-07-25	17_JULG	Summer 23	B - FL	268	268	0.31	7.08	TRUE
2017-07-27	17_JULH	Summer 17	A - SA	346	266	0.49	3.31	FALSE
2017-07-27	17_JULH	Summer 17	B - FL	341	341	0.39	6.33	TRUE
2017-07-29	17_JULI	Summer 17	A - SA	334	266	0.42	3.02	FALSE
2017-07-29	17_JULI	Summer 17	B - FL	328	328	0.37	5.96	TRUE
2017-07-31	17_JULK	Summer 23	A - SA	375	249	0.38	2.84	FALSE
2017-07-31	17_JULK	Summer 23	B - FL	360	360	0.32	5.27	TRUE
2017-08-02	17_AUGA	Summer 23	A - SA	391	391	0.35	3.63	TRUE
2017-08-02	17_AUGA	Summer 23	B - FL	396	396	0.29	8.2	TRUE
2017-08-06	17_AUGB	Summer 23	A - SA	330	330	0.35	4.02	TRUE
2017-08-06	17_AUGB	Summer 23	B - FL	334	334	0.37	9.64	TRUE
2017-08-09	17_AUGC	Summer 23	A - SA	371	371	0.36	4	TRUE
2017-08-09	17_AUGC	Summer 23	B - FL	373	373	0.33	8.01	TRUE
2017-08-14	17_AUGD	Summer 23	A - SA	396	242	0.39	3.2	FALSE

2017-08-14	17_AUGD	Summer	23	B - FL	389	389	0.35	7.39	TRUE
2017-08-17	17_AUGE	Summer	23	A - SA	300	256	0.37	2.97	FALSE
2017-08-17	17_AUGE	Summer	23	B - FL	299	299	0.32	7.46	TRUE
2017-08-19	17_AUGF	Summer	23	A - SA	324	237	0.36	3.21	FALSE
2017-08-19	17_AUGF	Summer	23	B - FL	323	323	0.32	7.42	TRUE
2017-08-21	17_AUGG	Summer	23	A - SA	238	195	0.37	2.99	FALSE
2017-08-21	17_AUGG	Summer	23	B - FL	238	238	0.31	6.68	TRUE

C.4 Turbidity profiles for filter runs divided by backwash rate & feed water.

Replication of individual facets from profiles plotted for pilot trials at WTW A shown below but not labelled.

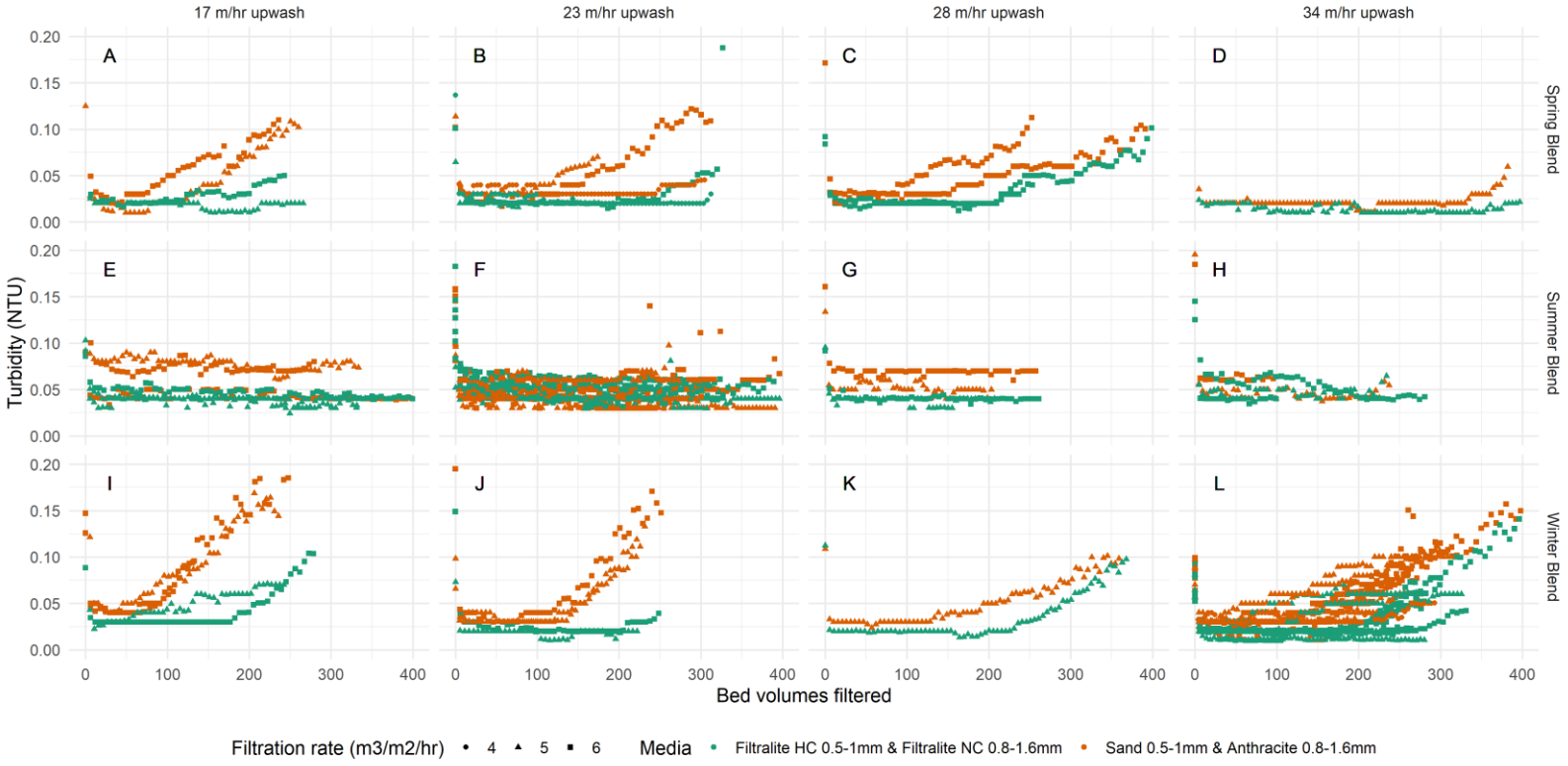

Figure_Apx 54 Comparison of turbidity profiles from pilot trials at WTW A. Media bed of Filtralite HC 0.5-1 mm & Filtralite NC 0.8-1.6 mm is compared to Sand 0.5-1 mm and Anthracite 0.8-1.6 mm at backwash rates of 17,23,28 & 34 m/hr over three seasons

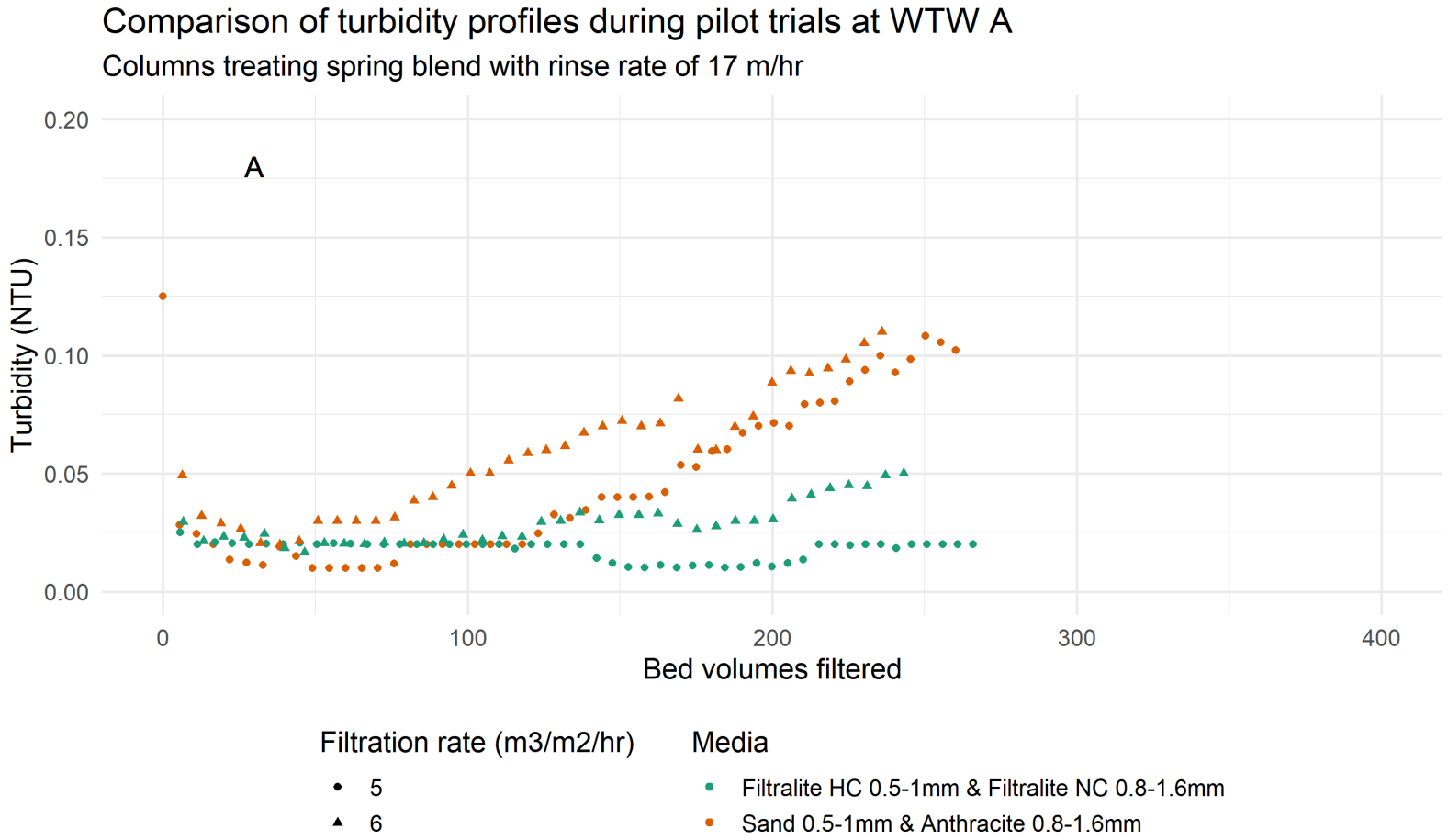

Figure_Apx 55 Enlargement of figure Figure_Apx 53 A turbidity profiles for pilot filter trials of the spring blend backwashed at 17 m/hr

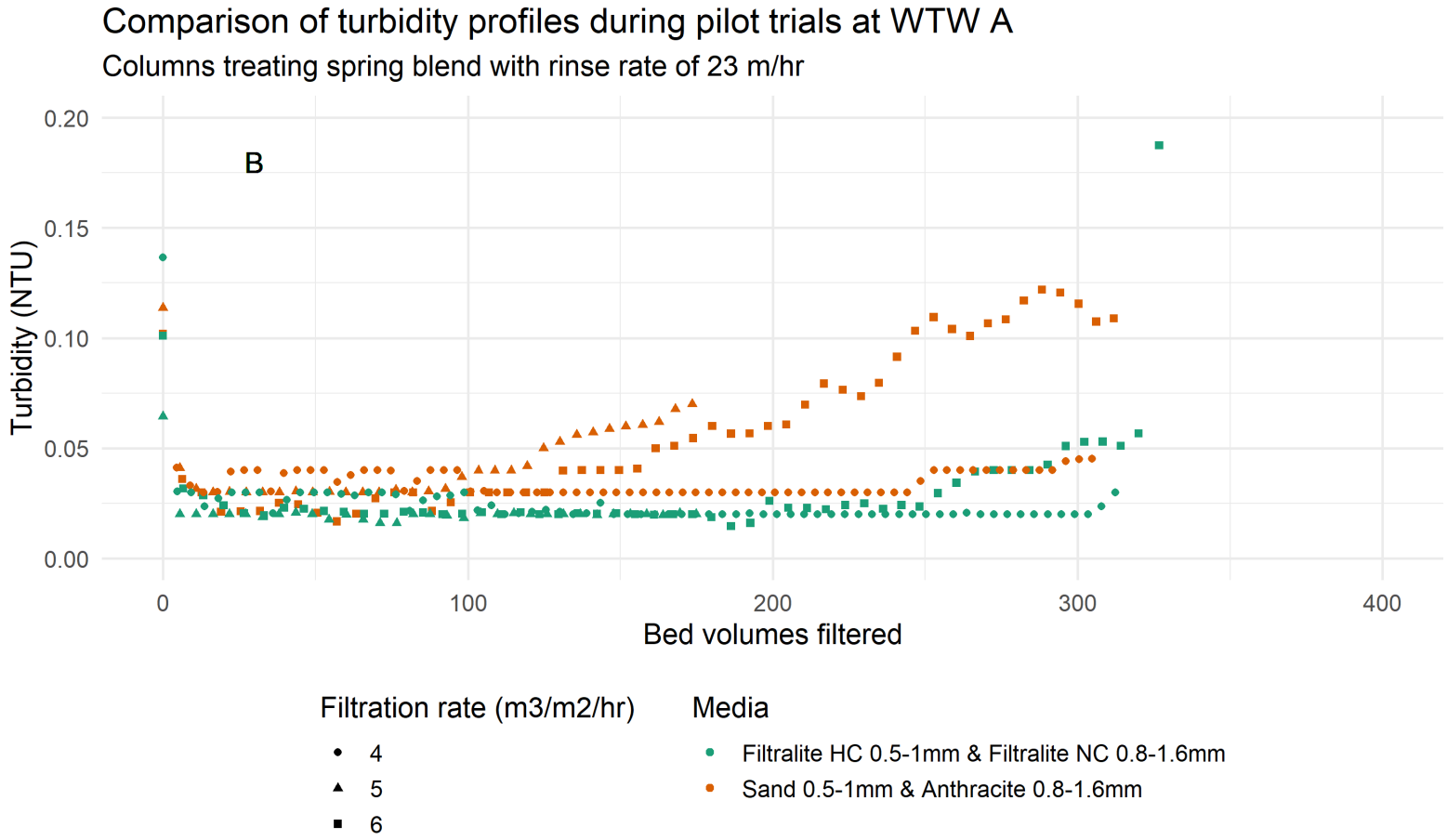

Figure_Apx 56 Enlargement of figure Figure_Apx 53 B turbidity profiles for pilot filter trials of the spring blend backwashed at 23 m/hr

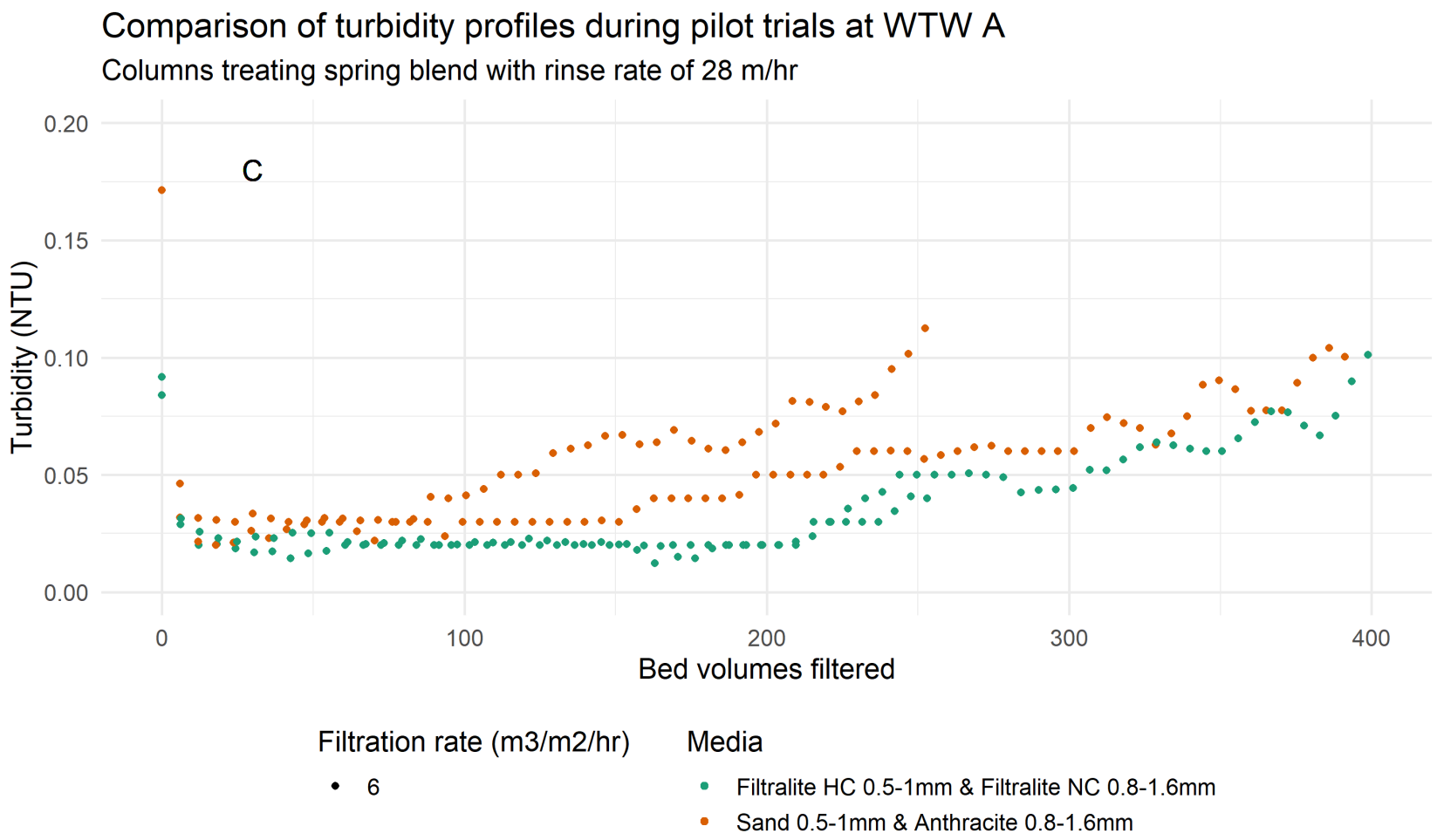

Figure_Apx 57 Enlargement of figure Figure_Apx 53 C turbidity profiles for pilot filter trials of the spring blend backwashed at 28 m/hr

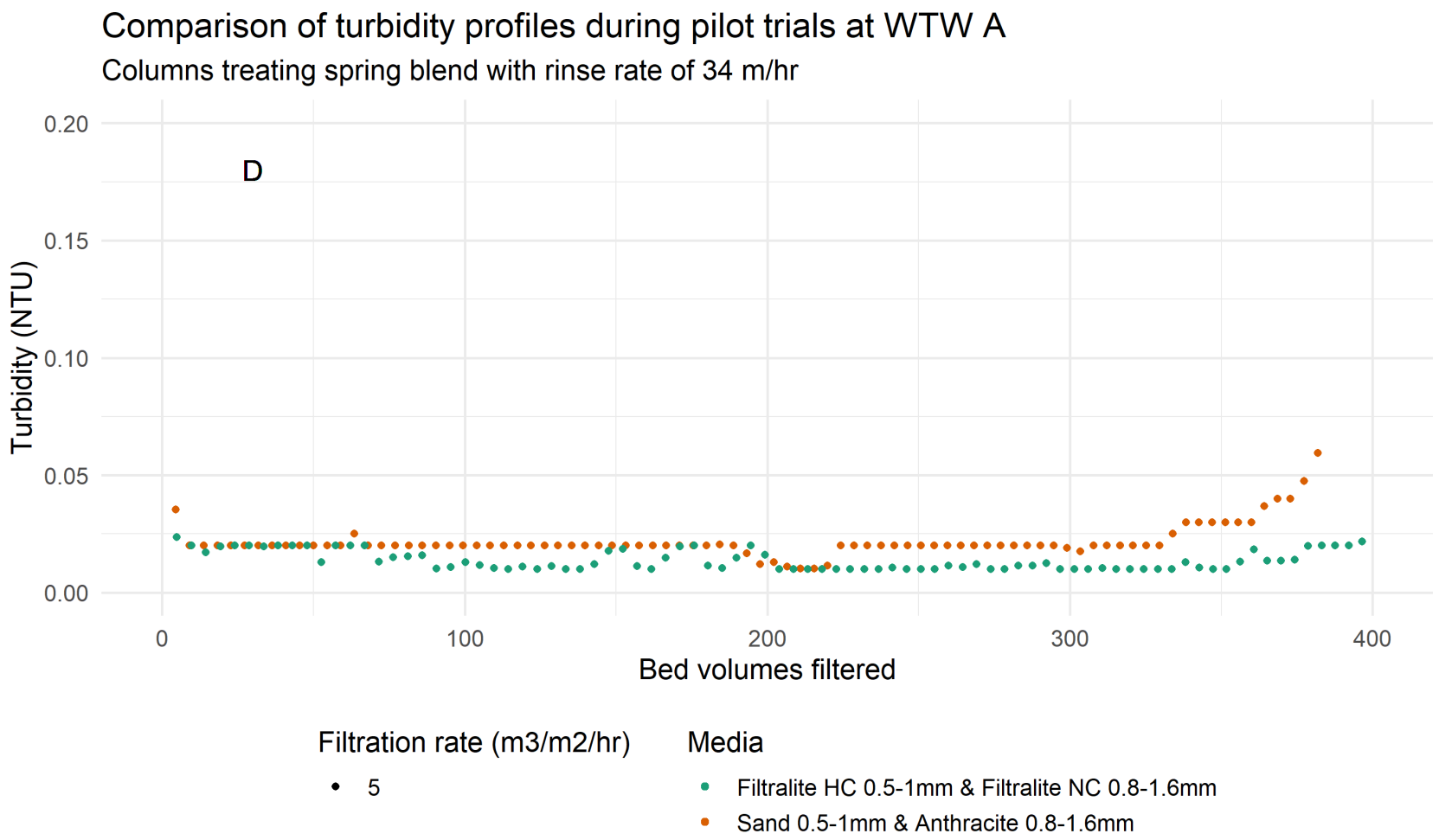

Figure_Apx 58 Enlargement of figure Figure_Apx 53 D turbidity profiles for pilot filter trials of the spring blend backwashed at 34 m/hr

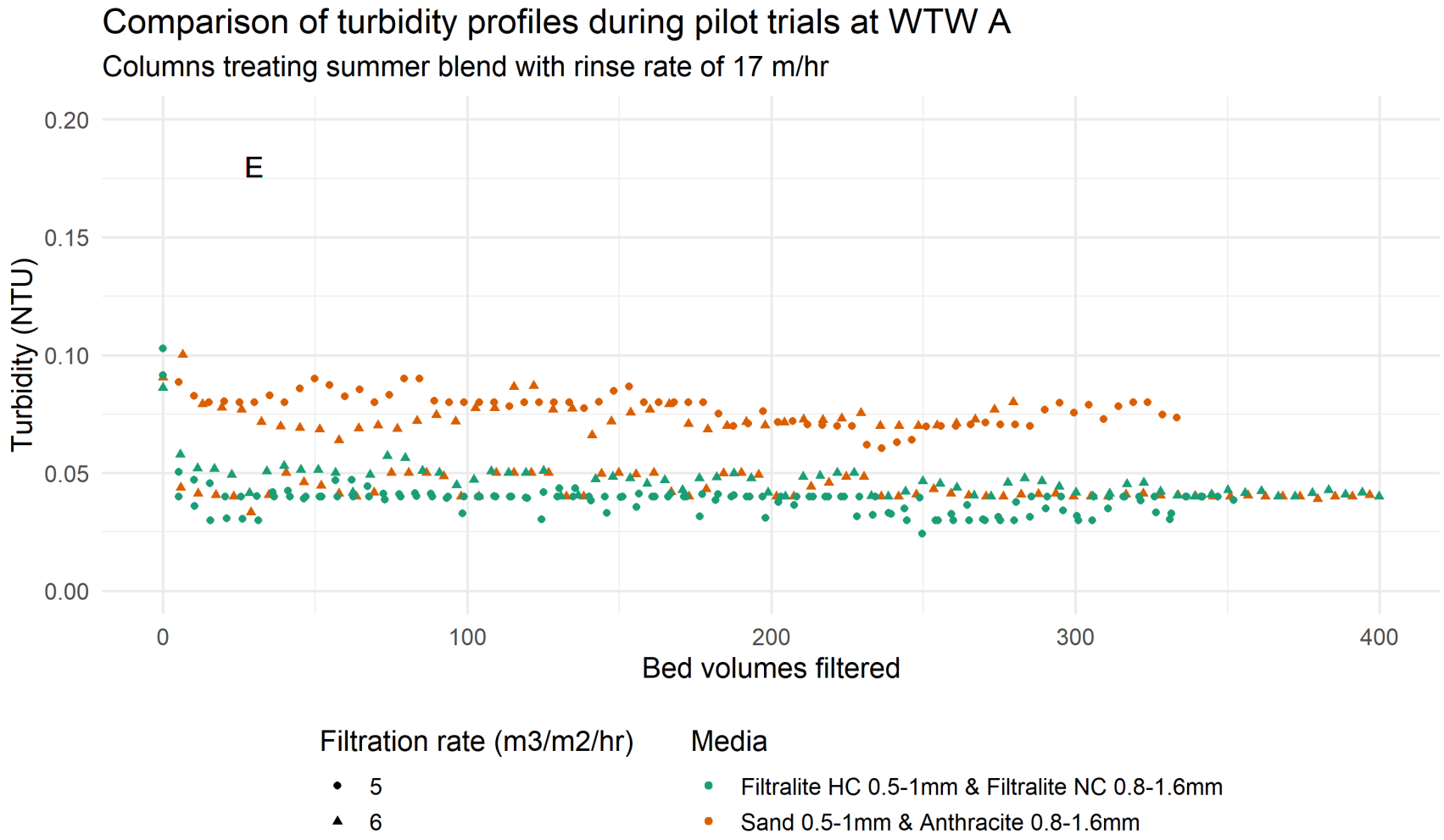

Figure_Apx 59 Enlargement of figure Figure_Apx 53 E turbidity profiles for pilot filter trials of the summer blend backwashed at 17 m/hr

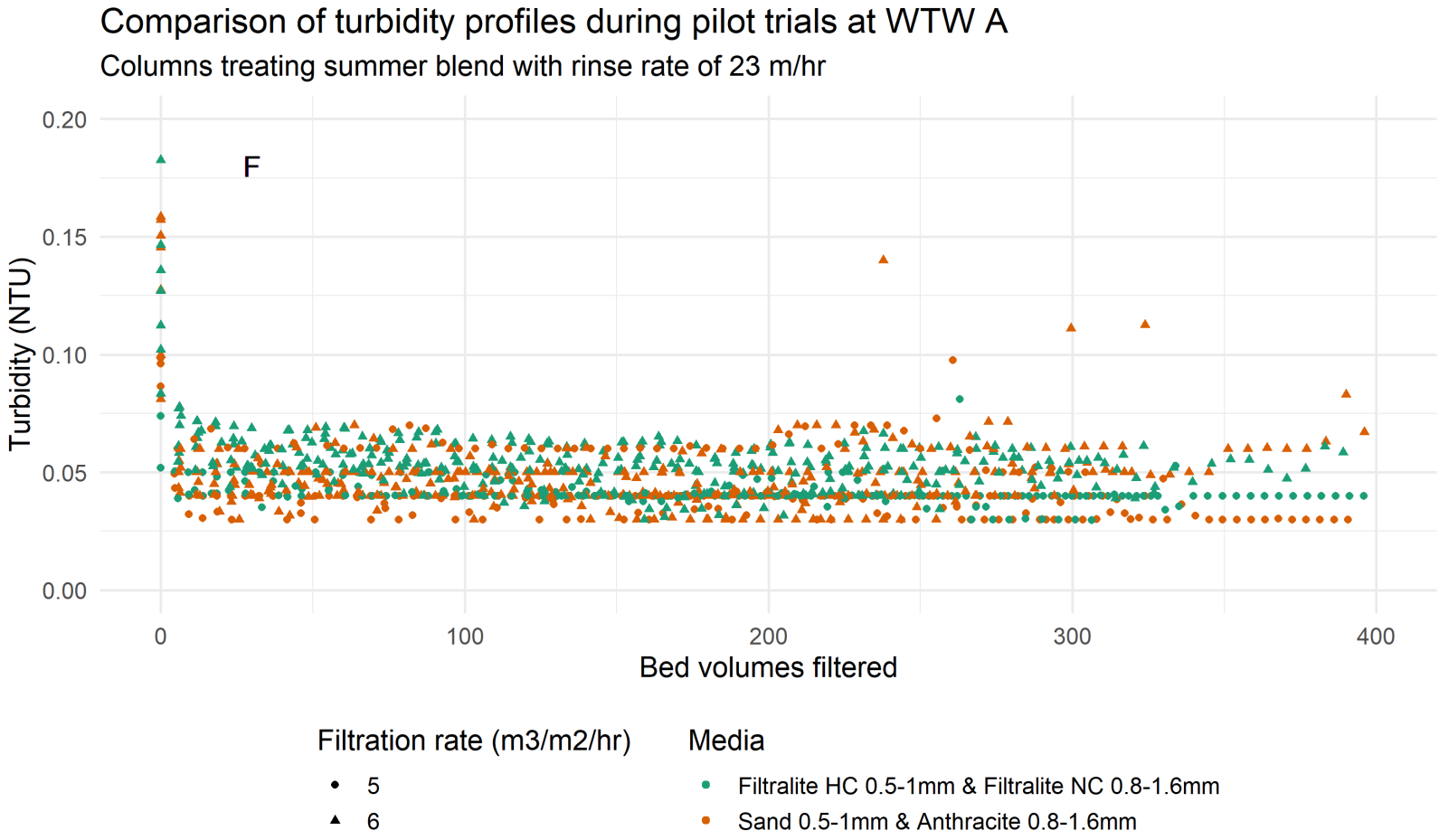

Figure_Apx 60 Enlargement of figure Figure_Apx 53 F turbidity profiles for pilot filter trials of the summer blend backwashed at 23 m/hr

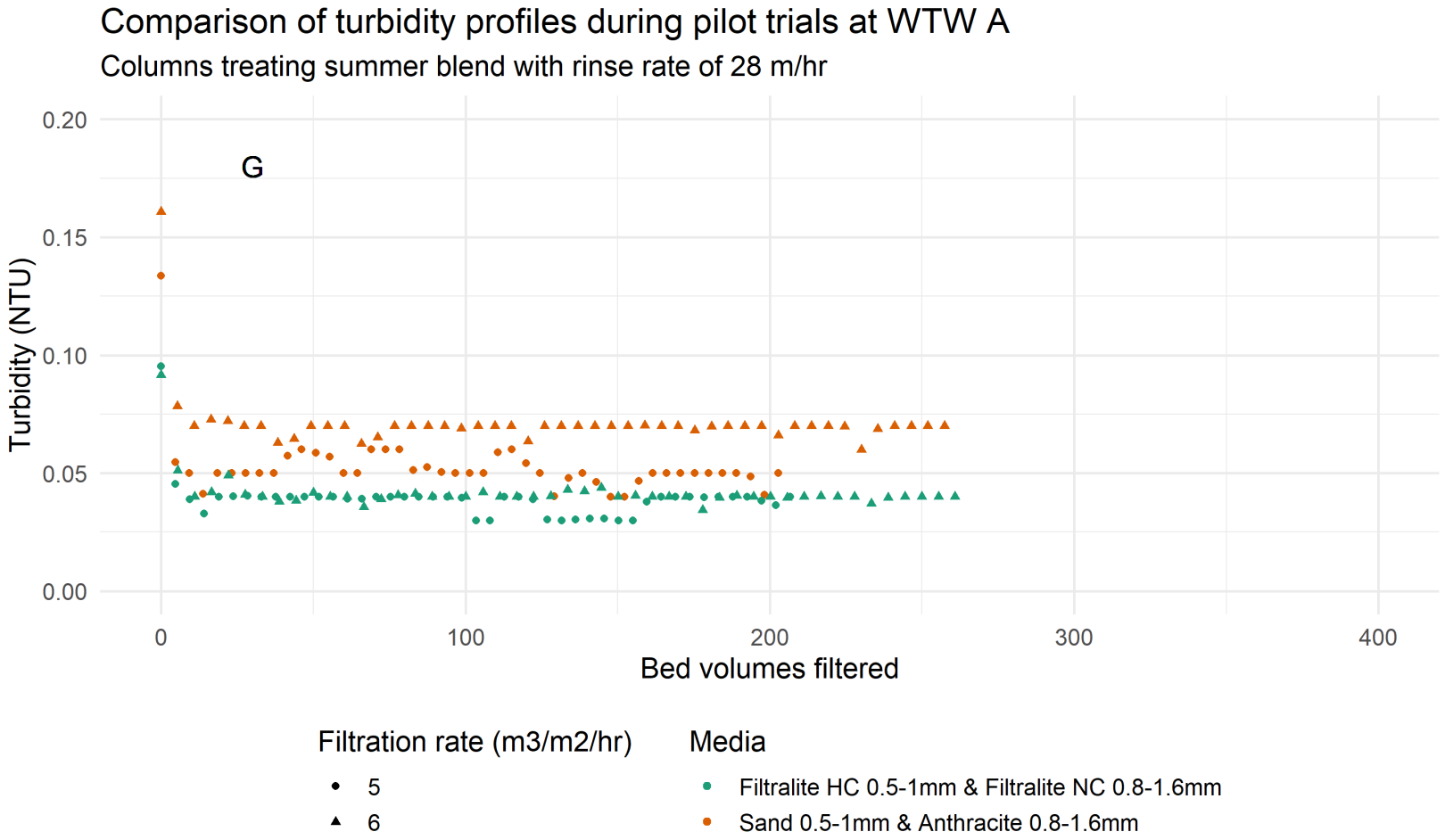

Enlargement of figure Figure_Apx 53 G turbidity profiles for pilot filter trials of the summer blend backwashed at 28 m/hr

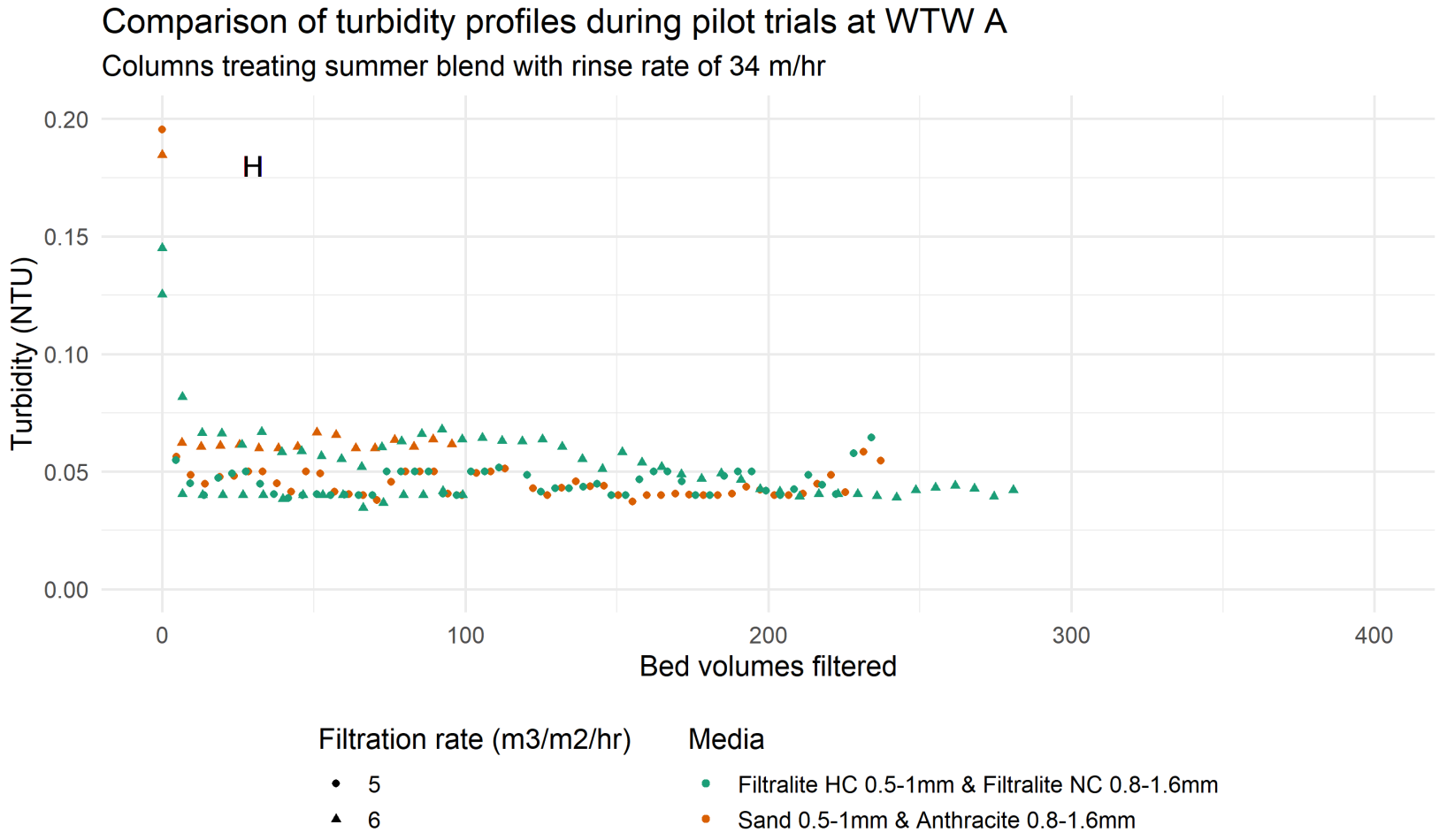

Enlargement of figure Figure_Apx 53 H turbidity profiles for pilot filter trials of the summer blend backwashed at 34 m/hr

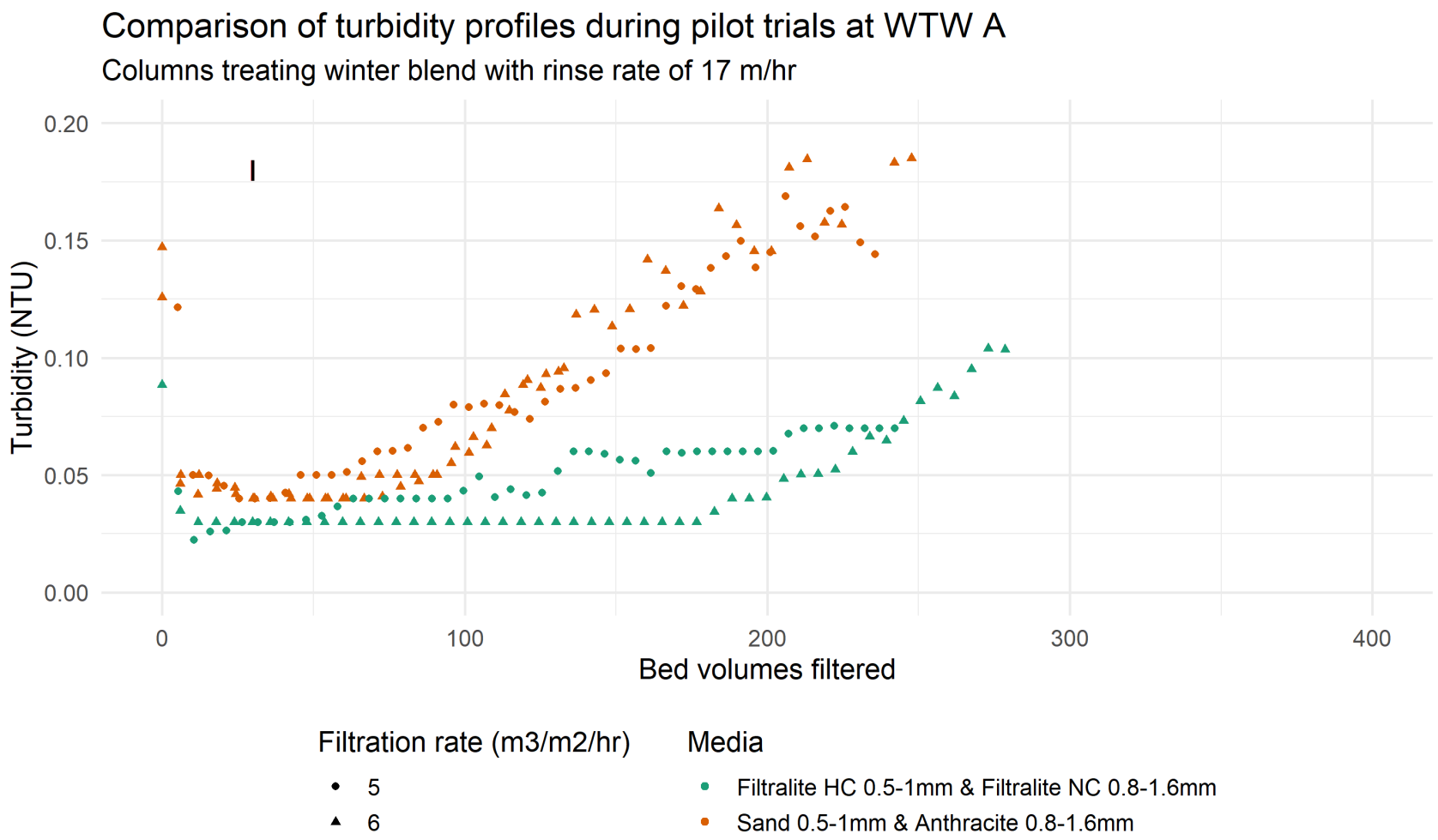

Figure_Apx 61 Enlargement of figure Figure_Apx 53 I turbidity profiles for pilot filter trials of the winter blend backwashed at 17 m/hr

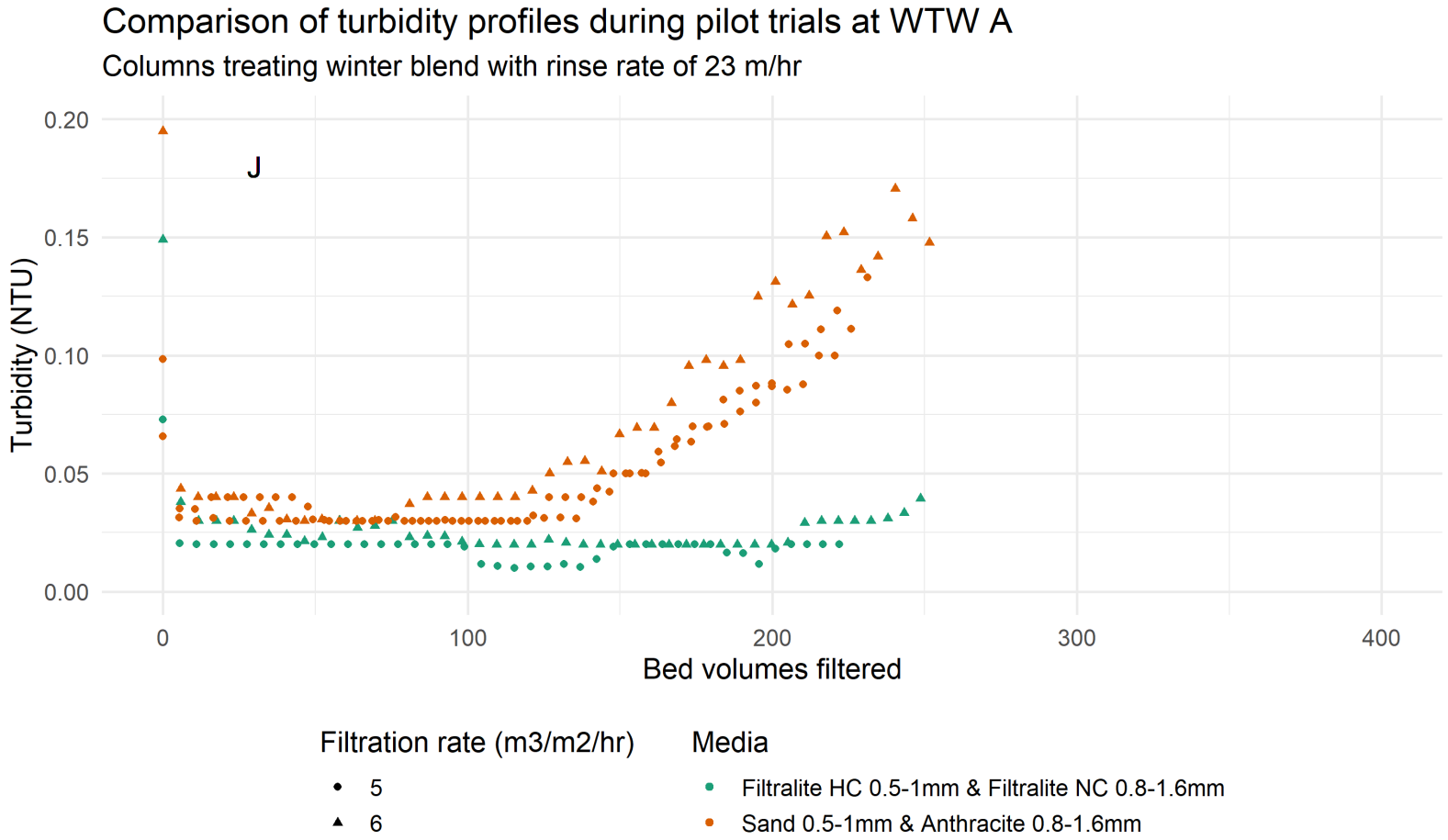

Figure_Apx 62 Enlargement of figure Figure_Apx 53 J turbidity profiles for pilot filter trials of the winter blend backwashed at 23 m/hr

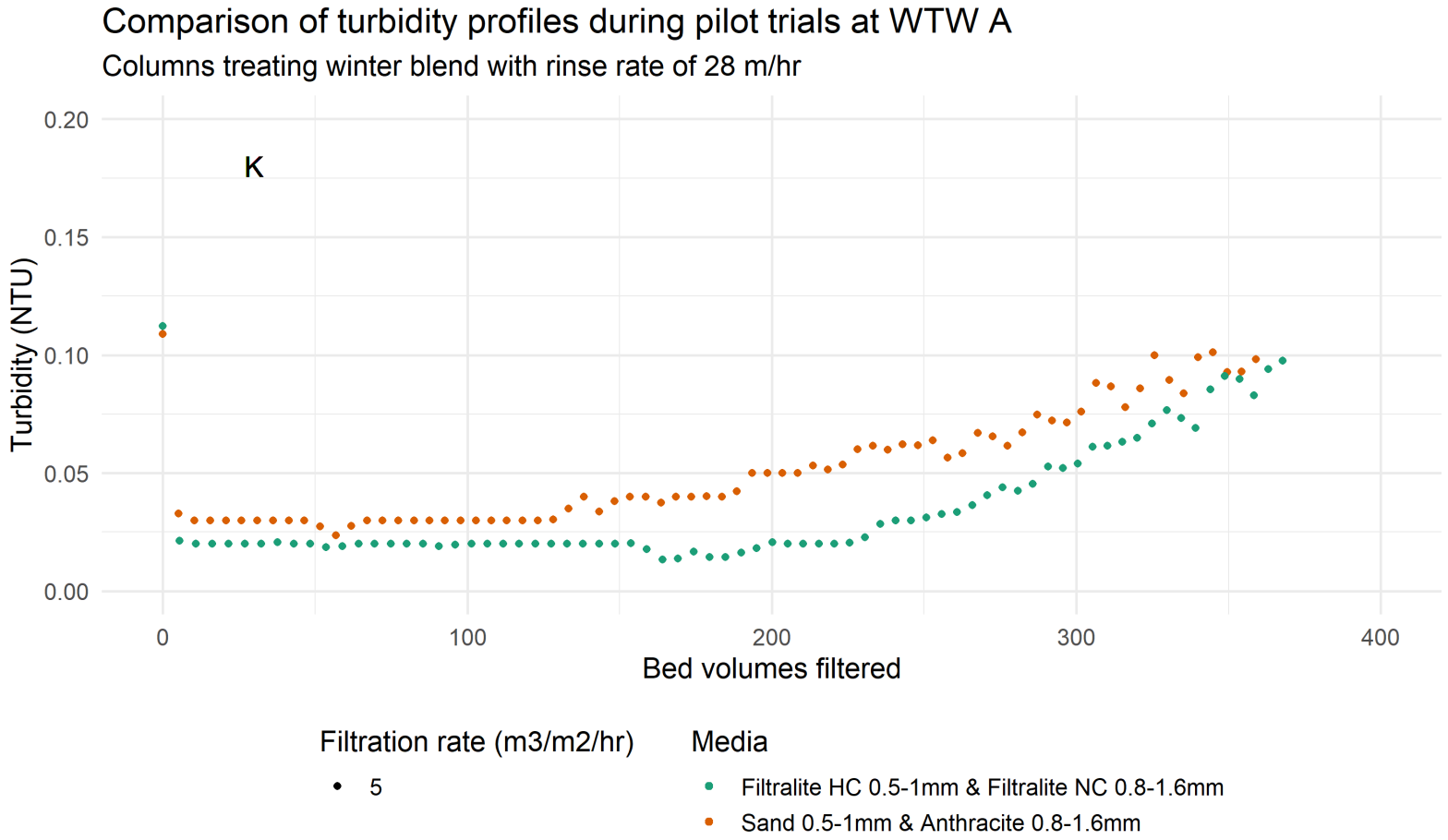

Figure_Apx 63 Enlargement of figure Figure_Apx 53 K turbidity profiles for pilot filter trials of the winter blend backwashed at 28 m/hr

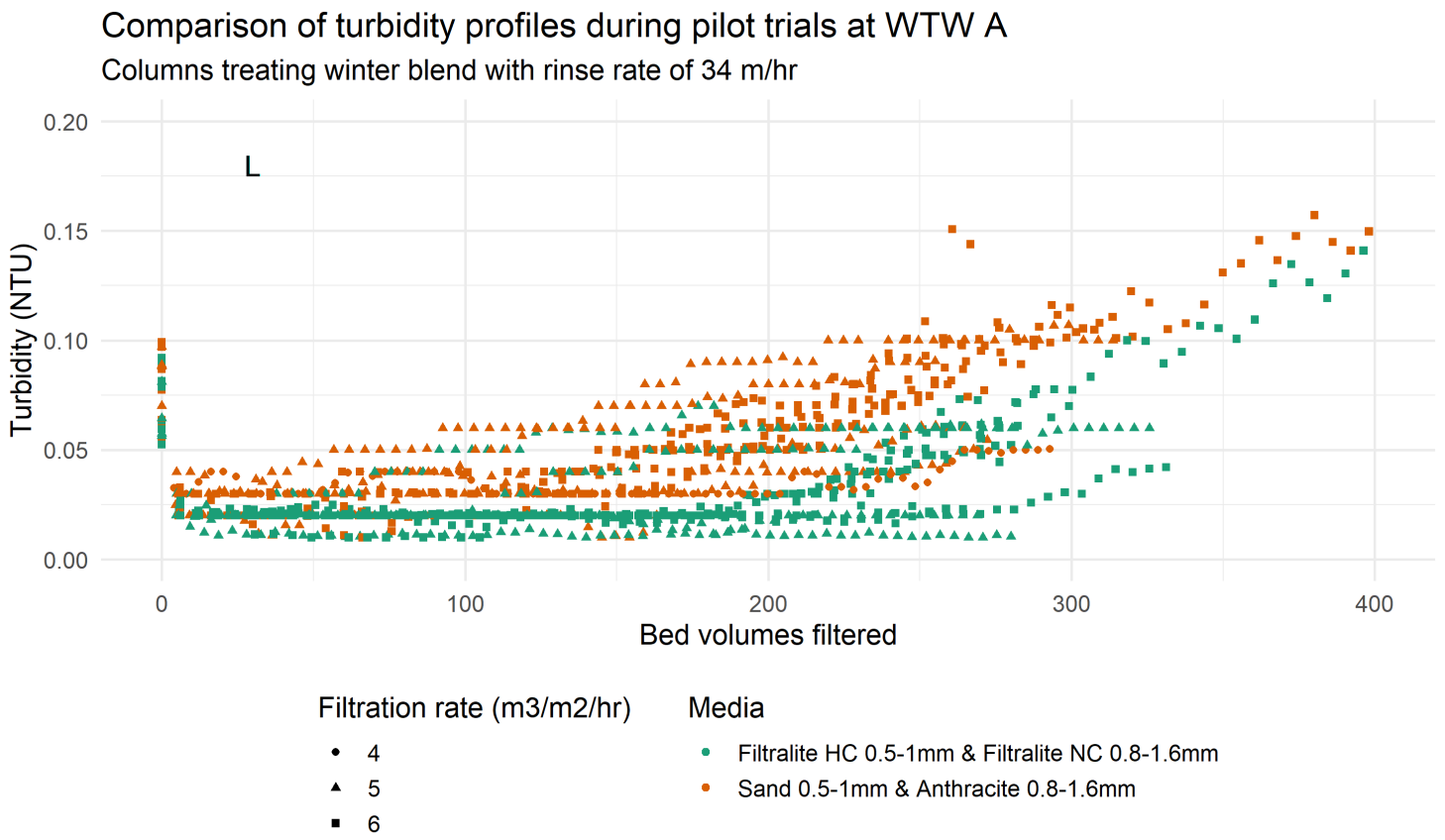

Figure_Apx 64 Enlargement of figure Figure_Apx 53 L turbidity profiles for pilot filter trials of the winter blend backwashed at 34 m/hr

C.5 Head loss profiles for filter runs divided by backwash rate & feed water.

Replication of individual facets from profiles plotted for pilot trials at WTW A shown below but not labelled.

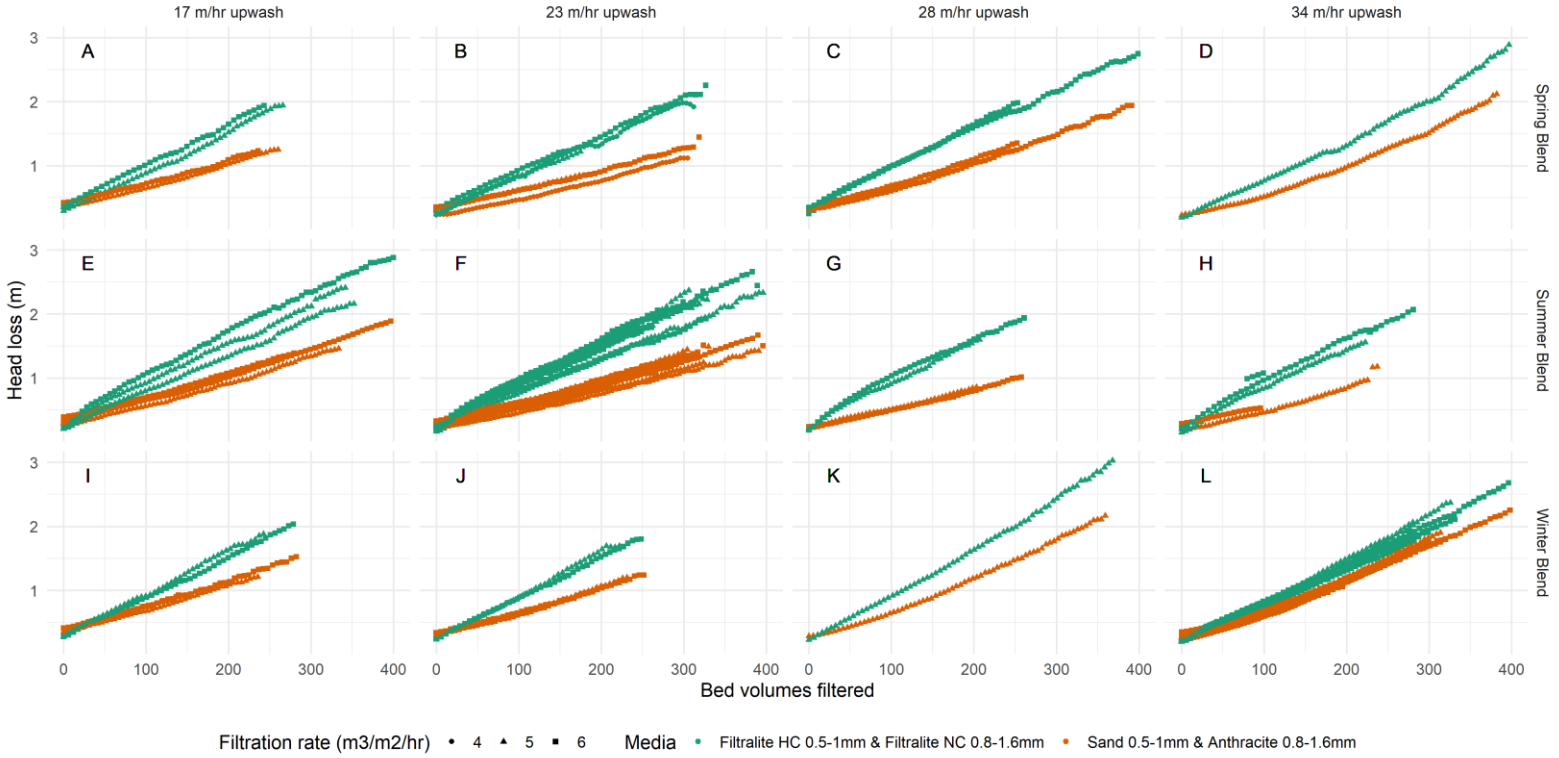

Figure_Apx 65 Comparison of head loss profiles from pilot trials at WTW A. Media bed of Filtralite HC 0.5-1 mm & Filtralite NC 0.8-1.6 mm is compared to Sand 0.5-1 mm and Anthracite 0.8-1.6 mm at backwash rates of 17,23,28 & 34 m/hr over three seasons.

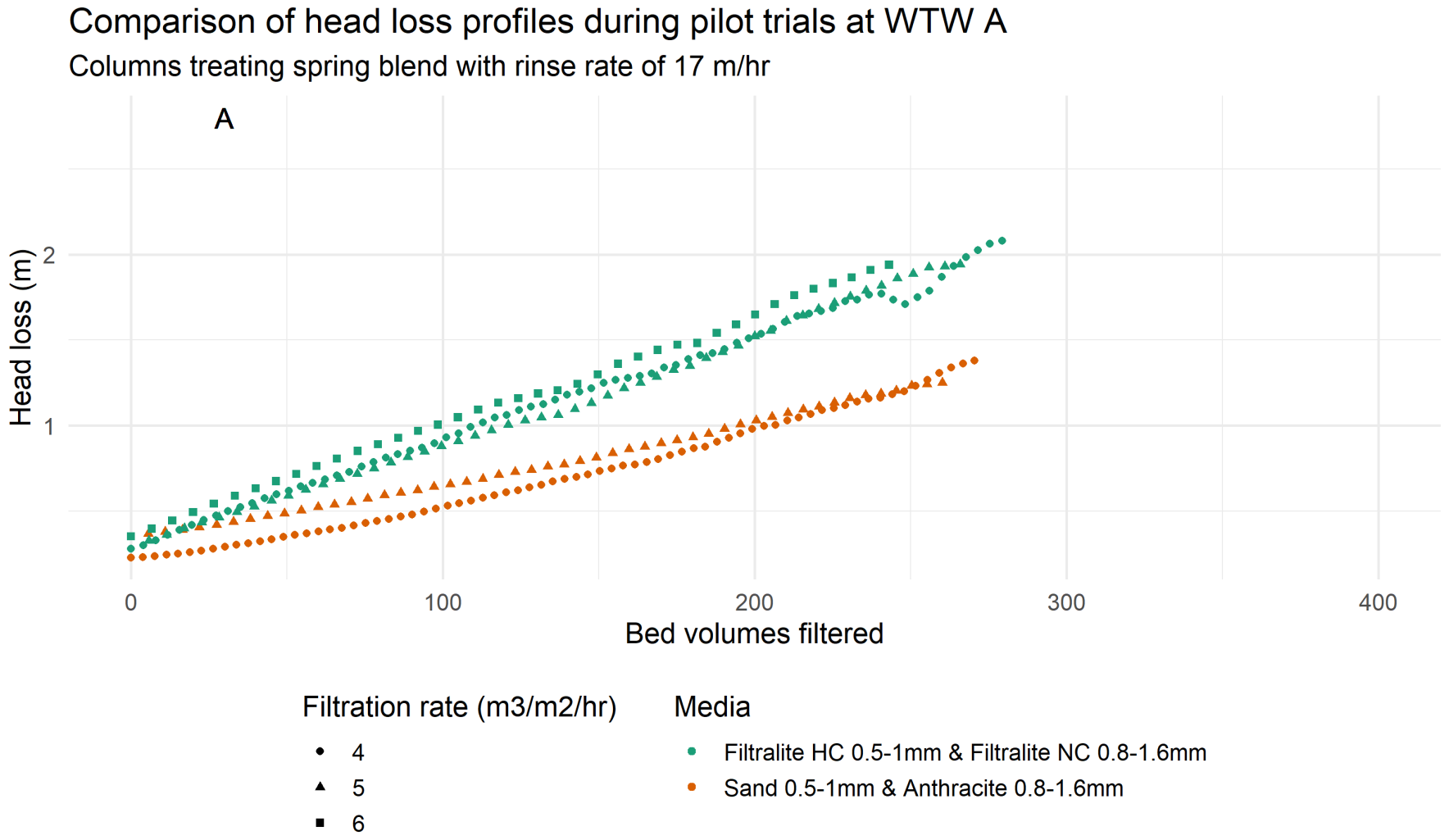

Figure_Apx 66 Enlargement of figure Figure_Apx 64 A head loss profiles for pilot filter trials of the spring blend backwashed at 17 m/hr

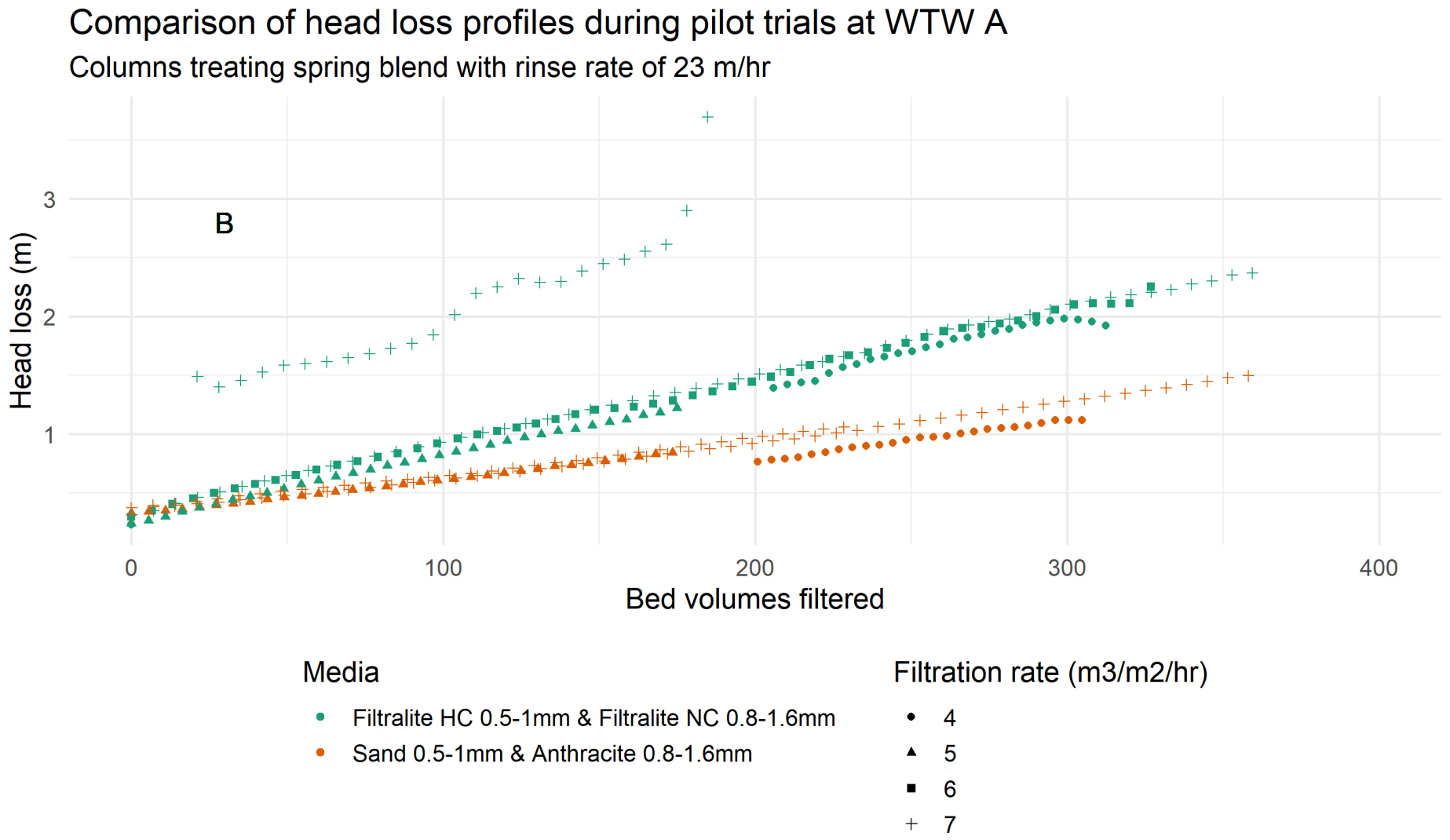

Figure_Apx 67 Enlargement of figure Figure_Apx 64 B head loss profiles for pilot filter trials of the spring blend backwashed at 23 m/hr

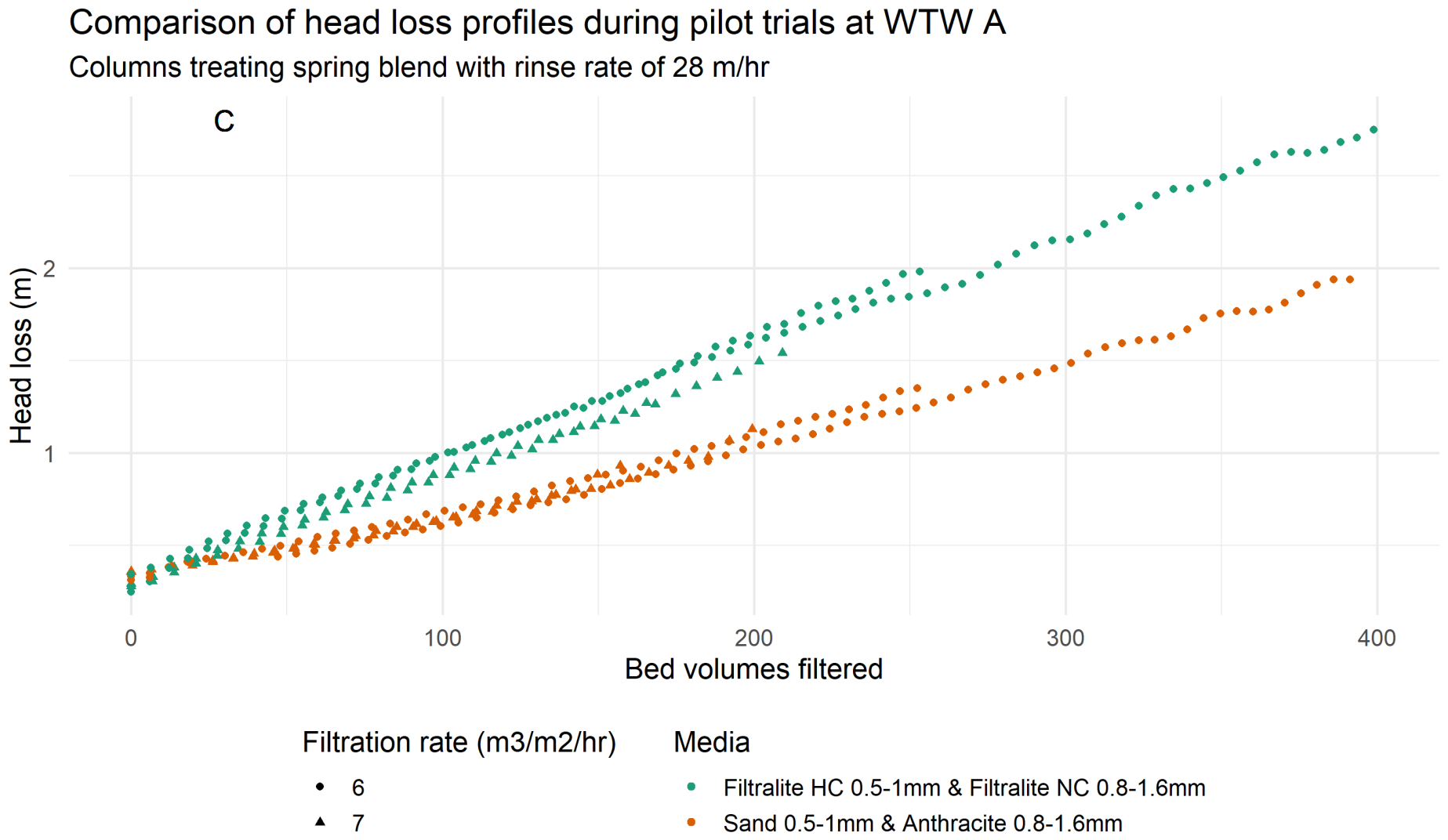

Figure_Apx 68 Enlargement of figure Figure_Apx 64 C head loss profiles for pilot filter trials of the spring blend backwashed at 28 m/hr

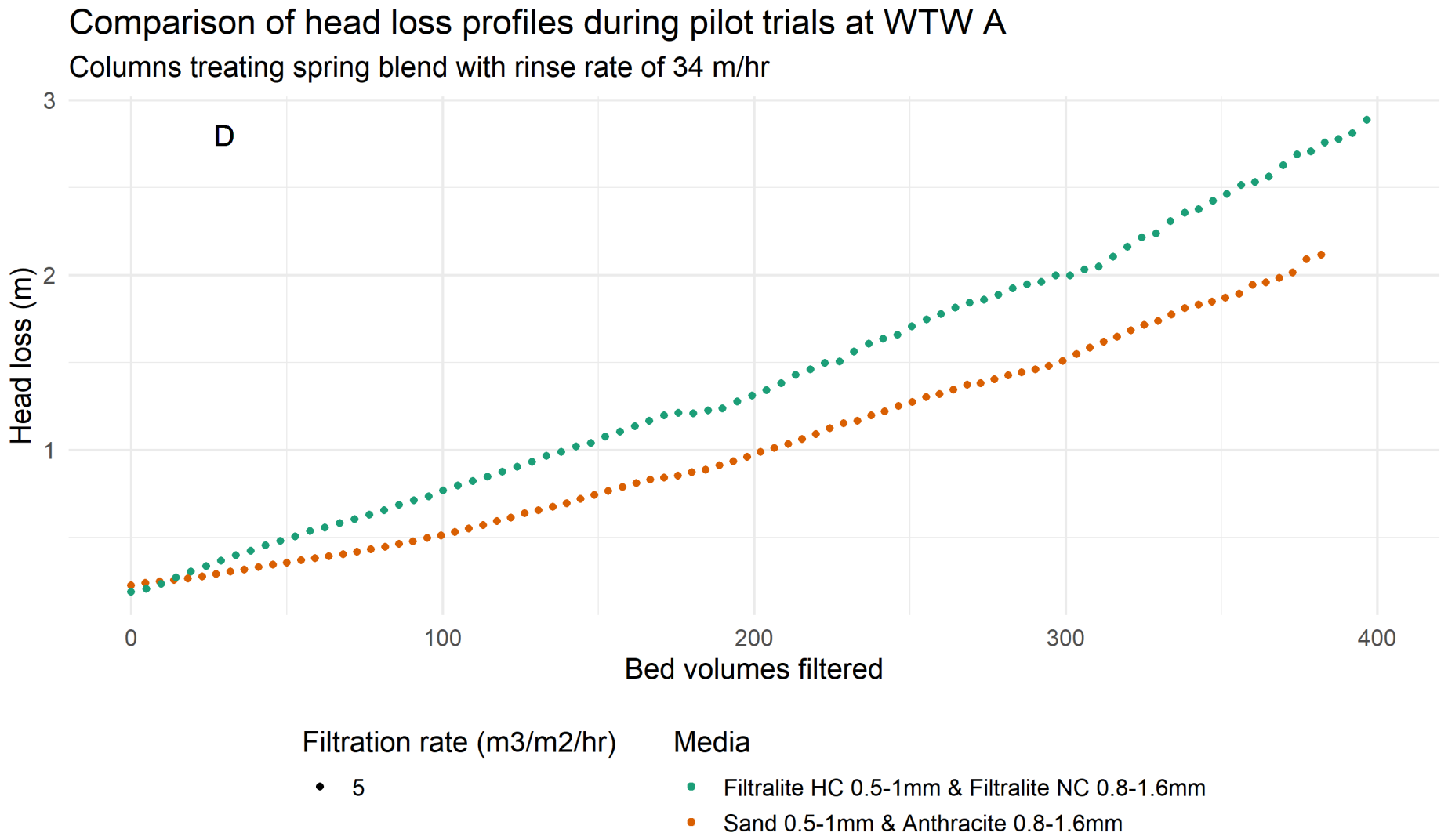

Figure_Apx 69 Enlargement of figure Figure_Apx 64 D head loss profiles for pilot filter trials of the spring blend backwashed at 34 m/hr

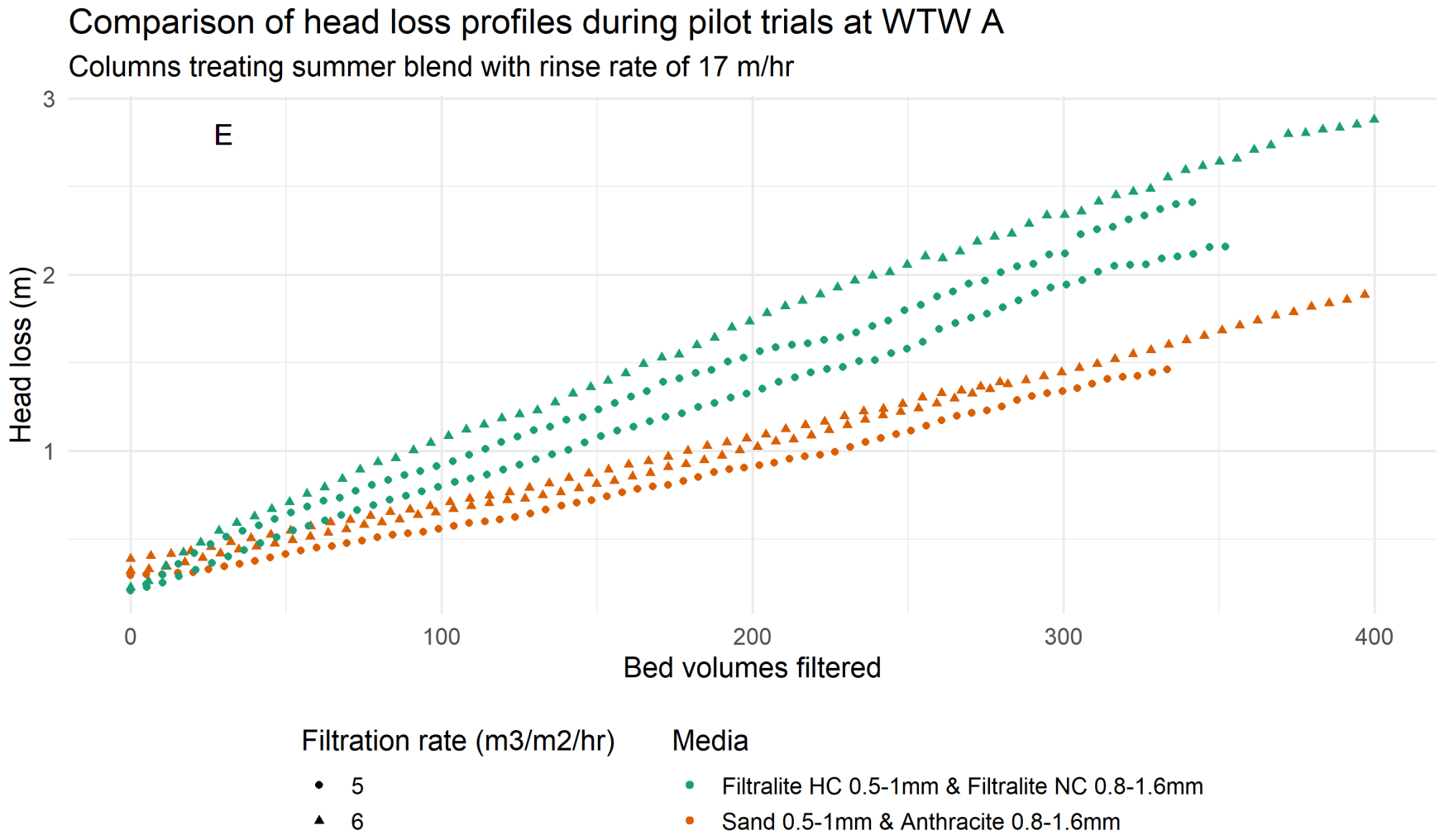

Figure_Apx 70 Enlargement of figure Figure_Apx 64 E head loss profiles for pilot filter trials of the summer blend backwashed at 17 m/hr

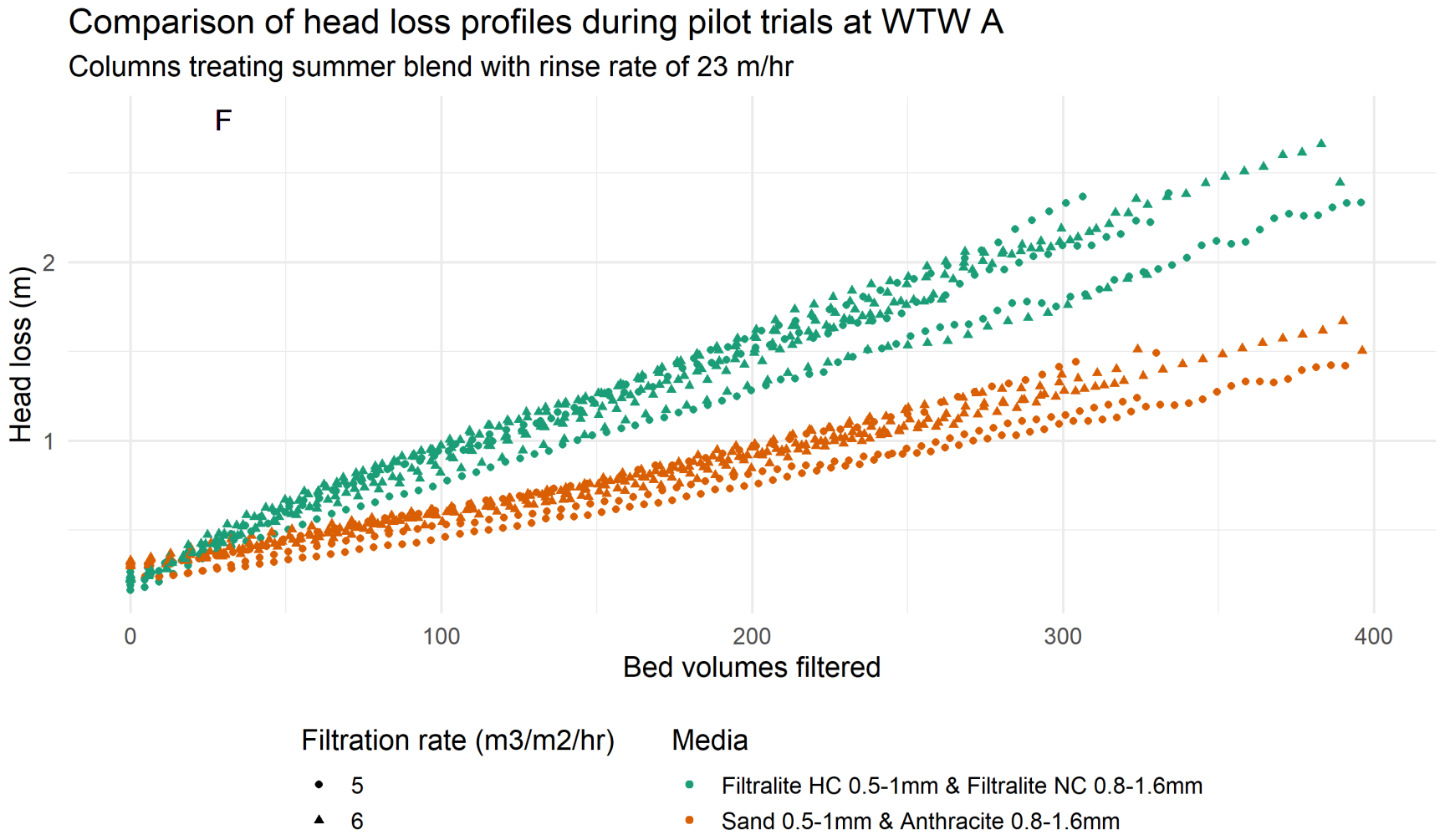

Figure_Apx 71 Enlargement of figure Figure_Apx 64 F head loss profiles for pilot filter trials of the summer blend backwashed at 28 m/hr

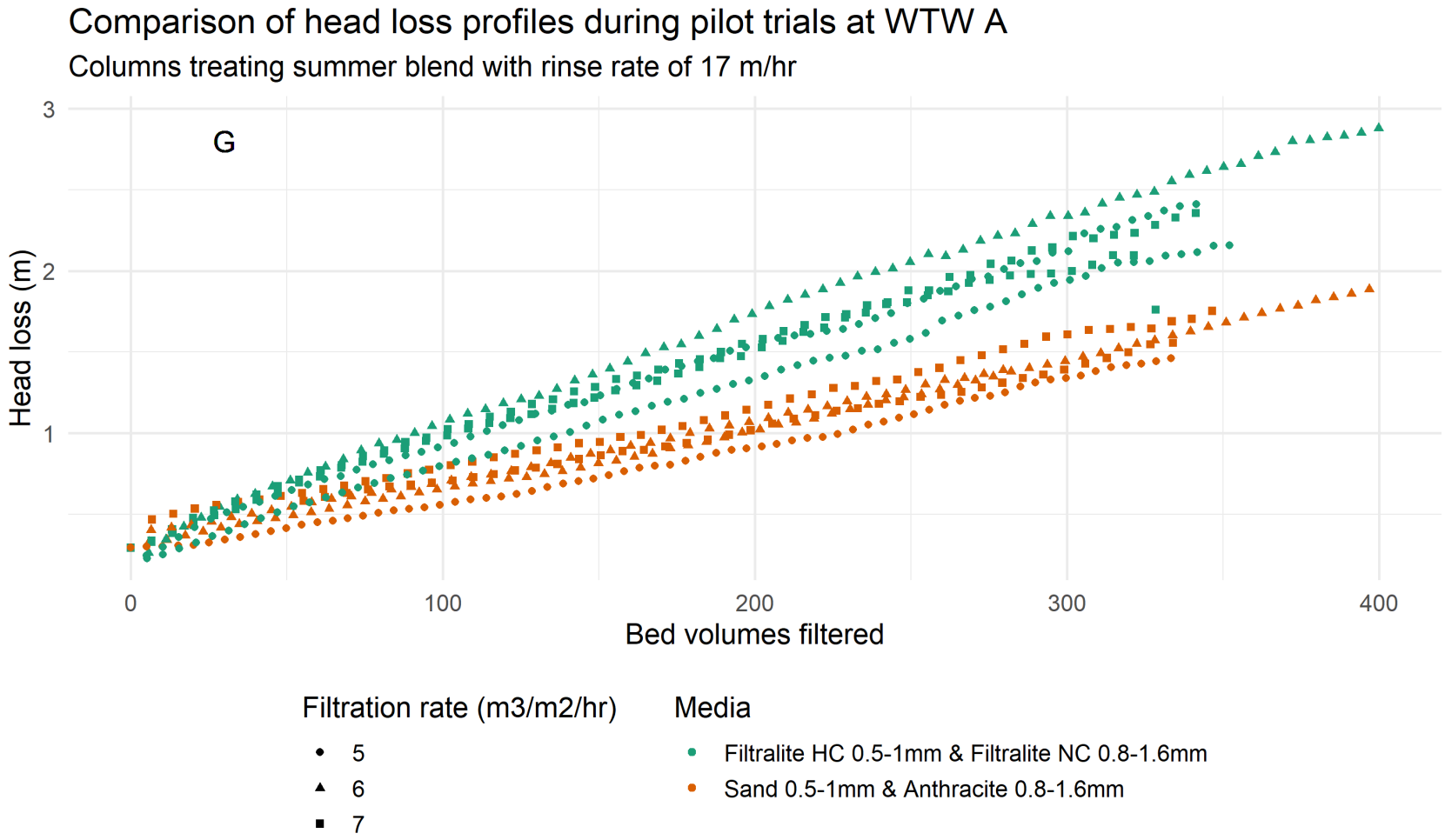

Figure_Apx 72 Enlargement of figure Figure_Apx 64 G head loss profiles for pilot filter trials of the summer blend backwashed at 28 m/hr

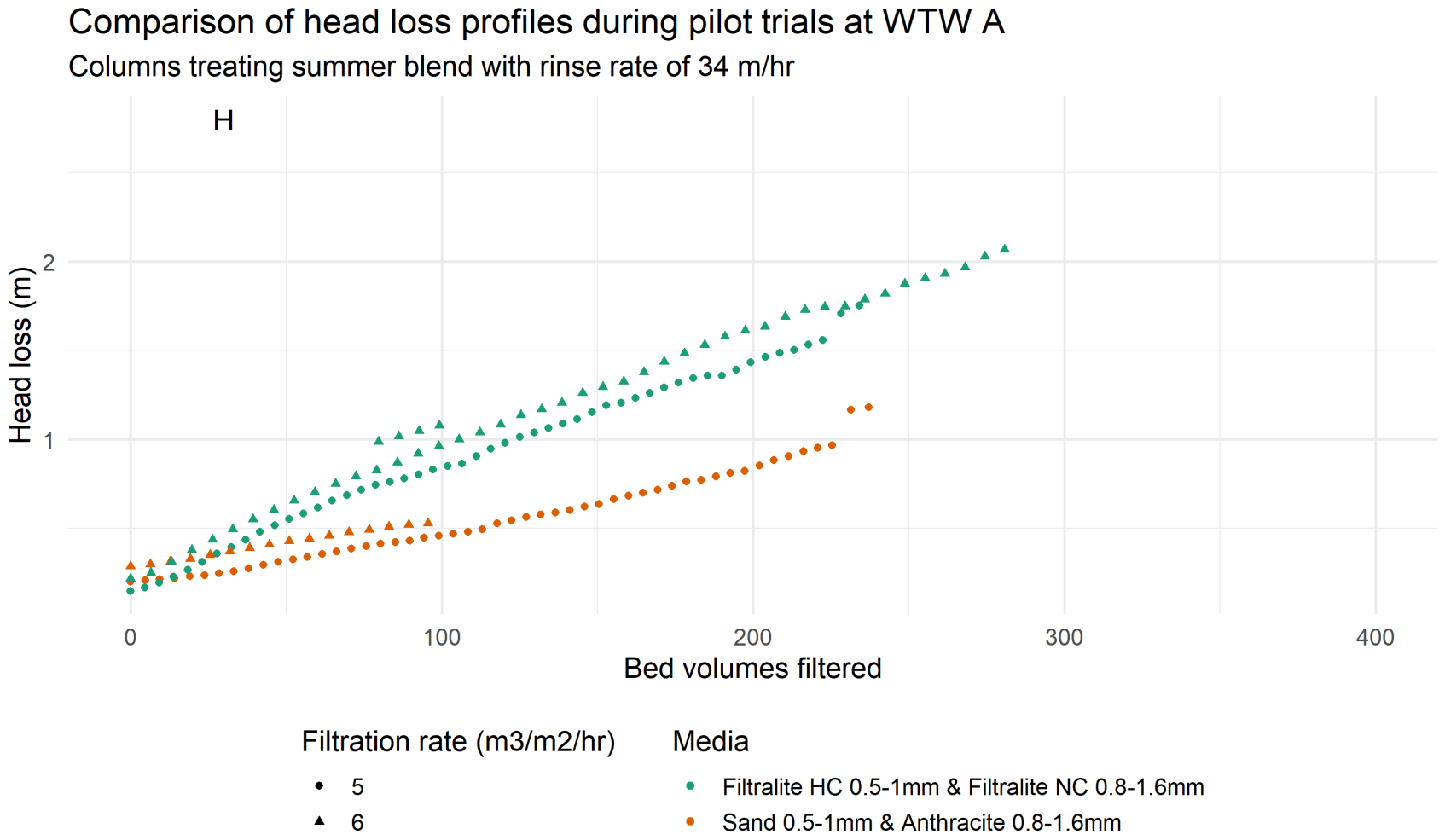

Figure_Apx 73 Enlargement of figure Figure_Apx 64 H head loss profiles for pilot filter trials of the summer blend backwashed at 34 m/hr

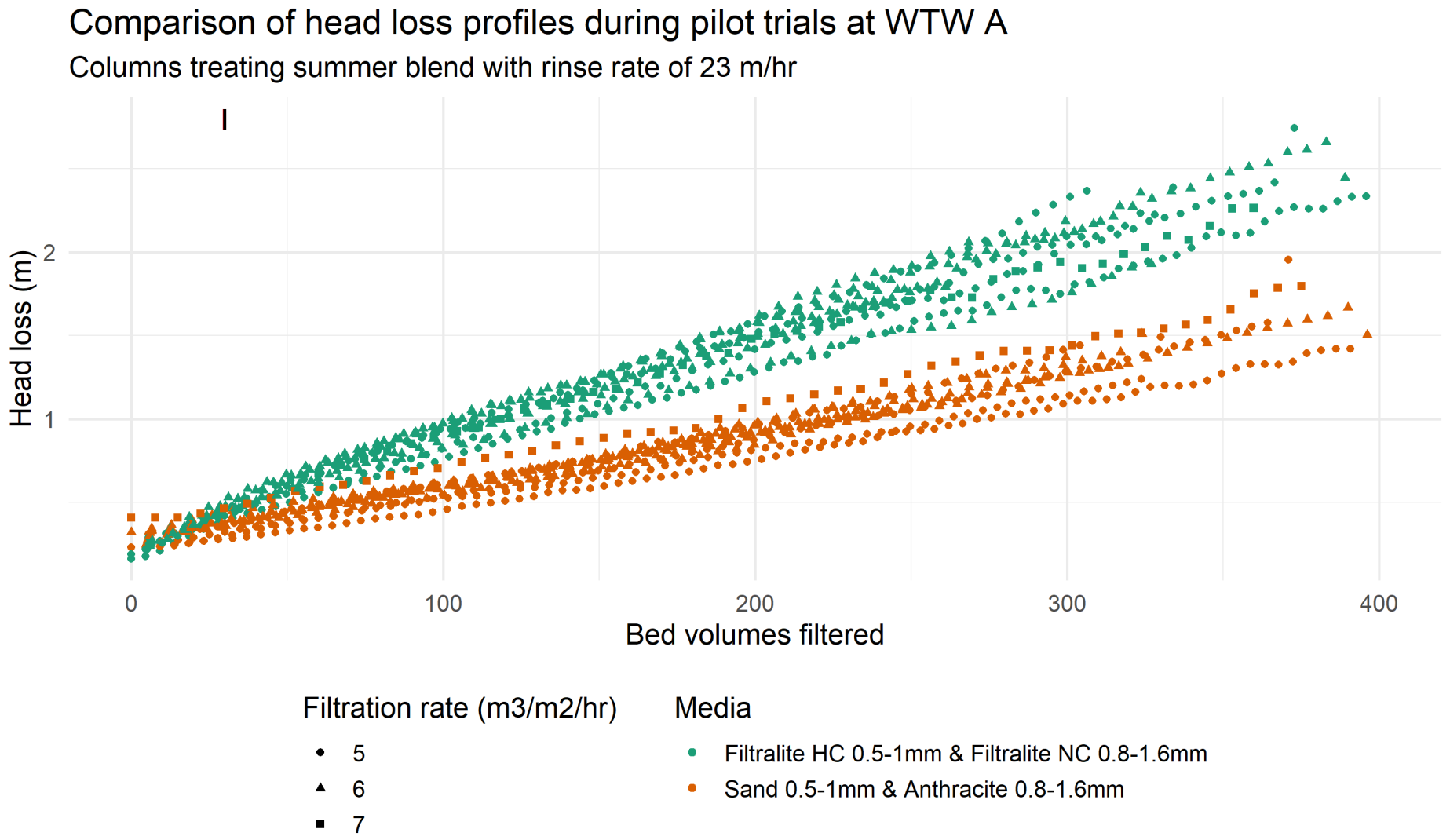

Figure_Apx 74 Enlargement of figure Figure_Apx 64 I head loss profiles for pilot filter trials of the winter blend backwashed at 17 m/hr

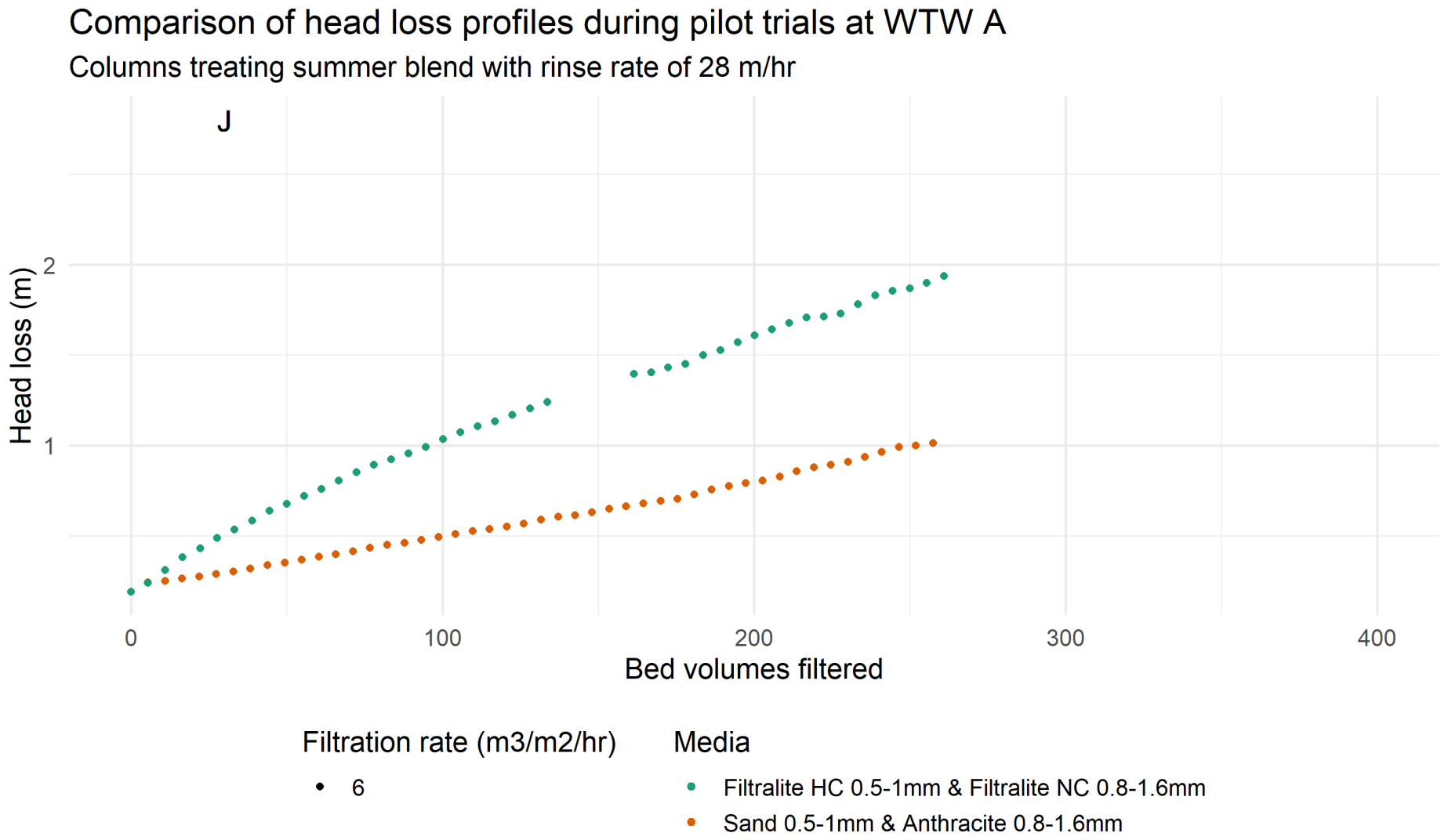

Figure_Apx 75 Enlargement of figure Figure_Apx 64 J head loss profiles for pilot filter trials of the winter blend backwashed at 23 m/hr

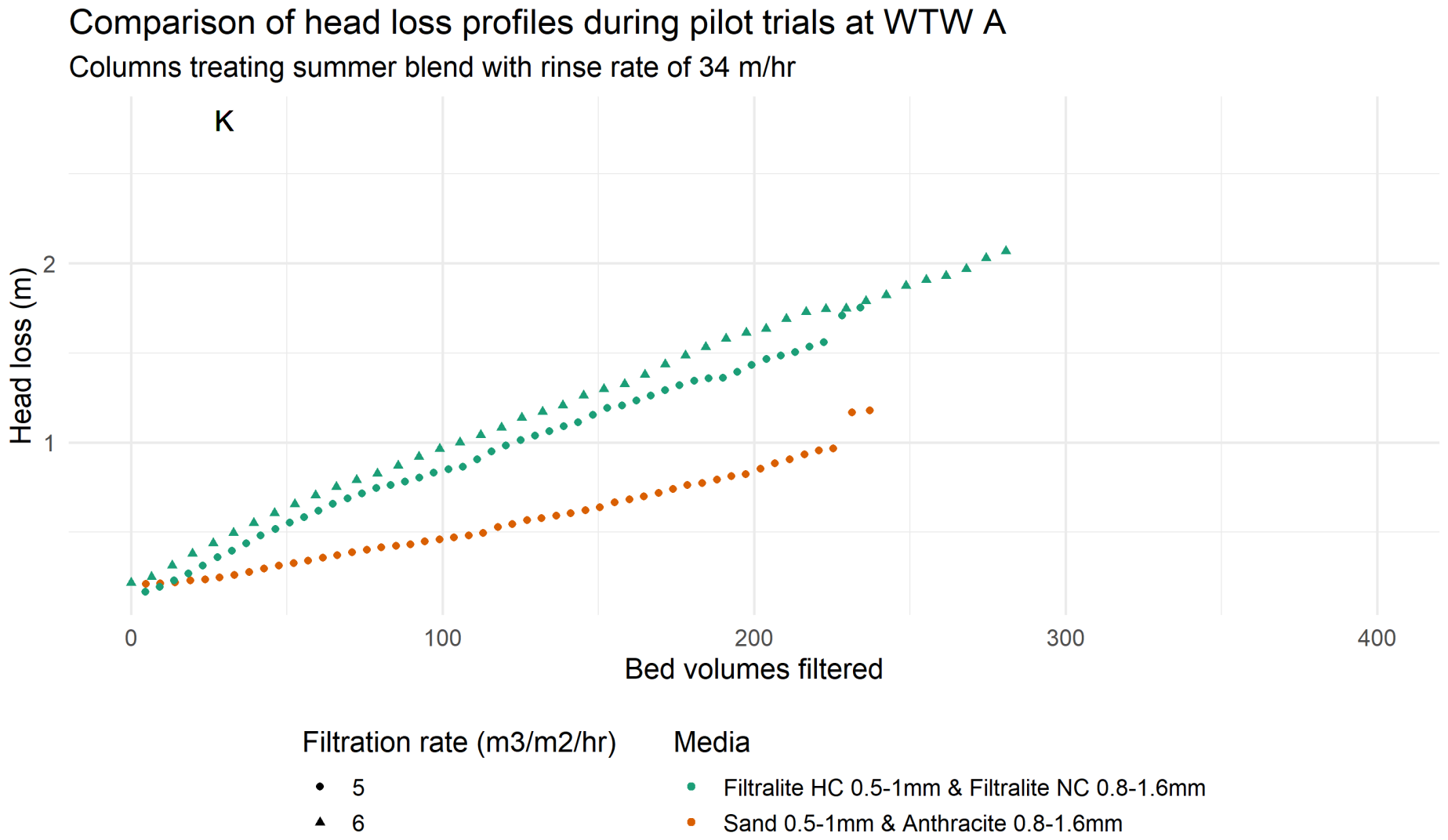

Figure_Apx 76 Enlargement of figure Figure_Apx 64 K head loss profiles for pilot filter trials of the winter blend backwashed at 28 m/hr

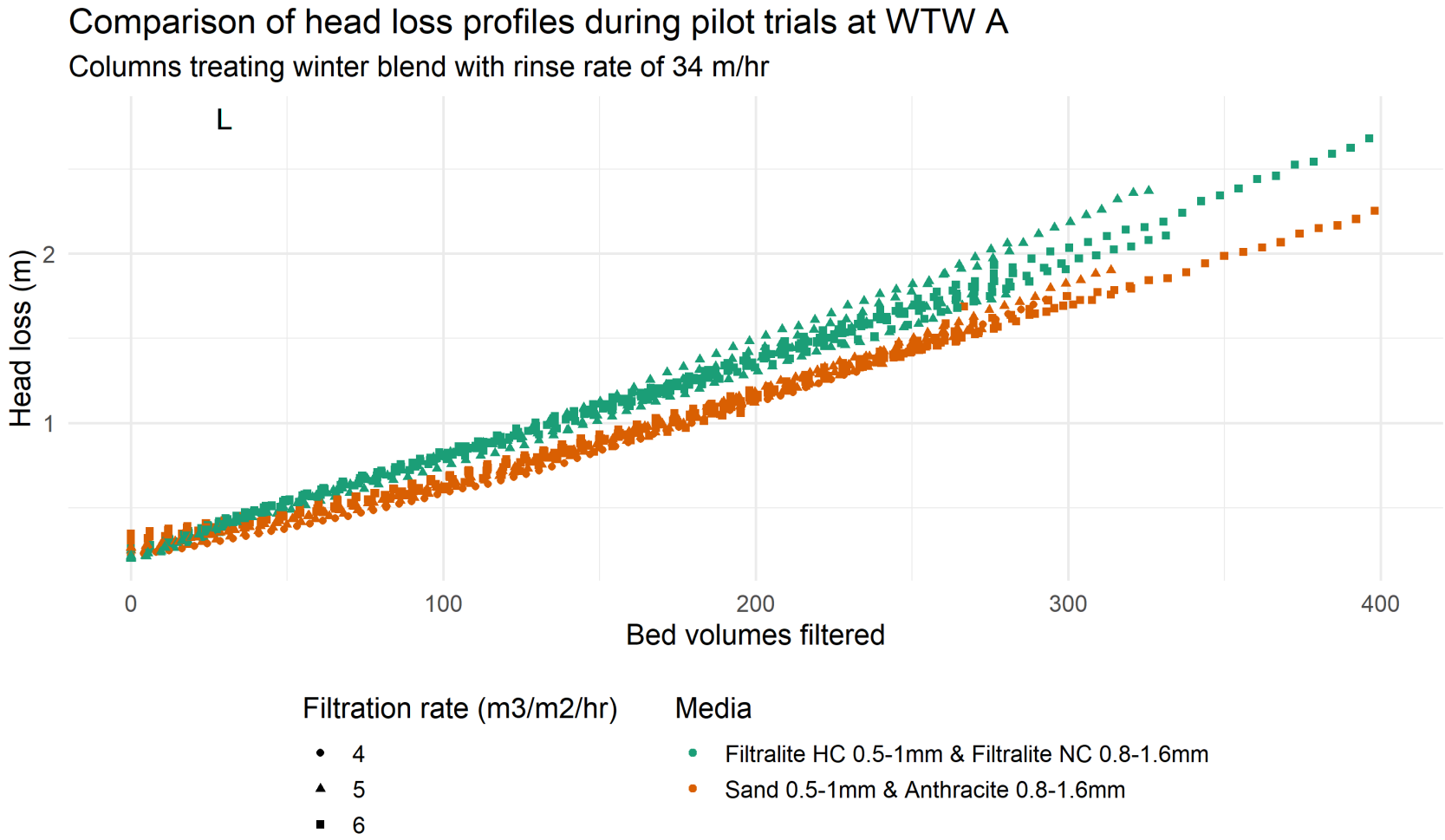

Figure_Apx 77 Enlargement of figure Figure_Apx 64 L head loss profiles for pilot filter trials of the winter blend backwashed at 34 m/hr

C.6 Summary data for full scale trials of Filtralite – anthracite media at WTWA

Table_Apx 4 Summary table of performance of Filtralite (0.5-1 mm) – anthracite (0.8-1.6 mm) media in comparison to neighbouring filter containing sand (0.6-1.2 mm) and pumice (unknown). Values presented as mean (min – max).

Summary of performance during full scale trial								
signal	Phase 1		Phase 2		Phase 3		Phase 4	
	Phase 1 Filtralite - Anthracite	Phase 1 Sand - Pumice	Phase 2 Filtralite - Anthracite	Phase 2 Sand - Pumice	Phase 3 Filtralite - Anthracite	Phase 3 Sand - Pumice	Phase 4 Filtralite - Anthracite	Phase 4 Sand - Pumice
Clarified turbidity (NTU)	0.7 (0.65-0.78)	0.69 (0.65-0.79)	0.77 (0.72-0.83)	0.77 (0.71-0.85)	0.86 (0.72-0.99)	0.86 (0.75-1)	0.59 (0.24-1.18)	0.58 (0.24-1.13)
Filtration rate (m3/m2/hr)	3.2 (2.92-4.31)	3.28 (3-3.82)	3.34 (3.08-4.23)	3.35 (3.15-3.59)	3.96 (3.51-4.25)	3.3 (2.89-3.59)	4.83 (3.94-5.96)	3.54 (2.98-4.71)
NCBHL (m)	0.07 (0.04-0.11)	0.28 (0.23-0.32)	0.12 (0.09-0.14)	0.25 (0.21-0.27)	0.13 (0.12-0.15)	0.2 (0.16-0.25)	0.16 (0.13-0.34)	0.22 (0.13-0.34)
Run time (hrs)	30.27 (20.82-36.76)	30.37 (22.79-35.77)	42.41 (34.08-47.97)	24.69 (20.48-47.75)	22.28 (19.42-43.79)	21.78 (17.8-24.38)	28.22 (14.33-39.78)	29.56 (14.43-43.83)
Temp (C)	9.38 (6.98-11.12)	9.41 (7-11.13)	5.21 (3.79-6.91)	5.38 (3.7-6.94)	3.05 (1.89-4.96)	3.05 (1.89-4.96)	8.21 (1.07-15.15)	8.3 (1.07-15.15)
Terminal NHL (m)	0.87 (0.56-1.35)	0.75 (0.5-0.9)	1.25 (1.02-1.48)	0.58 (0.53-0.64)	0.5 (0.42-0.59)	0.54 (0.37-0.63)	0.6 (0.39-0.8)	0.69 (0.47-0.97)
Turbidity 95thpctile (NTU)	0.04 (0.03-0.05)	0.05 (0.03-0.14)	0.09 (0.03-0.24)	0.1 (0.05-0.19)	0.04 (0.03-0.1)	0.13 (0.04-0.26)	0.05 (0.03-0.25)	0.07 (0.02-0.42)
Turbidity 95thpctile first 4 EBVs (NTU)	0.18 (0.03-0.6)	0.04 (0.02-0.07)	0.09 (0.04-0.16)	0.05 (0.04-0.12)	0.1 (0.04-0.29)	0.07 (0.04-0.17)	0.06 (0.03-0.14)	0.04 (0.03-0.15)
Turbidity mean (NTU)	0.03 (0.03-0.04)	0.03 (0.02-0.07)	0.04 (0.03-0.06)	0.04 (0.03-0.07)	0.03 (0.02-0.05)	0.05 (0.03-0.1)	0.04 (0.03-0.08)	0.04 (0.02-0.13)
Turbidity mean last hour (NTU)	0.03 (0.03-0.04)	0.04 (0.01-0.12)	0.14 (0.03-0.48)	0.08 (0.05-0.17)	0.03 (0.02-0.07)	0.1 (0.03-0.32)	0.05 (0.02-0.17)	0.05 (0.02-0.32)
UFRV (m3/m2/run)	96.45 (64.14-117.98)	99.3 (71.59-119.61)	140.9 (119.46-157.22)	82.59 (73.41-157.89)	88.08 (78.89-175.53)	71.71 (59.23-79.9)	136.12 (64.45-181.43)	104.24 (50.6-158.56)
VNHL (mm/EBV)	8.08 (5.66-11.08)	5.54 (4.5-6.57)	6.58 (5.09-7.48)	4.99 (3.61-6.5)	4 (2.87-5.58)	6.54 (4.06-13.93)	3.35 (1.45-9.52)	6.89 (4.13-13.09)

Appendix D Supplementary materials for Chapter 5

Table_Apx 5 Estimated velocities to achieve fluidisation and bed expansion based on media properties at 15°C. Minimum fluidisation velocities for the 60th & 90th percentile grain size shown, where a dual media is presented the highest fluidisation velocity of the two media is provided. Expansion is estimated based on the 10th percentile grain size. For brevity dual media are assumed to have two layers of equal depth. Expansion of individual media layers was assumed to be independent and additive.

Media Bed material & size (mm)	Vmf D_{60} (m/hr)	Vmf D_{90} (m/hr)	V 5% D_{10} Expansion (m/hr)	V 20% D_{10} Expansion (m/hr)
Dual Anthracite 0.60 - 1.18 Filtralite NC 0.8-1.6	8	10	16	23
Dual Anthracite 0.60 - 1.18 Filtralite NC 1.5-2.5	15	12	17	28
Dual Anthracite 0.60 - 1.40 Filtralite NC 0.8-1.6	10	10	16	24
Dual Anthracite 0.60 - 1.40 Filtralite NC 1.5-2.5	15	12	18	32
Dual Anthracite 0.80 - 1.60 Filtralite NC 0.8-1.6	14	10	20	29
Dual Anthracite 0.80 - 1.60 Filtralite NC 1.5-2.5	15	12	27	39
Dual Anthracite 0.85 - 1.60 Filtralite NC 0.8-1.6	14	10	20	32
Dual Anthracite 0.85 - 1.60 Filtralite NC 1.5-2.5	15	12	29	42
Dual Anthracite 1.18 - 2.50 Filtralite NC 1.5-2.5	25	19	32	47
Dual Anthracite 1.40 - 2.50 Filtralite NC 1.5-2.5	27	22	33	52
Dual Filtralite HC 0.5-1 Anthracite 0.60 - 1.40	10	13	15	23
Dual Filtralite HC 0.5-1 Anthracite 0.80 - 1.60	14	13	17	28
Dual Filtralite HC 0.5-1 Anthracite 0.85 - 1.60	14	13	17	30
Dual Filtralite HC 0.5-1 Anthracite 1.18 - 2.50	25	19	17	32
Dual Filtralite HC 0.5-1 Anthracite 1.40 - 2.50	27	22	17	33
Dual Filtralite HC 0.5-1 Filtralite MC 0.8-1.6	12	15	17	28
Dual Filtralite HC 0.5-1 Filtralite NC 0.8-1.6	8	13	16	23
Dual Filtralite HC 0.5-1 Filtralite NC 1.5-2.5	15	13	17	30
Dual Filtralite HC 0.8-1.6 Anthracite 1.18 - 2.50	25	28	31	47
Dual Filtralite HC 0.8-1.6 Anthracite 1.40 - 2.50	27	28	32	53
Dual Filtralite HC 0.8-1.6 Filtralite NC 1.5-2.5	23	28	28	40
Dual Filtralite MC 0.8-1.6 Filtralite NC 1.5-2.5	15	15	27	39
Dual Filtralite NC 0.8-1.6 Filtralite NC 1.5-2.5	15	12	20	31
Dual Sand 0.5-1 Anthracite 0.60 - 1.40	17	26	18	31
Dual Sand 0.5-1 Anthracite 0.80 - 1.60	17	26	25	40
Dual Sand 0.5-1 Anthracite 0.85 - 1.60	17	26	28	44
Dual Sand 0.5-1 Anthracite 1.18 - 2.50	25	26	31	49
Dual Sand 0.5-1 Anthracite 1.40 - 2.50	27	26	31	57
Dual Sand 0.5-1 Filtralite HC 0.8-1.6	23	28	26	41
Dual Sand 0.5-1 Filtralite MC 0.8-1.6	17	26	25	39
Dual Sand 0.5-1 Filtralite NC 0.8-1.6	17	26	20	30
Dual Sand 0.5-1 Filtralite NC 1.5-2.5	17	26	28	42

Dual Sand 0.6-1.2 Anthracite 0.60 - 1.40	28	33	18	31
Dual Sand 0.6-1.2 Anthracite 0.80 - 1.60	28	33	25	40
Dual Sand 0.6-1.2 Anthracite 0.85 - 1.60	28	33	28	45
Dual Sand 0.6-1.2 Anthracite 1.18 - 2.50	28	33	31	51
Dual Sand 0.6-1.2 Anthracite 1.40 - 2.50	28	33	33	59
Dual Sand 0.6-1.2 Filtralite HC 0.8-1.6	28	33	27	42
Dual Sand 0.6-1.2 Filtralite MC 0.8-1.6	28	33	26	40
Dual Sand 0.6-1.2 Filtralite NC 0.8-1.6	28	33	20	31
Dual Sand 0.6-1.2 Filtralite NC 1.5-2.5	28	33	28	42
Dual Sand 0.85-1.7 Anthracite 1.18 - 2.50	38	59	42	65
Dual Sand 0.85-1.7 Anthracite 1.40 - 2.50	38	59	49	77
Dual Sand 0.85-1.7 Filtralite NC 1.5-2.5	38	59	33	52
Dual Sand 1.0-2.0 Anthracite 1.18 - 2.50	59	74	43	67
Dual Sand 1.0-2.0 Anthracite 1.40 - 2.50	59	74	52	81
Dual Sand 1.0-2.0 Filtralite NC 1.5-2.5	59	74	33	53
Mono Anthracite 0.60 - 1.18	5	9	14	21
Mono Anthracite 0.60 - 1.40	10	6	15	24
Mono Anthracite 0.80 - 1.60	14	10	24	37
Mono Anthracite 0.85 - 1.60	14	10	30	45
Mono Anthracite 1.18 - 2.50	25	19	37	56
Mono Anthracite 1.40 - 2.50	27	22	50	77
Mono Filtralite HC 0.5-1	8	13	15	22
Mono Filtralite HC 0.8-1.6	23	28	27	40
Mono Filtralite MC 0.8-1.6	12	15	25	37
Mono Filtralite NC 0.8-1.6	8	10	17	25
Mono Filtralite NC 1.5-2.5	15	12	29	41
Mono Sand 0.5-1	17	26	25	43
Mono Sand 0.6-1.2	28	33	26	45
Mono Sand 0.85-1.7	38	59	49	77
Mono Sand 1.0-2.0	59	74	54	85
Mono Sand 1.2-2.8	74	109	84	125